

c. /

SYNOPTIC ESTIMATES OF  
AIR SEA FLUXES  
by  
RICHARD FRANK MARSDEN  
B.Sc., Royal Military College Of Canada, 1972

A THESIS SUBMITTED IN PARTIAL FULFILLMENT OF  
THE REQUIREMENTS FOR THE DEGREE OF  
DOCTOR OF PHILOSOPHY  
in  
THE FACULTY OF GRADUATE STUDIES  
(Department of Physics)

We accept this thesis as conforming  
to the required standard

THE UNIVERSITY OF BRITISH COLUMBIA

October 1980

(C) Richard Frank Marsden, 1980

In presenting this thesis in partial fulfilment of the requirements for an advanced degree at the University of British Columbia, I agree that the Library shall make it freely available for reference and study.

I further agree that permission for extensive copying of this thesis for scholarly purposes may be granted by the Head of my Department or by his representatives. It is understood that copying or publication of this thesis for financial gain shall not be allowed without my written permission.

Department of OCEANOGRAPHY

The University of British Columbia  
2075 Wesbrook Place  
Vancouver, Canada  
V6T 1W5

Date 15 Oct 1980

ABSTRACT

Synoptic and climatological dynamic studies generally rely on bulk aerodynamic flux formulae to describe air-sea heat and momentum exchange on synoptic and climatological scales. Barometric pressure maps (which involve an intrinsic temporal averaging of the wind) and wind roses provide two sources of spatial and temporal wind information for flux calculations. Several investigators have shown that, due to the non-linear dependence of the bulk aerodynamic formulae on the winds, time-averaged estimates of the fluxes based on vector averaged winds systematically underestimate the actual time-averaged fluxes.

Using 10 to 21 years of three-hourly sampled sea surface meteorological observations from 9 weatherstations in the North Atlantic Ocean and 2 weatherstations in the North Pacific Ocean, the three-hourly stresses, latent heat fluxes and sensible heat fluxes were calculated. The sampled data and the calculated fluxes were then averaged over periods varying up to 28 days. The estimates of the averaged fluxes based on the vector averaged winds were then compared to the directly averaged values.

A simple analysis revealed that an upper bound for the difference in the two stress calculations was directly proportional to the sum of the x and y component wind variances lost through the averaging process (in agreement with Fofonoff, 1960) and inversely proportional to the square of the vector averaged wind speed. The wind averaged and directly averaged flux estimates were grouped according to the Beaufort wind speed

category and the period over which the variates were averaged. A multivariate regression was then performed to optimize a transformation from the wind averaged to the directly averaged case.

For all fluxes, the transformation dramatically improved the wind averaged estimates of the climatological means and variances of the directly averaged fluxes. The residual error between the two estimates was decreased up to a factor of 5 over the uncorrected case and the correlation coefficients showed a moderate increase. The regression coefficients showed similar values for all temperate latitude stations.

Based on consistencies observed in the wind speed and averaging period dependencies of the multivariate coefficients, an empirical formula was found which interpolated the wind speed and averaging dependence and duplicated the multivariate regression results. The data from the ten temperate latitude stations were grouped and a single formula found which only moderately increased the errors between the wind-averaged and directly averaged estimates. The geographically averaged formula was not applicable at Station N, located at the northern extremity of the North Pacific Trade Wind region.

Analysis of the 28 day wind-averaged flux spectral estimates showed that they underestimated the 28 day directly averaged flux spectral estimates. Application of the specific ship empirical formula greatly improved agreement between the two spectral densities and reduced the residual series power density at all frequencies. High latent heat flux errors at Station N, could be reduced by application of a seasonal

correction.

The data were also grouped into monthly wind rose configurations and the wind rose monthly flux estimates were compared to the directly calculated long-term monthly mean fluxes. In all cases, the wind rose fluxes compared favourably with the directly calculated fluxes.

TABLE OF CONTENTS

ABSTRACT .....	ii
TABLE OF CONTENTS .....	v
LIST OF TABLES .....	vii
LIST OF FIGURES .....	viii
LIST OF SYMBOLS .....	xii
ACKNOWLEDGEMENTS .....	xiv
CHAPTER I Introduction .....	1
CHAPTER II Data Preparation .....	10
2.1 Data Origin .....	10
2.2 Data Verification .....	10
2.3 Density Calculations .....	16
2.4 Assumptions .....	18
2.5 Analysis And Definitions .....	23
CHAPTER III Momentum Fluxes .....	29
3.1 Vector Averaged 3H And VA Stress .....	29
3.2 Previous Studies .....	38
3.3 Individual Ratios .....	43
3.4 Multiple Regression Analysis .....	54
3.5 Variance Underestimation .....	58
3.6 Wind Dependent Correction Factors .....	61
3.7 Accuracy Of Transformations .....	64
CHAPTER IV Heat Fluxes .....	69
4.1 Three-hourly Heat Fluxes .....	69
4.2 Uncorrected Test Results .....	73
4.3 Heat Regression .....	78
4.4 Wind Dependent Corrections Factors .....	81

4.5 Beaufort Grouped Test Results .....	83
CHAPTER V Empirical Formula And Temporal Variations .....	88
5.1 Introduction .....	88
5.2 Empirical Formula .....	89
5.3 Ship Parameter Estimates .....	97
5.4 Geographical Averaged Results .....	107
5.5 Intrinsic Temporal Variations .....	113
CHAPTER VI Wind Rose Measurements .....	129
6.1 Introduction .....	129
6.2 Analysis .....	130
6.3 Results .....	136
Stress Magnitude Errors .....	137
Stress Direction Errors .....	140
Heat Fluxes .....	142
CHAPTER VII Summary And Conclusions .....	146
BIBLIOGRAPHY .....	152
APPENDIX A .....	155
APPENDIX B .....	162
APPENDIX C .....	169
APPENDIX D .....	187
APPENDIX E .....	194
APPENDIX F .....	198
APPENDIX G .....	216
APPENDIX H .....	219
APPENDIX I .....	222
APPENDIX J .....	231

LIST OF TABLES

TABLE I	Details of the station locations and number of years of collected data .....	12
TABLE II	Out-of-range limits for the initial stage of data processing .....	13
TABLE III	Total number of missing, out-of-range, and erroneous (spiked) data points per time series and weatherstation. ....	16
TABLE IV	Years of eliminated data for each weatherstation .....	17
TABLE V	The x and y component 3H stress means and standard deviations for all ships and years examined. ....	33
TABLE VI	Symbols used in the figures throughout the text. ....	36
TABLE VII	The stress variances for both drag coefficients as a function of averaging period. ....	37
TABLE VIII	The S(L) readings for all years of data at Weatherstation A using the constant drag coefficient. ....	43
TABLE IX	Beaufort wind speed intervals .....	46
TABLE X	The mean and standard deviations of the x and y component wind velocities, the air-sea temperature differences, the air-sea humidity differences, and the latent and sensible heat fluxes. ....	72
TABLE XI	The absolute latent and sensible heat flux variances as a function of averaging period. ...	74
TABLE XII	The geographical average ships' regression coefficients $\gamma = 1 + \alpha(u^2+v^2)^{\beta/2} L^{\gamma}$ for the form .....	109
TABLE XIII	The summer and winter formula coefficients required at Station N for the heat fluxes at L=28.0 days. ....	122
TABLE XIV	Coding for the wind rose levels calculated in Chapter VI. ....	136

## LIST OF FIGURES

Figure 1.	The net transport in the Greenland and Norwegian Seas for February, 1965. ....	6
Figure 2.	Locations of the 11 weatherstations involved in the study. ....	11
Figure 3.	The dew point temperature at three levels of processing. ....	14
Figure 4.	X and Y components of the 3H stress at Weatherstation C as a function of year and month. ....	31
Figure 5.	The 3H stress as a function of month at Station C indicating standard deviations of the monthly means. ....	32
Figure 6.	3H versus VA stress at Station A, L=28.0 days. ....	34
Figure 7.	Example of the composite test functions for all ships, x component, constant drag coefficient with no correction applied. ....	35
Figure 8.	The ratio of the wind stress magnitude computed from wind data that are vector averaged over a period, T, to the directly calculated wind stress. ....	40
Figure 9.	$S(L)$ and $A(L)$ as functions of averaging period for Weatherships A and C. ....	42
Figure 10.	Histogram of $R_j(.25)$ at Weatherstation C using the constant drag coefficient. ....	47
Figure 11.	Histogram of $B_j(.25)$ at Weatherstation C using the constant drag coefficient. ....	48
Figure 12.	$\overline{R(L)}$ for all ships at representative averaging periods and wind speeds using the constant drag coefficient. ....	51
Figure 13.	Geographically averaged values of $\overline{R(L)}$ for the constant drag coefficient for all averaging periods and wind speeds. ....	54
Figure 14.	$\overline{B(L)}$ for representative averaging periods and wind speeds for all ships using the constant drag coefficient. ....	55
Figure 15.	Systematic variance underestimation for all ships using initial estimates of $\zeta_{k2}$ . ....	59

Figure 16.	The relative error induced in the residual by application of a correction factor to readjust for the systematic bias in the difference variances. ....	62
Figure 17.	Correction factors $1/\xi_{he}$ for the constant drag coefficient. ....	63
Figure 18.	The test functions obtained when the ships' individual $\xi_{he}$ values were used. ....	65
Figure 19.	Improvement in the test values over the raw test results after application of the individual ships' correction. ....	66
Figure 20.	The year-to-year and monthly variations of the mean heat fluxes. ....	70
Figure 21.	The test quantities with no correction applied to the VA heat fluxes. ....	75
Figure 22.	The sensible and latent $\Delta H$ versus VA heat fluxes at Station C, $L=28.0$ days. ....	79
Figure 23.	Ships' $1/\xi_{he}$ values for the heat fluxes. ....	82
Figure 24.	Test values with the individual ships' $\xi_{he}$ applied to the heat fluxes. ....	84
Figure 25.	Test value improvements over the uncorrected case. ....	85
Figure 26.	The $\xi_{he}-1$ values as a function of wind speed. ...	90
Figure 27.	The $\xi_{he}-1$ values as a function of averaging period. ....	92
Figure 28.	Differences between the $\xi_{he}$ and empirical formula residual variances with no correction applied for the DV bias. ....	98
Figure 29.	The difference means using the empirical formula. ....	103
Figure 30.	The difference variances using the empirical formula. ....	104
Figure 31.	The residual variances using the empirical formula. ....	106
Figure 32.	The correlation coefficients with the ships' empirical formula applied. ....	107
Figure 33.	The difference means using the geographically averaged empirical formula. ....	110

Figure 34.	The difference variances using the geographically averaged empirical formula.....	111
Figure 35.	The residual variances using the geographically averaged empirical formula.....	112
Figure 36.	The correlation coefficients using the geographically averaged empirical formula. ....	114
Figure 37.	The spectra of the uncorrected VA, residual and 3H heat flux time series at Station C and N for L=28.0 days.....	118
Figure 38.	The spectra of the corrected heat flux for the 3H, VA and residual series at Stations C and N. ....	119
Figure 39.	The corrected residual series at Stations N and C for the latent heat flux, L=28.0 days....	123
Figure 40.	The heat flux spectra using the seasonally adjusted corrections at Station N, L=28.0 days. ....	124
Figure 41.	The X and Y component stress spectra, linear drag coefficient, for the uncorrected and corrected VA series at Station D, L=28.0 days. ....	125
Figure 42.	The linear drag coefficient spectra at Station D, L=28.0 days, corrected with the geographically averaged formula. ....	127
Figure 43.	The stress spectra at Station N corrected with the Station N empirical formula, L=28.0 days, linear drag coefficient. ....	127
Figure 44.	Construction of the piecewise linear distribution for the direction interpolation. ...	132
Figure 45.	The magnitude mean errors and error standard deviations between the actual stress and wind rose stress as a function of ship and month. ...	138
Figure 46.	The direction mean errors and error standard deviations between the actual stress and wind rose stress as function cf ship and month. ....	141
Figure 47.	The mean errors and error standard deviations between the actual sensible heat fluxes and the wind rose sensible heat fluxes as a function of ship and month. ....	143
Figure 48.	The mean errcrs and error standard deviations between the actual latent heat fluxes and the	

wind rose latent heat fluxes as a function of  
ship and month. ..... 144

TABLE OF SYMBOLSConstants

Cd	Drag coefficient	Constant - $1.5 \times 10^{-3}$ linear (see Equation 2.5)
Cq	Dalton number	$1.5 \times 10^{-3}$
Ct	Stanton number	$1.5 \times 10^{-3}$
Cp	Specific heat of air at constant pressure	$1.0 \times 10^3 \text{ J kg}^{-1} \text{ }^{\circ}\text{C}^{-1}$
E	Latent heat of evaporation	$2.46 \times 10^6 \text{ J kg}^{-1}$

General Symbols

A(L)	shift in direction between the climatological three-hourly averaged stress and the climatological vector averaged stress.
Bj(L)	shift in direction between the j estimate of the vector averaged stress magnitude and the j estimate of the three-hourly averaged stress magnitude.
<u>B</u> (L)	climatological time average of Bj(L)
DM	difference means
DV	difference variances
Hs	sensible heat flux
Hl	latent heat flux
L	averaging period (days)
q'	fluctuating absolute air humidity ( $\text{kg/m}^3$ )
q	mean absolute air humidity ( $\text{kg/m}^3$ )
Rj(L)	ratio of the j estimate of the vector averaged stress magnitude and the j estimate of the three-hourly averaged stress magnitude.
<u>R</u> (L)	climatological average of Rj(L)
RV	residual variance
S(L)	ratio of climatological vector averaged stress magnitude and climatological three-hourly averaged stress
T	average stress magnitude (dPa)
t'	fluctuating air temperature ( $^{\circ}\text{C}$ )
u	x component of wind velocity ( $\text{m/sec}$ )
v	y component of wind velocity ( $\text{m/sec}$ )
u'	fluctuating microscale downstream wind velocity ( $\text{m/sec}$ )
V	vector averaged wind speed ( $\text{m/sec}$ )
VA	vector averaged
w'	fluctuating microscale vertical wind velocity ( $\text{m/sec}$ )
X	three-hourly averaged flux
X'	vector averaged flux
3H	three-hourly averaged flux

Greek Symbols

$\Delta Q$	air sea humidity difference ( $\text{kg/m}^3$ )
$\Delta T$	air sea temperature difference ( $^\circ\text{C}$ )
$\eta$	empirical formula used to transform a vector averaged quantity to a three-hourly averaged quantity
$\bar{\eta}$	geographically averaged form of $\eta$
$\xi_{ne}$	Beaufort category/averaging period grouped regression constant used to transform the VA flux to resemble a 3H flux
$\overline{\xi}_{ne}$	geographical average of $\xi_{ne}$
$\rho$	air density ( $\text{kg/m}^3$ )

Superscripts

'	vector averaged quantity
$\bar{}$	time average

Subscripts

i	member of the three-hourly sampled and constructed time series
j	member of the set of variates averaged over L days
k	$k^{\text{th}}$ Beaufort category
l	$l^{\text{th}}$ averaging period
x	x direction (east)
y	y direction (north)

ACKNOWLEDGEMENT

I should like to thank the persons involved in the completion of this project. These few lines cannot adequately express my gratitude to my supervisor, Dr. S. Pond, without whose knowledge, encouragement and assistance, this work could not have been completed.

The North Atlantic weathership data was supplied by Dr. R. Pcllard of the Institute of Oceanographic Sciences, Wormley and the Station N data was obtained from Dr. C. Dorman, San Diego State University. Mr. B. Walker performed the initial structuring of the computer tapes. Dr. W. Large offered many practical suggestions in processing the large amounts of data involved.

The project was supported by the United States Office of Naval Research (Contract N00014-76-C-0446 under Project 083-207) and by the Natural Science and Engineering Research Council of Canada (Grant A8301). I personally received a post graduate scholarship from NSERC.

## CHAPTER I INTRODUCTION

The spatial and temporal scales of the turbulent environment for air-sea coupled systems may vary over significant orders of magnitude. For example, trends in the long-term heating and cooling of the Earth's surface of consequence to Man may require many decades to determine while turbulent diffusion of momentum within the sea must be measured in fractions of a second.

Fiedler and Panofsky (1970) have suggested several overlapping temporal (and spatial) scale ranges to aid in the description of time-dependent meteorological phenomena. The first is the microscale ranging from less than a second to about one hour. The mesoscale ranges from several minutes to several days, the synoptic scales start at about one day and extend to several weeks. The seasonal and climatic scales are longer than the synoptic scales.

Wind stress and sensible and latent heat fluxes can be described as the vertical transfer of horizontal momentum, temperature, and humidity from the air to the sea. Microscale experimental techniques are required to measure them. Among the techniques developed are the eddy-correlation, profile and dissipation methods. A detailed discussion of them may be found in the turbulence literature. Briefly, however, the vertical and downstream wind components and temperature and humidity fluctuations are sampled at a high rate (usually several Hertz) for periods up to one hour. The transport fluxes are determined through correlation of the vertical velocity fluctuations with

the downstream wind component, temperature and humidity fluctuations as shown below:

$$T = -\rho \overline{w'u'}$$

1.1 (a)

$$H_s = \rho C_p \overline{w't'}$$

1.1 (b)

$$H_e = E \overline{w'q'}$$

1.1 (c)

where  $T$  is the microscale wind stress,  $\rho$  is the air density,  $H_s$  is the sensible heat flux,  $H_l$  is the latent heat flux,  $w'$  is the vertical velocity,  $u'$  is the downstream velocity fluctuation,  $t'$  is the absolute air temperature fluctuation,  $q'$  is the absolute humidity fluctuation,  $E$  is the latent heat of vaporization ( $2.46 \times 10^6 \text{ J kg}^{-1}$ ),  $C_p$  is the specific heat of air at constant pressure ( $1.0 \times 10^3 \text{ J kg}^{-1} \text{ }^\circ\text{C}^{-1}$ ) and the overbar represents the ensemble average where all units are assumed to be S.I. Normally ergodicity is invoked and in practice a time average is actually used.

Equations 1.1 are exact. The rapid sampling required, however, (about 10 Hertz in the atmosphere) generates too much data for long time scale studies. Measuring the vertical fluctuation in particular and the rapidity of measurements in general necessitates using highly sophisticated equipment that is generally beyond the scope of the synoptic scale investigator.

The microscale fluxes can be related to the average of mesoscale measurements of one hour (or less) of sampling

duration through the bulk parameterizations given by (eg. Roll, 1965) :

$$T = \rho C_d V^2$$

1.2 (a)

or in components:

$$(T_x, T_y) = \rho C_d (u, v) V$$

1.2 (b)

$$H_s = \rho C_p C_t V \Delta T$$

1.2 (c)

$$H_e = C_q E V \Delta Q$$

1.2 (d)

where,  $T$  is the wind stress magnitude,  $T_x$  and  $T_y$  are the  $x$  and  $y$  components of the wind stress,  $V$  the mesoscale vector-averaged wind speed,  $u$  and  $v$  are the  $x$  and  $y$  components of the mesoscale averaged wind velocity,  $\Delta T$  is the average air-sea temperature difference,  $\Delta Q$  is the average air-sea absolute humidity difference.  $C_d$ ,  $C_t$  and  $C_q$  are nondimensional transfer coefficients commonly known as the drag coefficient, and Stanton and Dalton numbers respectively. They relate the mesoscale mean variables of Equation 1.2 to the microscale fluctuations of Equation 1.1.

Except for specific turbulence studies, hourly wind measurements are seldom available. Many calculations of transport fluxes are derived from quantities that are effectively averaged over periods much longer than one day. If we let overbars denote a time average then an estimate of the

average x component stress is:

$$\bar{T}_x = \frac{1}{I} \sum_{i=1}^I \rho_i C_{di} u_i (u_i^2 + v_i^2)^{1/2} \quad 1.3$$

where there are I observations and the subscript i denotes the set of wind components, air densities and drag coefficient observations.

An estimate of the x component of stress based on the component averaged winds is given by:

$$\bar{T}_x = \left( \frac{1}{I} \sum_i \rho_i \right) \left( \frac{1}{I} \sum_i C_{di} \right) \left( \frac{1}{I} \sum_i u_i \right) \times \\ \left\{ \left( \frac{1}{I} \sum_i u_i \right)^2 + \left( \frac{1}{I} \sum_i v_i \right)^2 \right\}^{1/2} \quad 1.4$$

It is evident that Equation 1.3 and 1.4 are not identical. By similar arguments the averaged heat fluxes calculated from Equations 1.2(c) and (d) will differ from the estimates of the averaged heat fluxes based on the product of the averaged constituent variables.

Malkus (1962) examined 59 three-hourly sampled wind observations from the Caribbean Sea and found that the fluxes (including momentum, latent heat, and sensible heat) calculated from the averaged constituents (Equation 1.4) underestimated the directly averaged fluxes (Equation 1.3) by only 7.0%. Similar calculations for the stresses, performed on three-hourly sampled winds at Weatherstation C revealed that the averaged constituent variables predicted a stress magnitude of only 35% of the directly calculated value. She attributed the differences in reduction to the steadiness of the Trade Winds where the long-term climatological averages are indicative of the short-term

mesoscale and synoptic scale conditions. Over middle latitude oceans, the winds are much more variable, being dominated by four to seven day cyclonic storms, and the long-term wind averages do not adequately indicate shorter period activity.

The wind stress input for many oceanographic calculations is derived from estimates of the geostrophic surface winds calculated from averaged barometric pressure maps. These maps are constructed through large spatial scale samples taken several times daily then temporally averaged over periods of up to a month or more.

Fofonoff(1960) in calculating oceanic transports in the North Pacific Ocean based on geostrophic winds derived from monthly pressure maps suggests that the difference between the monthly stress and the stress calculated from averaged pressures is proportional to the variance of the pressure gradient. The variance of the pressure gradient is equivalent to the sum of the u and v wind component variances over the period in which the pressure was averaged.

Aagaard(1970) provided a particularly striking example of the effect of using monthly averaged pressure maps in calculating transports in the Norwegian and Greenland Seas. Starting with six-hourly averaged pressure maps, he calculated the six-hourly Sverdrup transports following Fofonoff(1960). The six-hourly transports were then averaged over February 1965 to arrive at a monthly average transport which appears in Figure 1(a). He then averaged the barometric pressures over the same period and recalculated a pressure averaged estimate of the total transport for February 1965. This result appears in

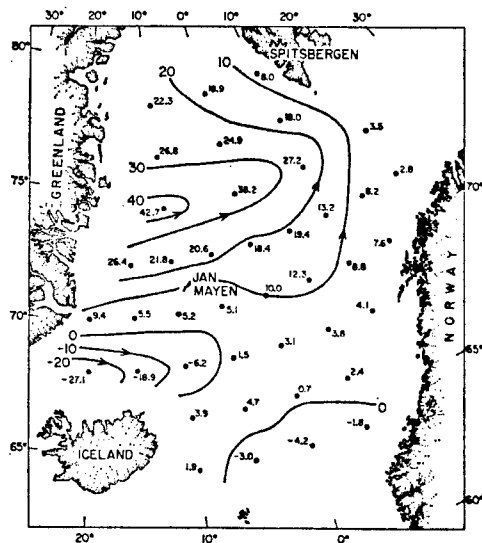


Figure 1(a)

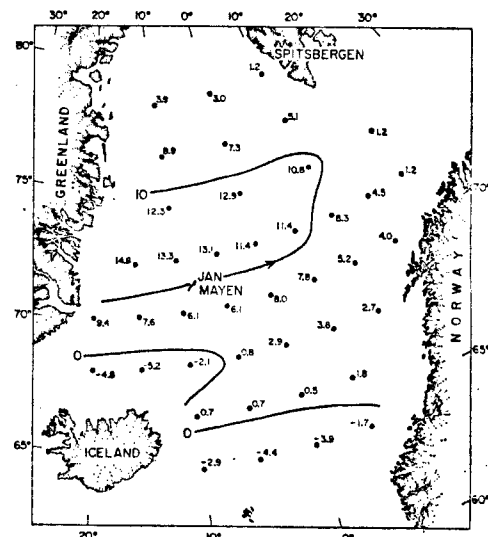


Figure 1(b)

Figure 1. The net transport in the Greenland and Norwegian Seas for February, 1965 based on six-hourly barometric pressure maps. Figure 1(a) shows the month average of the six-hourly transports and Figure 1(b) shows the transports based on the month average of six-hourly barometric pressures. Transport units are  $10^6 \text{ m}^3 \text{ sec}^{-1}$ . (from Aagaard, 1970)

Figure 1(b). It is quite evident that in regions of large average transport, the mean pressure approach underestimates the mean transport approach by a factor of four to five.

Willebrand(1978) used twelve-hourly averaged pressure maps to calculate spatial and temporal wind stress spectra on the North Atlantic and North Pacific Oceans. Although the overall spectral shapes may be qualitatively correct, the stress power density estimates are probably low.

Many oceanographic phenomena such as the reversal of the current regime in the Indian Ocean, the onset of El Niño in the Pacific Ocean, the reversal of the California and Davidson currents off the Western United States, and the onset of coastal upwelling have been linked with the temporal dependence of the wind stress forcing. A point of contention is whether the large scale (cf the order of 100 km) wind field and consequently

Sverdrup transports (curl of the wind stress) are important or whether local wind stresses (about 30 km) and Ekman transports are controlling mechanisms. In the case of El Niño, it has been demonstrated that the total oceanic stress is important (see McCreary, 1976 and Hurlburt, et.al. 1976) while the local Ekman transports are important for coastal upwelling (Allen, 1980).

For coastal phenomena the local winds, sampled at about hourly intervals, can be readily obtained from coastal stations. Open ocean wind field data are much more difficult to obtain (O'Brien, 1971) and geostrophic wind calculations from barometric pressure maps at present are the only viable source of wind information covering long time and large spatial scales. In the future satellite scatterometry may present an alternative source of wind information but at present these measurements are still in their infancy.

It is only recently that time-dependent meteorological conditions have been used to drive simulation models of the flow in large oceanic basins. Among others, a recent attempt in this vein has been the work of Huang(1978 and 1979) in modelling climatological and seasonal variations of the North Pacific Ocean. Two stages of his model have been presented. First, the model was spun up to quasi-steady state using an initial set of data based on climatologically averaged (over 20 years) stress, latent heat flux and sensible heat flux. The stress field resembled that of Hellerman(1967). In the next stage, a second set of data was used based on monthly estimates of the three fluxes at each grid point from monthly averaged values of air temperature, vapour pressure and zonal and meridional winds. A

quasi-deterministic annual cycle was then calculated at each grid point by fitting the first three harmonics of the annual cycle to the second data set and accepting the climatological information of the first data set for the constant term. It is evident that his technique should lead to the errors outlined by Aagaard (1970) shown in Figure 1. Some of the inherent averaging errors in Huang's model have been compensated by using a drag coefficient of  $2.5 \times 10^{-3}$  which is approximately double the more recent estimates (eg. Large 1979, Smith and Banke 1974).

Thus an objective of this thesis is to quantify on the mesoscale and synoptic scale, the reductions in air sea fluxes occurring when estimates are made using averaged wind and temperature data.

Fissel (1975) made an initial attempt at quantifying the discrepancy using as a data base ten years of meteorological observations at Weatherstation P. He found that the stress calculated through Equation 1.4 consistently underestimated that calculated through Equation 1.3 and that the reductions were quite regular for averaging periods up to two years.

The present study examines a data base of meteorological observations sampled at three-hourly intervals from nine weatherstations on the Atlantic Ocean and two weatherstations on the Pacific Ocean to determine the extent of the discrepancies referred to above and any generalities which may be projected from the results.

Normally climatological wind stress information is based on a wind rose analysis as outlined by Hellerman (1965). Here irregularly sampled wind measurements are sorted into discrete

wind speed and direction categories. The probability distribution of the wind components can be calculated and used to obtain estimates of the monthly or annual wind stress. Calculations of this sort have been used particularly for the steady state momentum flux inputs of large-scale ocean circulation numerical models.

The data base of the eleven weatherships' meteorological observations could be readily sorted into various choices of wind rose configurations. The "wind rose" fluxes were then compared to the actual individually determined fluxes (using Equation 1.3) to investigate the error induced by intrinsic wind rose averaging of the winds and thus errors in the estimates of the climatological wind stress fields.

## CHAPTER II DATA PREPARATION

### 2.1 Data Origin

The data base for the study originated from meteorological observations at Ocean Weatherstations Alpha, Bravo, Charlie, Delta, Echo, India, Juliet, Kilo, Mike, November and Papa which will henceforth be referred to by the capital letter only of the station (eg. Weatherstation E). The quantities recorded at each station were wind speed and direction, barometric pressure, wet and dry bulb temperatures and sea surface temperature which were sampled at three-hourly intervals. Maps of the weathership locations appear in Figure 2.

Data from Stations A through M were transferred from IBM punch cards to seven-track magnetic tape at the University of Southampton, England while Station N data were transferred to seven track magnetic tape at Oregon State University. The wet and dry bulb temperatures were converted to a dew point temperature on these tapes. The Station P data were entirely processed at the University of British Columbia and details of the editing can be found in Hertzman, et. al. (1974). A resume of the number of years of data, country responsible for collection, and latitude and longitude of the stations can be found in Table I. Further details of data collection techniques can be found by addressing inquiries to the national weather bureau services of the responsible countries.

### 2.2 Data Verification

In order for tapes from the University of Southampton and

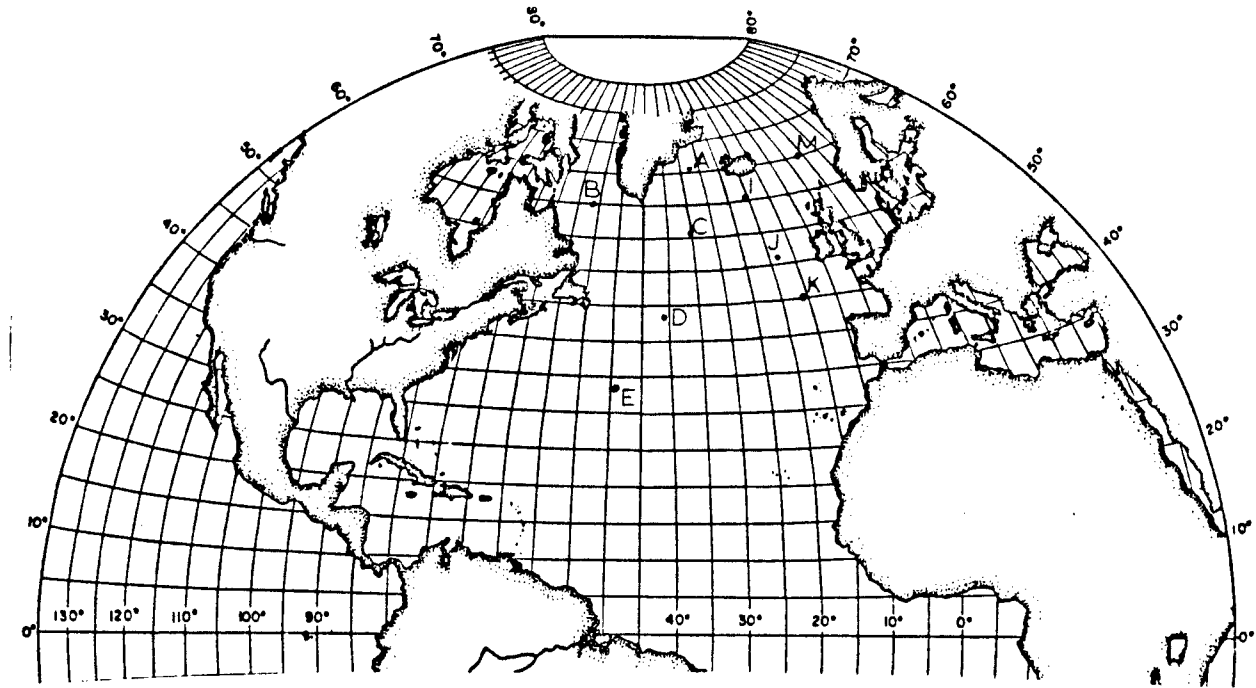


Figure 2(a) North Atlantic Stations.

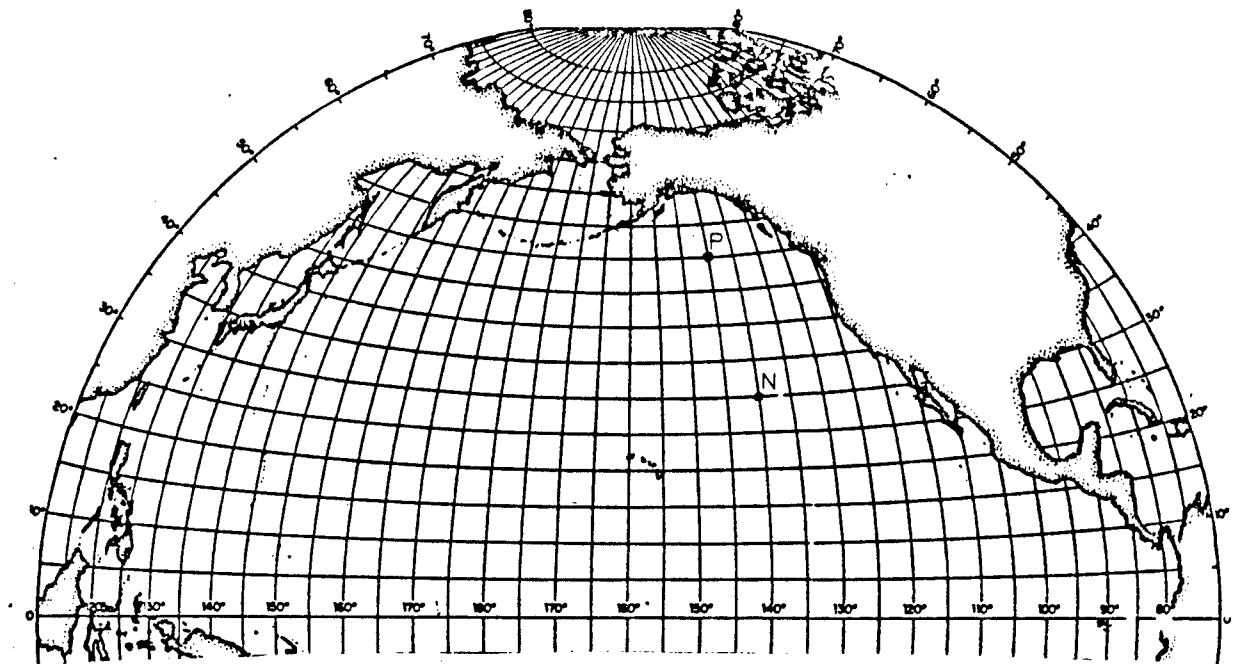


Figure 2(b) North Pacific Stations.

Figure 2. Locations of the 11 weatherstations involved in the study.

TABLE I

Details of the stations locations and number of years of data that were collected. The start date is 1 January of the start year and the end date is 31 December of the end year.

STATION	COUNTRY	LATITUDE	LONGITUDE	START	END
				RESPONSIBLE	DATE
A	Netherlands -U.S.	61-63 °N	31-35 °W	1949	1965
B	Canada -U.S.	55.5-57.5 °N	49.5-52.5 °W	1949	1967
C	U.S.	51.5-53.5 °N	34-37 °W	1949	1967
D	U.S.	43-45 °N	40-42 °W	1949	1967
E	U.S.	34-36 °N	47-49 °W	1949	1967
I	U.K.	59-61 °N	18-21 °W	1949	1964
J	Netherlands - U.S.	52.3-54.3 °N	17.8-20.8 °N	1949	1965
K	Netherlands -France	44-46 °N	15-17 °W	1949	1961
M	Norway	65-67	0-4 °E	1949	1963
N	U.S.	28.5-31.5 °N	138-142 °W	1949	1969
P	Canada	48.5-51.5 °N	142.6-147.6 °W	1958	1967

Oregon State University to be compatible with the University of British Columbia computer systems, the original data tapes had to be reformatted from seven to nine tracks. Simultaneously, missing data were identified and flagged by replacing the missing values with -999.9. The reconstructed time series were then compared, point-by-point, to extreme values as outlined in Table II. Any data which had values outside these ranges were considered to be in error and these were also eliminated from calculations by flagging them with -999.9. An example of the dew point temperature time series for Weatherstation A at this level of processing is shown in Figure 3(a). At this stage, the u and v wind velocity component time series were produced from the wind direction and speed choosing the positive x and y directions as east and north respectively.

TABLE II

Out-of-range limits for the initial stage of data processing.

QUANTITY	UNITS	LOWER LIMIT	UPPER LIMIT
Wind Direction	° from N	-180	180
Wind Speed	m/sec	0	70
Barometric Pressure	millibars	900	1060
Air Temperature	°C.	-20	40
Dew Point Temperature	°C.	-20	40
Sea Surface Temperature	°C.	-10	40

Because the data analysis required a continuous three-hourly time series, the flagged data of all channels were replaced by a value which was linearly interpolated between the nearest preceding good point and the next anteceding good point. The wind u and v components were interpolated and the speed and direction then calculated from the components. Figure 3(b) shows the interpolated time series reconstructed from Figure 3(a). There were two main types of errors present. The blackened areas of Figure 3(a) correspond to every second or third measurement being either missing or out-of-range. When these values are replaced, the corresponding sections in Figure 3(b) are virtually indistinguishable from the remainder of the time series. The arrow in Figure 3(a) indicates where data are missing for seven days corresponding to instrument malfunction or the ship being off station. As can be seen in Figure 3(b),

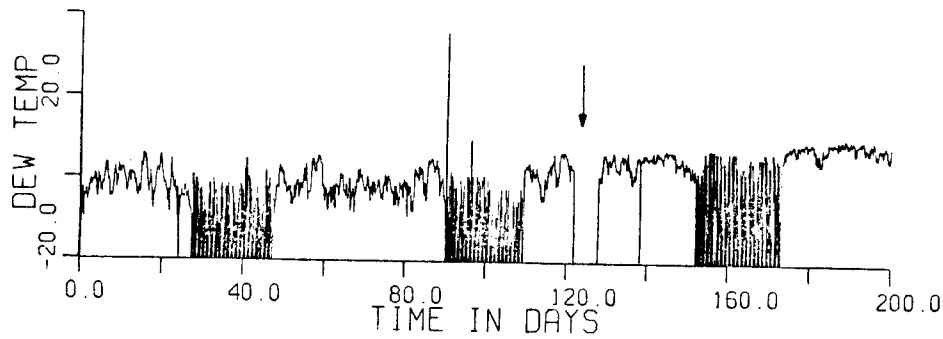


Figure 3(a). Missing and out-of-range flagged data.

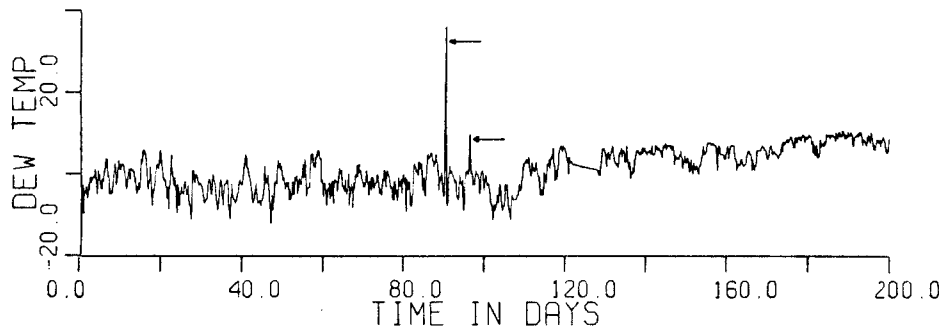


Figure 3(b). Same as above with bad data interpolated. The arrows indicate spikes.

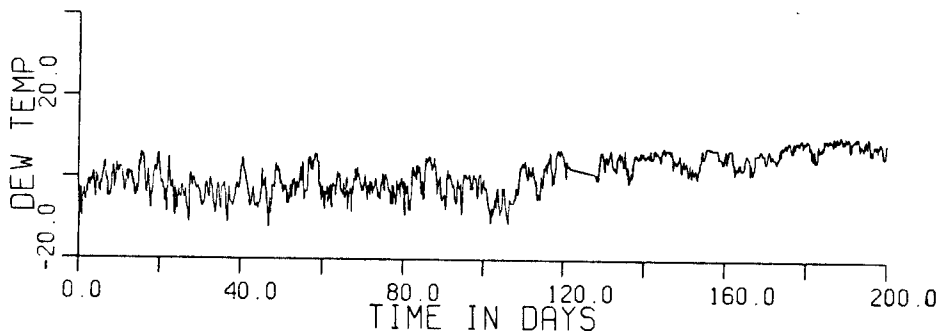


Figure 3(c). Same as above with the spikes identified and interpolated.

Figure 3. The dew point temperature at three levels of processing for Station A from Jan 1 1951 to July 20, 1951.

the linear interpolation results in a flattened region where the variance has been markedly reduced.

The arrows in Figure 3(b) illustrate examples of "spikes" or regions where the data are discontinuous and obviously erroneous even though within the limits of Table II. In the more prominent case, the dew temperature rises from -4.8°C to 36.1°C and back to -3.9°C in twelve hours. Consequently all the data were visually monitored on the UBC Department of Oceanography PDP - 12 computer. Obvious spikes were identified and the points replaced by interpolated values. At this stage an eight bit flag recorded each data point which had been interpolated. Table III gives the total number of missing, erroneous, and out-of-range data points for each of the measured quantities. The Station P information was extracted from Fissel(1975).

With the exception of Weatherstation I, the dew point temperature displays the largest number of interpolated points. This is representative of a large number of missing readings rather than spikes. Weathership A, for example, has dew point measurements for every second reading only for the period 1952 to 1954. Similar situations exist for the other weatherships.

Analyses attempted in the study required yearly blocks of data that closely approximated the actual times series. The regularly missing (that is, every second or third point) data presented little problem because major features such as the diurnal cycle remained intact. Large blocks of missing data severely distorted the time series to the extent that it was felt that they could influence the final results. For any

TABLE III

Total number of missing, cut-of-range, and erroneous (spiked) data points per time series and weatherstation. The total column signifies the total number of samples taken (ie. the number of days studied times 8).

SHIP	WIND METER	TIME SERIES					TOTAL
		BARO AIR TEMP.	DEW TEMP.	SEA TEMP.	TOTAL		
A	4911	4618	4620	8668	5659	49672	
E	2043	2029	2061	17730	6341	55512	
C	1702	1692	1708	17654	3102	55512	
D	1567	1532	1523	17851	5955	55512	
E	1677	1678	1642	17683	5921	55512	
I	2466	2395	2377	2405	2577	46752	
J	3703	3837	3669	4325	3636	49672	
K	1704	1591	1619	4767	4758	37984	
M	2778	2780	2938	4605	2879	43824	
N	1432	1278	1298	17814	5754	64280	
P	235	238	231	233	244	29216	

variate which contained more than 125 consecutive missing data points in any given month, the entire year of data for that variable was rejected. Table IV shows the years of rejected data for each ship.

### 2.3 Density Calculations

Page F-9 of the Handbook of Physics and Chemistry (59th edition) gives an empirical formula for the density of moist air as:

$$\rho = 1.2929(273.13/T_a)(P - 0.3783e/760)$$

2.1

where  $\rho$  is the air density in  $\text{kg/m}^3$ ,  $T_a$  is the dry air temperature in  $^\circ\text{K}$ ,  $P$  is the barometric pressure in  $\text{mmHg}$ , and  $e$

TABLE IV

The year(s) of eliminated data for each weatherstation.

SHIP	STRESS	HEAT FLUXES
A	1950	1950
B	-	52,53
C	-	1953
D	-	52,53
E	-	52,53
I	1952	1952
J	1952	52,57
K	1953	49,50,51 53,54
M	1949	1949
N	-	52,53
P	-	-

is the vapour pressure of the moisture in mmHg. Hertzman et. al. (1974) give a formula to calculate the absolute humidity based on values in the CRC Handbook of Physics and Chemistry (51st edition):

$$q = 6.4038 \times 10^8 \exp(-5107.4/T_d) \quad 2.2$$

where  $q$  is the absolute humidity in  $\text{gm/m}^3$  and  $T_d$  is the dew point temperature in  $^{\circ}\text{K}$ . By the ideal gas law:

$$e/T_a = qR \quad 2.3$$

where  $R$  is the ideal gas constant =  $8.0143 \text{ J mol}^{-1} ({}^{\circ}\text{K})^{-1}$  and  $T_a$  is the air temperature in  ${}^{\circ}\text{K}$ . The quantities recorded are the barometric pressure in millibars and the air and dew-point temperatures in degrees Celsius. Making appropriate unit

conversions, and substituting Equation 2.3 in 2.2 gives:

$$\epsilon = 2.2158 \times 10^6 \times (T_a) \times \exp(-5107.4/T_d) \quad 2.4$$

After obtaining the vapour pressure Equation 2.4 was substituted in Equation 2.1 to give the air density.

#### 2.4 Assumptions

The most sensitive parameters in the bulk aerodynamic flux formulae of Equations 1.2 are the transfer coefficients. For example, the form of the drag coefficient has undergone considerable debate. Estimates vary from a constant value (Pond et al. 1971), to a step function of wind speed (Rossby and Montgomery 1935), to a linear function of wind speed (Smith and Banke, 1975). Traditionally mesoscale and synoptic scale dynamic studies have employed the constant form. Recent estimates (eg. Large, 1979) at wind speeds greater than 15 m/sec have indicated that the linear form may be appropriate. Consequently for this study two drag coefficient formulations were used -- a constant form of  $1.5 \times 10^{-3}$  (after Pond, 1971) and a linear form (from Large, 1979):

$$C_d = 1.14 \times 10^{-3} \quad 0 < V < 10 \text{ m/sec} \quad 2.5$$

$$C_d = (0.49 + 0.065V) \times 10^{-3} \quad V > 10 \text{ m/sec}$$

where V is the wind velocity averaged over one hour.

The Stanton and Dalton numbers are less well understood than the drag coefficient. Large lists instrument contamination

from sea spray as a major impediment in their measurement. Thus a value of  $1.5 \times 10^{-3}$  after Pond et al. (1974) was taken.

Normally the transfer coefficients are assumed to be calculated at a reference level of 10m and under conditions of neutral stability. Neither of these conditions is met by most of the data used in this study. The anemometer level, for example, at Station P is at 22m. Over most of the Northern temperate oceans the sea is generally warmer than the air and the sea surface saturation is generally greater than the absolute humidity of the surrounding air indicating that generally unstable conditions exist.

Large(1979) and Turner(1973) give the corrections required to the transfer coefficients to account for non-normal conditions. Corrections applied in turbulence studies require the calculation of a flux Richardson number involving the correlation of the vertical velocity fluctuations with the air temperature fluctuations and the air absolute humidity fluctuations at microscale sampling rates. A bulk stability parameter could be estimated from the data. Large(1979) indicates that certain oceanic conditions (eg. an air-sea temperature difference of 5.0 °C and a wind speed of 10.0 m/sec) could induce about a 10% error in the transfer coefficients due to stability. Averaging the fluxes would lead to much smaller errors and because the study will be concerned with ratios of fluxes, such errors will further cancel. Furthermore, the relationship between the stability and the flux ratios at Station A for 1949 was investigated and no correlation was evident. Thus stability considerations are left as minor errors

in the data. Non-standard height is not corrected because it would involve a direct multiplication factor to the stresses (Fissel et al. 1977). Since this study will be concerned with ratios of stress, the height corrections cancel. (Indeed any constant formulation of the transfer coefficients cancels). Thus it is assumed that the transfer coefficients defined in Equations 1.3 and 1.4 are at 10m reference height and at neutral stability.

In order to calculate the latent heat flux it was necessary to find the sea surface saturation and absolute air humidity difference. The absolute air humidity is given by Equation 2.2. The sea saturation was assumed to be at the sea surface temperature. Ts was used in place of Td to calculate the sea surface humidity. This value was then multiplied by 0.98 to account for the depression of the saturation point due to the presence of salt.

Throughout the thesis, the air-sea humidity differences and not the constituent sea surface and dew point temperatures were averaged. For usual climatic calculations, however, averaged humidity differences are seldom available. Rather, the normal information is the averaged constituent variables. Consequently a systematic error is induced in most calculations.

If we consider a single estimate of q to be based upon a mean temperature  $\bar{T}$  and a deviation from the mean  $T'$  then (see Equation 2.2):

$$q = C_1 \exp(C_2 / (\bar{T} + T'))$$

2.6

Assuming that the mean temperature is much greater than the fluctuation, the exponential can then be re-expressed as :

$$q = C_1 \exp \left\{ \frac{C_2}{\bar{T}} \left[ 1 - \frac{\bar{T}'}{\bar{T}} + \left( \frac{\bar{T}'}{\bar{T}} \right)^2 \right] \right\}$$

which becomes:

$$q = C_1 \exp \left( \frac{C_2}{\bar{T}} \right) \exp \left\{ \frac{C_2}{\bar{T}} \left[ \left( \frac{\bar{T}'}{\bar{T}} \right)^2 - \frac{\bar{T}'}{\bar{T}} \right] \right\} \quad 2.7$$

A typical ratio of  $\bar{T}'^2/\bar{T}^2$  for the dew point temperatures was found to be  $1.2 \times 10^{-4}$ . Allowing a fluctuation of 5 standard deviations and a value of  $C_2/T = -18.0$  (ie.  $T=273$  °K), the terms above in the exponential are correct to  $O(10^{-2})$ .

Expanding Equation 2.7 in a Taylor series and keeping all terms of  $O(>10^{-2})$  gives:

$$\begin{aligned} q &= C_1 \exp \left( \frac{C_2}{\bar{T}} \right) \left\{ 1 + \frac{C_2}{\bar{T}} \left[ \left( \frac{\bar{T}'}{\bar{T}} \right)^2 - \frac{\bar{T}'}{\bar{T}} \right] + \right. \\ &\quad \frac{1}{2} \left( \frac{C_2}{\bar{T}} \right)^2 \left[ \left( \frac{\bar{T}'}{\bar{T}} \right)^2 - 2 \left( \frac{\bar{T}'}{\bar{T}} \right)^3 \right] + \\ &\quad \left. \frac{1}{6} \left( \frac{C_2}{\bar{T}} \right)^3 \left[ 3 \left( \frac{\bar{T}'}{\bar{T}} \right)^4 - \left( \frac{\bar{T}'}{\bar{T}} \right)^3 \right] + \frac{1}{24} \left( \frac{C_2}{\bar{T}} \right)^4 \left[ \left( \frac{\bar{T}'}{\bar{T}} \right)^4 + \dots \right] \right\} \end{aligned} \quad 2.8$$

Averaging both sides of Equation 2.8 and recognizing that  $C_1 \exp(C_2/\bar{T})$  is the absolute humidity determined from the average temperature ( $q(\bar{T})$ ) then :

$$\bar{q} = q(\bar{T}) \left\{ 1 + \frac{C_2}{\bar{T}} \left[ \frac{\bar{T}^{12}}{\bar{T}^2} - \frac{\bar{T}^4}{\bar{T}} \right] + \right. \\ \left. \frac{1}{2} \left( \frac{C_2}{\bar{T}} \right)^2 \left[ \frac{\bar{T}^{12}}{\bar{T}^2} - 2 \frac{\bar{T}^{13}}{\bar{T}^3} \right] + \right. \\ \left. \frac{1}{6} \left( \frac{C_2}{\bar{T}} \right)^3 \left[ 3 \frac{\bar{T}^{14}}{\bar{T}^4} - \frac{\bar{T}^{13}}{\bar{T}^3} \right] + \frac{1}{24} \left( \frac{C_2}{\bar{T}} \right)^4 \left[ \frac{\bar{T}^{14}}{\bar{T}^4} + \dots \right] \right\} \quad 2.9$$

If the distribution is reasonably Gaussian then:

a.  $\bar{T}^n - n \text{ cdd} = 0.0$

b.  $\bar{T}^4 = 3 \times (\bar{T}^2)^2$

The terms in  $\bar{T}^4/\bar{T}^2$  are all 0 ( $< 10^{-3}$ ) and Equation 2.9 reduces to:

$$\bar{q} = q(\bar{T}) \left\{ 1 + \left( \frac{\bar{T}^{12}}{\bar{T}^2} \right) \left( \frac{C_2}{\bar{T}} \right) \left( \frac{1}{2} \frac{C_2}{\bar{T}} + 1 \right) \right\} \quad 2.10$$

Taking  $(C_2/\bar{T}) = -18.0$  and  $\bar{T}^{12}/\bar{T}^2 = 1.2 \times 10^{-4}$  (a typical value) we see that:

$$q = q(\bar{T}) (1 + 0.02)$$

Since the maximum averaging period is 28 days, an upper limit on the systematic error induced in averaging the humidities over averaging the dew point temperatures is approximately 2.0%. Furthermore, the  $\bar{T}^{12}/\bar{T}^2$  ratio for the sea surface temperatures was about one half that of the dew point temperatures. This gives a systematic sea surface humidity bias of about 1.0%. Since the two biases are subtracted in the latent heat flux, this gives a negative systematic air-sea humidity difference bias of only 1.0%. This was considered negligible in comparison with the probable sampling errors in the data.

## 2.5 Analysis And Definitions

Because each ship contained a varying number of years of data, they were reconstructed into yearly blocks of 2912 observations each. The 2912 figure was chosen because it was evenly divisible by multiples of 2, 4, and 13 allowing semi-annual and lunar monthly divisions of the year. The eight (or 16 for a leap year) observations at the end of each year were omitted from calculations. This is unlikely to significantly influence the final results.

From the raw three-hourly data set, the three-hourly densities, absolute humidities, stresses and heat fluxes were calculated. The sampled and calculated variates were then averaged in sets of 2, 4, 8, 16, 32, 56, 112, and 224 readings, corresponding to averaging over 0.25, 0.5, 1.0, 2.0, 4.0, 7.0, 14.0, and 28.0 days. Thus for a one year sample, the set of variates averaged over 224 three-hourly readings contains  $2912/224=13$  members. The length of time over which the three-hourly data set was averaged will be referred to as the averaging period, will be denoted by the capital letter L, and will be expressed in days. Thus averaging 224 three-hourly measurements yields an averaging period of  $L=28.0$  days.

The fluxes were then recalculated using the averaged constituent data. The winds and fluxes calculated in this manner will referred to as the vector averaged or VA winds and fluxes. The VA fluxes were then compared to the directly averaged fluxes from the original three-hourly time series. The directly averaged fluxes will be referred to as the three-hourly averaged or 3H fluxes.

An example using the stress components should clarify these definitions. Defining the positive x and y directions as east and north respectively, the 3H stress vector components averaged over L days are:

$$(T_{xj}, T_{yj}) = \left( \frac{1}{I} \sum_{i=1}^I \rho_i C_{di} (u_i^2 + v_i^2)^{1/2} u_i , \frac{1}{I} \sum_{i=1}^I \rho_i C_{di} (u_i^2 + v_i^2)^{1/2} v_i \right) \quad 2.11$$

where I=L days x 8 measurements/day,  $u_i$  and  $v_i$  are the constituent wind components from the raw three-hourly series,  $\rho_i$  are the three-hourly air densities,  $C_{di}$  are the three hourly drag coefficients, and  $T_{xj}$  and  $T_{yj}$  are the 3H x and y stress components. The VA wind vectors over the same averaging period are:

$$(u_j, v_j) = \left( \frac{1}{I} \sum u_i , \frac{1}{I} \sum v_i \right) \quad 2.12$$

where  $u_j$  and  $v_j$  are the VA wind components averaged over L days. A VA stress can then be calculated from the VA winds by :

$$(T'_{xj}, T'_{yj}) = (\rho_j C_{dj} (u_j^2 + v_j^2)^{1/2} u_j , \rho_j C_{dj} (u_j^2 + v_j^2)^{1/2} v_j) \quad 2.13$$

$\rho_j$  is the density averaged over I days,  $C_{dj}$  is the drag coefficient based on the VA wind and  $T'_{xj}$  and  $T'_{yj}$  are the VA stress component estimates.

Throughout the text, the subscript i will refer to a member of the raw three-hourly data set and the subscript j will refer to a member of the data set obtained from averaging the three-

hourly set in L day groups. The 3H fluxes will appear without primes and the VA fluxes will appear with primes.

The analysis of the differences between the VA and 3H fluxes requires three distinct steps. First, the raw VA and 3H variates must be evaluated statistically to determine the inherent differences between the two estimates. Next, since the 3H variate is the more accurate flux estimate, transformations must be found for the VA variate so that it more closely approximates the 3H variate. Once a suitable transformation has been found, it must be applied to the VA variate and the statistics re-evaluated. Thus, the analysis involves two distinct calculations -- computing the statistical relationship between the VA and 3H variates and computing the transformation itself.

Let  $X_j$  and  $X'_j$  be members of the 3H and VA flux variates respectively for an averaging period L. The  $X'_j$  may or may not include the transformation step and  $X_j$  and  $X'_j$  define generally the x or y components of stress or the latent or sensible heat fluxes. The long-term means ( $\bar{X}, \bar{X}'$ ) are defined as:

$$(\bar{X}, \bar{X}') = \left( \frac{1}{J} \sum_{j=1}^J X_j, \frac{1}{J} \sum_{j=1}^J X'_j \right) \quad 2.14$$

where J is the total number of averagings available in the record for a given averaging period L. Similarly the long term variances,  $\sigma_x^2$  and  $\sigma_{x'}^2$ , are defined as:

$$(\sigma_x^2, \sigma_{x'}^2) = \left( \frac{1}{J} \sum_{j=1}^J (X_j - \bar{X})^2, \frac{1}{J} \sum_{j=1}^J (X'_j - \bar{X}')^2 \right) \quad 2.15$$

The relationship between the 3H and VA variates is then defined in terms of four statistical quantities which will collectively be called the test functions. First, the effectiveness of determining the long term mean flux is defined by:

$$\Delta x = |\bar{x} - \bar{x}'| \quad . \quad 2.16$$

This will be referred to as the difference mean (or DM). A measure of the conservation of the total variance, in the transformation, is given by:

$$\Delta \sigma_x^2 = \frac{(\sigma_x^2 - \sigma_{x'}^2)}{\sigma_x^2} \quad 2.17$$

and will be referred to as the difference variance (DV). The effectiveness of the transformation on a point-by-point basis is given by the residual variance (RV), defined as:

$$\delta_x^2 = \frac{\left\{ \frac{1}{J} \sum_{j=1}^J (x_j - x'_j)^2 - (\Delta x)^2 \right\}}{\sigma_x^2} \quad 2.18$$

Finally, the correlation coefficient determines the statistical dependence of one variate on the other and is defined by:

$$R_x = \frac{\left\{ \frac{1}{J} \sum_{j=1}^J X_j X'_j - \bar{X} \bar{X}' \right\}}{\left\{ \sigma_x^2 \sigma_{x'}^2 \right\}^{1/2}}$$

2.19

Assuming that the atmosphere has a climatological steady state, the DMs indicate whether the climatological mean of the VA variate approaches that of the 3H variate. For spectral studies such as Willebrand(1978) both the total variance and the frequency-by-frequency power spectral densities for the two variates should match. The former condition is determined by the DVs; the latter condition will be investigated in Chapter V. The RVs determine the relationship between the VA and 3H variates on a point-by-point basis (ie. on the time scales of the averaging period itself). Finally, the correlation coefficients determine statistically the ability of one variate to infer the other. It is quite conceivable, for example, to find a scale factor which will effectively reduce the DMs, DVs, and RVs, while leaving the correlation coefficients unchanged.

The DVs, RVs and correlation coefficients have been normalized by the 3H variance for ease of inter-comparison between ships. This effectively removes the height correction (discussed in Section 2.4) from the statistics since it would appear to the same power in the numerator and denominator in all three cases. The DMs have not been normalized because an appropriate normalizing factor would be the mean 3H flux value. At certain locations, however, it approached 0 dPa for the stress (DeciPascals are used for units and are numerically equivalent to dynes/cm<sup>2</sup>) and 0 Watts/m<sup>2</sup> for the heat fluxes.

The absolute value is used in the DM calculation because we are concerned that the climatological  $3H$  value be estimated irrespective of sign. Recent information (Large, personal communication, 1980) indicates that the Stanton and Dalton numbers used in this study ( $1.5 \times 10^{-3}$ ) are about 20.0% high. Furthermore, the non-standard height and the stability assumptions outlined in Section 2.4 may induce a further 20.0% error in the data. Thus, when a DM or a mean  $3H$  flux is quoted, the values given may be biased high.

A discussion of the VA transformation procedures forms an integral part of the text and will be discussed in more detail later. In all cases, however, the test functions defined in Equations 2.16 to 2.19 will be used to evaluate the effectiveness of the transformations.

### CHAPTER III MOMENTUM FLUXES

The processed data base outlined in Chapter II was analysed to determine the extent of the expected underestimation of stress when using winds averaged over times longer than one hour. The reductions are studied both for calculations of climatological values of long term net stresses, (based on wind data averaged over a month or more) and for calculating actual time history values for which data might be averaged to about one month. Climatological stresses are used as an input in numerical models attempting to calculate the steady state oceanic circulation. The temporal variations are required for such studies as that by Willebrand (1978) for calculations of the stress spectra using vector averaged winds derived from pressure maps or for models attempting to examine the effects of time-dependent wind stress forcing. The bulk aerodynamic formulae for the calculation of the stresses are given in Equations 1.2(a) and (b).

#### 3.1 The Vector Averaged $3H$ And $VA$ Stress

The  $3H$  stress provides an estimate of the 'true' stress and will be examined first. The annual cycle, in terms of monthly  $3H$  means and standard deviations will be examined using 224 points per month giving 13 lunar months per year.

Due to the enormous amount of data analysed, not all of the results can be presented in this thesis. All ships exhibited a winter maximum and summer minimum both in the average stress and in the stress variability of which Weatherstation C is an

example. This pattern is indicative of a winter storm season typical of the northern temperate latitudes.

A plot of the stress components for Weatherstation C appears in Figures 4(a) through (d). The error bars are  $\pm 1$  standard deviation about the mean. It is readily apparent that the standard deviations may be as much as one order of magnitude larger than the mean stress value (and thus the variance to mean squares ratio of order 100) in either component for any given year. Over the whole record, the x component mean value is positive with an overall average value of about 1.0 dPa (which is numerically equivalent to 1.0 dynes  $\text{cm}^{-2}$ ) while the y component average value is about 0.20 dPa and the x component standard deviation is about 1.25 times greater than the y component standard deviation. The maximum difference in standard deviation between years appears in the x component between 1952 and 1959 where the ratio is about 2. Figures 4(c) and (d) demonstrate the annual cycle in variability; the ratio of standard deviations between month 1 (January) and month 7 (July) is about 3.

The standard deviation of the monthly means was also calculated and appears in Figure 5 to show the inter-annual variability of the monthly stress mean. The annual cycle of the mean stress is evident particularly in the x component which varies from about 1.5 dPa in the winter to about 0.5 dPa in the summer. An annual cycle in the mean y stress is not evident. A comparison between the standard deviations of Figures 5 and 4(c) and (d) indicates that they have been reduced by a factor of two to three, not the factor of 15 one might expect if the 224

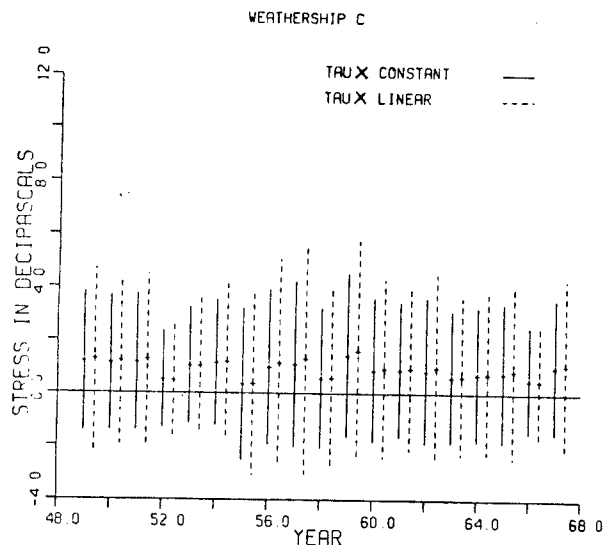


Figure 4 (a)

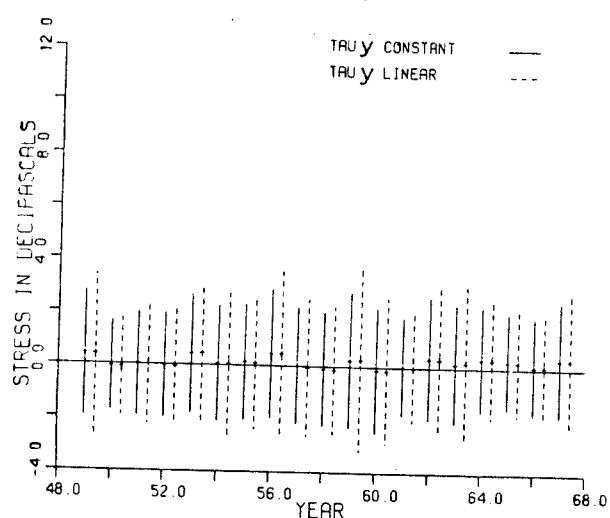


Figure 4 (b)

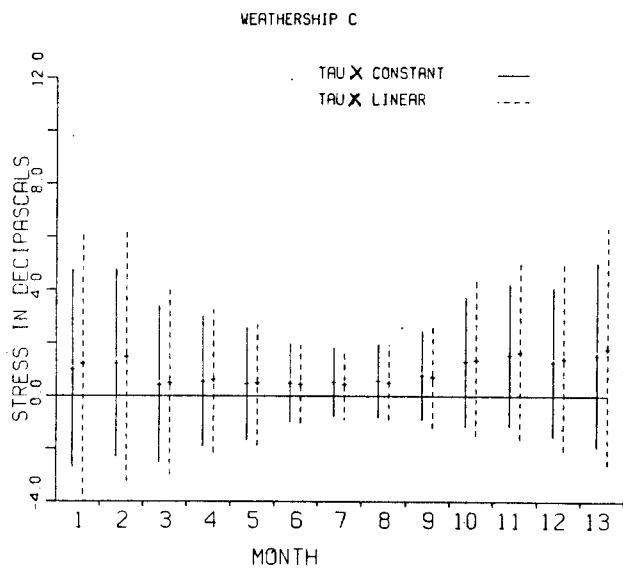


Figure 4 (c)

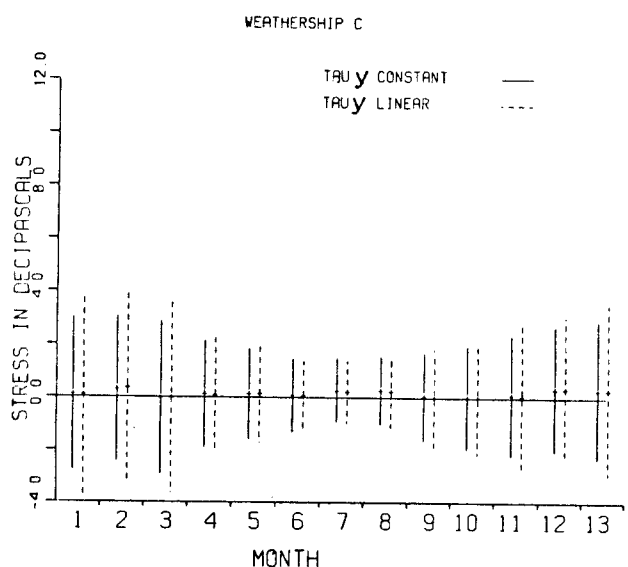


Figure 4 (d)

Figure 4. X and Y components of the 3H stress at Weatherstation C as a function of year and month. The solid line shows  $\pm 1$  standard deviation using the constant drag coefficient and the dashed line  $\pm 1$  standard deviation using the linear drag coefficient. Means are indicated by horizontal bars.

three-hourly values on which each monthly mean is based were statistically independent. The result suggests that measurements about 3 to 7 days apart are independent which is

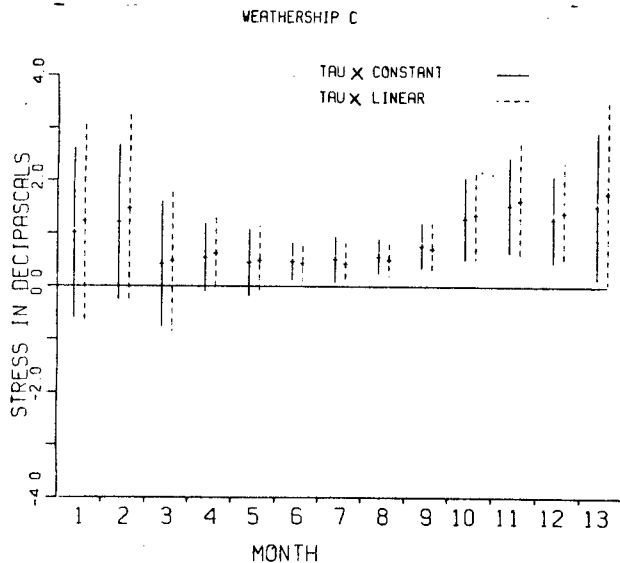


Figure 5 (a)

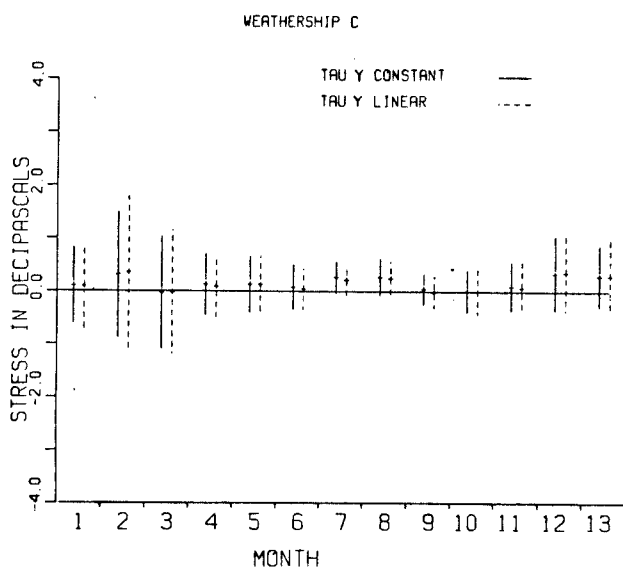


Figure 5 (b)

Figure 5. The 3H stress as a function of month at Station C. The solid line is  $\pm 1$  standard deviation of the monthly means using the constant drag coefficient and the dashed line  $\pm 1$  standard deviation of the monthly means using the linear drag coefficient. The means are indicated by the horizontal bars.

similar to the time scales of storms in the mid-latitudes.

Table V gives the averages and standard deviations of the entire record for all the stations examined. Note that Station

TABLE V

The x and y components of 3H stress means and standard deviations for all ships and years examined. The standard deviation  $\sigma_k = (\bar{T}k^2 - \bar{T}\bar{k}^2)^{1/2}$  where k denotes the x or y component. All measurements are in dPa.

SHIP	CONSTANT DRAG				LINEAR DRAG COEFFICIENT			
	T <sub>x</sub>	$\bar{\sigma}_x$	T <sub>y</sub>	$\bar{\sigma}_y$	T <sub>x</sub>	$\bar{\sigma}_x$	T <sub>y</sub>	$\bar{\sigma}_y$
A	.074	2.47	-.035	2.35	.128	3.21	-.029	2.97
B	.438	2.58	-.298	2.36	.473	3.38	-.375	3.02
C	.902	2.62	.161	2.17	1.06	3.55	.156	2.82
D	1.01	2.43	.204	2.24	1.18	3.39	.197	2.88
E	.478	1.48	.199	1.50	.510	1.81	.170	1.72
I	.497	2.56	.544	2.25	.575	3.22	.591	2.84
J	.925	2.33	.492	2.07	1.03	2.96	.513	2.51
K	.614	1.98	-.045	1.81	.673	2.43	-.038	1.81
M	.338	1.93	.065	2.21	.394	2.30	.058	2.70
N	-.311	.845	-.126	.847	-.238	.800	-.091	.825
P	.805	1.99	.330	1.71	.910	2.69	.304	2.19

N values of the standard deviation are 1/3 to 1/2 of those of the other weatherships (or the variance is 1/9 to 1/4 of the others).

In Figure 6, the 3H stress components are plotted versus the VA stress components for the constant drag coefficient and L=28.0 days for Station A. The diagonal solid line indicates the equivalence line between the 3H and VA stress. Rather than scattering around this line, the absolute value of the VA stress is consistently less than that of the 3H stress although they are fairly well correlated.

Figure 7, shows estimates of the four test functions defined in Equations 2.16 - 2.19 for the x component, constant drag coefficient when no correction to the VA stress has been

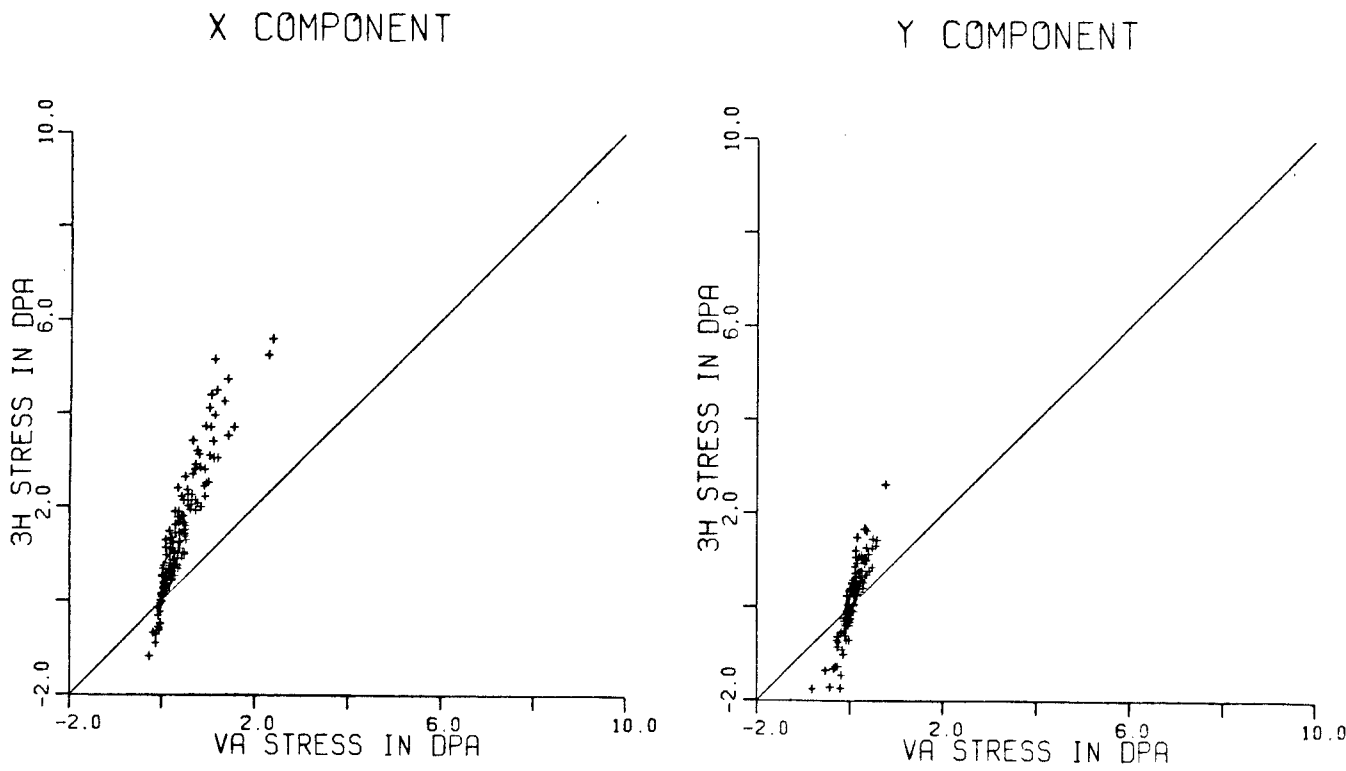


Figure 6. 3H versus VA stress for the constant drag coefficient at Station A, L=28.0 days with no corrections applied.

applied. The actual values for both components and drag coefficients are given in Appendix B. Symbols that will be used in the figures throughout the text to indicate ship are given in Table VI.

In Figure 7(a), the difference means are small for short averaging periods indicating that the VA stress closely approximates the long term 3H mean. As the averaging period increases, the VA estimates become increasingly inaccurate and the errors appear to increase approximately exponentially with averaging period. There is a distinct ordering in the DMs by ship through all averaging periods. A comparison of Appendix B and Table V indicates that the ordering may be dependent upon the mean 3H stress component value averaged over the entire

X COMPONENT

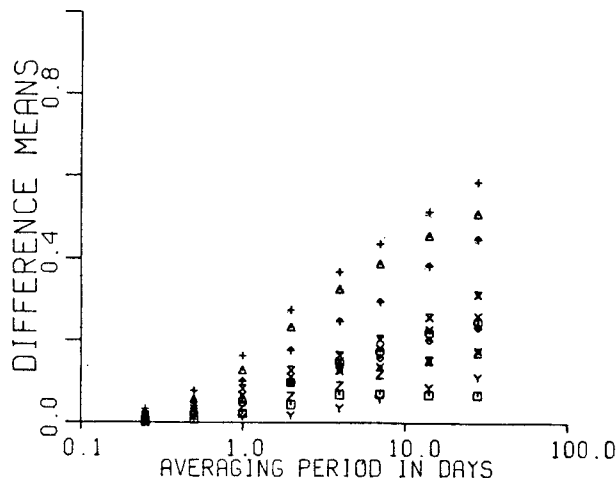


Figure 7(a) DMS in dPa.

X COMPONENT

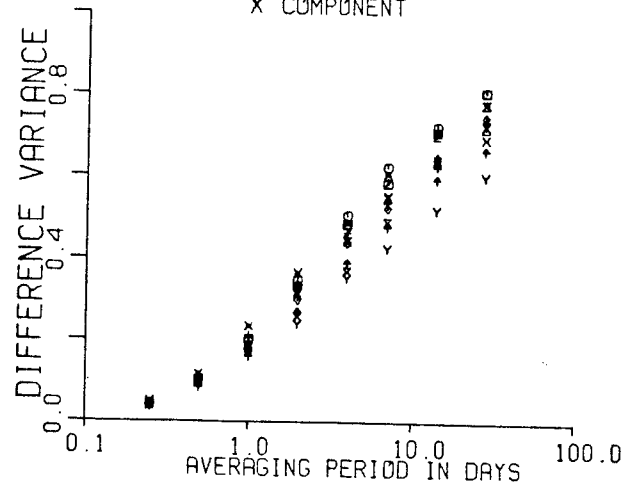


Figure 7(b)

X COMPONENT

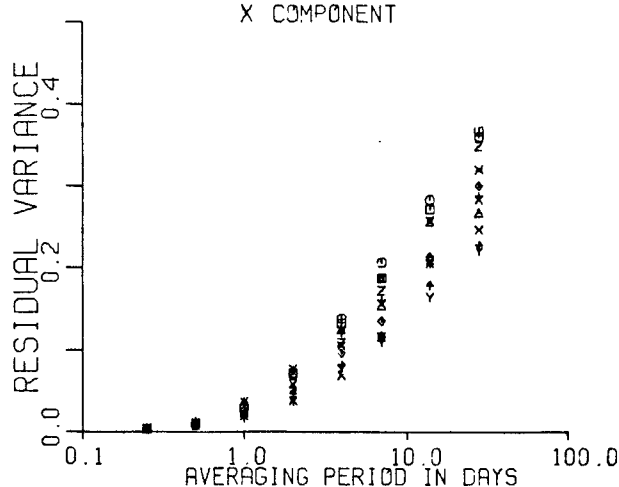


Figure 7(c)

X COMPONENT

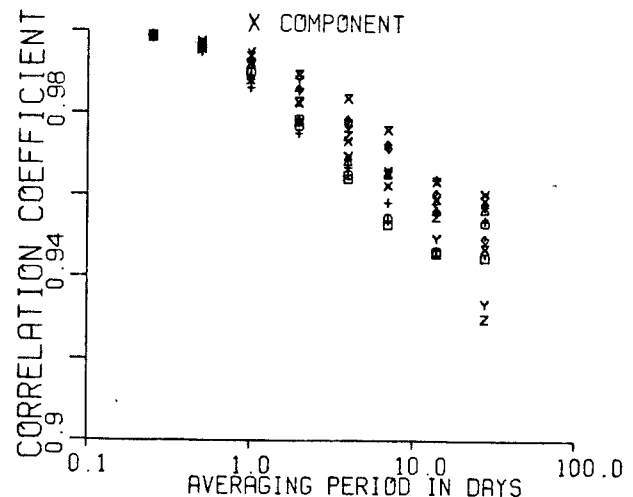


Figure 7(d)

Figure 7. Example of the composite test functions for all ships, x component, constant drag coefficient with no correction applied.

record. Those ships with larger initial  $3H$  values appear to have large difference mean stresses.

The difference variances appear in Figure 7(b). For

TABLE VI

Symbols used in the figures throughout the text.

SHIP	SYMBOL
A	□
B	○
C	△
D	+
E	×
I	◊
J	◆
K	✗
M	Ζ
N	Υ
P	✗

Note: When it is indicated that Station N is excluded from the figure, Station P is indicated by Υ .

reference, the 3H stress variances for all averaging periods appear in Table VII. Again the VA variance closely approximates the 3H variance for small averaging periods. By  $L=1.0$  days, however, the VA variance underestimates the 3H variance by about 20%. At  $L=28$  days, the variance reduction is 60 to 80%. The ship-to-ship DVs are more tightly grouped than the difference means. The relative position of each ship appears to shift as the averaging period increases.

The residual variances appear in Figure 7(c). At  $L=0.25$  days, the residuals are less than 1.0% of the total 3H variance. By  $L=4.0$  days this rises to a mean of about 10% and by 28 days the value is between 20 and 40% of the total 3H variance.

Overall, the correlation coefficients shown in Figure 7(d) are quite high. At  $L=0.25$  days, all values are greater than 0.99 while at  $L=28.0$  days all values lie between 0.93 and 0.97.

Although only the x component, constant drag coefficient appears here, the range of values for the y component constant

TABLE VII

The stress variances for both drag coefficients as a function of averaging period. The columns refer to the averaging length in days and the variances are in (dPa)<sup>2</sup>.

SHIP	X COMPONENT CONSTANT D.C.							
	0.25	0.50	1.0	2.0	4.0	7.0	14.0	28.0
A	5.535	5.000	4.169	3.160	2.288	1.725	1.165	0.705
B	6.388	5.829	4.924	3.759	2.703	1.975	1.325	0.902
C	6.458	5.825	4.843	3.685	2.648	2.093	1.446	1.018
D	5.531	4.973	4.094	3.135	2.349	1.859	1.324	0.862
E	2.203	2.030	1.779	1.440	1.144	0.886	0.662	0.501
I	5.849	5.347	4.626	3.739	2.889	2.244	1.494	0.907
J	4.919	4.514	3.919	3.195	2.487	1.990	1.309	0.914
K	3.556	3.317	2.972	2.533	2.044	1.548	0.948	0.585
M	3.200	2.922	2.515	2.010	1.495	1.133	0.704	0.447
N	0.708	0.658	0.598	0.513	0.406	0.331	0.220	0.144
P	4.579	4.093	3.349	2.508	1.788	1.318	0.870	0.525
Y COMPONENT CONSTANT D.C.								
SHIP	0.25	0.50	1.0	2.0	4.0	7.0	14.0	28.0
A	5.084	4.692	4.084	3.260	2.441	1.801	1.174	0.772
B	5.278	4.806	4.021	2.925	1.900	1.359	0.824	0.474
C	4.241	3.726	3.000	2.150	1.425	1.032	0.644	0.406
D	4.462	3.835	2.964	1.999	1.196	0.771	0.468	0.266
E	2.054	1.838	1.498	1.086	0.684	0.472	0.285	0.159
I	4.503	4.109	3.529	2.788	2.065	1.582	1.010	0.664
J	3.843	3.442	2.857	2.172	1.572	1.156	0.730	0.477
K	2.821	2.501	2.041	1.575	1.162	0.850	0.545	0.304
M	3.932	3.632	3.157	2.546	1.837	1.385	0.826	0.494
N	0.710	0.649	0.570	0.465	0.340	0.261	0.180	0.121
P	5.597	4.998	4.103	3.057	2.141	1.575	1.002	0.661
X COMPONENT LINEAR D.C.								
SHIP	0.25	0.50	1.0	2.0	4.0	7.0	14.0	28.0
A	7.762	6.841	5.514	4.039	2.871	2.117	1.424	0.862
B	9.090	8.132	6.684	4.982	3.478	2.517	1.648	1.102
C	10.00	8.858	7.206	5.283	3.647	2.856	1.958	1.381
D	9.106	8.010	6.346	4.708	3.427	2.715	1.966	1.304
E	2.704	2.440	2.077	1.625	1.257	0.960	0.715	0.538
I	7.896	7.078	5.973	4.708	3.575	2.775	1.816	1.110
J	6.571	5.912	4.993	3.949	2.986	2.378	1.547	1.077
K	4.429	4.036	3.530	2.891	2.254	1.679	1.025	0.625
M	3.676	3.305	2.773	2.165	1.579	1.193	0.739	0.475
N	0.536	0.491	0.439	0.369	0.285	0.232	0.150	0.097
P	6.128	5.372	4.231	3.089	2.150	1.538	1.012	0.615

TABLE VII (continued)

SHIP	Y COMPONENT LINEAR D.C.								
	0.25	0.50	1.0	2.0	4.0	7.0	14.0	28.0	
A	6.768	6.138	5.220	4.048	2.961	2.167	1.416	0.931	
B	7.183	6.422	5.239	3.716	2.349	1.662	0.985	0.557	
C	5.880	5.039	3.910	2.753	1.785	1.273	0.779	0.495	
D	6.093	5.074	3.754	2.482	1.462	0.936	0.572	0.327	
E	2.201	1.931	1.514	1.075	0.661	0.451	0.267	0.149	
I	5.848	5.221	4.346	3.351	2.415	1.830	1.148	0.748	
J	4.667	4.074	3.293	2.442	1.728	1.262	0.785	0.506	
K	3.344	2.889	2.253	1.691	1.211	0.871	0.557	0.309	
M	4.449	4.017	3.394	2.671	1.868	1.418	0.816	0.478	
N	0.568	0.510	0.442	0.353	0.253	0.192	0.131	0.088	
P	8.383	7.310	5.831	4.208	2.835	2.075	1.313	0.870	

drag coefficient are similar to those quoted above with differences occurring only in the detail of the scatter. The difference means, difference variances and residual variances are greater for all ships and averaging periods using the linear drag coefficient than when using the constant drag coefficient while the correlation coefficients are consistently smaller.

### 3.2 Previous Studies

Fissel (1975) analysed 10 years of data from Station P. He divided his data into five two-year blocks of 5832 data points each and quantified the reduction in terms of two functions which I define as :

$$S(L) = \frac{\{(T_x')^2 + (T_y')^2\}^{1/2}}{\{(T_x)^2 + (T_y)^2\}^{1/2}}$$

$$A(L) = \text{Arctan} \left( \frac{\bar{T}_x}{\bar{T}_y} \right) - \text{Arctan} \left( \frac{\bar{T}'_x}{\bar{T}'_y} \right)$$

3.2

where  $\bar{T}'_x$  and  $\bar{T}'_y$  are the x and y component VA estimates of the two-year mean stresses for an averaging period of L days and  $\bar{T}_x$  and  $\bar{T}_y$  are the two-year mean 3H stress components. One  $S(L)$  and  $A(L)$  value was calculated for each 5832 point block, and the sample means and standard deviations were calculated over the five blocks.

The Fissel results appear in Figure 8. (Fissel used the linear Cd form of Deacon and Webb (1962) rather than the one used here). The 95% confidence zones (equal to  $\pm 2$  standard deviations of the two-year means) were typically of the order 0.1 times the mean value of  $S(L)$  and  $2^\circ$  for  $A(L)$ .

$S(L)$  determines the ratio of the climatological average VA stress magnitude to the average 3H stress magnitude and  $A(L)$  determines the average difference between the 3H and VA stress directions. Exact long-term mean 3H stress from VA stresses within the two-year averaging block should result from the application of  $S(L)$  and  $A(L)$  to the VA stresses. The test functions were calculated by applying  $S(L)$  and  $A(L)$  to the data and the DMs were substantially improved but the other test quantities remained nearly identical to those in Figure 7 where no correction was applied.

This technique was attempted on the North Atlantic ship data. In the present study, it was found that one-yearly blocks of 2912 data points simplified the analysis when using data of a varying number of years. For most weatherstations, the Station P results were well replicated as shown in Figures 9(a) and (b).

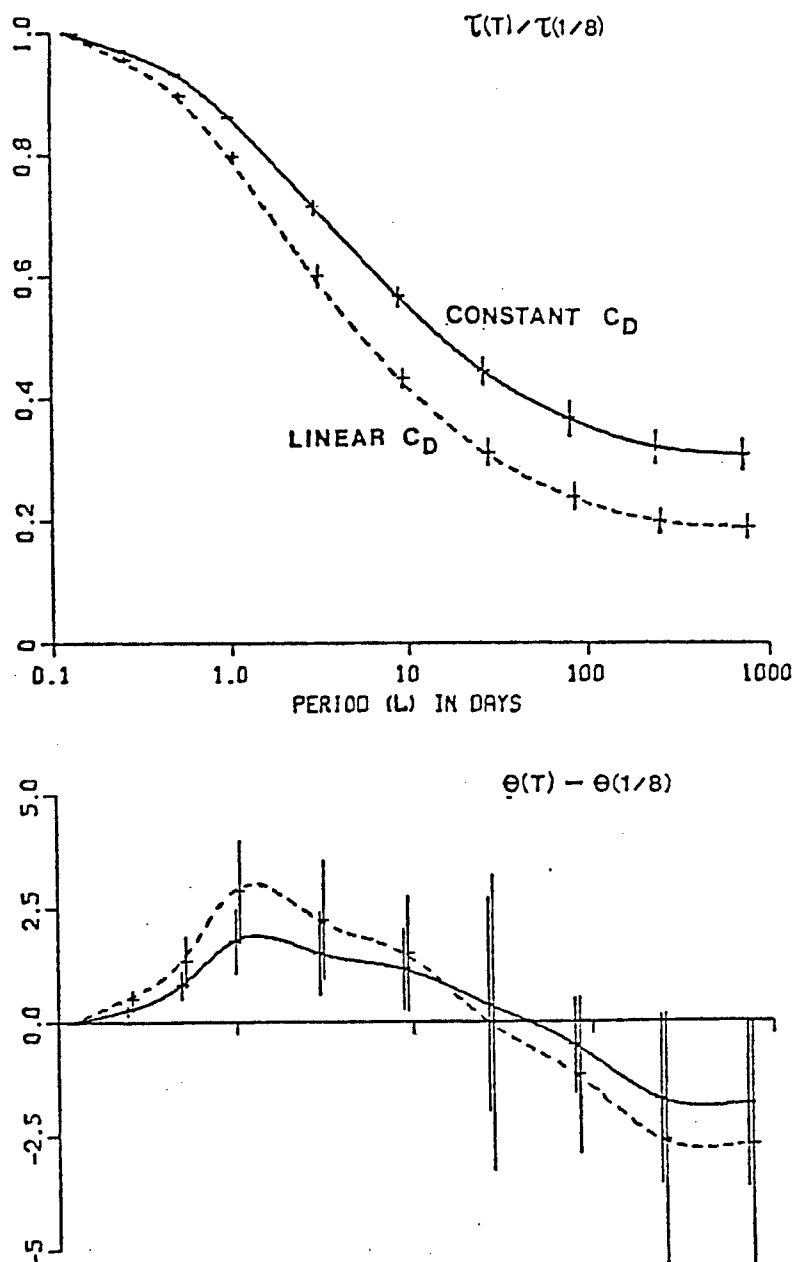


Figure 8. The ratio of the wind stress magnitude computed from wind data that are vector averaged over a period,  $T$  to the directly calculated wind stress. The lower plot represents the difference between the direction of the directly calculated wind stress and the direction of the wind stress computed from the vector averaged data. The vertical error bars represent approximate 95% confidence intervals of the mean. (From Fissel (1975))

for Station C. The  $S(L)$  values at Weatherstation A (Figures 9 (c) and (d)), however, differ markedly from the other ships. Whereas Stations P and C,  $S(L)$  values are consistently less than 1.0, Station A has several values significantly greater than 1.0. The standard deviations for averaging periods from 0.5 to 28.0 days are as much as 100 times larger at A than C and are large compared to the mean  $S(L)$  values. Station A has direction shifts ( $A(L)$ ) of up to  $30^\circ$  for averaging periods greater than 14 days. For a large value to arise in  $S(L)$ , the denominator of Equation 3.1 may tend to 0 while the numerator remains finite. One would expect high values of  $S(L)$  to occur for low values of the average 3H stress magnitude. The yearly values of  $S(L)$  at Station A are listed in Table VIII along with the yearly averaged 3H stress magnitudes.

From Table VIII it is clear that generally low yearly averaged stress values lead to  $S(L) > 1$  (also true for the linear drag coefficient). This is not, however, a sufficient condition. The 1955 stress magnitude is 0.3 dPa while  $S(0.25) = 1.0005$ ; in 1952 the stress is 0.107 dPa but  $S(0.25) < 1.0$ . The highest stress value for which  $S(L)$  is greater than 1.0 is at Weatherstation B in 1965 where the stress was 0.372 dPa. In general, however, small vector averaged 3H stress magnitudes lead to large values of  $S(L)$ . Furthermore the lower the 3H stress, the more averaging periods are affected. All values of  $S(L)$  greater than 2.0 have vector averaged 3H stress magnitudes less than 0.05 dPa.

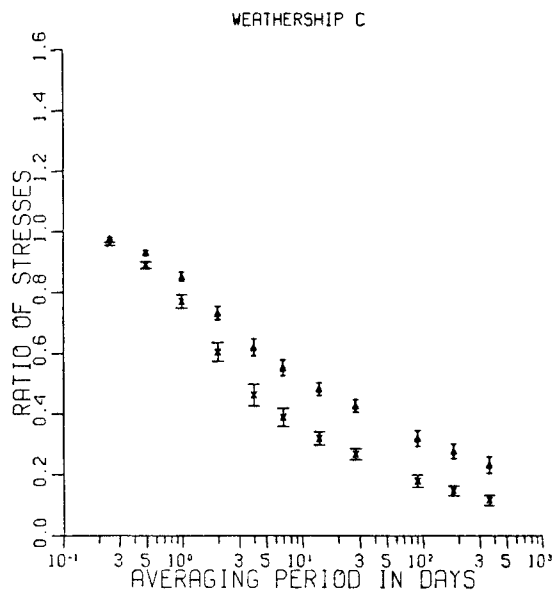


Figure 9(a) S(L)

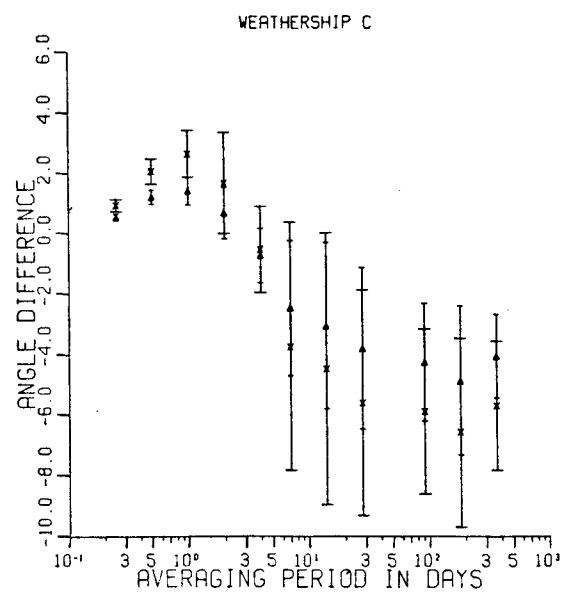


Figure 9(b) A(L)

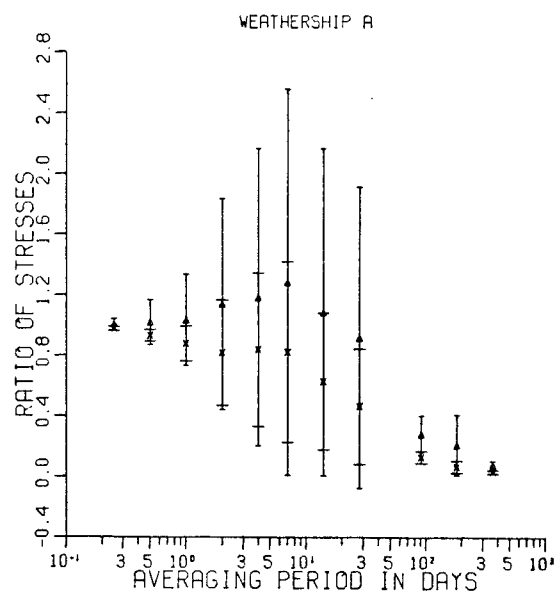


Figure 9(c) S(L)

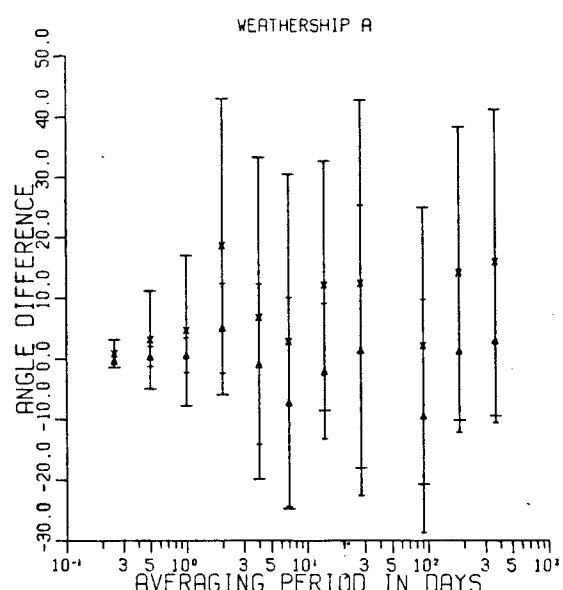


Figure 9(d) A(L)

Figure 9. S(L) and A(L) (in Degrees) as functions of averaging period for Weatherships A and C. The mean for the constant drag coefficient is indicated by ▲ with ±1 standard deviation of the yearly means by the narrow horizontal lines. The mean for the linear drag coefficient is indicated by X and ±1 standard deviation of the yearly means by the wide horizontal lines.

TABLE VIII

The S(L) readings for all years of data at Weatherstation A using the constant drag coefficient. The 3H vector averaged stress magnitude is in dPa.

YEAR	AVERAGING PERIOD IN DAYS							
	0.25	1.5	1.0	2.0	4.0	7.0	14.0	28.0
WEATHERSTATION A								
1949	0.48	0.96	0.92	0.84	0.74	0.59	0.61	0.52
1951	0.39	0.96	0.95	0.89	0.80	0.59	0.68	0.53
1952	0.11	0.98	0.98	0.72	0.77	0.57	0.28	0.16
1953	0.51	1.00	0.95	0.88	0.77	0.57	0.49	0.47
1954	0.36	0.99	0.95	0.88	0.85	0.70	0.50	0.43
1955	0.30	1.00	0.98	0.96	0.84	0.70	0.68	0.27
1956	0.67	0.99	0.93	0.87	0.80	0.70	0.59	0.52
1957	0.01	1.28	2.12	3.30	6.46	8.67	10.98	9.26
1958	0.12	1.06	1.07	1.09	0.88	0.77	0.60	0.54
1959	0.27	0.98	0.89	0.78	0.57	0.53	0.53	0.60
1960	0.47	1.00	0.99	0.97	0.91	0.86	0.71	0.50
1961	0.08	0.96	0.86	0.79	0.73	1.04	1.54	1.68
1962	0.12	0.97	0.84	0.78	0.59	0.33	0.32	0.33
1963	0.21	1.00	0.99	1.03	0.97	0.92	0.79	0.56
1964	0.33	0.98	0.94	0.88	0.74	0.71	0.62	0.51
1965	0.47	1.00	0.95	0.92	0.80	0.72	0.65	0.51

### 3.3 Individual Ratios

In attempting to quantify the reduction in stress due to vector averaging the wind, the functions S(L) and A(L) have several disadvantages. First, in regions of small average stress, the functions may assume radically different values from one year to the next, indicating that they may not be generally applicable to years other than those over which the initial averaging was done. Second, the S(I) and A(L) functions do not improve the RVs and correlation coefficients. For calculations of actual time variations it is necessary to estimate the accuracy of the individual stress values. Consequently two functions Rj(L) and Bj(L) were defined as:

$$R_j(L) = \frac{\left\{ (T_{xj}^*)^2 + (T_{yj}^*)^2 \right\}^{1/2}}{\left\{ (T_{xj})^2 + (T_{yj})^2 \right\}^{1/2}} \quad 3.3$$

$$B_j(L) = \text{Arctan} \left( \frac{T_{xj}^*}{T_{yj}^*} \right) - \text{Arctan} \left( \frac{T_{xj}}{T_{yj}} \right) \quad 3.4$$

where  $T^*x_j$  and  $T^*y_j$  are the sets of VA x and y component stress estimates and  $Tx_j$  and  $Ty_j$  are the sets of 3H x and y component stress estimates for an averaging period of L days following the notation given in Section 2.5.

The  $R_j(L)$  for any given averaging period can be examined mathematically to gain some insight into its expected behaviour. Equation 3.3 for the constant drag coefficient can be rewritten as:

$$R_j(L) = \frac{u_j^2 + v_j^2}{\left[ \left[ \frac{1}{I} \sum_i (u_i^2 + v_i^2)^{1/2} u_i \right]^2 + \left[ \frac{1}{I} \sum_i (u_i^2 + v_i^2)^{1/2} v_i \right]^2 \right]^{1/2}} \quad 3.5$$

with the approximation that the air density and the drag coefficient are constant. Applying the Schwartz inequality (see Pfeiffer, 1965, pp. 223) to the denominator and rearranging terms, a lower bound for the function can be established:

$$R_j(L) \geq \frac{1}{1 + \frac{\sigma_{xj}^2 + \sigma_{yj}^2}{u_j^2 + v_j^2}} \quad 3.6$$

Where:  $\sigma_{xj}^2$  and  $\sigma_{yj}^2$  are the x and y wind velocity component variances in averaging period j. Thus the lower bound for any particular averaging period increases for higher vector averaged mean winds and lower variances.

$R_j(L)$  has no upper bound. If one takes the set  $u = v = \{3, 4, -5\}$  and substitutes into Equation 3.5, then the numerator is finite and the denominator is 0.0, or  $R_j(L) = \infty$ . The probability of such an occurrence is remote. Whenever the 3H stress averaged exactly to 0.0, leading to  $R_j(L) = \infty$ , the particular averaging values were eliminated from calculations. After imposing this criterion, in over 750,000 cases (all ships, averaging periods and drag coefficients) examined, not one instance of  $R_j(L)$  greater than 1.0 appeared. Furthermore, in all cases where the 3H stress was 0, the mean VA stress was also 0.

The smoothed wind data as encountered in surface pressure maps, hides the internal variance through the averaging process, but the square of the vector averaged wind is not only readily calculable but essential in determining the  $j^{th}$  value of VA fluxes. Although the value of any single  $R_j(L)$  and the lower bound may not coincide, an average value ( $\bar{R}(L)$ ) may be wind speed dependent. Consequently the effect of grouping  $R_j(L)$  value according to the vector averaged wind speed was investigated.

$R_j(L)$  and  $B_j(L)$  were sorted into twenty equally spaced divisions according to value. For each  $R_j(L)$  and  $B_j(L)$  reading the vector averaged wind speed  $(u_j^2 + v_j^2)^{1/2}$  was determined and the functions were further sorted into thirteen divisions according to the Beaufort number of the  $j^{th}$  value of the vector averaged wind speed. The Beaufort wind speeds according to the Marine Climatic Atlas, U.S. Office of Naval Operations are given in Table IX.

TABLE IX  
BEAUFORT WIND SPEED INTERVALS

BEAUFORT #	SPEED INTERVAL	MEAN
	m/sec	m/sec
1	0.0-0.4	0.2
2	0.4-1.6	1.0
3	1.6-3.4	2.5
4	3.4-5.5	4.45
5	5.5-8.0	6.75
6	8.0-10.8	9.4
7	10.8-13.9	12.35
8	13.9-17.2	15.55
9	17.2-20.8	19.0
10	20.8-24.5	22.65
11	24.5-28.5	26.5
12	28.5-33.5	31.0
13	> 33.5	35.0

Figure 10 is the histogram of  $R_j(L)$  and Figure 11 the histogram for  $B_j(L)$  for the constant and linear drag coefficients respectively at Weatherstation C. Beaufort numbers 2 (1.0 m/sec), 6 (9.4 m/sec), and 10 (22.65 m/sec) for an averaging period of  $L=0.25$  days were selected as being representative. The standard deviation was calculated from all the values of  $R_j(L)$  and  $B_j(L)$  in each wind speed-averaging period category and will be referred to as the sample standard deviation and its square will be referred to as the sample variance.

As seen in Figure 10 at 1.0 m/sec,  $R_j(L)$  has a distinct mode between 0.45 and 0.50 with an average value of 0.530. The rest of the distribution is nearly flat. At 9.40 m/sec the distribution of  $R_j(L)$  becomes markedly skewed towards 1.0. The standard deviation has also significantly decreased. At 22.65 m/sec, the skewness becomes even more pronounced to 1.0 with 93%

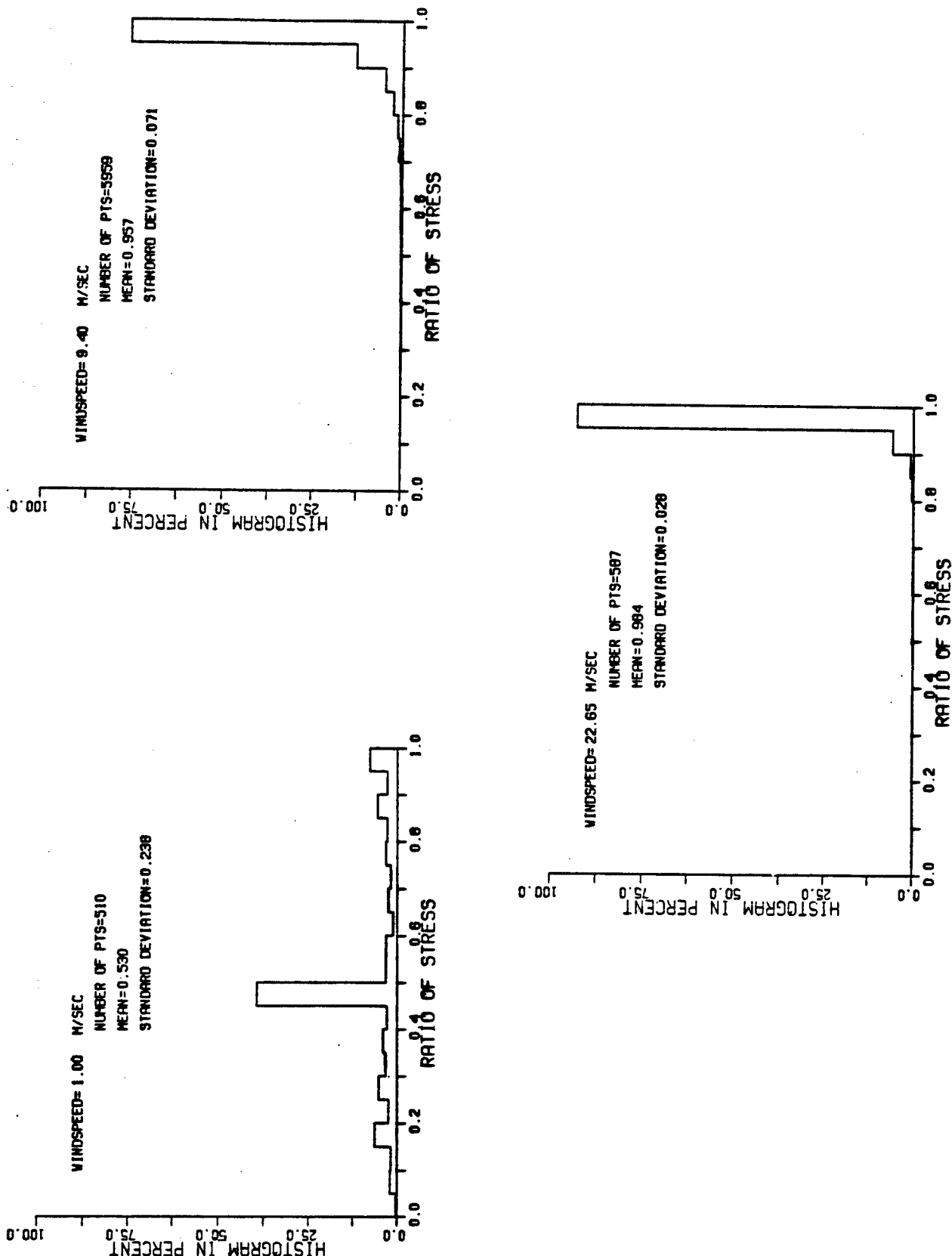


Figure 10. Histogram of  $R(0.25)$  at Weatherstation C using the constant drag coefficient.

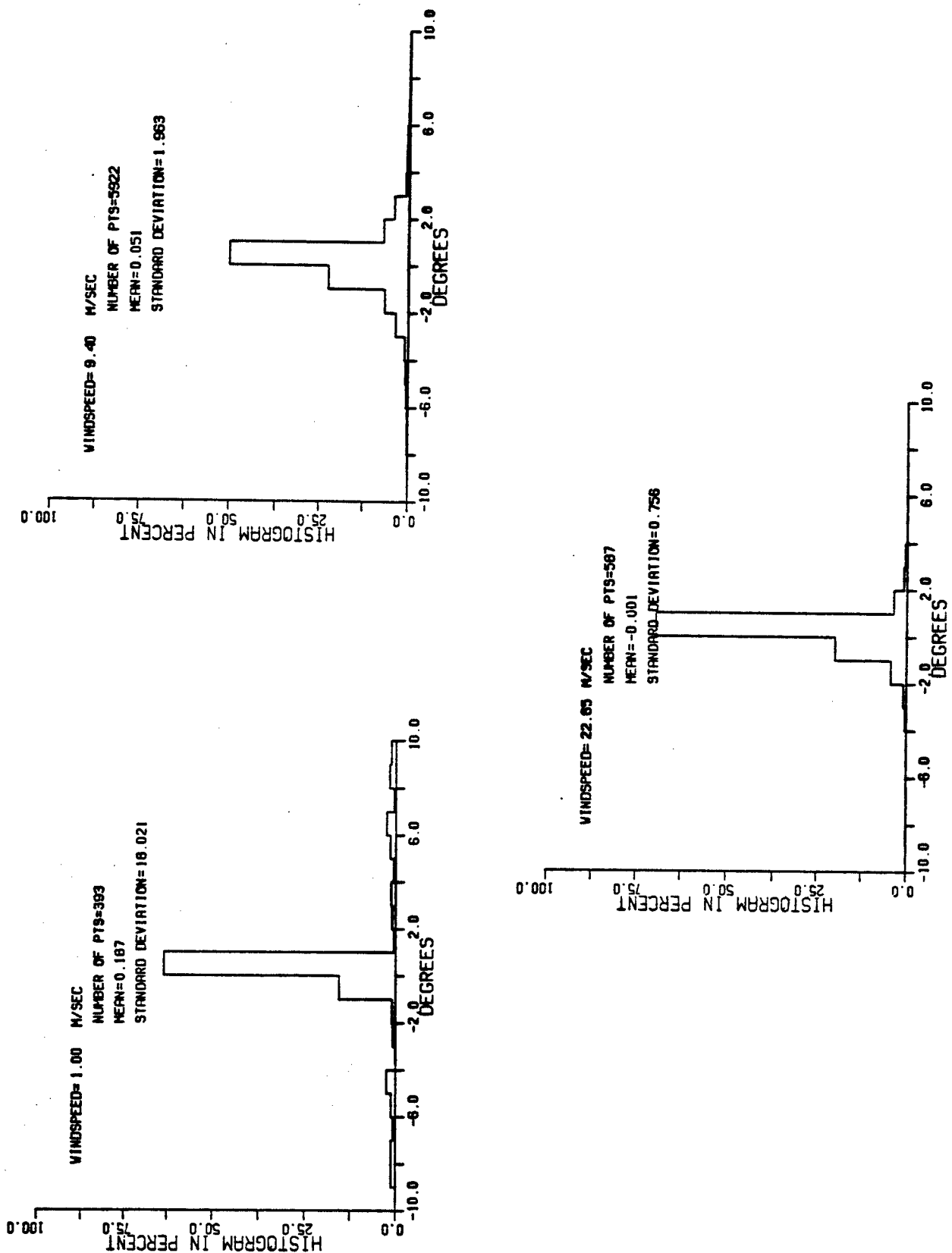


Figure 11. Histogram of  $B(0.25)$  at Weatherstation C using the constant drag coefficient.

of the distribution in the 0.95 to 1.0 slot. Because of the increasing concentration of values to the high end of the distribution, the standard deviation continues to decrease with averaging speed. The trend to higher  $\bar{R}(L)$  values and lower standard deviations for increasing wind speed is generally true for all averaging periods.

$Bj(L)$  has a distinctly spiked distribution at low wind speeds. The histogram for 1.0 m/sec has 64% of the total number of 383 points in the 0 to  $1.0^\circ$  direction shift slot. There are, however, an additional 59 points from  $-10^\circ$  to  $-180^\circ$  and an additional 68 points from  $10^\circ$  to  $180^\circ$  accounting for the large  $18.021^\circ$  standard deviation. As the wind speed increases to 9.40 m/sec, the mean remains very close to  $0.00^\circ$ . The number of exterior points decreases causing the sample standard deviation to decrease so that at 22.65 m/sec the distribution appears approximately Gaussian.

The joint histogram for  $Rj(L)$  and  $Bj(L)$  was calculated for all ships. The arithmetic means,  $\bar{R}(L)$  and  $\bar{B}(L)$ , were then calculated for each Beaufort category and averaging period. Thus each ship was assigned  $\bar{R}(L)$  and  $\bar{B}(L)$  values that were functions of windspeed and averaging period.

The mean  $\bar{R}(L)$  values for all the ships appear in Figure 12 while the means  $\bar{B}(L)$  values appear in Figure 14. Two standard deviations are also shown. Particularly for larger VA wind speeds and longer averaging periods,  $\bar{R}(L)$  and  $\bar{B}(L)$  may be calculated from differing numbers of measurements. First, weights proportional to the number of estimates within each Beaufort-averaging period category were applied to the ship

means values of  $\overline{R(L)}$  and  $\overline{B(L)}$  to arrive at an estimate of the standard deviations of the geographic means. This is the standard deviation of the means shown in the figures and it is indicated by the dashed lines. Next similar weights were applied to the sample variances to arrive at an average sample variance. This indicative of the average sample variability about any single  $\overline{R(L)}$  estimate and is indicated by the solid line in Figures 12 and 14. Finally, it will be shown that Station N differs markedly from other locations and its values are excluded entirely from standard deviation estimates.

Figure 12(a) shows  $\overline{R(0.25)}$  (the 0.25 indicates  $L=0.25$  days) as a function of wind speed. The value of  $\overline{R(0.25)}$  approaches 0 for very small wind speeds. For larger vector averaged winds  $\overline{R(0.25)}$  rapidly increases. At 7 m/sec  $\overline{R(0.25)}$  is 0.90. As the wind speed increases, the values approach 1.0. Both the standard deviations of the sample and the standard deviations of the ships' means have maxima at low wind speeds and then decrease gradually as the wind speed increases. For all wind speeds, the average error in the sample is much larger than the error in the means indicating that the value of  $\overline{R(0.25)}$  may be independent of geographical location.

The results can be explained in terms of Equation 3.6. An averaging period of 0.25 days contains only two three-hourly measurements. Lower vector averaged winds result from simultaneous cancellation of the x and y wind components. Thus the variances will be much greater than the means of the components resulting in a lower bound that approaches 0. For higher wind speeds one expects a strong steady wind to blow for

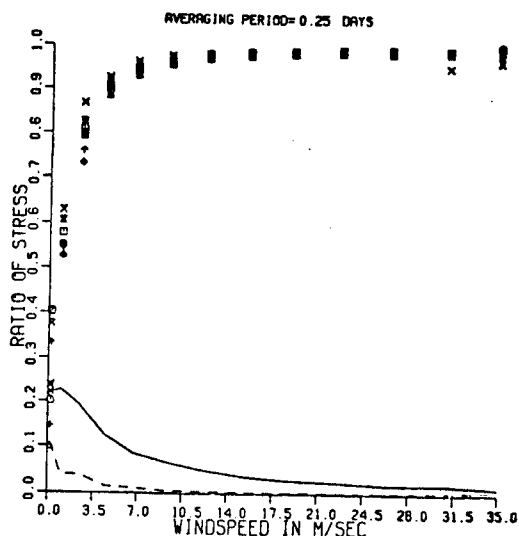


Figure 12 (a)

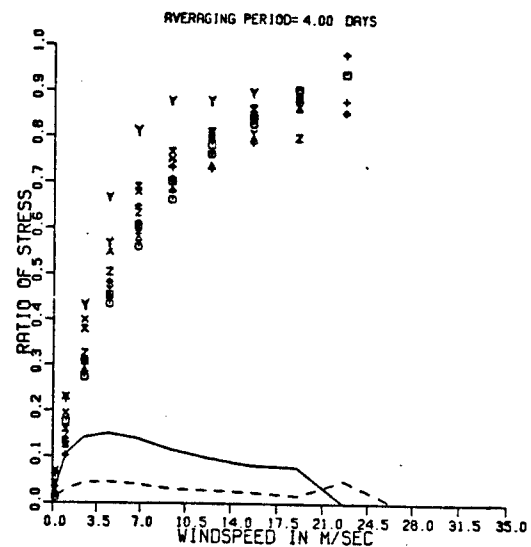


Figure 12 (b)

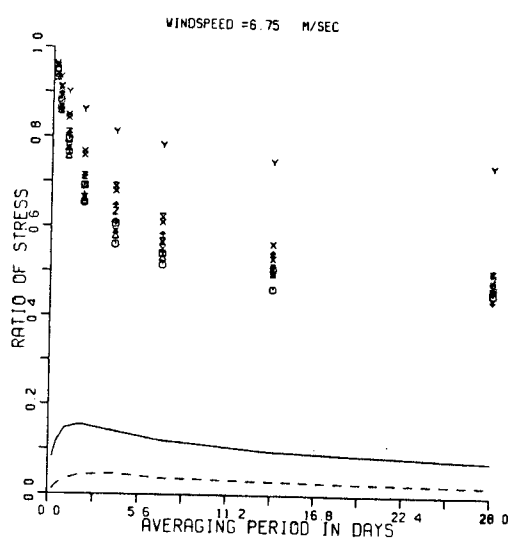


Figure 12 (c)

Figure 12. Plots of  $R(L)$  for representative averaging periods and wind speeds of all ships using the constant drag coefficient.  $\gamma$  denotes Weatherstation N. The solid line is a weighted mean sample standard deviation and the dashed line is the standard deviation of the ships' means. Since N differs from the other ships, its values were not included in the calculation of the standard deviations.

a relatively long length of time in which case the variance of the two components is small compared to the vector averaged wind and the lower bound in Equation 3.6 approaches 1.  $\overline{R(4)}$  approaches 0 as the wind speed goes to 0 m/sec. The value of  $\overline{R(4)}$  increases with wind speed. The scatter in measurements for both the mean and sample values is larger than for  $\overline{R(0.25)}$ . At the largest wind speed, the scatter in the means appears to be more significant than the scatter in the individual estimates. The four values at 21 m/sec, however, comprise less than 1% of the total number of points measured and this value cannot be considered statistically reliable. From 0 to 14 m/sec, Weathership N has systematically higher values than the others.

Figure 12(c) exhibits further evidence of the higher values of  $\overline{R(L)}$  for Weathership N. Here,  $\overline{R(L)}$  for varying averaging periods is plotted for a constant wind speed of 6.75 m/sec. The Station N  $\overline{R(L)}$  values are more than two standard deviations of the mean larger than any other ship indicating that its values are significantly larger than the other stations. The scatter in the individual measurements reaches a maximum for an averaging period of two days and then decreases slowly with increasing averaging period. The scatter in the ships' means increases rapidly to two days and then maintains a relatively constant value.

The anomaly in  $\overline{R(L)}$  at Station N is consistent both with Equation 3.6 and the findings of other researchers. Malkus (1962) notes that Station N is at the northern extremity of the Northern Pacific Trade Wind region characterized in both direction and magnitude by moderate and steady winds. This is

confirmed in Table V where the total  $3H$  variance is about  $1/10$  times that of the more northerly stations. Thus Equation 3.6 predicts that one should get systematically larger values of  $R_j(L)$  and hence  $\overline{R(L)}$ . This is confirmed by Malkus where substantially smaller discrepancies between the  $3H$  and VA stress over a single monthly averaging were found in the Caribbean Sea at  $19^{\circ}$  N,  $66^{\circ}$  W than were found at Station C. Thus the corrections required for the tropics and subtropics may be much less than those required for temperate latitudes.

Figure 13 shows the geographic (ie. average of all the stations) average values of  $\overline{R(L)}$  for the constant drag coefficient, excluding N, as a function of wind speed. The weighting outlined above was employed in the calculation of these geographically averaged values. All the curves appear to be regular with the exception of the highest wind speeds. This may be a result of there being too few averagings at the higher wind speeds to yield a representative value of  $\overline{R(L)}$ .

The scatter and behaviour of  $\overline{B(L)}$  as a function of averaging period are indicated in Figure 14. There is a high degree of scatter at a wind speed of  $0.2$  m/sec for both the sample and between ships. There does not appear to be a systematic difference between ships. At  $6.75$  m/sec, the sample standard deviation is reduced from  $35^{\circ}$  to about  $15^{\circ}$  and the variability between ships is nearly zero. Figure 14(c) clearly indicates that non-zero values of  $\overline{B(L)}$  occur only for low wind speeds. For winds greater than about  $3$  m/sec,  $\overline{B(L)}$  averages to exactly zero. It is not clear whether the large values of  $\overline{B(L)}$  for low wind speeds are statistically significant since the low

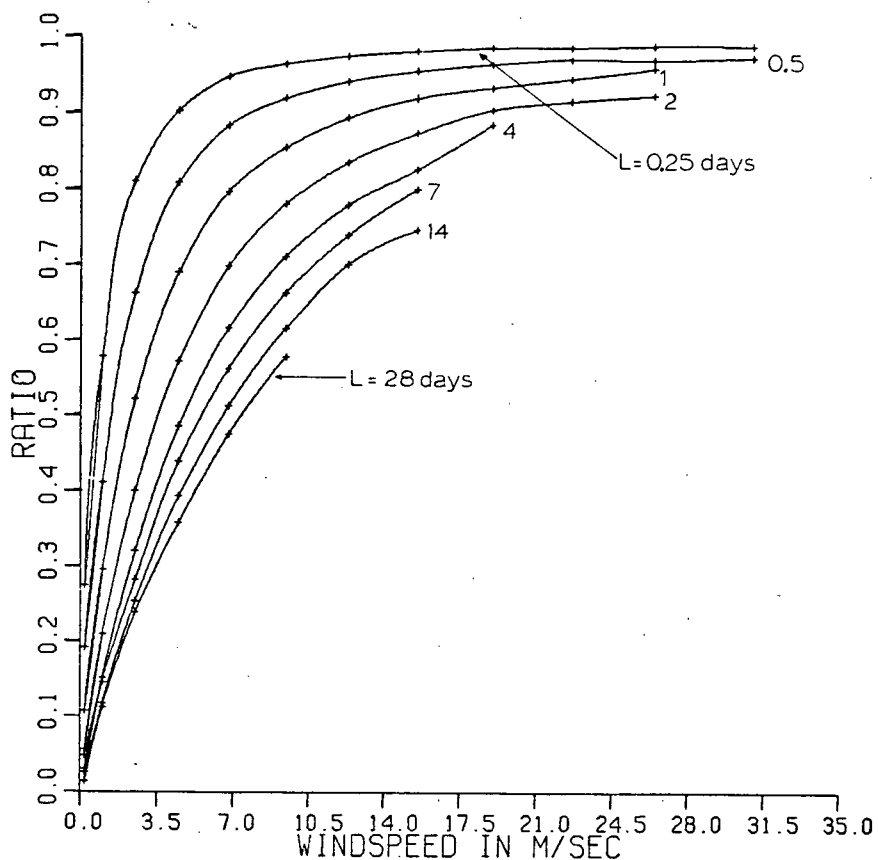


Figure 13. Geographically averaged  $R(L)$  values for all wind speeds and averaging periods. The numbers indicate lines of equal averaging periods (in days). Station N has been excluded from the averaging.

wind speeds account for only a very small percentage of the total number of wind measurements made.

### 3.4 Multiple Regression Analysis

From the previous discussion it is evident that the reduction in stress due to vector averaging of winds varies with the averaging period and the measured VA winds. For wind speeds greater than 3.0 m/sec the average shift in direction is  $0^\circ$  indicating that, on average, there may not be significant differences between the transformations required for the x and y components. This implies that a single transformation based on

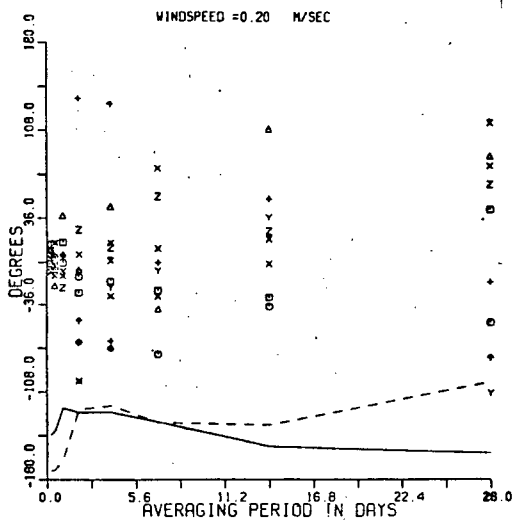


Figure 14 (a)

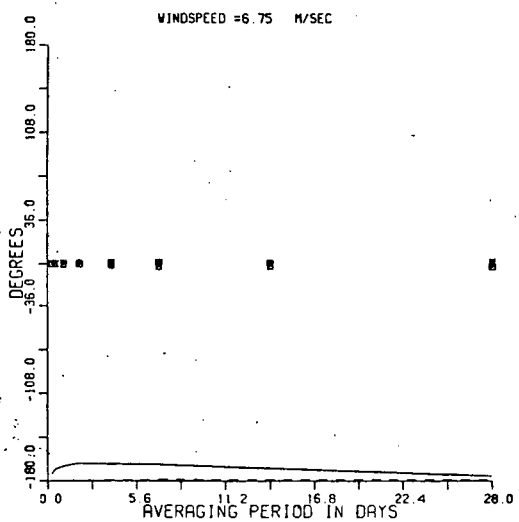


Figure 14 (b)

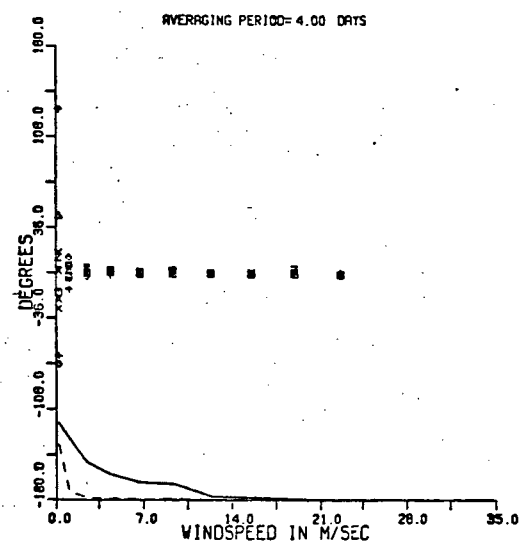


Figure 14 (c)

Figure 14. Plots of  $\overline{B}(L)$  for representative averaging periods and wind speeds for all ships using the constant drag coefficient. The solid line denotes the average standard deviation of the sample and the dashed line is one standard deviation of the ships' mean values.

the stress magnitude is feasible. A single set of correction factors equally applicable to both components reduces the required parameters by a factor of 2.

The object of any transformation is to reduce the differences means, difference variances, and residual variances to predict accurately the long-term and point-by-point 3H stress from the VA stress. Specifically, if the point-by-point 3H stress (as quantified by the residual variance) can be accurately determined then the difference variances and means should also be reduced. The residual variance can be optimally reduced by a least squares fit.

To this end the 3H and VA stress magnitudes were calculated and sorted according to the Beaufort interval as previously outlined. For each averaging period, the following quantity:

$$\bar{T}_{eT}^2 S_{eT}^2 = \frac{1}{N} \sum_{k=1}^{13} \sum_{j=1}^{J_k} (T_{kj} - \bar{\xi}_{ke} T'_{kj})^2 \quad 3.7$$

was minimized by :

$$\frac{\partial (\bar{T}_{eT}^2 S_{eT}^2)}{\partial \bar{\xi}_{ke}} = 0 \quad 3.8$$

giving :

$$\bar{\xi}_{ke} = \frac{\sum_{j=1}^{J_k} T_{kj} T'_{kj}}{\sum_j T'^2_{kj}} \quad 3.9$$

where  $T_{kj}$  and  $T'_{kj}$  are the 3H and VA stress magnitudes,  $S_{eT}^2$  is the stress magnitude residual variance for the  $l^{th}$  averaging period,  $\bar{\xi}_{ke}$  is a multiplicative factor which minimizes the

residuals in Beaufort category k and the  $l^{th}$  averaging period, N is the total number of averagings available in the record and  $J_{k_l}$  is the number of averagings within Beaufort category k.

$\xi_{k_l}$  is the slope of a stress magnitude regression line passing through the origin. This is not a bad assumption in light of Figure 6, where the scatter of the x and y stress components becomes constricted at the origin. Appendix A gives an outline of some of the relationships between the difference variances, residual variances, and correlation coefficients for the regression analysis. Notice that Equation 3.7 unlike Equation 2.18 excludes the mean terms. They were excluded because as demonstrated in Figure 4 and Table V, the stress component fluctuations dominate the mean. Appendix A.1 includes the influence of the linear term on the residuals. This form of the regression will be applied presently to the heat fluxes. In fact a regression of the type outlined in Appendix A.1, including the mean stress magnitude was tried on the stress magnitudes. Up to Beaufort interval 3, some of the  $\xi_{k_l}$  values were found to be negative in contradiction with Equation 3.3. Furthermore, the component residual variances were significantly larger than when the means were excluded.

An estimate of 95% confidence zone of the slope was made by:

$$\Delta \xi_{k_l} = \frac{t_{k_l, .025}}{\left\{ \frac{(J_{k_l}-2) \sum T_{k_l j}^2}{\sum_{j=1}^{J_{k_l}} (T_{k_l j} - \bar{\xi}_{k_l} T_{k_l j})^2} \right\}^{1/2}} \quad 3.10$$

where  $t_{k_l, .025}$  is the Student t statistic with  $J - 1$  degrees of freedom at a 0.95 level of significance. This is not a precise

estimate of the error because as shown in the previous section, the distribution of  $R_j(L)$  is highly skewed around the mean for most averaging periods and wind speeds and consequently the statistics are not Gaussian.

### 3.5 Variance Underestimation

The  $\xi_{ke}$  values were calculated for each ship and the four test functions outlined in Section 2.6 were then found by applying  $\xi_{ke}$  to the VA stress components.

The difference variances using the constant drag coefficient are shown in Figure 15. Values for all ships, components and drag coefficients are greatly reduced from the values shown in Figure 7. All values are positive definite which implies that the long term 3H variance is systematically larger than the long term corrected VA variance. Although only the constant drag coefficient results are shown, every case examined showed a positive difference variance.

This is an artifact of the regression analysis. Appendix A.1 shows that when the optimal  $\xi_{ke}$  is applied, the difference variance and the residual variances must be identical. Note that even though Appendix A.1 applies to including the long-term difference means in the calculation of  $\xi_{ke}$ , identical results can be obtained by setting the DMs to 0. Since the residual variance must be positive definite, so is the difference variance. For this result to be exactly applicable in the stress components, the x and y components must be regressed independently and a separate set of transformations found for each component. Here the stress magnitude was regressed and  $\xi_{ke}$

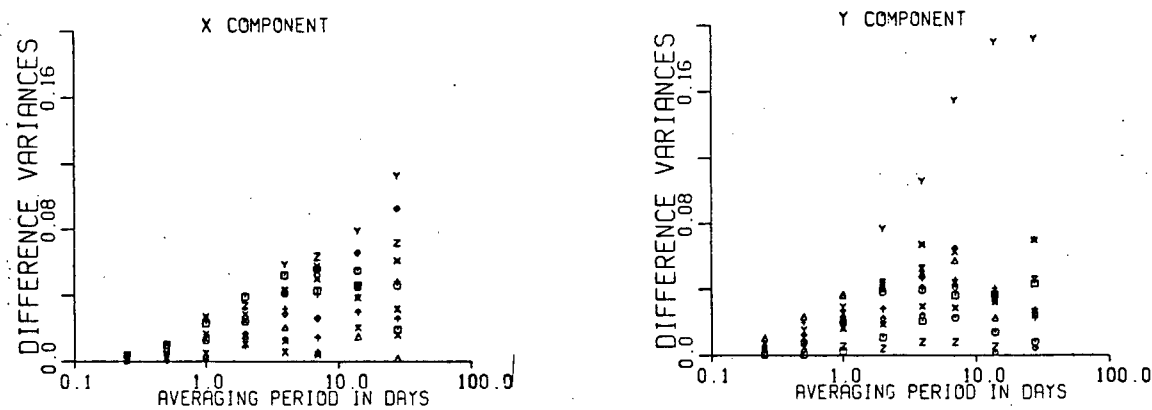


Figure 15. Systematic variance underestimation for all ships, constant drag coefficient using the initial estimates of  $\Sigma_{ke}$ . Station N is represented by Y.

applied identically to each component. Thus the applied transformation may differ from the optimal component transformation. The fact that the DV corrections in this section are positive definite indicates that the calculated  $\Sigma_{ke}$  based on the stress magnitudes approximates the optimal component corrections reasonably well. Finally, this suggests that a trade-off occurs in which one can either reduce the RVs to a minimum value and accept a systematic error in the long-term variance or minimize the DVs and accept an increase in the residuals.

If the difference variances for each component were identical then this bias could be made exactly 0 by multiplying  $\Sigma_{ke}$  by either  $\sigma_x / \sigma_{x'}$  or  $\sigma_y / \sigma_{y'}$  where  $(\sigma_x, \sigma_y)$  and  $(\sigma_{x'}, \sigma_{y'})$  are the component SH and VA standard

deviations with the transformation applied to the VA variate. This is not exactly the case. Consequently a new  $\bar{\epsilon}_{ke}^1$  term was found by :

$$\bar{\epsilon}_{ke}^1 = \frac{1}{2} \left( \frac{\bar{\epsilon}_x}{\bar{\epsilon}_{x1}} + \frac{\bar{\epsilon}_y}{\bar{\epsilon}_{y1}} \right) \bar{\epsilon}_{ke}$$

3.11

The  $\bar{\epsilon}_{ke}$  has been multiplied by the mean correction required for both the x and y VA stress components.

The DVs for the corrected transformation appear in Appendix D, and the specific constant drag coefficient results will be shown later. The variance differences are now randomly scattered positive and negative. Appendix D shows that for all ships, components, drag coefficients and averaging periods, a positive difference variance in the x component implies that the y component DV is, within several tenths of a percent, the exact negative.

Since the objective has been to minimize the RV, the correction applied to  $\bar{\epsilon}_{ke}$  to remove the systematic bias from the variance differences perturbs the residual variance so that it is no longer a minimum. The amount of this perturbation can be calculated under two different sets of assumptions as outlined in Appendices A.2 and A.3. If we define:

$$(1+\epsilon) = \bar{\epsilon}_{ke1}^1 / \bar{\epsilon}_{ke}$$

3.12

and assume that  $\bar{\epsilon}_x/\bar{\epsilon}_{x1} = \bar{\epsilon}_y/\bar{\epsilon}_{y1}$ , then it is demonstrated in Appendix A.3 that:

$$\frac{\delta_{eT}^{12} - \delta_{eT}^2}{\delta_{eT}^2} = \epsilon - \{(\epsilon^1 + \epsilon^2)/[2(1+\epsilon)(1-R_T) + \epsilon^2]\}$$

3.13

where  $\delta_{eT}^{12}$  is the RV after  $(1+\epsilon)$  has been applied. The relative increase in the RV can be determined in terms of the applied correction and the correlation coefficient. Figure 16 shows this function for the ranges of  $\epsilon$  and  $R_T$  associated with this problem. Excluding Station N, Figure 15 indicates that the largest DV values are about 0.08 which gives a typical value of 0.04 for  $\epsilon$ . A low estimate of the correlation coefficient is 0.95. When Equation 3.13 is then evaluated, the relative increase in RV is 2.4%. Allowing for a residual variance as high as 50%, the absolute change in RV is about 1%. (The initial residual variances are, in fact, significantly less than 10%). The actual change in RV was calculated and in all cases was substantially less than 1.0%.

Henceforth, the primes will be dropped and it will be understood that  $\xi_{ke}$  includes the DV correction.

### 3.6 Wind Dependent Correction Factors

The correction factors  $\xi_{ke}$  for all ships, averaging periods and wind speeds are given in Appendix C - Part I. The corresponding error estimates of the 95% confidence intervals on these values as estimated by the Student 't' test are given in Appendix C - Part II. Figure 17 shows the inverse of correction factors ( $1/\xi_{ke}$ ) as functions of wind speed and averaging period. The inverse is plotted for ease of comparison with Figure 12. Also, the inverse ratio is bounded between 0 and 1.0. Since  $\xi_{ke}$  increases as the wind speed approaches 0 m/sec, the inverse

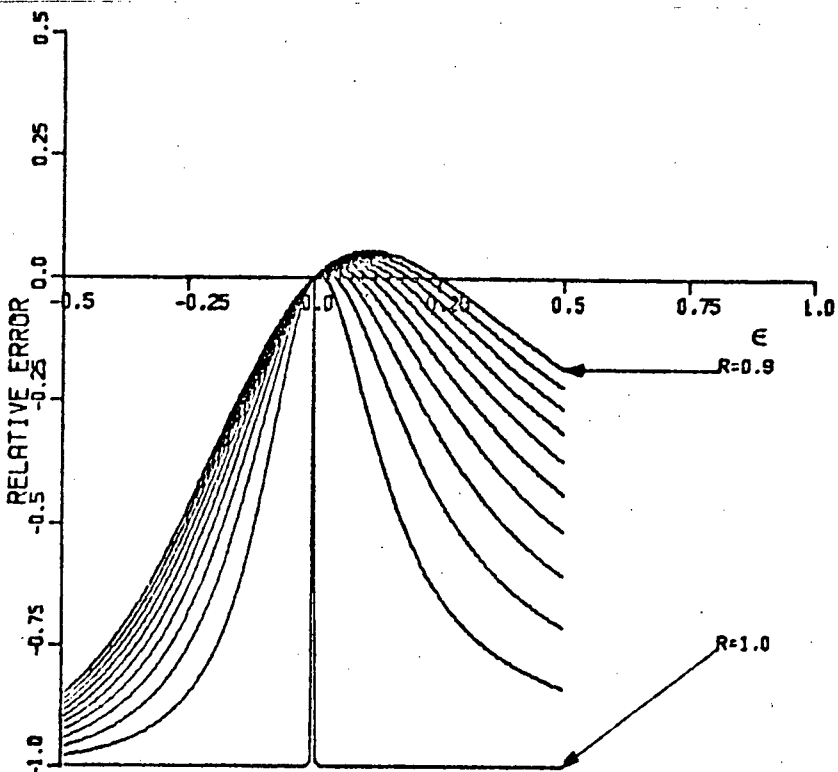


Figure 16. The relative error induced in the residual variances by application of a correction factor  $(1+\epsilon)$  to readjust for the systematic bias in the difference variances.

ratio is more convenient for plotting.

In all respects, the regressed correction factors are qualitatively similar to the average ratio of stresses  $\bar{R}(L)$  defined before). The mean ship values are nearly identical. The disparity of Station N at  $L=4.0$  days and  $6.75 \text{ m/sec}$  plots is also evident. The geographic standard deviations are similar in shape and magnitude. Finally an examination of Appendix C - Part II reveals that the error in the slope is larger than the scatter between ships and has the largest values for low wind speeds.

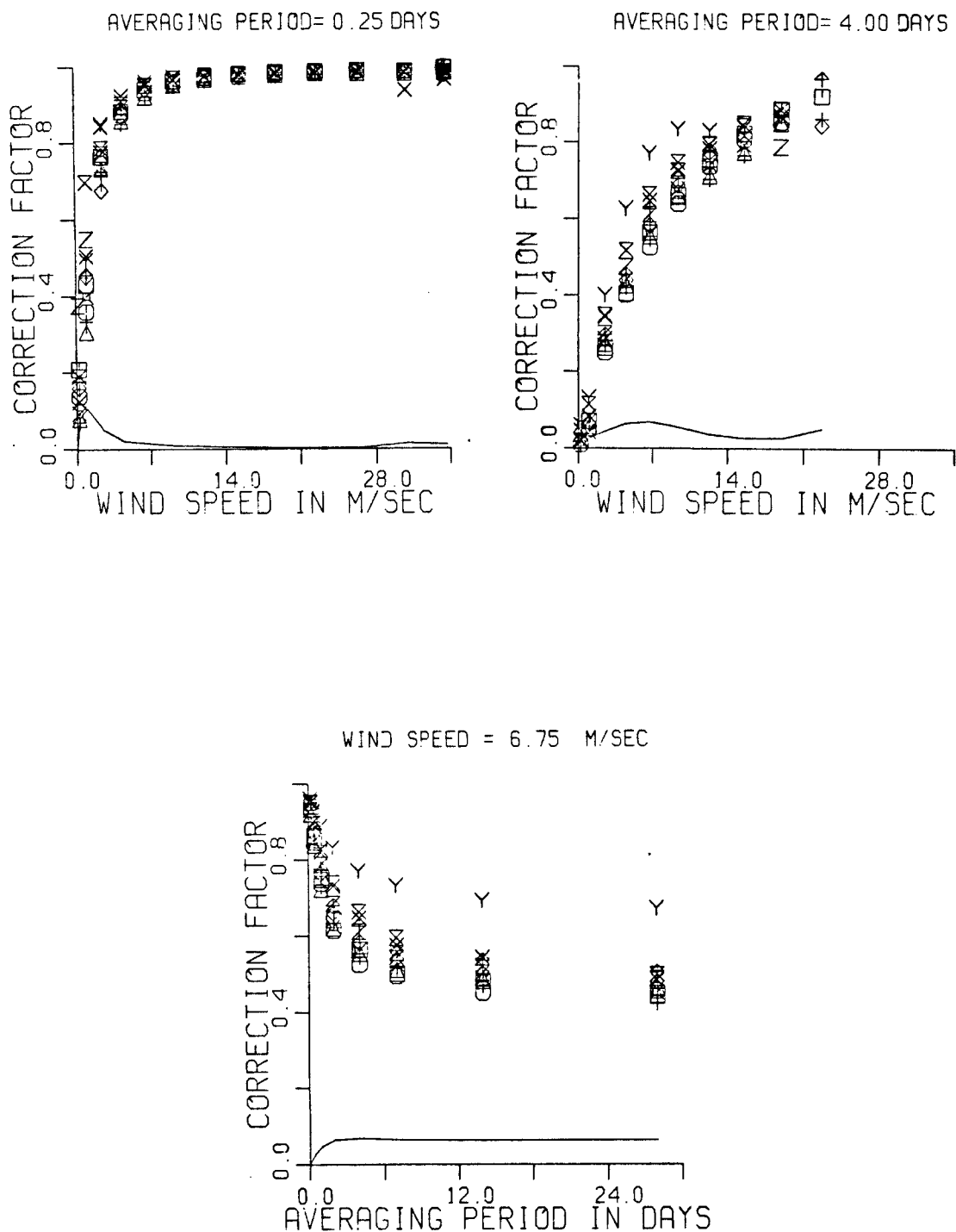


Figure 17. Correction factors  $\frac{1}{\xi_{\text{re}}}$  for the constant drag coefficient. Station N is Y. The solid line is  $\pm 1$  standard deviation of the geographically averaged mean value.

### 3.7 Accuracy Of Transformations

The difference means, difference variances, residual variances and correlation coefficients were determined by applying  $\xi_{ke}$  and the results appear in Appendix D. These quantities will be examined in light of their actual values and the arithmetic difference between the unimproved values of Appendix B and the improved values of Appendix D.

As an example, the difference means for the x component, constant drag coefficient appear in Figure 18(a). A comparison with Figure 7 illustrates several interesting features. First, the difference means have been reduced by a factor of about 10. Second, there appears to be an inverse relation in the amount of reduction achieved. In Figure 7 Stations A and N, with no correction applied, have the smallest difference means. In Figure 18, after application of  $\xi_{ke}$ , they now have the largest difference mean values. Conversely, Stations C and D have the highest difference means with no correction, but are less than 0.02 dPa for all averaging periods after correction. The improvements appear in Figure 19(a) for the x component, constant drag coefficient. In all cases there was some improvement. An inspection of Appendices B and D indicates that the most dramatic improvements occur where the uncorrected values were initially large -- in particular for longer averaging periods and the linear drag coefficient.

The difference variance values are now randomly scattered and bounded between about  $\pm 6\%$  using the constant drag coefficient and about  $\pm 10\%$  using the linear drag coefficient -- again a 10 fold improvement over the uncorrected values. The

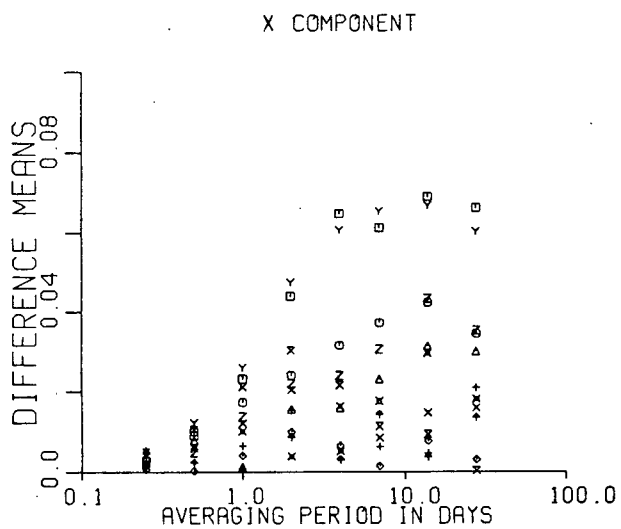


Figure 18 (a)

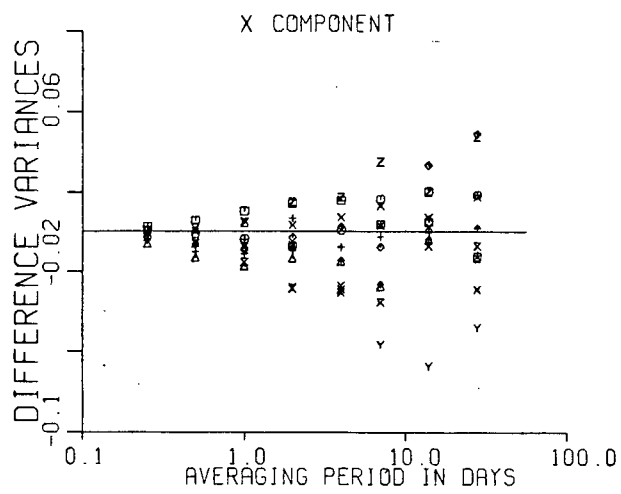


Figure 18 (b)

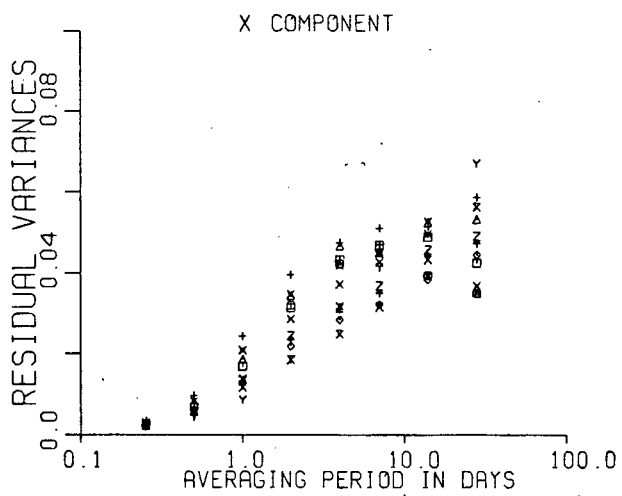


Figure 18 (c)

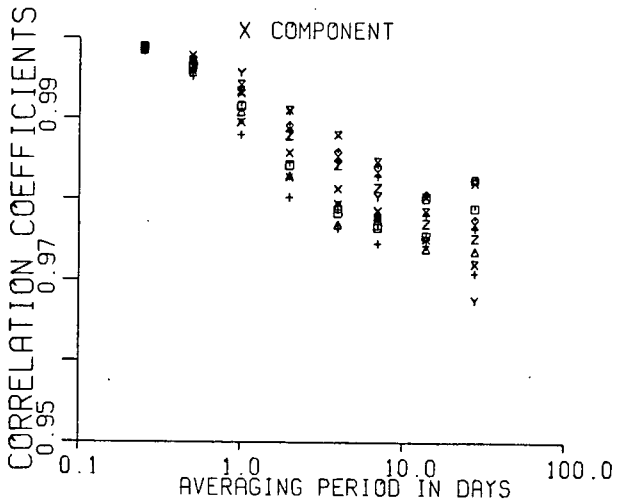


Figure 18 (d)

Figure 18. The test functions obtained when the ships' individual  $\xi_{be}$  values were used. The example is for the x component constant drag coefficient. Station N is Y.

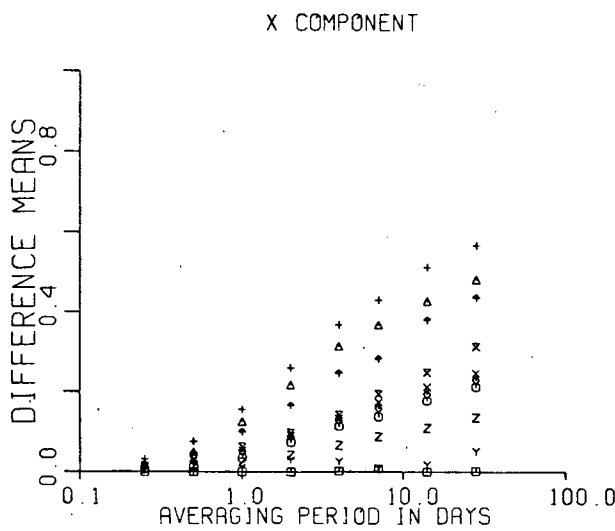


Figure 19 (a)

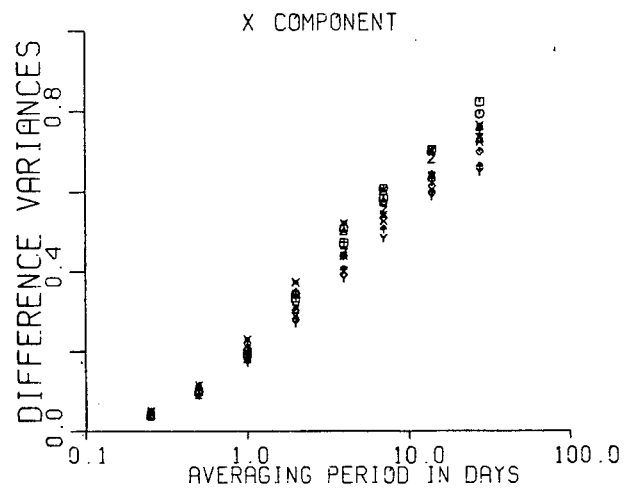


Figure 19 (b)

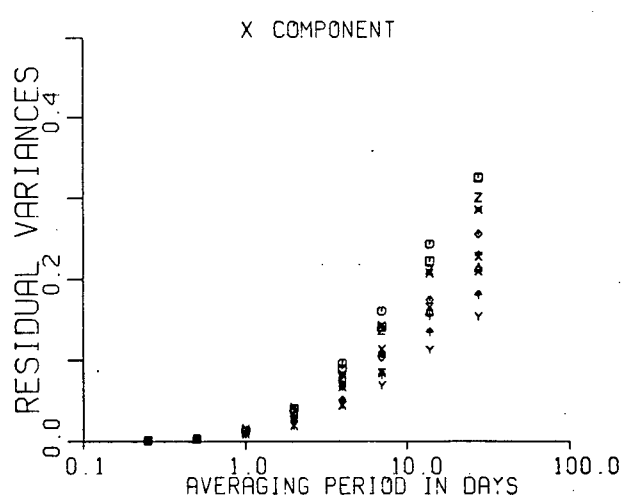


Figure 19 (c)

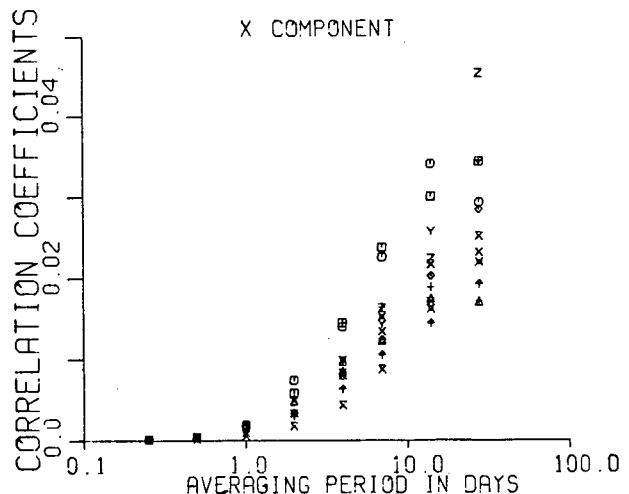


Figure 19 (d)

Figure 19. Improvement in the test values over the raw test results after application of the individual ships'  $\zeta_{ke}$  correction factor for the x component constant drag coefficient.

most accurate values occur, not unexpectedly, for the lower averaging periods. The differences between Figures 18 and 7 for each averaging period appear in Figure 19(b). Again all changes are positive, indicating that the corrections have improved the long-term variance. Indeed for L=28 days there are improvements up to 85% in the 3H variance.

Figure 18(c) shows the final calculated residual variances for the x component constant drag coefficient. Note that the RV axis scale has been increased by a factor of 5.0 from Figure 7(c). With the exception of Station N all values are less than 6%. Figure 19(c) indicates the improvements achieved. For low averaging periods, the differences are quite small. By L=4 days, however, an improvement of about 5% has been achieved. These improvements increase to L=28 days where improvements of the order of 20% for the constant drag coefficients and 30% for the linear drag coefficients values are common.

Figure 18(d) shows the final correlation coefficients. Because the raw correlation coefficients are all quite high ( $>0.90$ ), the broad features of 19(d) are not significantly different from the raw values. The high initial correlations account for the large reductions in the residual variances that can be achieved with only a linear regression. Figure 19(d), however, demonstrates the improvements achieved over the raw correlation coefficients. In all cases the improvements are small for low averaging periods and rise to values of up to 0.05 at L=28 days. An examination of Appendix B reveals that at L=2 days there are no values less than 0.99. Since the correlation coefficient is bounded by 1.0, there is little room for

improvement at the low averaging periods.

For averaging periods of greater than 1.0 days, the VA estimates of the long-term variances as quantified by the DV and the point-by-point variance as quantified by the RV can be substantially improved through application of the  $\xi_{ke}$  corrections given in Appendix C. In regions where the unimproved estimates of the climatological VA fluxes differed greatly from the EH fluxes (as quantified by the DMs), dramatic improvements resulted with application of the  $\xi_{ke}$  factor. The major strength of the multivariate regression is to increase the correlation coefficients particularly at longer averaging periods. If a similar regression had been performed irrespective of wind speed grouping no improvements would have resulted because the correlation coefficient is independent of an overall scale change.

## CHAPTER IV HEAT FLUXES

This chapter describes the effects of averaging winds, temperatures, and absolute humidities on the sensible and latent heat fluxes. The sensible heat flux is a measure of the heat transferred by convection into or out of the sea surface while the latent heat flux is a measure of the heat lost or gained by the evaporation or condensation. The bulk aerodynamic formulae for their calculation are given in Equations 1.2(c) and (d).

### 4.1 Three-hourly Heat Fluxes

Similar to the 3H momentum fluxes, the 3H heat fluxes had summer minima and winter maxima average values of which station C was chosen as an example.

Plots for Station C of the yearly and monthly latent and sensible 3H heat fluxes with error bars indicating  $\pm 1$  sample standard deviation appear in Figures 20 (a) and (b). Similar graphs with  $\pm 1$  standard deviation of the monthly means appear in Figures 20(c) and (d) respectively. In this section, the sensible heat results will be quoted in parentheses following the latent heat results. The extreme values in the means are much greater between months than between years. Between months the maximum values are 80.8 (34.7) Watts/m<sup>2</sup> in December (January) and the minimum values are 12.4 (-7.4) Watts/m<sup>2</sup> in July (July). The minus sign indicates a net transport of heat from the air to the sea. This may be due to advection of warm continental air in the summer to the mid-Atlantic. Between years the

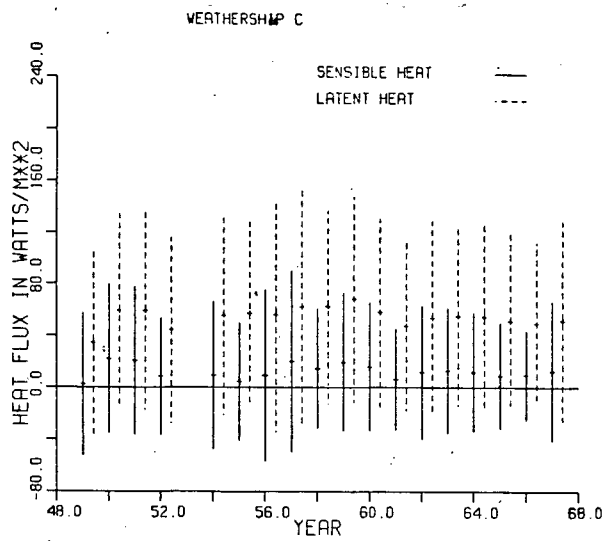


Figure 20 (a)

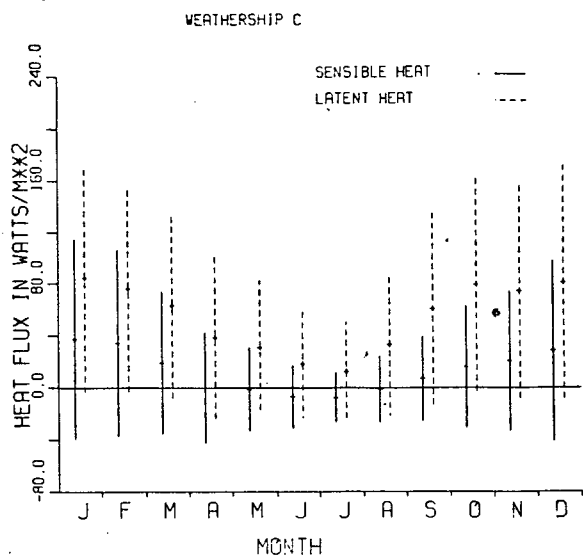


Figure 20 (b)

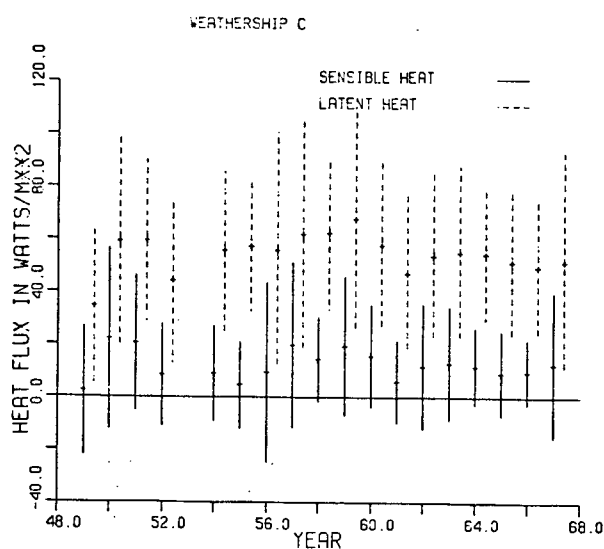


Figure 20 (c)

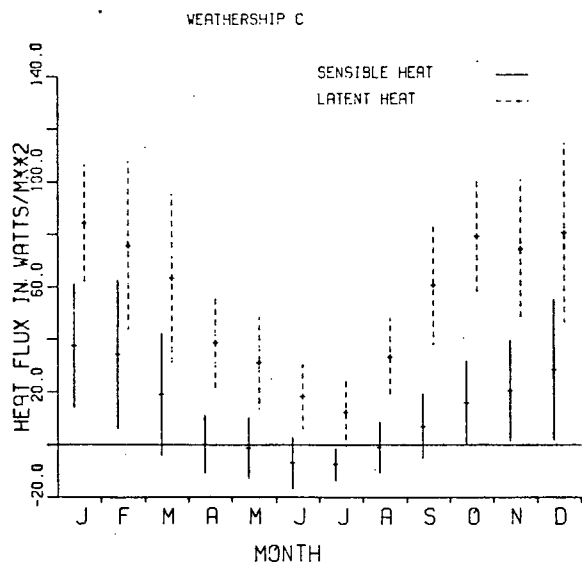


Figure 20 (d)

Figure 20. The year-to-year and monthly variations of the mean heat fluxes at Station C. The error bars are  $\pm 1$  sample standard deviation in Figures 20(a) and (b) and  $\pm 1$  standard deviation of the monthly means in Figures 20(c) and (d).

latent(sensible) heat fluxes have maxima in 1959(1957) of 67.9(19.9) Watts/m<sup>2</sup> and minima in 1949(1949) of 34.5(2.3) Watts/m<sup>2</sup>.

It is clear from Figure 20 that the standard deviations in the yearly heat values are fairly constant. The maximum yearly standard deviations for the latent (sensible) heat fluxes are 90.3 (69.8) Watts/m<sup>2</sup> for 1957(1957) while the minimum values are 62.2(34.4) Watts/m<sup>2</sup> in 1956(1950). The standard deviations of the monthly means for both heat fluxes are approximately one-half of the total standard deviations based on all the three-hourly flux readings indicating that about one-quarter of the total variance may be in periods of greater than one month.

Figures 20(b) and (d) show the difference in standard deviation between the summer and winter months. The December heat flux standard deviation is 91.1(69.5) Watts/m<sup>2</sup> while the July values are 38.3(19.0) Watts/m<sup>2</sup>. The standard deviations of the monthly means vary from 34.0(26.8) Watts/m<sup>2</sup> in December to 12.8(6.3) Watts/m<sup>2</sup> in July indicating that the annual cycle is present in the means and the variances.

The total ships' means and standard deviations of the velocity components, air-sea temperature, air-sea absolute humidity difference, latent heat and sensible fluxes appear in Table X. The mean heat fluxes are all of the same order as the standard deviations.

Oceanographically, the data may be divided into four main regimes. Stations A, B, C, and M are in Sub-Arctic regions. They are characterized by sea surface temperatures of about 10° C and colder air temperatures. As one proceeds south the air

TABLE X

The mean and standard deviations of the x and y component wind velocities, the air-sea temperature differences, the air-sea humidity differences and the latent and sensible heat fluxes. The first line for each ship is the mean value and the second line is standard deviation.

SHIP	$U$ m/sec	$V$ m/sec	$\Delta T$ °C	$\Delta Q$ g/m <sup>3</sup>	$H_s$ W/m <sup>2</sup>	$H_e$ W/m <sup>2</sup>
A	-0.1	0.0	1.6	1.7	34.4	62.8
	7.8	8.0	2.2	1.3	60.5	65.3
B	-0.8	1.7	1.8	1.5	41.4	58.9
	7.8	8.3	2.9	1.2	79.6	64.5
C	0.7	3.1	0.5	1.4	12.0	54.1
	7.3	8.2	2.0	1.5	51.3	74.5
D	1.1	3.9	2.1	3.6	45.9	140.1
	7.6	7.6	3.1	2.9	85.4	150.7
E	1.3	2.0	0.9	4.4	14.0	124.7
	6.3	6.1	1.7	2.7	34.7	116.2
I	2.0	1.6	1.6	2.0	32.9	78.1
	7.5	8.3	1.8	1.3	49.9	69.8
J	2.0	3.4	1.0	1.9	20.3	73.7
	7.3	7.7	1.5	1.5	38.8	72.8
K	-0.2	2.1	0.3	2.2	5.3	71.8
	6.8	7.3	1.7	1.9	32.6	80.6
M	0.3	1.0	1.9	2.0	34.9	69.1
	7.6	6.9	2.1	1.3	50.0	59.7
N	-0.8	-2.5	1.2	4.8	14.4	110.1
	4.6	4.7	1.2	1.9	19.5	75.0
P	4.0	1.4	0.3	1.1	5.8	42.4
	7.6	7.5	1.2	1.2	31.1	57.5

temperature increases, decreasing the air-sea temperature difference.

Station D lies at the transition region between the Gulf Stream and North Atlantic Drift. Here the water is relatively

warm (about 5-10°C) accounting for large air-sea temperature differences. The advection of large horizontal sea surface temperature gradients and invasions of continental air account for large standard deviations in the heat fluxes.

Stations E and N lie in the middle of the large Atlantic and Pacific sub-tropic gyres. They are characterized by moderate air-sea temperature differences and by dry prevailing winds thus accounting for moderate sensible heats and large latent heat flux values. Station N is the Trade Wind region, where steady summer winds account for the small heat flux standard deviations in comparison to Station E.

Stations I, J, and K lie on the eastern boundary of the Atlantic Ocean. Proceeding south, the air temperature becomes warmer more quickly than the corresponding increase in sea surface temperature accounting for lower sensible heat fluxes. The three stations show similar air-sea humidity differences and moderate latent heat flux values.

#### 4.2 Uncorrected Test Results

The difference means, difference variances, residual variances and correlation coefficients as defined in Equations 2.16-2.19 were calculated with no correction factors applied. The results appear in Figures 21(a) through (h) while the raw values are in Appendix E. Table XI contains the 3H heat flux variance at each averaging period so the difference variances and residual variances can be converted to absolute quantities.

As in the wind stress case, the heat flux difference means (DMs) appear to be dependent upon the average 3H heat flux value

TABLE XI

The absolute latent and sensible heat flux variances as a function of averaging period. The columns refer to the averaging period in days and the variances are in (Watts/m<sup>2</sup>)<sup>2</sup> x 10<sup>3</sup>.

VARIANCES - SENSIBLE HEAT FLUX									
SHIP	0.25	0.50	1.0	2.0	4.0	7.0	14.0	28.0	
A	3.511	3.303	2.982	2.508	2.035	1.669	1.331	0.994	
B	6.154	5.900	5.461	4.870	4.142	3.684	3.077	2.530	
C	2.496	2.314	2.020	1.626	1.263	1.045	0.797	0.566	
D	6.947	6.512	5.725	4.646	3.679	3.084	2.479	1.892	
E	1.133	1.057	0.921	0.759	0.573	0.451	0.326	0.245	
I	2.374	2.219	1.998	1.687	1.383	1.133	0.867	0.670	
J	1.423	1.316	1.160	0.968	0.747	0.602	0.412	0.325	
K	1.001	0.941	0.860	0.764	0.672	0.589	0.510	0.442	
M	2.398	2.266	2.058	1.775	1.453	1.200	0.900	0.706	
N	0.341	0.302	0.275	0.236	0.192	0.162	0.124	0.081	
P	0.896	0.806	0.708	0.577	0.448	0.345	0.240	0.181	

VARIANCES - LATENT HEAT FLUX									
SHIP	0.25	0.50	1.0	2.0	4.0	7.0	14.0	28.0	
A	4.078	3.785	3.343	2.751	2.179	1.812	1.426	1.064	
B	4.017	3.795	3.443	2.989	2.484	2.161	1.812	1.518	
C	5.326	4.951	4.330	3.495	2.663	2.154	1.639	1.233	
D	21.51	20.15	17.70	14.71	11.67	9.680	7.830	6.171	
E	12.79	12.01	10.74	9.036	7.008	5.693	4.237	3.295	
I	4.600	4.205	3.655	2.933	2.318	1.879	1.373	1.029	
J	5.010	4.582	3.966	3.112	2.242	1.732	1.132	0.836	
K	6.155	5.753	5.165	4.351	3.500	2.847	2.091	1.668	
M	3.374	3.122	2.747	2.297	1.838	1.502	1.133	0.884	
N	5.084	4.701	4.213	3.542	2.732	2.157	1.481	0.870	
P	3.115	2.853	2.509	2.034	1.580	1.253	0.957	0.750	

and with mincr exceptions, increase approximately exponentially with averaging period. A comparison of Table X and Appendix E indicates that the sizes of the difference means are well correlated with the average 3H heat flux. At L=28.0 days, the sensible heat fluxes fall into two distinct groups -- Stations A, B, D, I, and M with average DMs greater than 18 Watts/m<sup>2</sup> and

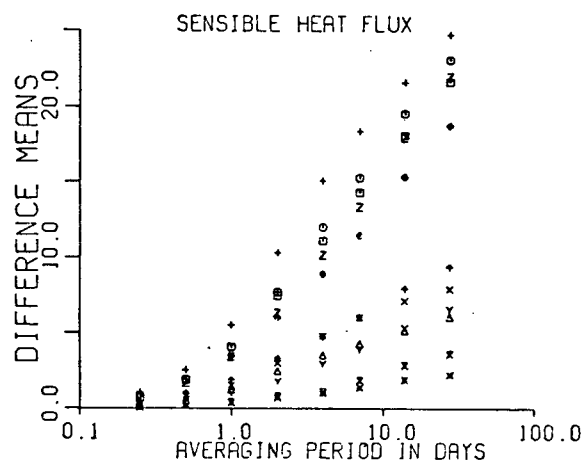
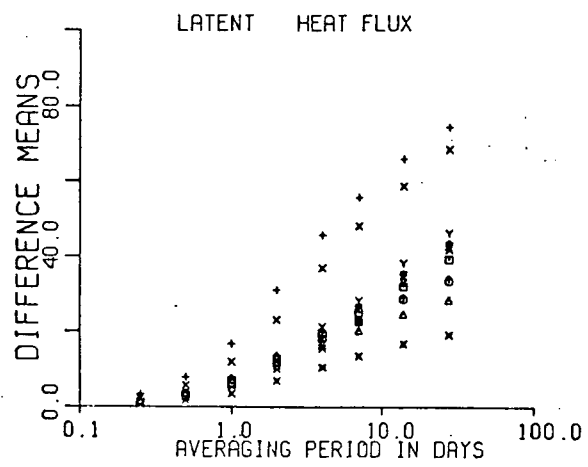
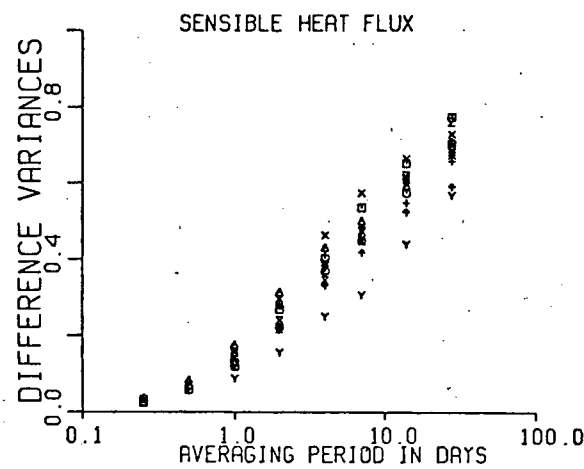
Figure 21(a) DMs in Watts/m<sup>2</sup>Figure 21(b) DMs in Watts/m<sup>2</sup>

Figure 21(c)

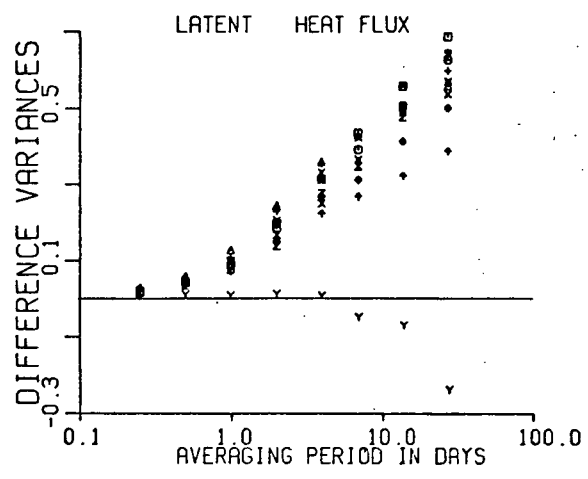


Figure 21(d)

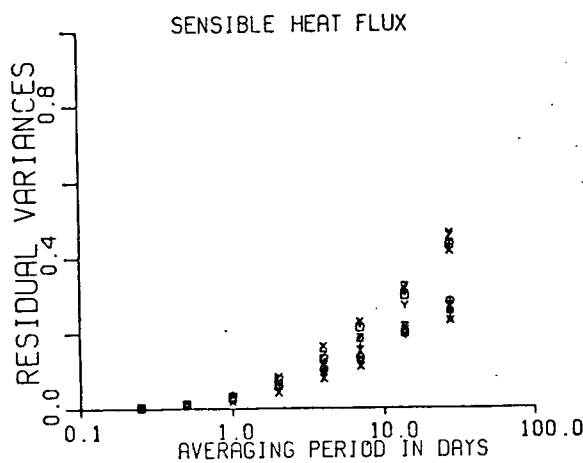


Figure 21(e)

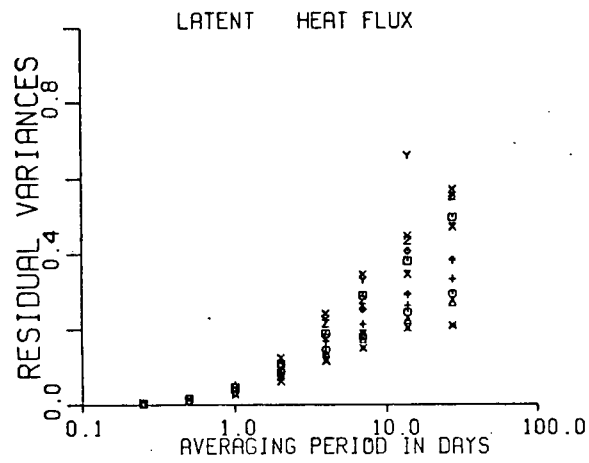


Figure 21(f)

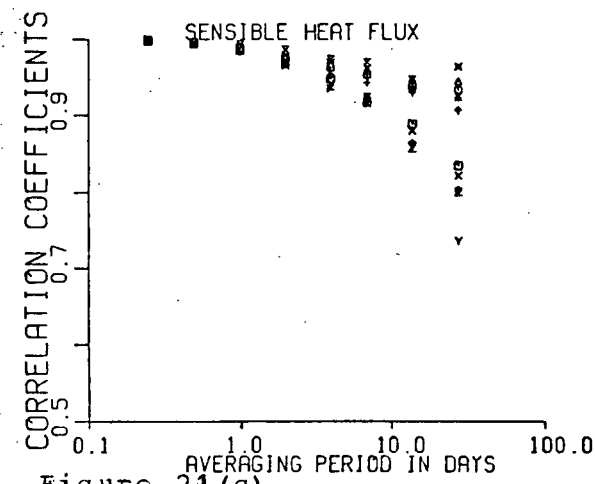


Figure 21(g)

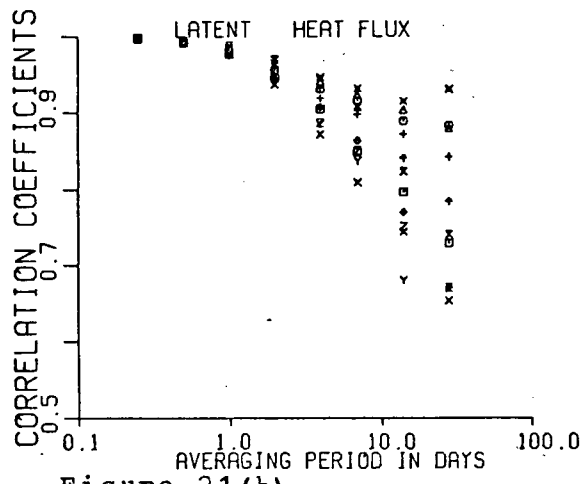


Figure 21(h)

Figure 21. The test quantities with no correction applied to the VA heat fluxes.

Stations C, D, E, J, N, and P having DMs less than 10 Watts/m<sup>2</sup>. The latent heat fluxes have three distinct groups. Stations D and E have uncorrected DMs greater than 60 Watts/m<sup>2</sup>. At L=28.0 days, Stations A, B, C, I, J, K, M and N have DMs in the range of 20 to 60 Watts/m<sup>2</sup>; Station P has distinctly smaller DMs at less than 20.0 Watts/m<sup>2</sup>. The same groupings occur in the 3H mean flux values shown in Table X indicating that the larger climatological errors occur in regions with the higher initial mean flux.

The difference variances (DVs) for all ships excluding Station N differ only slightly. Both heat fluxes show increases from near 0 at L=0.25 days to mean maximum values of about 0.55 to 0.65 at L=28.0 days. Station N has markedly lower DVs from L=1.0 to L=14.0 days in the sensible heat flux. For the latent heat flux, Stations N's values are nearly 0.0 Watts/m<sup>2</sup> up to L=4.0 days and then go negative -- in contrast to all the other ships.

All ships have similar residual variances (RVs) up to L=4 days. The sensible heat fluxes then split into two distinct groups. The first includes Stations A, E, I, M, and N having RV values of greater than 40.0% at L=28.0 days. The others have RVs less than 30.0%. The latent heat flux RVs are generally larger (except at Station F) than for the sensible heat fluxes. The average value at L=28.0 days is about 35%. Up to L=7.0 days, the Station N values are indistinguishable (although biased high) from the other values. At L=14.0 days, however, the Station N values are much greater than the other ships. Indeed, at L= 28.0 days the Station N RV is greater than 100.0%

which is not shown in Figure 21.

The correlation coefficients for the heat fluxes are lower than for the momentum fluxes. Those for the latent heat flux are lower than for the sensible heat flux. At  $L=28.0$  days Station N has the lowest correlation coefficient of 0.438 (not shown) for the latent heat flux and 0.736 for the sensible heat flux. After  $L=14.0$  days, the sensible heat flux correlation coefficients divide into the same two groups as for the RV values -- Stations A, E, I, M, and N with values less than 0.835 (at  $L=28.0$  days) and the rest having correlation coefficients greater than 0.900.

#### 4.3 Heat Regression

Figure 22 shows an example of the 3H heat flux plotted against the VA heat flux for Station A,  $L=28$  days. Similar to the stress case, shown in Figure 6, the scatter increases for extreme positive and negative values. As the VA flux approaches 0.0 Watts/m<sup>2</sup>, the scatter becomes more constricted. Note, however, that there is a bias towards positive heat fluxes.

Two important differences exist between the heat flux regression and the momentum flux regression. First, the analysis of the raw 3H values revealed that the latent and sensible heat fluxes are statistically quite distinct quantities. Consequently the regression was performed separately on each flux. Thus, no attempt was made to assume that the fluxes might be similar and thus produce a single transformation applicable to both. Second, as shown in Table X, the means are of the same magnitude as the standard deviations.

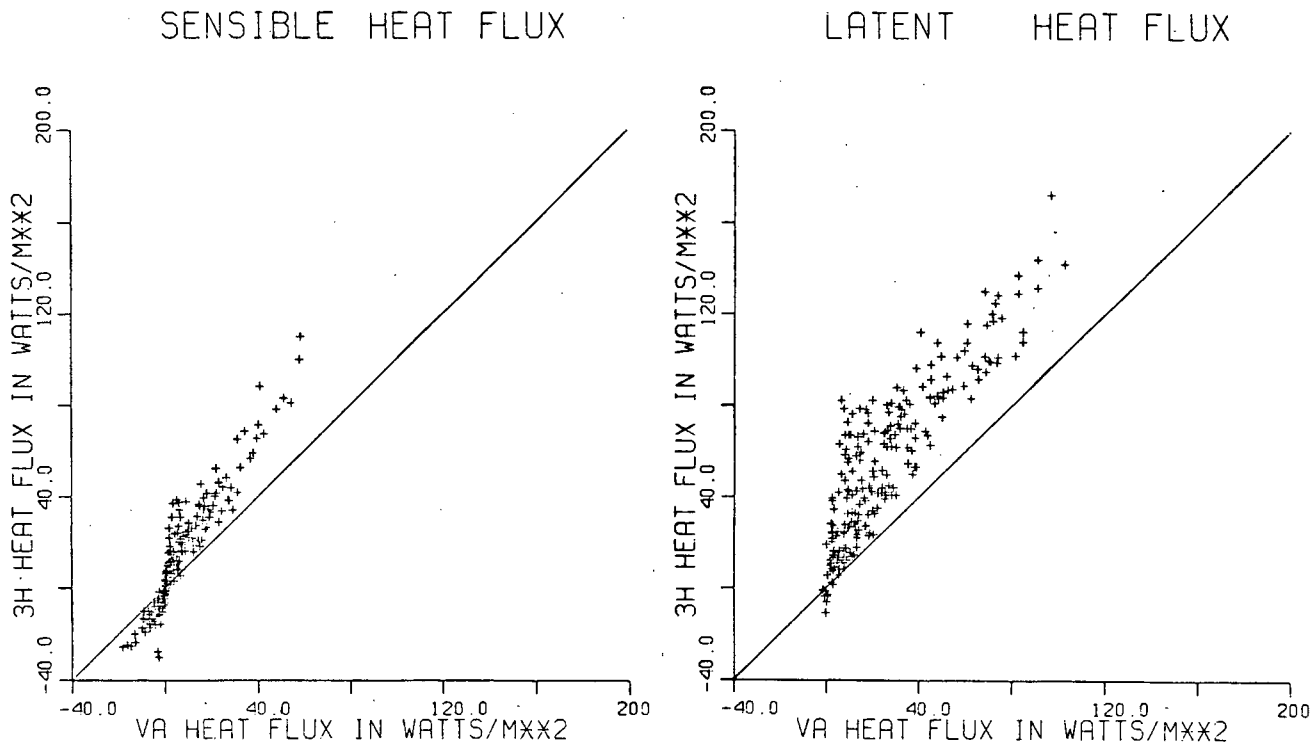


Figure 22. The sensible and latent 3H versus VA heat fluxes at Station C, L=28.0 days.

Consequently the following quantity:

$$\sigma_x^2 \delta_{ex}^2 = \frac{1}{N} \sum_{k=1}^{13} \sum_{j=1}^{J_{1k}} (X_{kj} - \bar{X}_{ke} X'_{kj})^2 - \left\{ \left( \sum_{k=1}^{13} \sum_{j=1}^{J_{1k}} \frac{X_{kj}}{N_j} \right) - \left( \sum_{k=1}^{13} \sum_{j=1}^{J_{1k}} \bar{X}_{ke} \frac{X'_{kj}}{N_j} \right) \right\}^2 \quad 4.1$$

was minimized as outlined in Appendix A.1 where X and X' are the 3H and VA variates for either the latent or sensible heat fluxes. This gives:

$$\bar{X}_{ke} = \frac{\sum_{j=1}^{J_{1k}} X_{kj} X'_{kj} - \sum_{j=1}^{J_{1k}} X_{kj} \left[ \frac{1}{N} \sum_{k=1}^{13} \sum_{j=1}^{J_{1k}} (X_{kj} - \bar{X}_{ke} X'_{kj}) \right]}{\sum_{j=1}^{J_{1k}} X'_{kj}^2} \quad 4.2$$

where all variates are defined in Section 2.5. This is a matrix

equation of the form

$$\bar{x} = \bar{b} + \underline{A} \bar{x}$$

4.3

where  $\bar{x}$  and  $\bar{b}$  are vectors with components corresponding to 13 Beaufort categories and  $\underline{A}$  is a  $13 \times 13$  matrix. The solution was obtained by Gaussian elimination followed by iterative improvement until a relative error of less than .001 was found.

Appendix A.1 shows that the DVs were exactly equal to the RVs and the systematic positive DV bias again exists. This fact provided a convenient check to ensure that the computer programmes were running correctly. The systematic bias was eliminated by :

$$\xi'_{ke} = \frac{\nabla_x}{\nabla_{x'}} \xi_{ke}$$

4.4

where  $\nabla_x$  is the 3H standard deviation,  $\nabla_{x'}$  is the VA standard deviation with  $\xi_{ke}$  applied and  $X$  represents either the latent or sensible heat. An attempt was made to correct  $\xi_{ke}$  on a Beaufort category basis (ie.  $\xi'_{ke} = \frac{\nabla_{x'k}}{\nabla_{x'n}} \xi_{ke}$ ). However, in many cases the required iterations failed to converge.

Appendix A.3 shows that when readjusting from the minimum RV value, the correction given in Equation 4.4 induces a further error in RV given by:

$$\delta_{ex}^2 - \delta_{eX}^2 = \left( \frac{\nabla_x - \nabla_{x'}}{\nabla_x} \right)^2 = (1 - R_x)^2$$

4.5

Thus for correlation coefficients of 0.9 or greater, the induced

error is less than 1.0%.

Again, the primes will be dropped and it will be understood that  $\xi_{ke}$  includes the DV correction.

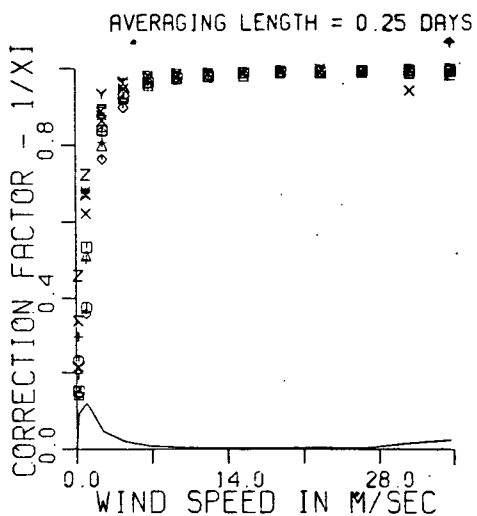
#### 4.4 Wind Dependent Correction Factors

The  $\xi_{ke}$  for the heat fluxes were calculated and appear in Appendix F - Part I. Figure 23 shows the  $1/\xi_{ke}$  values as functions of wind speed and averaging period.

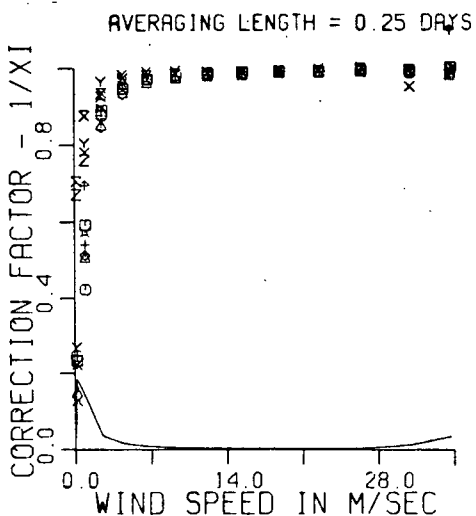
In general, the inverse heat corrections  $1/\xi_{ke}$  follow a similar pattern to the stress values. For low wind speeds  $1/\xi_{ke}$  approaches 0.0 ( $\xi_{ke}$  approaches  $\infty$ ). As the wind speed increases,  $1/\xi_{ke}$  approaches 1.0 for all averaging periods. In general Appendix F indicates that the corrections required for the sensible heat fluxes are larger than those required for the latent heat fluxes. Furthermore, a comparison with Appendix C indicates that the stress corrections are larger than both the heat corrections.

An estimate of the error in  $\xi_{ke}$  was obtained by employing the Student 't' test as outlined in Equation 3.10. The results appear in Appendix F - Part II. These results should be viewed somewhat skeptically as no attempt was made to assure that the scatter about the regression was Gaussian. Similar patterns to the stress errors, however, are exhibited in the heat flux errors. For the lowest wind speed categories, the 95% confidence zone is large compared to the  $\xi_{ke}$  values. By Beaufort interval 3 (1.6 - 3.4 m/sec<sup>2</sup>) errors in the calculations are reduced to less than 10% of the calculated  $\xi_{ke}$  value for all averaging periods. In general, the errors

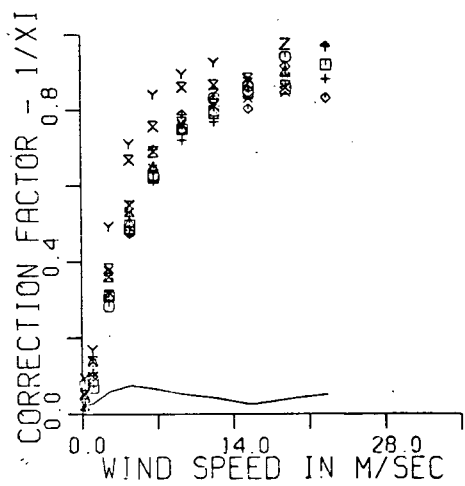
## SENSIBLE



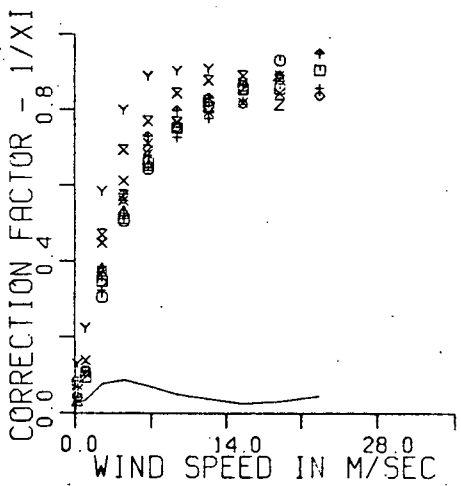
## LATENT



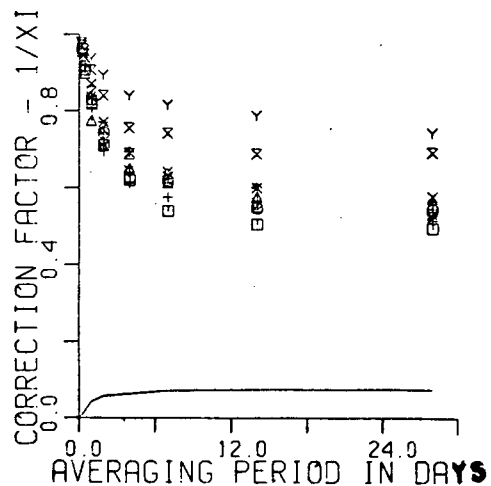
AVERAGING LENGTH = 4.00 DAYS



AVERAGING LENGTH = 4.00 DAYS



WINDSPEED = 6.75 M/SEC



WINDSPEED = 6.75 M/SEC

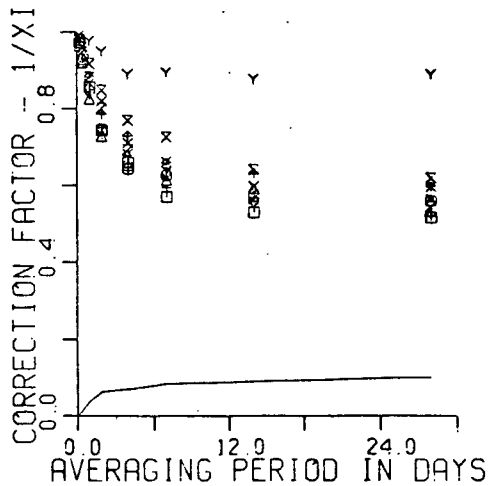


Figure 23. Ships'  $1/\xi_{\text{sc}}$  values for the heat fluxes. The line at the bottom indicates  $\pm$  one standard deviation of the means excluding Station N. Station N is Y, Station K is X.

increase as the averaging period increases.

The  $\xi_{ke}$  heat corrections for all ships are fairly tightly grouped. Station N shows significantly larger  $1.0/\xi_{ke}$  (smaller  $\xi_{ke}$ ) values at averaging periods greater than 0.5 days. Station K also shows significantly larger  $1.0/\xi_{ke}$  values for the sensible heat flux -- lying between the Station N values and the main ship grouping. An inspection of the sensible heat raw statistics in Table X does not reveal anything either to distinguish Station K from the other ships or to show any consistencies with Station N to account for the difference. In the latent heat fluxes, the Station K values are biased towards high values in the  $1.0/\xi_{ke}$  plots but can be considered within the general ships' geographic grouping and are far below those of Station N.

#### 4.5 Beaufort Grouped Test Results

The three test quantities were calculated for the  $\xi_{ke}$  values given in Appendix F. The results appear in Appendix G and are shown in Figure 24. The arithmetic differences between Figures 24 and 21 are shown in Figure 25. The difference variances are not considered in this section because the correction for the systematic bias forced all values to exactly 0.0.

The difference means have improved markedly after the application of  $\xi_{ke}$ . A comparison of Figures 24 and 21 indicates that both the latent and sensible heat flux DMS have been improved by a factor of 5.0. Climatological errors are now less than 3.5 Watts/m<sup>2</sup> for the sensible heat flux and 17.7 Watts/m<sup>2</sup>

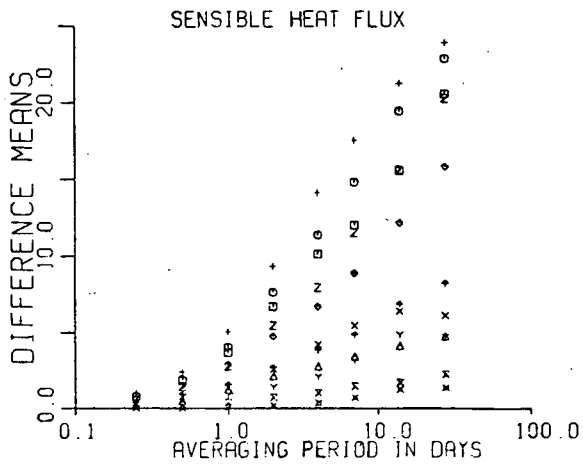


Figure 24 (a) DMs in  
Watts/m<sup>2</sup>

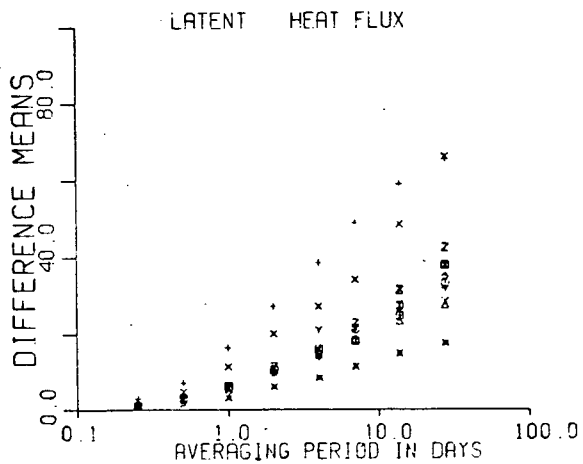


Figure 24 (b)  
Watts/m<sup>2</sup>

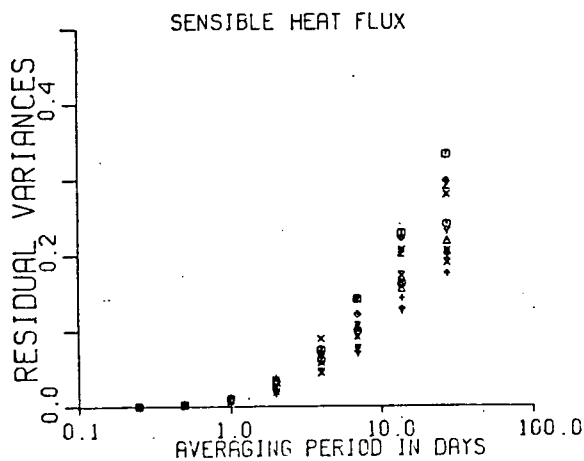


Figure 24 (c)

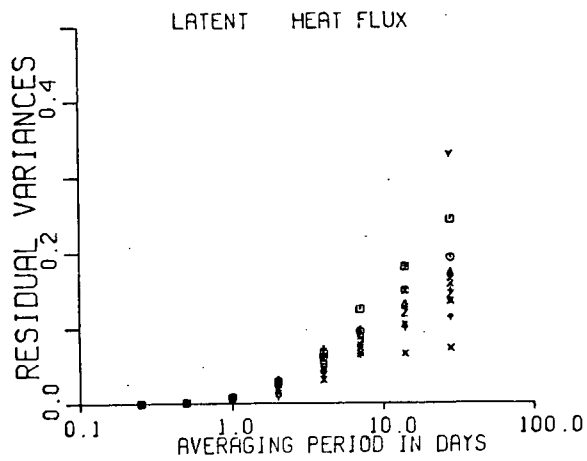


Figure 24 (d)

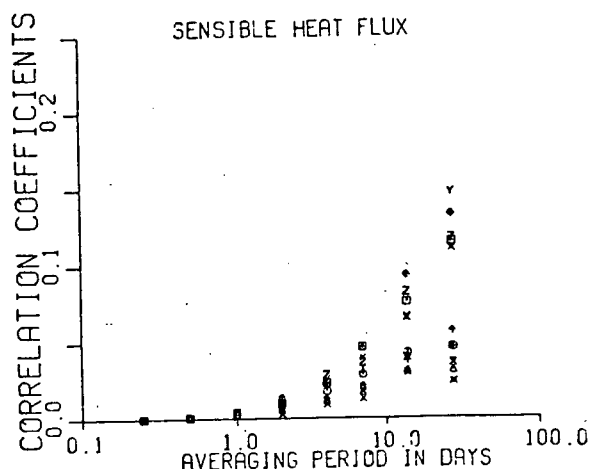


Figure 24 (e)

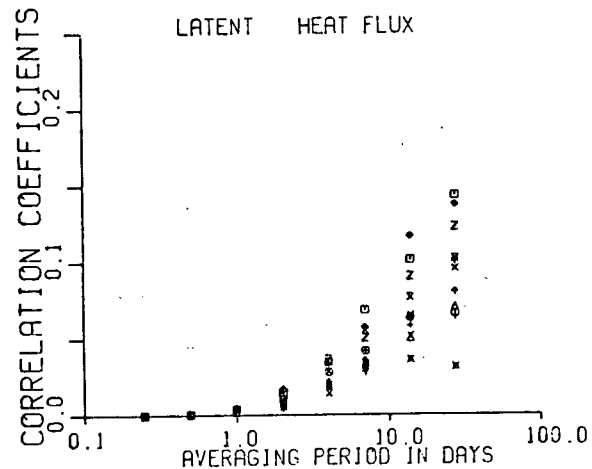


Figure 24 (f)

Figure 24. Test values with individual ships'  $\Sigma_{\text{be}}$  applied to the heat fluxes.

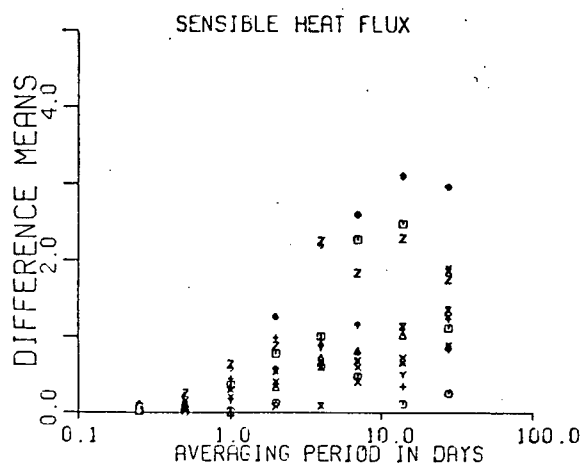
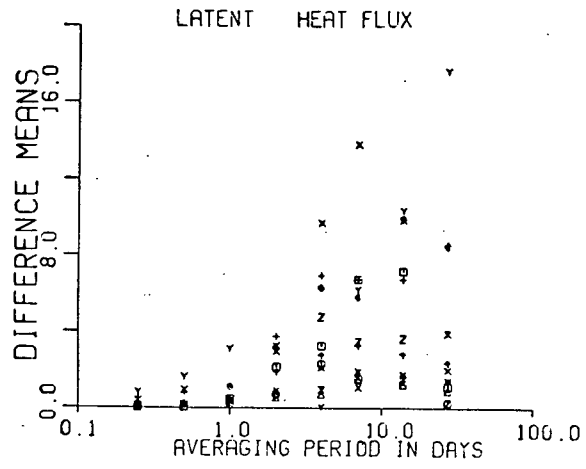
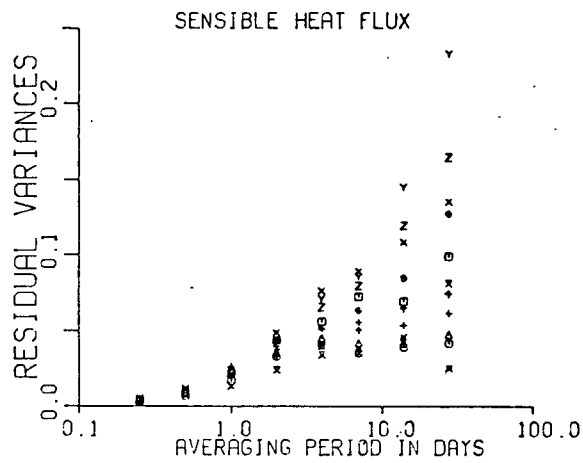
Figure 25 (a) DMS in Watts/m<sup>2</sup>Figure 25 (b) DMS in Watts/m<sup>2</sup>

Figure 25 (c)

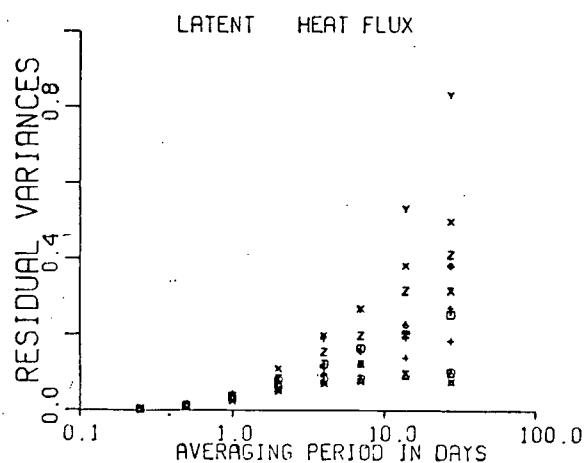


Figure 25 (d)

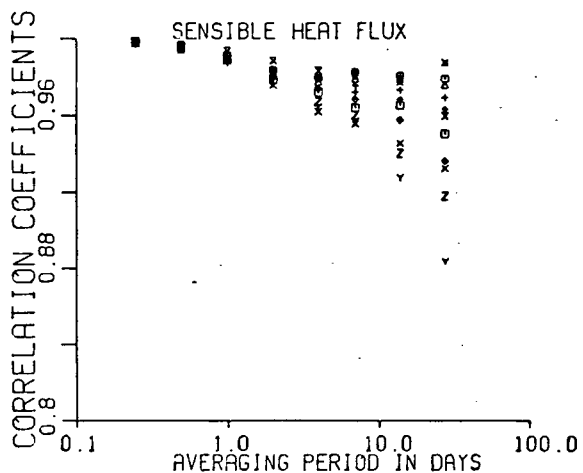


Figure 25 (e)

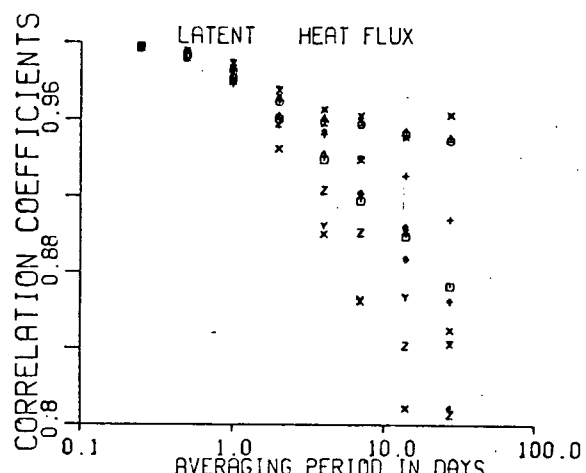


Figure 25 (f)

Figure 25. Test value improvements over Figure 21, the uncorrected case.

for the latent heat flux. Ignoring Stations E and N for the latent heat flux, the DM errors are then all less than 10.0 Watts/m<sup>2</sup>. The improvements shown in Figure 25 and are virtually a replication of Figure 21 indicating that the greater the initial DM error, the greater the improvements that can be obtained.

The residual variance errors are somewhat less encouraging for longer averaging periods. Station N in particular, has extremely high (up to 0.23 for the sensible heat and 0.83 for the latent heat flux) RVs at L=14.0 and L=28.0 days. If one considers 10% to be an acceptable noise level then an appreciable number of ships lie above this level at L=14.0 days for the sensible heat flux and at L=4.0 days for the latent heat flux. The application of  $\xi_{k\theta}$  has markedly improved the final residual variances over the initial raw values. The RVs at long averaging periods are now about one-half the uncorrected values. Figure 25 indicates that improvements of 0.25 for the sensible heat flux and 0.15 for the latent heat flux at L=28.0 days are typical.

The application of  $\xi_{k\theta}$  has improved the correlation coefficients. The sensible heat flux correlations, with the exception of Station N, L=28.0 days, are all above 0.90. The latent heat flux correlations are above 0.90 up to L=4.0 days after which some stations fall off, for example, to values as low as of 0.583 at Station N and 0.750 at Station E (both not shown) for L=28.0 days. According to Equation 4.8, this partly explains the large RVs at Stations N and E. If the DVs were not corrected, the RVs would be reduced by 17.4% and 6.25%

respectively. The improvements shown in Figure 25 have similar ranges for both the latent and sensible heat fluxes. There is a tendency for the stations with the lower initial correlation coefficients to show the most improvement. For example, in Figure 21, the sensible heat flux raw correlations at Stations A, E, I, M and B are distinctly grouped lower than the others. Figure 25 shows these same stations grouped with the most improvement.

## CHAPTER V EMPIRICAL FORMULA AND TEMPORAL VARIATIONS

### 5.1 Introduction

In the previous two chapters it has been established that systematic reductions occur in the 3H momentum and heat fluxes when estimated through VA parameters. In Chapter III it was shown that the  $1/\xi_{ke}$  optimally regressed stress reductions were qualitatively similar to the set of averaged corrections  $\bar{R}(L)$ . With the exception of Station K, sensible heat flux, it was noted that the  $1/\xi_{ke}$  optimal corrections for the heat fluxes were similar to the corresponding  $1/\xi_{ke}$  corrections found in the stress.  $R_j(L)$  of Equation 3.14 can be rewritten as:

$$\frac{1}{R_j(L)} \leq 1 + \frac{\sigma_{xj}^2 + \sigma_{yj}^2}{u_j^2 + v_j^2} \quad 5.1$$

using notation previously defined. As stated previously the variance information is lost to the averaging process, however, the VA wind speeds,  $(u_j^2 + v_j^2)^{1/2}$ , are required for the estimates of all the VA fluxes. Given these arguments, an expected wind speed dependence of  $\xi_{ke}$  for all fluxes is:

$$\xi_{ke} = 1 + \alpha(u_j^2 + v_j^2)^{\beta/2} \quad 5.2$$

where  $\alpha$  and  $\beta$  are constants to be determined.

The temporal aspects of the reductions have also not been investigated. These may manifest themselves in two ways. First, there may be consistent variations between averaging periods which will be called functional temporal variations.

Establishing consistencies in these variations would aid greatly in interpolating the reductions to averaging periods not specifically investigated. Second, the  $\xi_{ke}$  transformations may be influenced by time scales greater than the averaging period. For example, the corrections required in December may be markedly different from those required in July. These will be called intrinsic temporal variations.

Finally, it was shown in Chapters III and IV that the optimal corrections  $\xi_{ke}$  (with the exception of Station N for all fluxes, and Station K for the sensible heat flux) do not differ markedly from one ship location to the next. If a formula which is applicable at most ship locations can be found, then the ease of applying the tranfcrmations would be greatly enhanced.

## 5.2 Empirical Formula

To verify the arguments of the previous section, the  $\xi_{ke}$  values of Appendix C for the stresses and of Appendix F for the heat fluxes for each ship were weighted and averaged (excluding Station N) according to the method outlined in Section 3.3 to arrive at a geographically averaged estimate  $\overline{\xi_{ke}}$  of the corrections. The results appear at the ends of Appendices C and F - Parts I.

$(\overline{\xi_{ke}} - 1)$  was initially plotted versus  $(u_j^2 + v_j^2)^{1/2}$  on a log scale and the results for all fluxes appear in Figure 26. The horizontal line indicates where a correction of 10% or greater is required. In all cases the curves are quite linear in the range 0.5 to 20 m/sec except in the linear drag coefficient case where a discontinuity in the slope occurs at 10 m/sec. This is

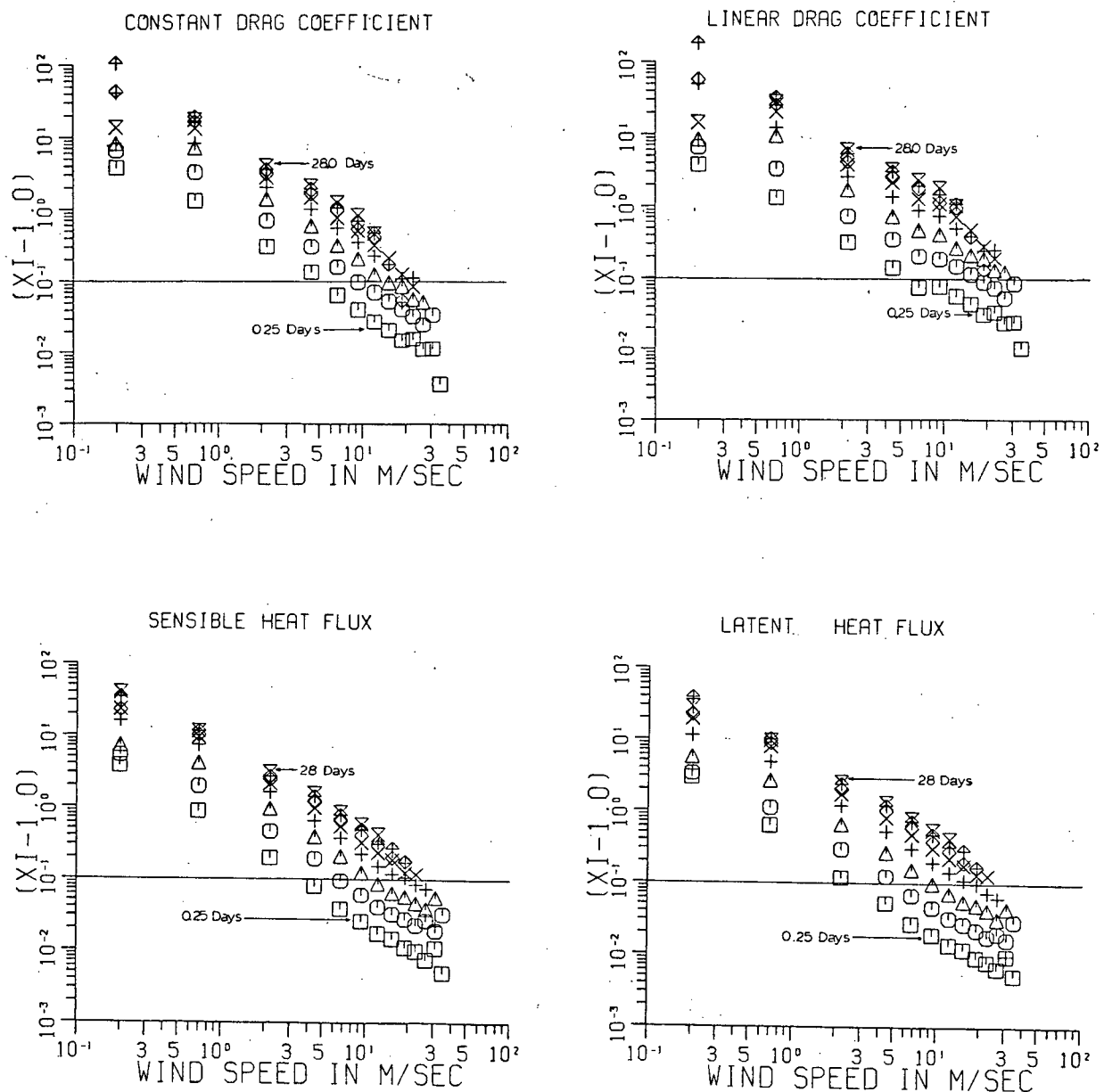


Figure 26. The  $\xi_{re} - 1$  values as a function of wind speed. All points above the horizontal line require greater than 10% correction. The inset numbers indicate averaging period in days.

the wind speed at which the drag coefficient changes form (see Equation 2.5). For wind speeds greater than 20 m/sec, the points become scattered. This may be due to there being

substantially fewer averagings in this regime. The slopes for all curves appear to be similar for all averaging periods. Note that typical wind speeds of 1-10 m/sec at L=28.0 days yield corrections of about 1 to 8 which are of the correct order to improve the transport calculations by Aagaard shown in Figure 1(b). The individual ships' plots of  $(\bar{\xi}_{ne}-1)$  versus  $(u_j^2+v_j^2)^{1/2}$  were examined and were all qualitatively similar to the geographically averaged case.

Next,  $(\bar{\xi}_{ne}-1)$  was plotted versus averaging period (L) on a log scale to determine any functional temporal variations which appear in Figure 27. Again all fluxes show similar patterns. All points above the horizontal line require at least 10% correction. Beaufort interval 1 (0.2 m/sec) is more scattered than the others. This extends to Beaufort interval 2 (1.0 m/sec) on the individual ships  $(\bar{\xi}_{ne}-1)$  versus L plots. This is not surprising since the extremities in wind speed contain the fewest number of points and the lowest wind speeds have the largest inherent errors of Appendices C and F - Parts II. At L=2.0 days, the \* represents Beaufort category 12 (26.0 m/sec) and appears distinct from the pattern of the rest of the points. This point was determined from only four out of approximately one million total possible averagings and cannot be considered statistically valid.

All other curves appear to increase systematically. From L=0.25 to L=2.0 days (which I call Region I) the slopes are steeper than from L=4.0 to L=28.0 days (which I call Region II). The vertical line at L=3.0 days demarcates the two regions. Within each region the slopes do not appear to change

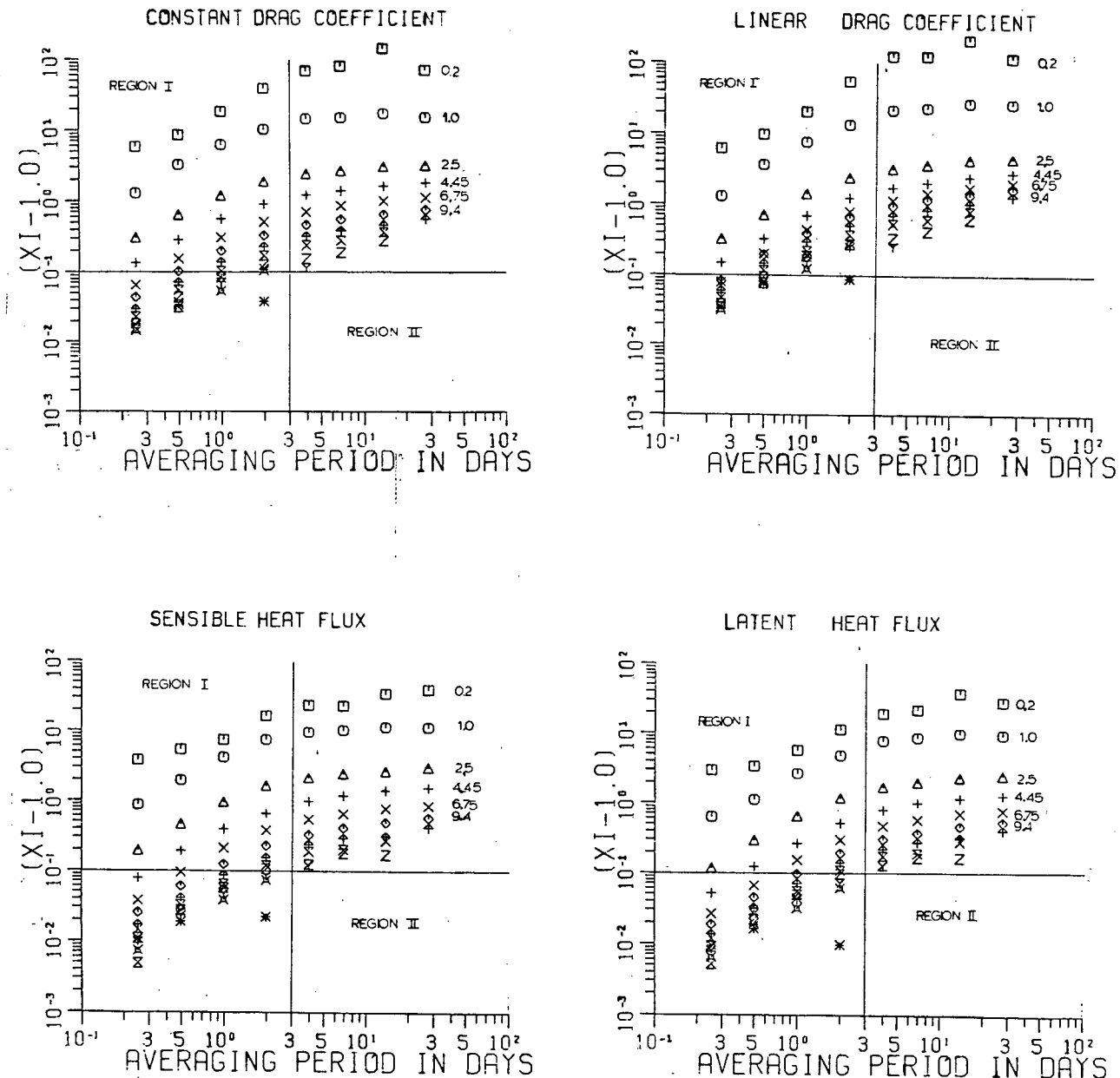


Figure 27. The  $\xi_{ke} - 1$  values as a function of averaging period. The vertical line demarcates the division between Regions I and II and all points above the horizontal line require greater than 10% correction. The inset numbers indicate wind speed in m/sec.

dramatically from one Beaufort category to the next.

Figure 26 indicates a power law behaviour of  $(\xi_{ke} - 1)$  with wind speed which appears to be independent of averaging period

and Figure 27 indicates a power law behaviour of  $(\bar{E}_{\text{ke}} - 1)$  with averaging period which appears to be independent of wind speed. It is assumed a priori that the correction  $\eta$  is of the form:

$$\eta = 1 + \alpha (u_j^2 + v_j^2)^{\beta/2} L^\gamma \quad 5.3$$

where  $(u_j^2 + v_j^2)^{1/2}$  is the vector averaged wind speed and  $L$  is the averaging period in days.

The assumed form of the  $X(3H)$  variate and  $X'(VA)$  residual is :

$$\bar{\sigma}_x^2 \delta_x^2 = \overline{(X - \eta X')^2} \quad 5.4$$

where the overbar indicates averaging over all Beaufort categories and averaging periods which can be rewritten as:

$$\bar{\sigma}_x^2 \delta_x^2 = \overline{[(X - X') - (\eta - 1) X']^2}$$

which immediately leads to :

$$\bar{\sigma}_x^2 \delta_x^2 = \overline{[(X - X') - \alpha (u_j^2 + v_j^2)^{\beta/2} L^\gamma X']^2} \quad 5.5$$

Note that we now regress the assumed form directly to the data. This is a non-linear regression of the form:

$$\bar{\sigma}_x^2 \delta_x^2 = \overline{(Y - f(\lambda_i; (u_j^2 + v_j^2)^{1/2}, L) X')^2} \quad 5.6$$

where  $Y = X - X'$ ,  $\lambda_i = \alpha, \beta, \gamma$  for  $i=1, 2, 3$  and

$f(\lambda_i; (u_j^2 + v_j^2)^{1/2}, L) = \alpha(u_j^2 + v_j^2)^{\beta/2} L^\gamma$ . If we have an initial guess  $f(\lambda_{i_0})$ , Equation 5.6 can be expanded in a Taylor series to first order as follows:

$$\nabla_x^2 \delta_x^2 = \overline{\left[ Y - \left( f(\lambda_{i_0}) + \sum_{i=1}^3 \frac{\partial f}{\partial \lambda_i} \Big|_{\lambda_{i_0}} \cdot \Delta \lambda_i \right) x' \right]^2} \quad 5.7$$

The quantity  $\Delta \lambda_j$  can then be minimized giving:

$$0 = \overline{\left[ x x' - x'^2 - f(\lambda_0) x'^2 \right] \frac{\partial f}{\partial \lambda_j} \Big|_{\lambda_{j_0}}} - \overline{\sum_{i=1}^3 \frac{\partial f}{\partial \lambda_i} \Big|_{\lambda_{i_0}} \Delta \lambda_i \frac{\partial f}{\partial \lambda_j} \Big|_{\lambda_{j_0}} x'^2} \quad 5.8$$

this is a matrix equation of the form:

$$\bar{F} = \underline{A} \bar{x} \quad 5.9$$

where:

$$F_j = \overline{\left[ x x' - x'^2 - f(\lambda_{j_0}) x' \right] \frac{\partial f}{\partial \lambda_j} \Big|_{\lambda_{j_0}}}$$

$$A_{ij} = \overline{\frac{\partial f}{\partial \lambda_i} \Big|_{\lambda_{i_0}} \frac{\partial f}{\partial \lambda_j} \Big|_{\lambda_{j_0}} x'^2}$$

$$x_i = \Delta \lambda_i$$

By evaluating explicitly the derivatives in Equation 5.8, the  $\Delta\lambda_i$  can then be iterated until  $\Delta\lambda_i$  is small compared to  $\lambda_{i0}$ . Iteration was halted when  $|\Delta\lambda_i/\lambda_{i0}| < 0.001$ . Note that  $XX'$  and  $X'X$  are the cross products and squares of the individual variates and not the squares of the average within each Beaufort category. Furthermore, the difference means have been removed from the regression residuals. It will be demonstrated that this has little influence on the final result.

Since Figure 27 indicated a definite break in the slope at  $L=3$  days, the regression was performed piecewise with a separate set of constants for the two regions. A regression of this type greatly reduces the required number of constants to be stored; consequently a separate regression was performed on the x and y stress components. Thus the number of parameters were reduced from 104 per ship to 12 for the stresses and 6 for each of the heat fluxes.

To be rigorous, the regression should be performed directly against the VA and 3H estimates from each individual averaging. This would entail calculations involving as many as 50,000 points per ship and flux repeated over several iterations. The computer costs would be excessive in storage and processing time. The Beaufort-averaging period groupings of the sums, sums of squares and sums of cross products of the 3H and VA variates were stored during the  $\lambda$  calculations. By appropriately weighting these stored statistics, an approximation for the  $\alpha$ ,  $\beta$  and  $\gamma$  could be achieved requiring effectively only  $13 \times 8 = 104$  points per ship and flux.

A weighting matrix was created in order not to bias the

parameter estimates. First, each Beaufort category contained unequal numbers of points. The first order weight then was directly proportional to the number of 3H/VA averagings within each Beaufort category. By the nature of the averaging of the 3H and VA variates, the longer averaging periods had fewer estimates of the reduction which would tend bias the temporal power ( $\gamma$ ) in favour of the shorter averaging periods. However, we wish an unbiased estimate over all averaging periods. Consequently, the number of estimates within each Beaufort category and averaging period was expanded to the total number of raw three-hourly samples that went into the calculations of the statistics of each category. Thus, if Beaufort interval 8 at  $L=1.0$  days contained 4 3H/VA estimates, since there were 8 readings per day, the 4 readings were expanded to 32.

This type of regression minimizes the total residuals within each region. That is, each averaging period is no longer considered as a single block of data but the total residuals from  $L=0.25$  to  $L=2.0$  days (Region I) and from  $L=4.0$  to  $L=28.0$  (Region II) are now minimized. It will be shown that the regression performed in this manner did not significantly increase the residuals when compared with a direct regression.

The first guess ( $\lambda_{10}$ ) was made by performing a linear regression in log space. At several locations, the iteration failed to converge with this value. Fortunately, it was established that most ships converged to values of  $\beta = -1.0$  and  $\gamma = 1.0$  in Region I and  $\gamma = 0.25$  in Region II. Consequently these values as well as an arbitrary  $\alpha = 2.0$  were used as

initial guesses. Not only did all ships converge, but in cases where the iteration had previously succeeded, the convergence went to the same values in fewer recursions. This indicates that a linear regression in log space may not produce suitable estimates of the coefficients.

### 5.3 Ship Parameter Estimates

In light of the dramatic improvements in test results achieved by the  $\Sigma_{ke}$  calculations, they provided an acceptable means of comparison to determine the effectiveness of the  $\eta$  technique. If the  $\eta$  results compare favourably with the  $\Sigma_{ke}$  results, then the empirical formula would be an effective replacement. In this section, the residual variances were calculated by applying the regression coefficients against the stored Beaufort number-averaging period statistics outlined above and the empirical formula was not allowed to interpolate wind speed.

Figure 28 shows the  $\eta$  RV estimate minus the  $\Sigma_{ke}$  RV estimate in percent. For the stresses, nearly all results are within 1.5% of the  $\Sigma_{ke}$  values for all averaging periods. The only exception is Station D, L=7.0 days, linear drag coefficient, x component where the difference was 2.3% (not shown). Station N was also within 1.5% of the  $\Sigma_{ke}$  residuals. Many stations showed an improvement (ie. negative residual variances in Figure 28) in the stresses. This occurred because here a separate regression was performed on the components.

The heat flux RVs (Figures 28(e) and (f)) were generally within 4.0% of the  $\Sigma_{ke}$  RVs for all averaging periods. The

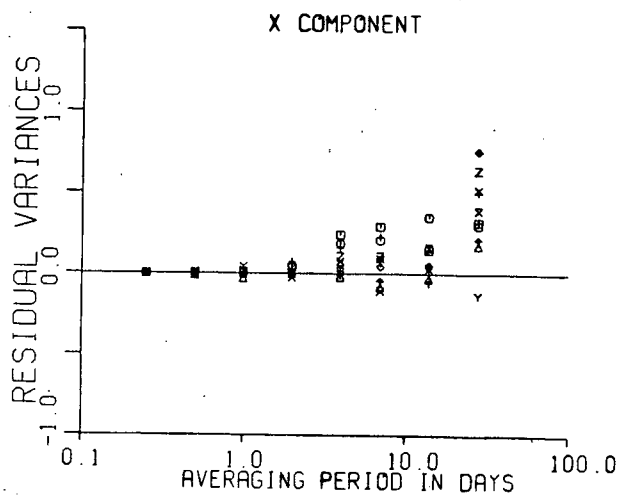


Figure 28 (a) Constant D.C.

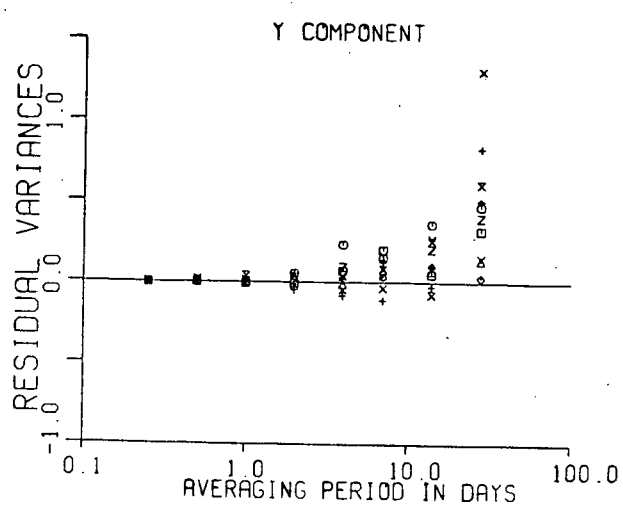


Figure 28 (b) Constant D.C.

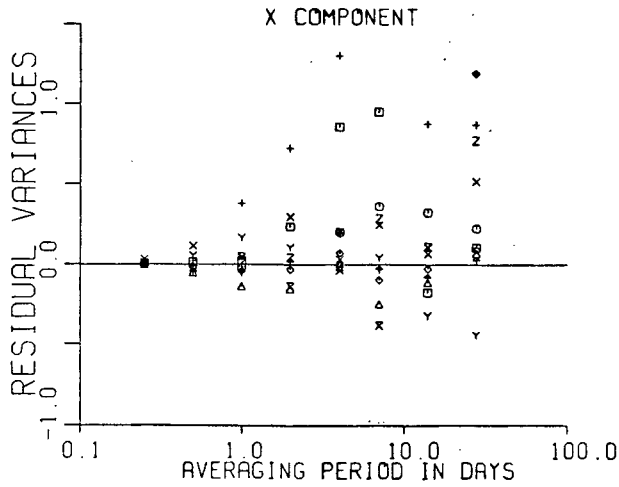


Figure 28 (c) Linear D.C.

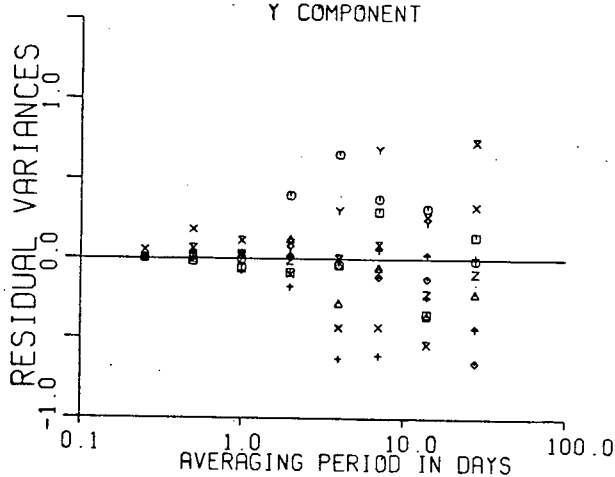


Figure 28 (d) Linear D.C.

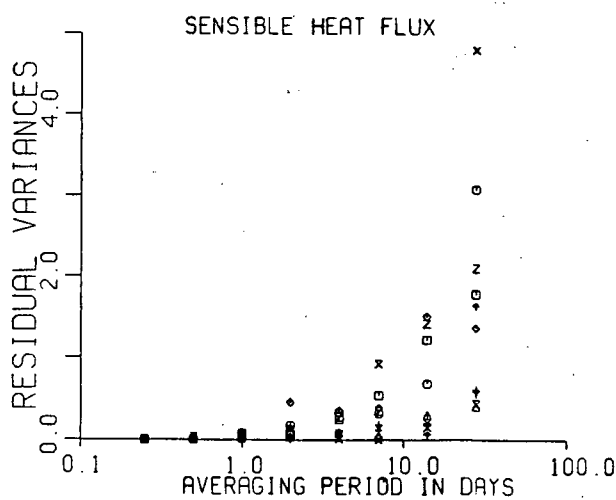


Figure 28 (e)

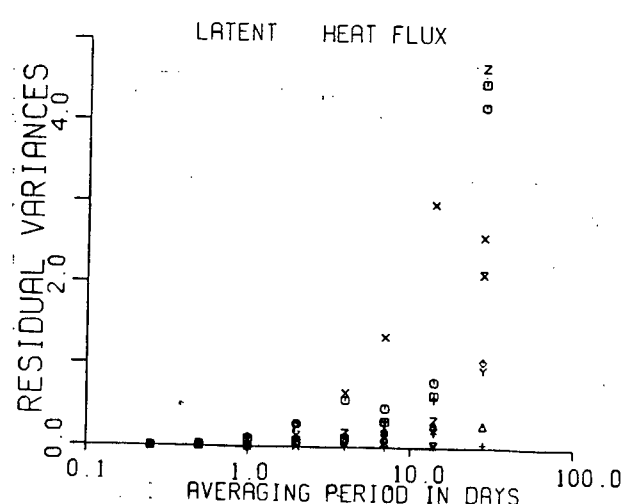


Figure 28 (f)

Figure 28. Differences between the  $\epsilon_{ke}$  and  $\epsilon_k$  residual variances with no correction applied for the DV bias. The values are in percent. D.C. denotes drag coefficient.

exceptions were Station N (not shown) where the results in Region II were generally poor and Station J,  $L=28.0$  days, latent heat flux where the regression induced a further error of about 10.0% (also not shown). Note, however, up to  $L=14.0$  days the differences were all within 1.5% of the  $\bar{X}_{ke}$  values.

As a further indication of the accuracy of the technique, all fluxes (momentum and heat) showed a positive bias in the difference variances (not shown). Although they were not identical to the residual variances, they were close enough to indicate that a DV/RV statistical biasing was occurring. Consequently, cf Equation 5.3 was adjusted by a multiplicative factor  $\mu_e$  to reduce the difference variances. Again considering the 3H variate to be  $X$  and the VA variate to be  $X'$ , the condition for 0 difference variance for each averaging period is :

$$\begin{aligned} (\sigma_x^2 \Delta \sigma_x^2)_e &= \sum_{k=1}^{13} \frac{x_{ke}^2}{N} - \sum_{k=1}^{13} \left[ \frac{(1+\mu_e f) X'_{ke}}{N} \right]^2 \\ &\quad \left[ \sum_{k=1}^{13} \frac{x_{ke}}{N} \right]^2 + \left[ \sum_{k=1}^{13} \frac{(1+\mu_e f) X'_{ke}}{N} \right]^2 = 0 \quad 5.10 \end{aligned}$$

where the summation is over 13 Beaufort intervals,  $f$  is the minimum approximation outlined in Equation 5.6,  $\mu_e$  is a multiplicative correction factor forcing the difference variance to 0 for each averaging period, and  $X'_{ke} = \sum_{j=1}^{J_h} X'_{kej}$ . This gives:

$$\begin{aligned} \mu_e^2 \left[ \sum_{k=1}^{13} \left( \frac{f X'_{ke}}{N} \right)^2 - \left( \frac{\sum f X'_{ke}}{N} \right)^2 \right] + \\ 2\mu_e \left[ \frac{\sum f X'^2}{N} \cdot \left( \frac{\sum f X'_{ke}}{N} \right) \left( \frac{\sum X'_{ke}}{N} \right) \right] - (\sigma_x^2 - \sigma_{x'}^2) = 0 \quad 5.11 \end{aligned}$$

where  $\sigma_{x_e}^2$ ,  $\sigma_{x'e}^2$  are the raw 3H and VA variances with no correction applied. This is then a quadratic in  $\mu_e$ . The correct root was chosen by comparison with the uncorrected difference mean value. The corrections for each averaging period within each region were then averaged to determine a mean regional correction.

After this correction was applied, the constants  $\alpha$ ,  $\beta$ , and  $\gamma$  of Equation 5.3 were calculated and the results appear in Appendix H. The  $\beta$  term for the linear drag coefficient ( $\approx -0.9$ ), constant drag coefficient ( $\approx -1.3$ ), and heat fluxes (-1.2 to -1.4) tend to decrease in this order, for most ships. The temporal power ( $\gamma$  coefficient) is regular for all ships excluding Station N. In Region I, it varies from a low of 0.860 to a high of 1.04 indicating that the corrections required in this region vary approximately linearly with averaging period. In Region II the  $\gamma$  coefficients vary from 0.166 to 0.359 with most lying between 0.20 and 0.30. Furthermore the temporal power is independent of type of flux. Thus the discontinuity in the time dependence is quite distinct between two and four days which appears to correspond to a discontinuity observed in the slope of the stress components spectra noted by Willebrand (1978).

The four test functions were then calculated. Calculation of the  $\zeta_{he}$  values required storing the sums, sums of squares, and sums of the cross products of the 3H and VA variates within each Beaufort category. These stored values served as the raw statistics from which the four test functions were calculated. The empirical formula allowed interpolation of the VA wind speed

correction within each Beaufort category. When the empirical formula was applied to each VA estimate individually, certain ships showed a dramatic decrease in residual variance. For example, Station N latent heat flux, had a  $\bar{Z}_{\text{re}}$  RV of 82.0% for L=28 days. When the empirical formula interpolated the velocities, the RV was only 58.9%. In the sensible heat flux, the change was from 23.3% to 12.6%. At L=28.0 days, 78% of the data is grouped in Beaufort categories 3 and 4. Consequently the interpolation of the correction within the two groups was important. At locations where the data were more evenly distributed among Beaufort categories (eg. Station C), the improvement by direct application of  $\gamma$  was less than 1.0%.

This immediately suggests that the empirical formula regression coefficients should also be calculated directly against the data rather than against the Beaufort grouped statistics. Since the regression involved several iterations of large amounts of data the only feasible method was to regress the data in Region II only. This was done for several ships including Station N, latent heat flux and in no case were the residuals improved more than 1.0%. In some cases the difference variances increased to values of about 30.0%. Since the regression against the data required several iterations over large amounts of information proving extremely costly in computer time and was of dubious value , this avenue was not pursued.

The four test functions were then calculated by applying  $\gamma$  to each VA flux and stress estimate. The complete results appear in Appendix I while the x component linear drag

coefficient and the heat fluxes appear in Figures 29 to 32.

The difference means appear in Figure 29. Except for Station A, all DMs are below 0.08 dPa for the linear drag coefficient. A comparison of Appendix I with Appendix D ( $\bar{E}_{ke}$  results) indicates that the values found by the empirical formula, although not identical to the  $\bar{E}_{ke}$  DMs, both show similar ranges of values. The heat flux DMs are generally 1.0-2.0 Watts/m<sup>2</sup> larger with the empirical formula than with the directly applied  $\bar{E}_{ke}$  technique. The sensible heat flux DMs, with the exception of Station I, L=28.0 days, are all less than 2.5 Watts/m<sup>2</sup> while the latent heat fluxes are mostly below 10 Watts/m<sup>2</sup>. Station E in Region II is a notable exception where the DMs are as large as 20 Watts/m<sup>2</sup>. According to Table X, Station E also has the second largest mean latent 3H heat flux at 124.7 Watts/m<sup>2</sup>.

The difference variances appear in Figure 30. Since the DVs at all averaging periods could not be set simultaneously to 0, they are all larger than those that appear in Appendix D for the stresses (the heat flux DVs are identically 0). Up to L=2.0 days the DV stress error for all components is bounded by  $\pm 5.0\%$ . This increases to  $\pm 10.0\%$  for the majority of ships by L=28.0 days. An exception is Station D L=28.0 days which will be investigated later. Up to L=7.0 days (with the exception of Station N), the DV heat flux errors are all bounded between  $\pm 10.0\%$ . From L=14.0 to L=28.0 days, particularly in the latent heat flux, the DV errors become quite large -- up to 30.7% at Station M. These are, however, all substantially lower than the 60-80% error in the uncorrected tests outlined in Figures 7 and

SENSIBLE HEAT FLUX

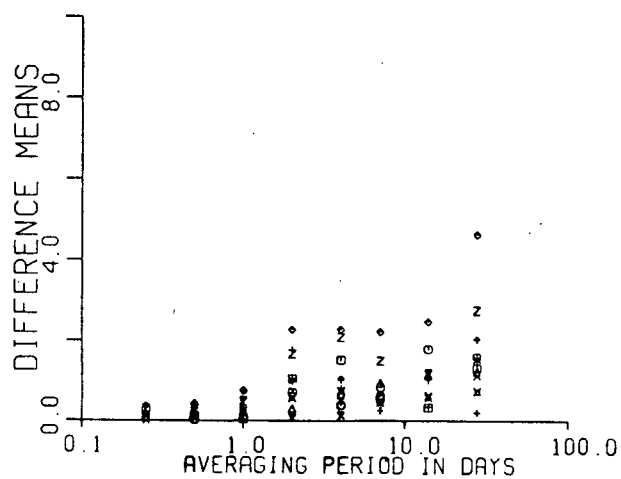


Figure 29 (a)

LATENT HEAT FLUX

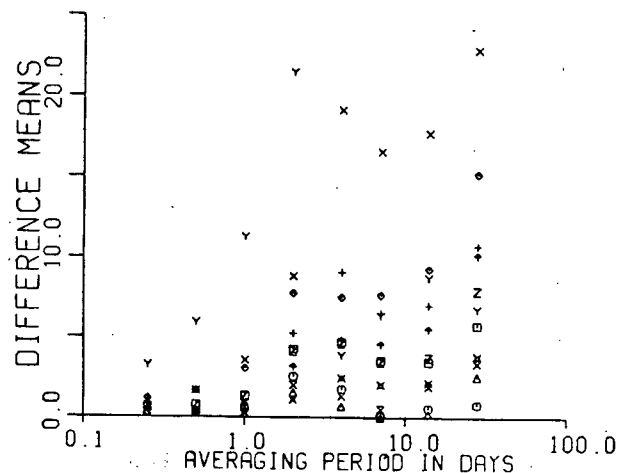


Figure 29 (b)

X COMPONENT

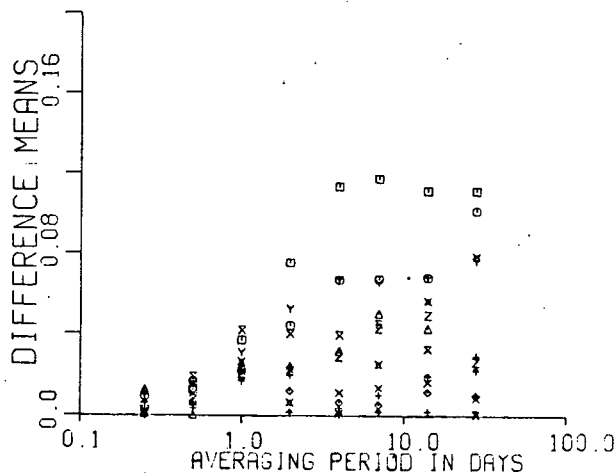


Figure 29 (c) Linear D.C.

Figure 29. The difference means using the empirical formula. The heat flux DMs are in Watts/m<sup>2</sup> while the stress DMs are in dPa. D.C. denotes drag coefficient.

21. The DV error in the stresses and sensible heat fluxes appears to oscillate. Generally the first and last points in each region (ie. L=.25, 2.0, 4.0, and 28.0 days) are biased lower than the middle points. This indicates that the adjustment to the constant ( $\propto$ ) term alone of Equation 5.12 may

SENSIBLE HEAT FLUX

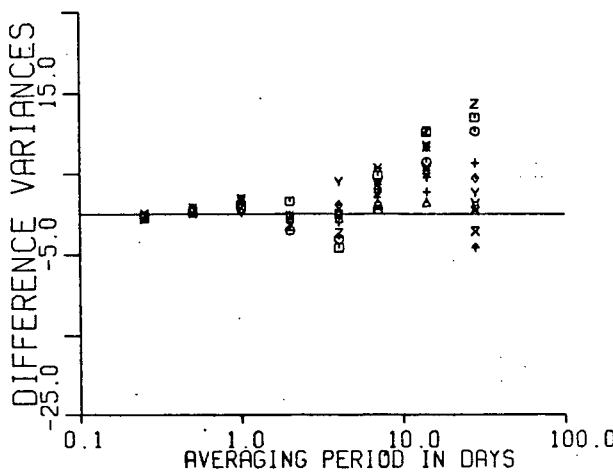


Figure 30 (a)

LATENT HEAT FLUX

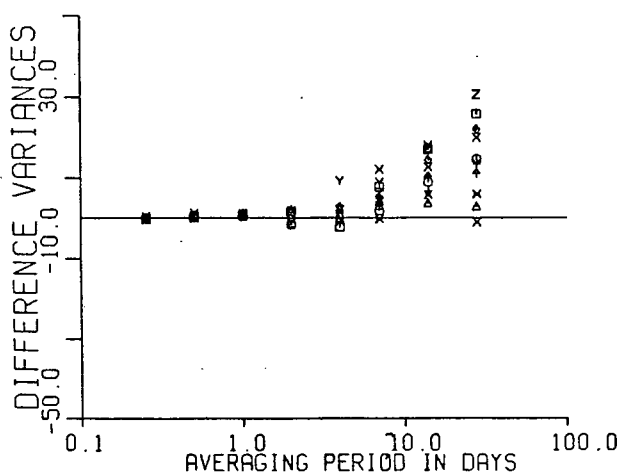


Figure 30 (b)

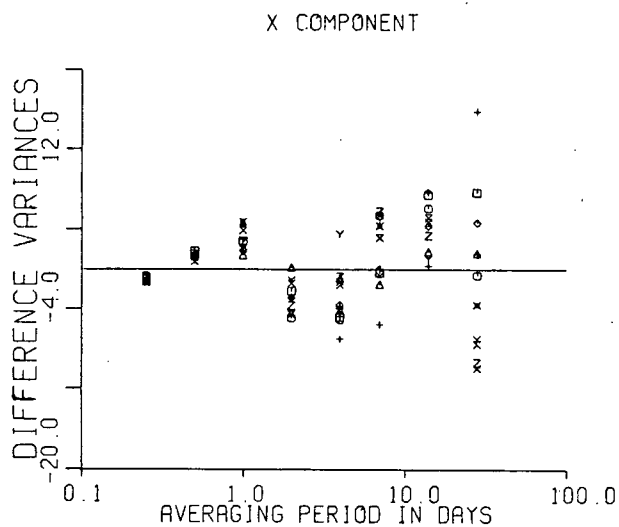


Figure 30 (c) Linear D.C.

Figure 30. The difference variances using the empirical formula. All values are in percent. D.C. denotes drag coefficient.

not be appropriate and that an adjustment of all three coefficients may be necessary to force all the DVs to zero. This was not attempted in light of their reductions over the uncorrected DVs.

The residual variances appear in Figure 31. For nearly

every ship, averaging period, and flux, the directly applied empirical formula registers an improvement over the  $\xi_{ke}$  RVs. In the stress case, the improvements are marginal -- being limited to about 1.0%. Both of the heat fluxes, however, show marked improvements. At  $L=28.0$  days, there are many instances where the empirical formula residuals are about one-half of the  $\xi_{ke}$  values. This is quite remarkable when one considers that the formula predicts both the temporal and velocity dependent corrections.

Generally, the linear drag coefficients RVs increase with averaging period in Region I while the scatter of values is a fairly constant in Region II. The x component RVs are between 6.0 - 12.0% in Region II while the y component values lie between 8.0 - 17.0%. The corresponding constant drag coefficient values are about one-half of the linear drag coefficient values. The sensible heat fluxes generally follow the pattern of the stress and, with the exception of Station N are less than 8.0%. The latent heat fluxes are somewhat less accurate with all stations except N, E, and M being less than 18.0%. Again a marked reduction from the uncorrected values has occurred.

The correlation coefficients appear in Figure 32. Those points having low RVs have high correlation coefficients and vice-versa. For the stresses the  $\eta$  correlations are marginally larger (ie. better) than the  $\xi_{ke}$  correlations, having improvements of several parts per thousand. More substantial improvements are shown in the heat fluxes where improvements of 0.05 to 0.1 are common.

SENSIBLE HEAT FLUX

LATENT HEAT FLUX

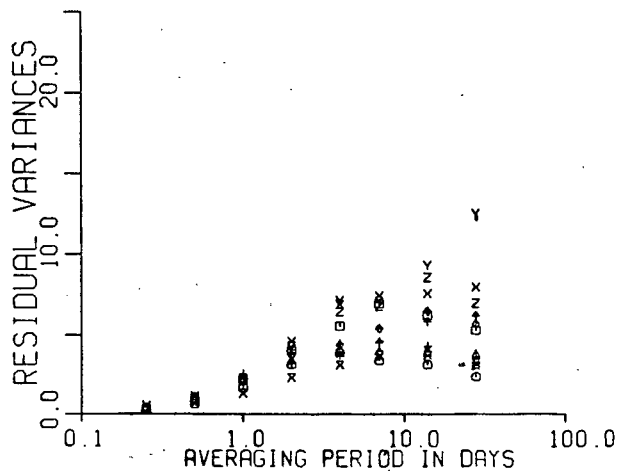


Figure 31(a)

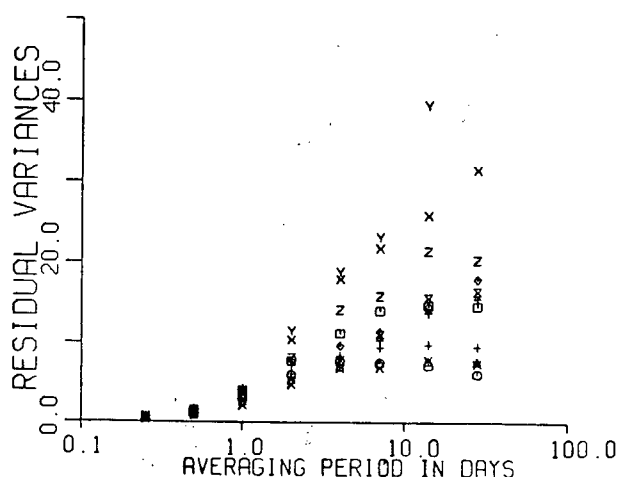


Figure 31(b)

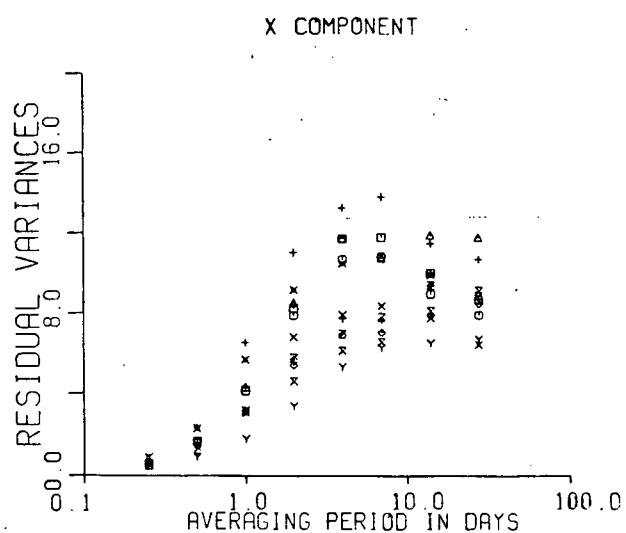


Figure 31(c) Linear D.C.

Figure 31. The residual variances with the empirical formula applied. All values are in percent. D.C. denotes drag coefficient.

Even though the mean was not included in the non-linear regression, all four test functions closely approximate the  $E_{ke}$  test results for the heat fluxes where the mean was included. The  $\mathcal{N}$  empirical formula offers substantial improvement over the uncorrected test results.

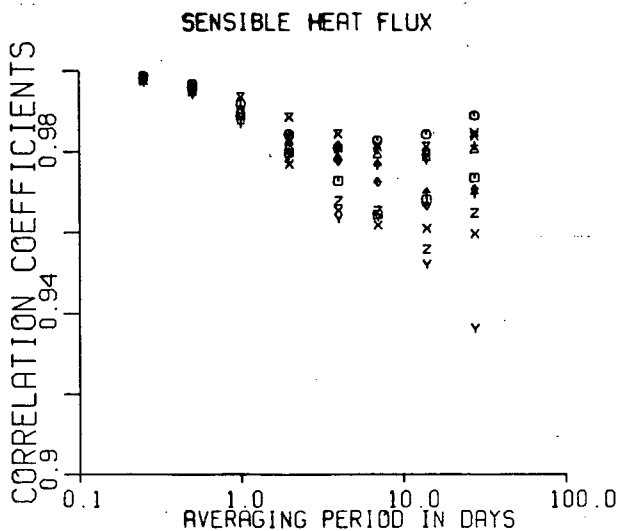


Figure 32(a)

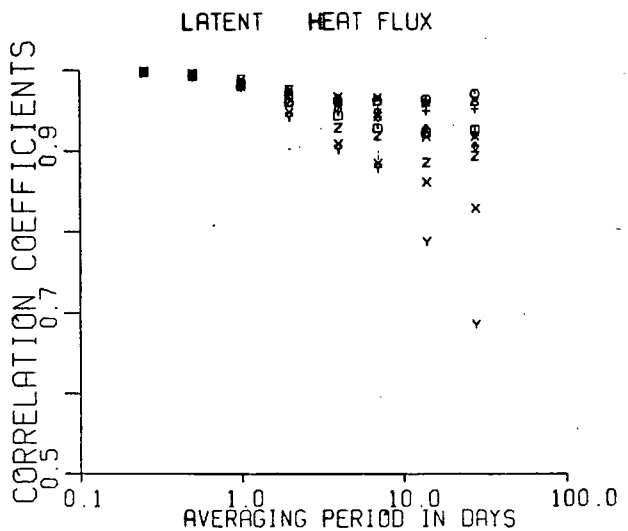


Figure 32(b)

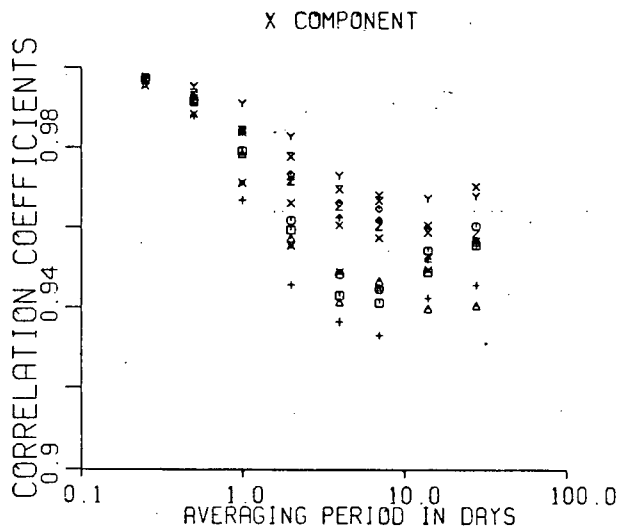


Figure 32(c) Linear D.C.

Figure 32. The correlation coefficients with the ships' empirical formula applied. D.C. denotes drag coefficient.

#### 5.4 Geographical Averaged Results

The sums, sums of squares, and the sums of the cross products of the VA and 3H variates were saved from the initial calculations and were then added (excluding Station N) to create a set of total statistics for all the ships. The non-linear regression (Equation 5.9) was then applied to achieve an

estimate of geographically averaged regression coefficients ( $\bar{\eta}$ ) and hence a single set of formulae applicable to most ship locations. The results appear on the AVG row of Appendix H and in Table XII.

The geographically averaged empirical formula ( $\bar{\eta}$ ) was then used to determine the four test functions at each location. The complete results for all ships including Station N and K, appear in Appendix J. Again only the x component linear drag coefficient and the heat fluxes will be presented.

The difference means are shown in Figure 33. In general the range of values is similar to those of the  $\eta$  results with most values being less than 0.1 dPa for the stress, and 5.0 and 12.0 Watts/m<sup>2</sup> for the sensible and latent heat fluxes. The inapplicability of  $\bar{\eta}$  at Station N is readily evident in the abnormally large DM values for all three fluxes (see Appendix J).

The difference variances appear in Figure 34 excluding Station N for all fluxes and Station K for the sensible heat flux. For all fluxes, the DV values have a range approximately twice that of the  $\Sigma_{\text{ge}}$  DVs. The oscillating behaviour is no longer evident. In the stress case, the DVs are dispersed fairly regularly around 0.0%. The heat fluxes, however, have a positive bias. Station K was not removed from averaging in the sensible heat fluxes. The effect of the geographical formula on Station K is reflected in its abnormally low DV values in the sensible heat flux (see Appendix J) -- indicating that the geographical averaged formula overestimated the 3H flux. There are two possible causes for the positive DV bias. The

TABLE XII

The geographically averaged ships' regression coefficients for the form  $\bar{\eta} = 1 + \alpha(u^2+v^2)^{\beta/2} L^Y$ . The C denotes the constant drag coefficient, the L denotes the linear drag coefficient, the X denotes the x component, the Y denotes the y component, the H denotes the heat fluxes, the S denotes the sensible heat flux and the L denotes the latent heat flux.

SHIP	TYPE	REGION I .25 - 2.0 DAYS			REGION II 4.0 - 28.0 DAYS		
		$\alpha$	$\beta$	$\gamma$	$\alpha$	$\beta$	$\gamma$
AVG	C X	3.337	-1.322	0.920	4.237	-1.150	0.261
	C Y	3.437	-1.336	0.901	4.639	-1.183	0.231
	L X	2.325	-0.910	0.967	3.276	-0.795	0.310
	L Y	2.322	-0.910	0.940	3.754	-0.853	0.275
	H S	2.874	-1.469	0.984	3.946	-1.244	0.244
	H L	1.365	-1.251	1.021	2.335	-1.108	0.263

geographical average,  $\bar{\eta}$ , may generally reduce the residuals sufficiently so the DV values begin to approach the RV values; or the effect of including Station K is to weight the statistics so the calculated regression coefficients slightly underestimate the required corrections. Since the positive bias is also felt in the latent heat flux where Station K did not differ radically from the other locations, the former is the probable cause of the bias.

The residual variances appear in Figure 35. The geographically averaged values are, with the exception of Station N, remarkably similar to the individual ship empirical formula  $\eta$  RV values. For the stresses and the sensible heat fluxes, the RVs at all averaging periods are within 1.0% of those listed in Appendices D and G. Station K sensible heat flux values show a 5.0% increase in the residuals at L=28 days over the individually calculated values. As noted in Chapter IV

## SENSIBLE HEAT FLUX

## LATENT HEAT FLUX

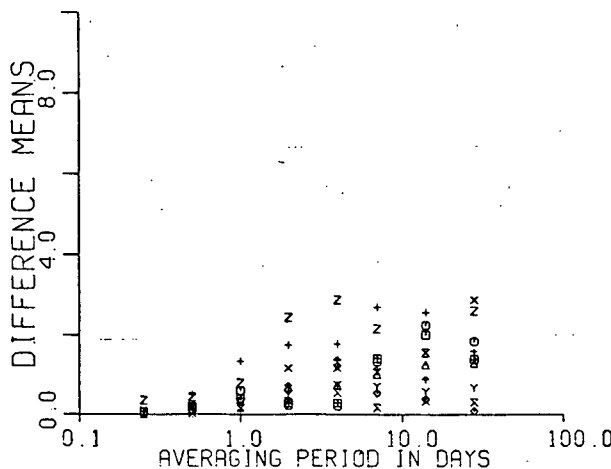


Figure 33 (a)

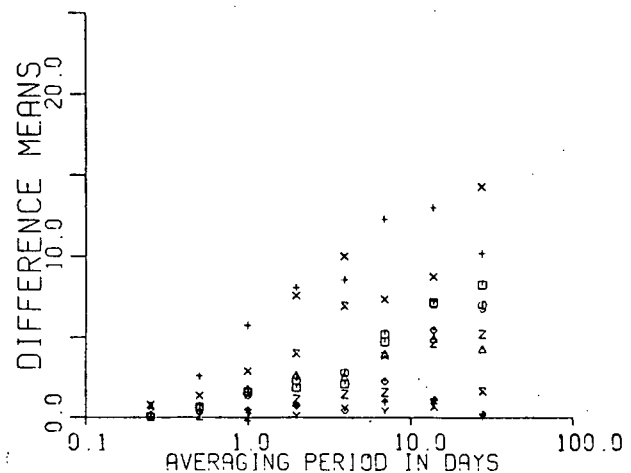


Figure 33 (b)

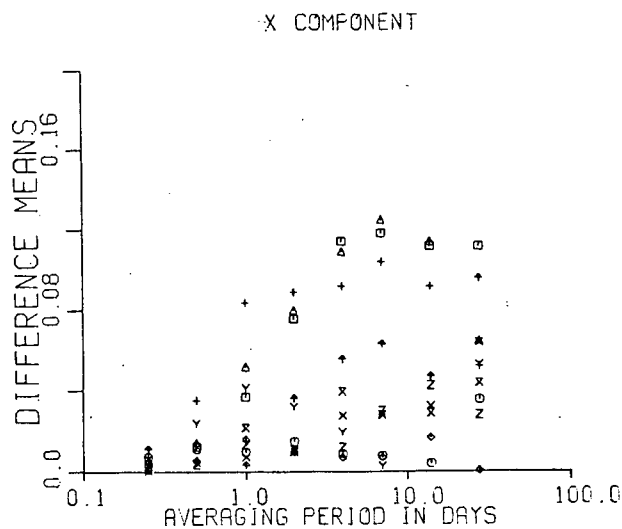


Figure 33(c) Linear DC

Figure 33. The difference means using the geographically averaged empirical formula. The heat flux DMs are in Watts/m<sup>2</sup> while the stress DMs are in dPa. DC denotes drag coefficient. The Station N values are omitted.

, the Station K  $\Sigma_{\text{he}}$  values differ quite markedly from the other ships' values. The 8.0% residual listed in Appendix J is not, however, markedly larger than those calculated for the other ships.

In several instances, the geographically averaged RVs show

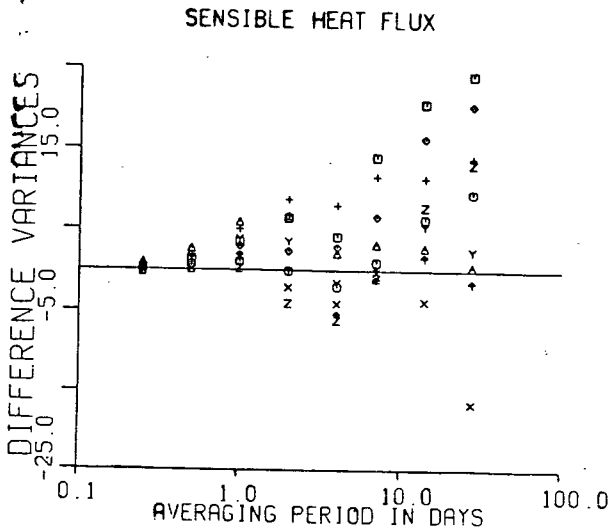


Figure 34 (a)

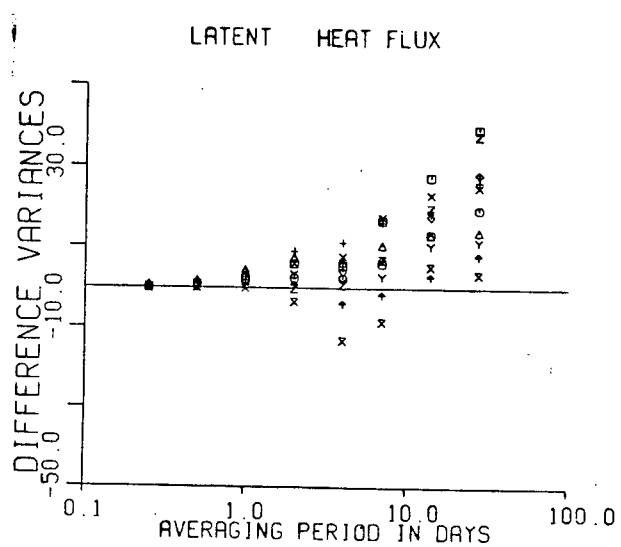


Figure 34 (b)

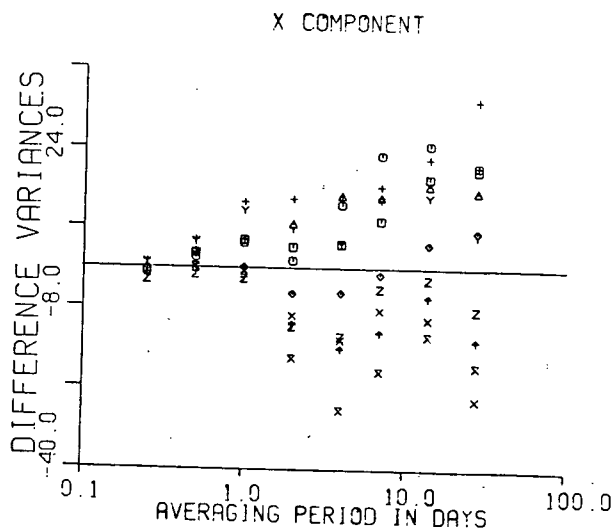


Figure 34(c) Linear DC

Figure 34. The difference variances using the geographically averaged empirical formula. All values are in percent. DC denotes drag coefficient. Station N is excluded in all fluxes and Station K is excluded from the sensible heat flux.

an improvement over the individual ship RVs. For example, at Station D  $L=4.0$  days, the geographically averaged latent heat flux RV is 12.2% while the individual RV is 13.3%. A comparison between the respective difference variances indicates a rise to 13.8% from -7.0%. Thus the geographic empirical formula has

SENSIBLE HEAT FLUX

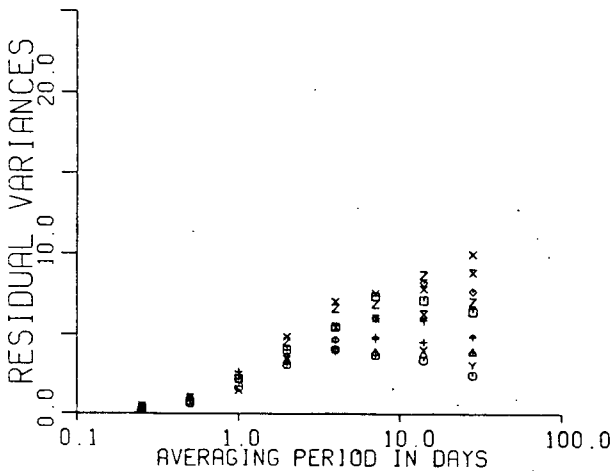


Figure 35(a)

LATENT HEAT FLUX

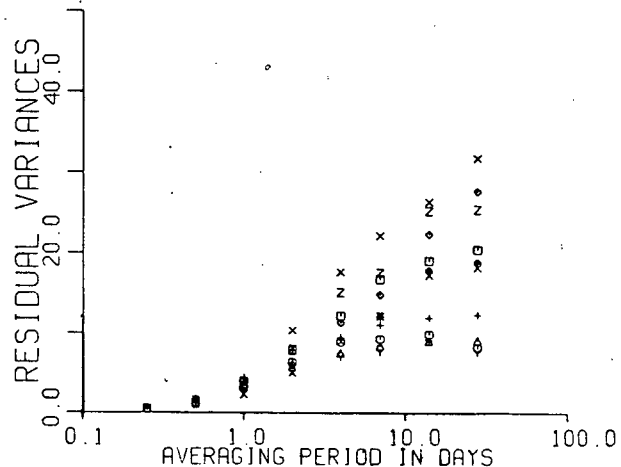


Figure 35(b)

X COMPONENT

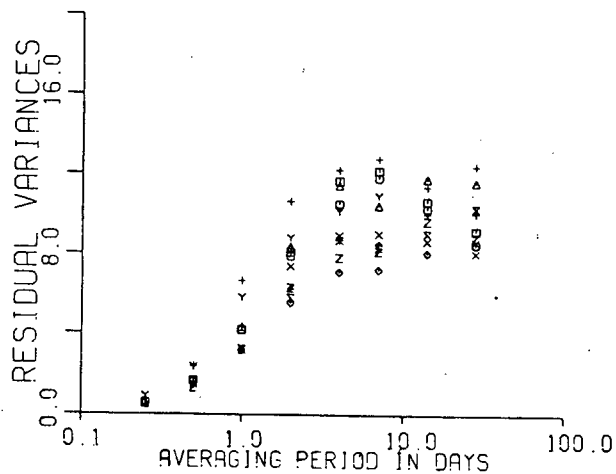


Figure 35(c) Linear DC

Figure 35. The residual variances using the geographically averaged empirical formula. All values are in percent. Station N is excluded. DC denotes drag coefficient.

more closely approached the least squares estimate of the Station D parameters and negated the DV bias correction.

The latent heat flux geographic  $\bar{\chi}$  residuals are substantially larger in several instances than the individually calculated values. For example, at Station I, the geographic

residuals at  $L=28.0$  days are 27.6% where the individual formula,  $\eta$ , gives 18.0%. In all other cases, the geographic residuals are within 5.0% of the individually calculated values.

The correlation coefficients appear in Figure 36. In all cases, the geographically averaged correlations are about 0.02 less than the  $\eta$  values.

The geographically averaged empirical formula approach, with two exceptions, appears to yield nearly identical results to the individual ships empirical formula. This approach is not viable for any of the fluxes at Station N and may not be the best estimate for the Station K sensible heat flux correction. For Station D, particularly at longer averaging periods, the geographical empirical formula shows RV improvement over the individual ships empirical formula because no attempt is made to remove the DV bias. This is also reflected in the general positive DV bias indicating that the geographical average may not predict the long-term 3H variance quite as accurately as the individual ships' empirical formula ( $\eta$ ).

### 5.5 Intrinsic Temporal Variations

The latent heat flux corrections at Station N are characterized by markedly larger residuals and lower correlation coefficients for averaging periods in Region II. When the empirical formula,  $\eta$ , is applied, at  $L=28.0$  days, the residuals are as high as 58.9% of the 3H variance. Although the sensible heat flux residuals are larger at Station N they are less pronounced than for the latent heat flux.

The required transformations may be inherently non-

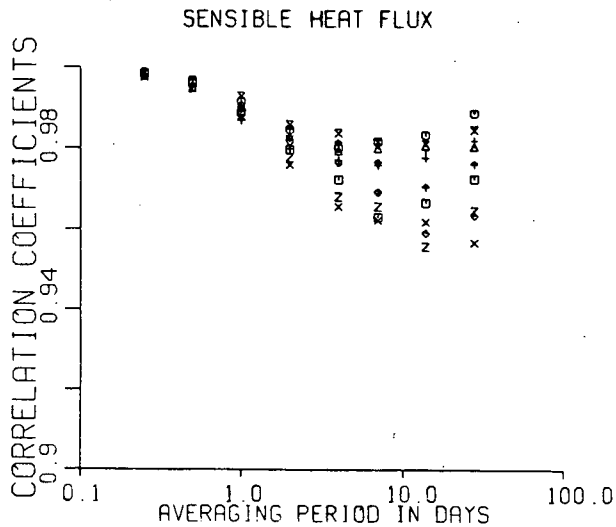


Figure 36 (a)

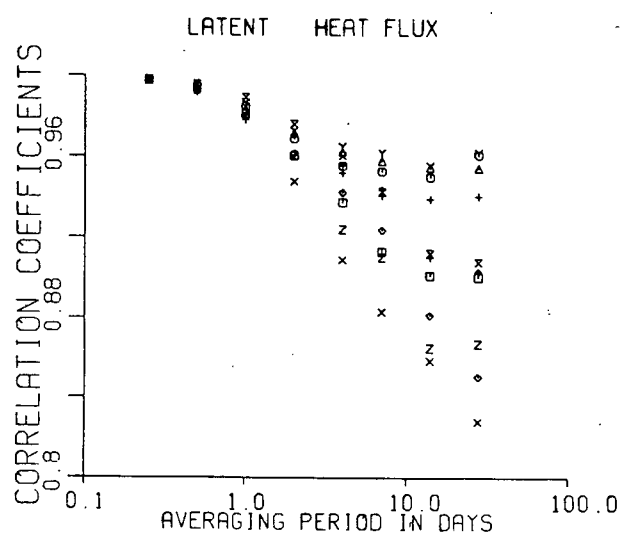


Figure 36 (b)

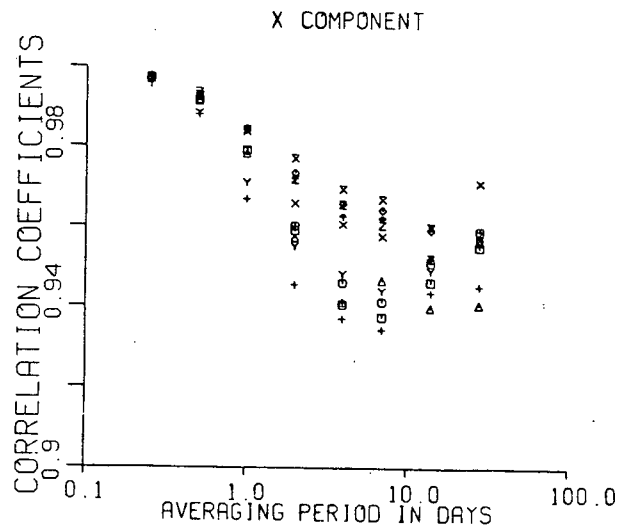


Figure 36 (c) Linear DC

Figure 36. The correlation coefficients using the geographically averaged empirical formula. DC denotes drag coefficient.

stationary. It has been assumed that the winter corrections, for example, are identical to the summer corrections. Dorman (1974) has demonstrated that at Station N there are large amounts of energy at the annual cycles for the winds, wind components, sea surface temperatures, air temperatures and dew

point temperatures. Except for sea surface temperatures, the character of all component variates changes markedly from winter to summer. Dorman also showed that the winter clockwise wind component power is more than four times that of the summer power. Some of the scatter that is evident between the 3H and VA variates may be due to seasonal changes in the required corrections.

One method to determine whether the annual cycle plays a dominant role in the required corrections is to examine the 3H and VA and residual (3H - VA) spectra. If a significant peak in the residual spectra occurs, then a seasonally dependent correction may be necessary. To this end Station C was selected as a control because it exhibits particularly stable heat flux residuals at  $L=28.0$  days -- 7.6% for the latent heat flux and 3.8% for the sensible heat flux as compared to 58.9% and 12.6% respectively at Station N after the ship's empirical formula,  $\eta$ , was applied. The data at both ships were averaged, and the lunar monthly 3H, VA and residual stresses were calculated. The three time series were then broken into 9 two-year blocks at Station C and 10 two-year blocks at Station N.

Each block of data was detrended and a cosine taper was applied (following Bendat and Piersol (1971)) to 10.0% of the data at each end of the blocks to reduce ringing from the convolution in frequency space of the box window inherent in the data. The spectral characteristics of the box window and the cosine taper can be seen in Bendat and Piersol (1971) pp. 324-325. The cosine taper also tends to reduce the power of the input signal. Consequently the variance was calculated before

and after the taper and all the output spectra multiplied by the appropriate correction at each frequency.

The twenty-six points within each block were then fast fourier transformed by the UBC FOURT programme and the square of the magnitude of each fourier sine/cosine pair was calculated. The spectral density estimates for all blocks were added and the mean power density estimate was found.

The error in the mean spectral density estimates follows a  $\chi^2$  distribution with  $2N$  degrees of freedom (Jenkins and Watts, 1972) where  $N$  is the number of blocks. The 95% confidence zone is determined from:

$$\frac{\nu s^2}{\chi^2_{\nu, 0.025}} \leq \sigma^2 \leq \frac{\nu s^2}{\chi^2_{\nu, 0.975}} \quad 5.12$$

where  $\nu$  is the number of degrees of freedom ( $2N$ ),  $\chi^2_{\nu, 0.025}$  and  $\chi^2_{\nu, 0.975}$  are the  $\chi^2$  statistics at 0.025 and 0.975 probabilities and  $\nu$  degrees of freedom,  $s^2$  is the spectral density estimate and  $\sigma^2$  is the actual unknown spectral density. Equation 5.12 is correct assuming that the input series is Gaussian and that the spectral estimates between blocks are independent. Deterministic signals, non-stationarity, and non-normality of the input series reduce the actual degrees of freedom causing an increase in the confidence zones. Sophisticated techniques have been developed to calculate the effective degrees of freedom. These will not be implemented because the aim is to determine only if outstanding peaks exist in the data. Consequently it will be assumed that  $2N$  is also the effective degrees of freedom and the factor  $(\frac{\nu}{\chi^2_{\nu, 0.025}}, \frac{\nu}{\chi^2_{\nu, 0.975}})$  will be quoted. For two degrees

of freedom (ie. one independent spectral estimate), this factor is approximately (.25, 4.0).

The spectra of the uncorrected latent and sensible heat fluxes at Stations C and N appear in Figure 37. In all cases, the annual cycle in the 3H flux is evident. At Station C, the VA power is always less than the 3H power and if one considers the 3H peaks to be a factor of 4.0 above the 3H noise level, they are significant to less than 2.0 degrees of freedom.

At Station N, however, the VA power densities often exceed the 3H values in the latent heat flux, consistent with the negative uncorrected DV values shown in Figure 21. In the sensible heat flux, the VA annual cycle is well within the VA noise level while the 3H annual cycle is well above the 3H noise level. Furthermore, the residual series power density for both fluxes at the annual cycle is much greater than the residual noise level. In fact, the annual cycle frequency band for the latent heat flux accounts for 42% of the total power of the residuals. The processes behind this power may also influence the semi-annual cycle causing slightly larger power densities at this frequency.

The individual empirical formula,  $\eta$ , was applied and the spectra for the heat fluxes recalculated. The results appear in Figure 38.

At Station C, sensible heat flux, the VA series closely matches the 3H series at all frequencies. At 0.5 cycles/year the VA series slightly under predicts the 3H series while at 3.5 cycles/year, it slightly over predicts the 3H series. The over and under predictions counter-balance accounting for the low

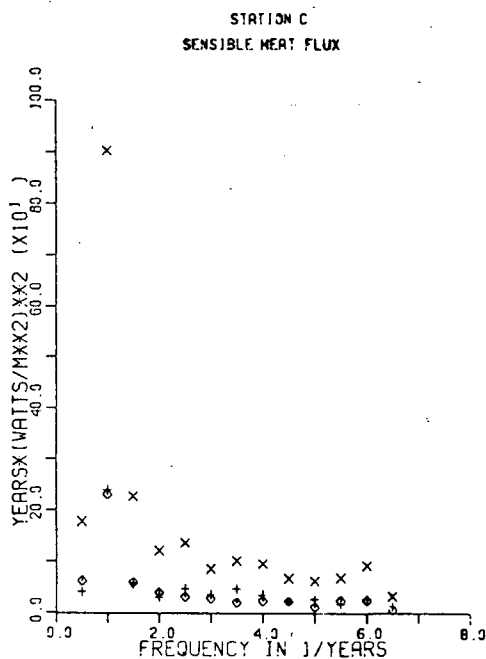


Figure 37 (a)

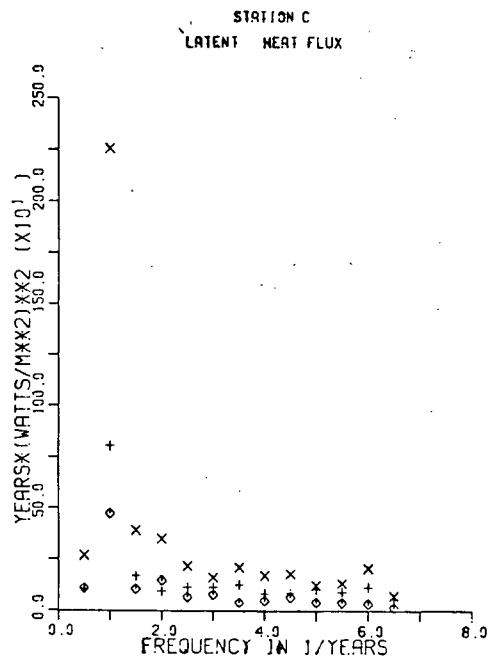


Figure 37 (b)

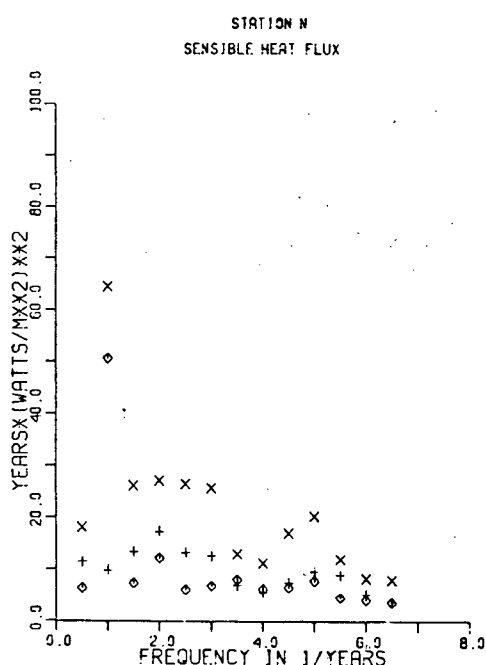


Figure 37 (c)

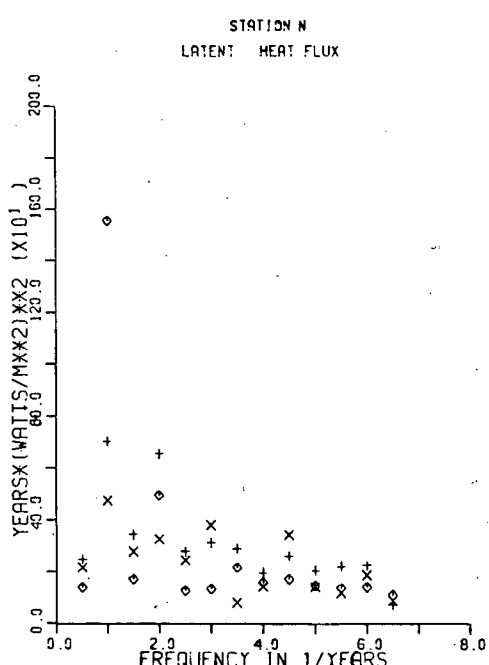


Figure 37 (d)

Figure 37. The spectra of the uncorrected VA, residual, and 3H heat flux time series at Stations C and N. The VA series is indicated by '+', the 3H series by 'x' and the residual series by '◊'. The 95% confidence limits are (.57, 2.19) for Station C and (.59, 2.08) for Station N.

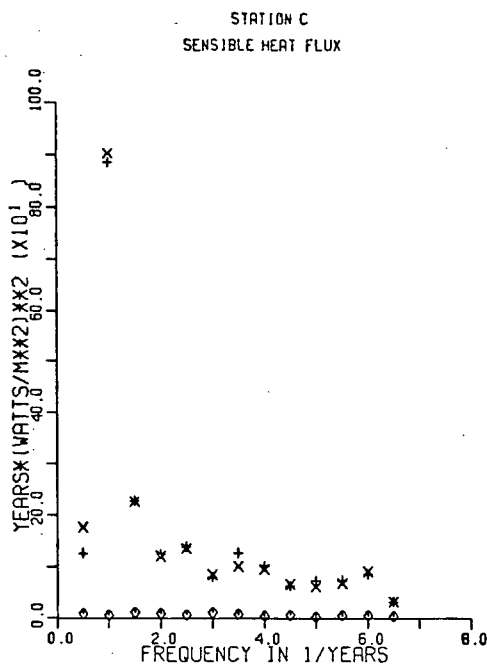


Figure 38 (a)

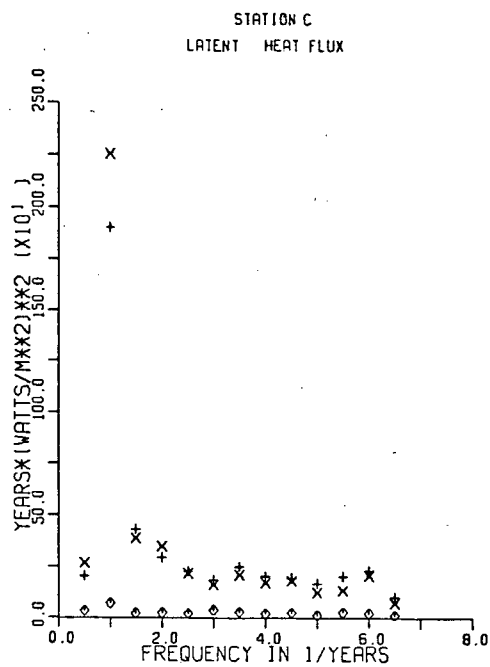


Figure 38 (b)

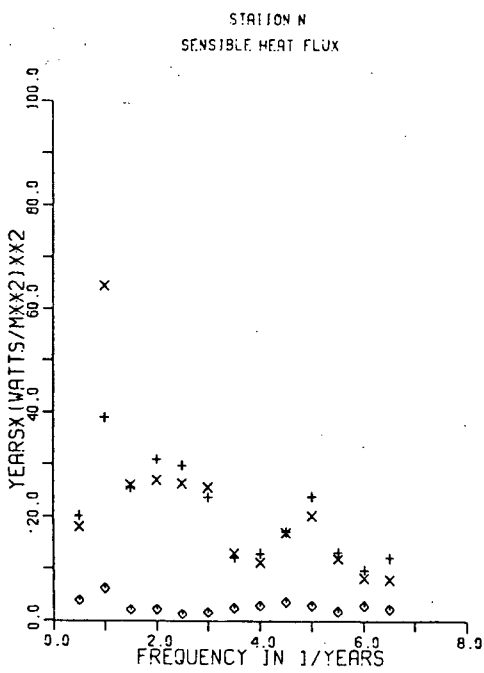


Figure 38 (c)

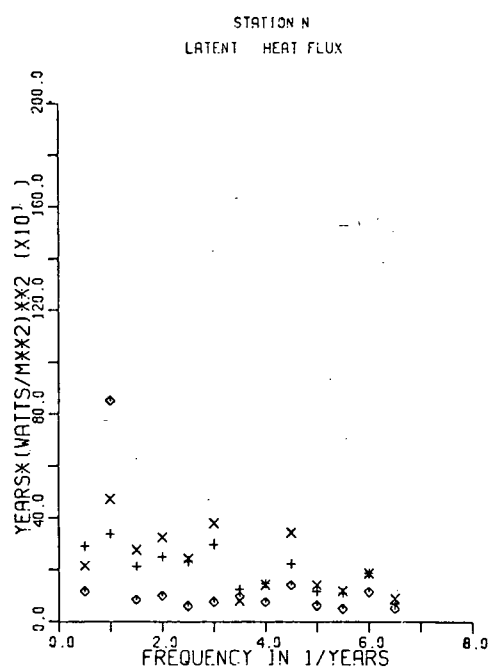


Figure 38 (d)

Figure 38. The spectra of the corrected heat flux for the 3H, VA and residual series at Stations C and N. The VA series is indicated by '+', the 3H series by 'x', and the residual series by '◊'. The confidence limits are (.57, 2.19) at Station C and (.59, 2.08) at Station N.

0.5% DV level shown in Appendix I. The residual series power is quite negligible at all frequencies compared to the 3H series. The latent heat flux VA series also closely approximates the 3H series for all but the annual cycle. The 350 (Watt/m<sup>2</sup>)<sup>2</sup> years difference at this frequency accounts for a large portion of the 3.0% difference variance. The residual series shows a slight increase at the annual cycle but it cannot be classified as significant. Thus, even though there is substantial power in the 3H and VA variates at the annual cycle there is no indication of a substantial peak in the residual series.

At Station N, the sensible heat flux results approximate the 3H results reasonably well at all frequencies except the annual cycle where the VA results underestimate the 3H results. At 8 other harmonics, the VA series slightly overestimates the 3H series. In attempting to reduce the DV error to 0.0, the variance difference at the annual cycle may have been increased to the detriment of the other frequencies. The residual series shows a slight rise at the annual cycle but is probably not significant in comparison to the error at the other frequencies. In the latent heat flux at Station N, the VA series underestimates the 3H spectral densities at most frequencies. At the annual cycle, the residual power density is more than 4 times that at any other frequency. Thus seasonal corrections may be required at Station N in the latent heat flux and this may in part account for its larger residual variances. The residual power density is approximately equal to the sum of the VA and 3H powers. It is demonstrated in Appendix A.4 that this can occur when there is a 90° phase shift between the 3H and

VA variates.

The time series of the residual latent heat flux at Station N with  $\eta$  applied is shown in Figure 39(a). The annual cycle is evident. In contrast, the Station C residuals are in Figure 39(b). As suggested in the spectra, there are no dominant signals.

An inspection of the data at Station N,  $L=28.0$  days, latent heat flux revealed that grouping months 1-5 and 11-13 inclusive reflected a positive bias in the residuals while months 6-10 inclusive reflected a negative bias in the residuals. The data were then arranged in these groups and a winter and summer empirical formula calculated for  $L=28.0$  days. The results appear in Table XIII. The summer  $\beta$  values of about -1.8 are substantially lower (more negative) than any other values. The latent heat residuals were calculated using these values and were reduced to 31.9% and the sensible heat residuals were reduced to 8.0%.

The spectra for the seasonally corrected fluxes at Station N appear in Figure 40. The 3H and VA series VA series now match more closely at the annual cycle. A comparison with Figure 38 reveals that a slight reduction in the power of the residuals at 2.0 cycles/year and a slight reordering of the relative positions of the VA and 3H spectral densities has occurred at most frequencies. The spectral density of the residual series at the annual cycle is well within the scatter of the other frequencies. The power of the residuals at all frequencies other than the annual cycle has remained, however, virtually unchanged.

TABLE XIII

The summer and winter formula coefficients required at Station N for the heat fluxes at L=28.0 days.

TYPE	WINTER		SUMMER	
	$\alpha$	$\beta$	$\alpha$	$\beta$
Sensible	5.337	-1.368	4.399	-1.730
Latent	4.997	-1.373	3.878	-1.824

Station D has the largest residuals for the y component, linear drag coefficient and the second largest residuals for the x component linear drag coefficient. Consequently, the spectra at this station were examined at L=28.0 days. Figures 41(a) and (b) are the x and y component spectra calculated from the uncorrected time series. The x component 3H and residual spectra both show distinct increases in spectral density at the annual cycle while the y component is quite white. In both components the residual spectra are larger at all frequencies than the VA spectra indicating that the error is greater than the actual VA estimate of the power. This indicates that severe errors may arise if geostrophic winds from barometric pressure maps averaged over periods of greater than perhaps four days are used to calculate stress spectra. One expects much smaller errors in the spectra calculated by Willebrand(1978) since the errors for the 28 day averaging period shown here is much larger than those for the 12 hourly averaging period upon which he based his study.

Figures 41(c) and (d) show the VA and 3H spectra with  $\gamma$  applied to the VA series. In the x component there is a definite mis-match between the 3H and VA spectra at the annual

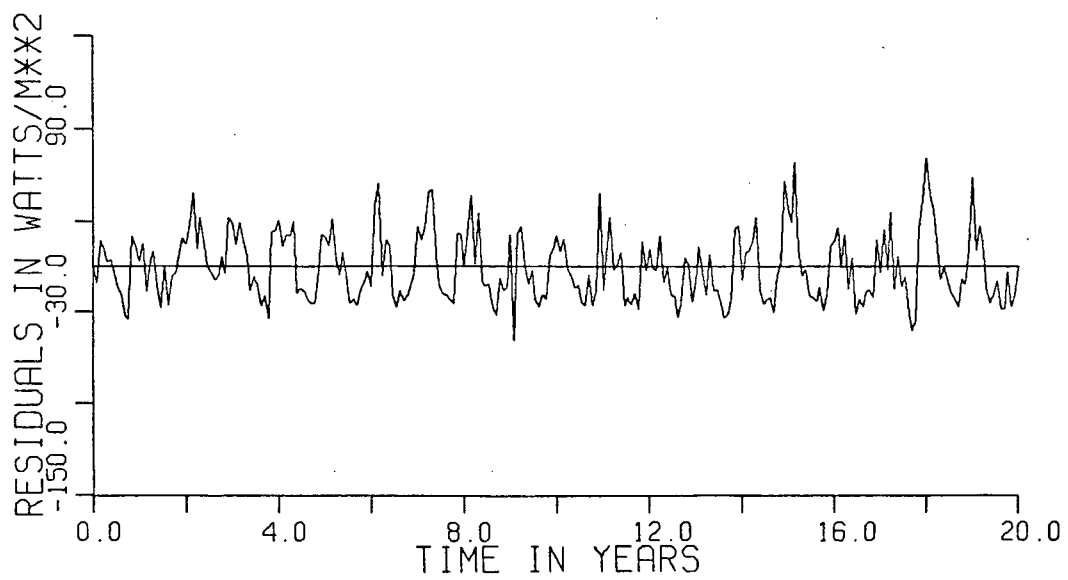


Figure 39 (a) Station N

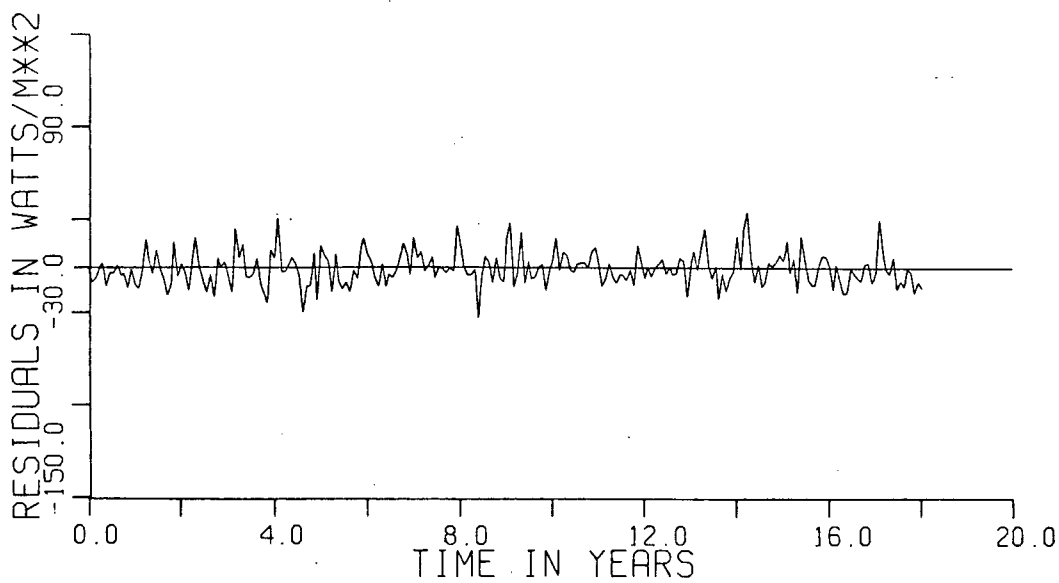


Figure 39 (b) Station C

Figure 39. The corrected residual series at Stations N and C for the latent heat flux, L=28.0 days.

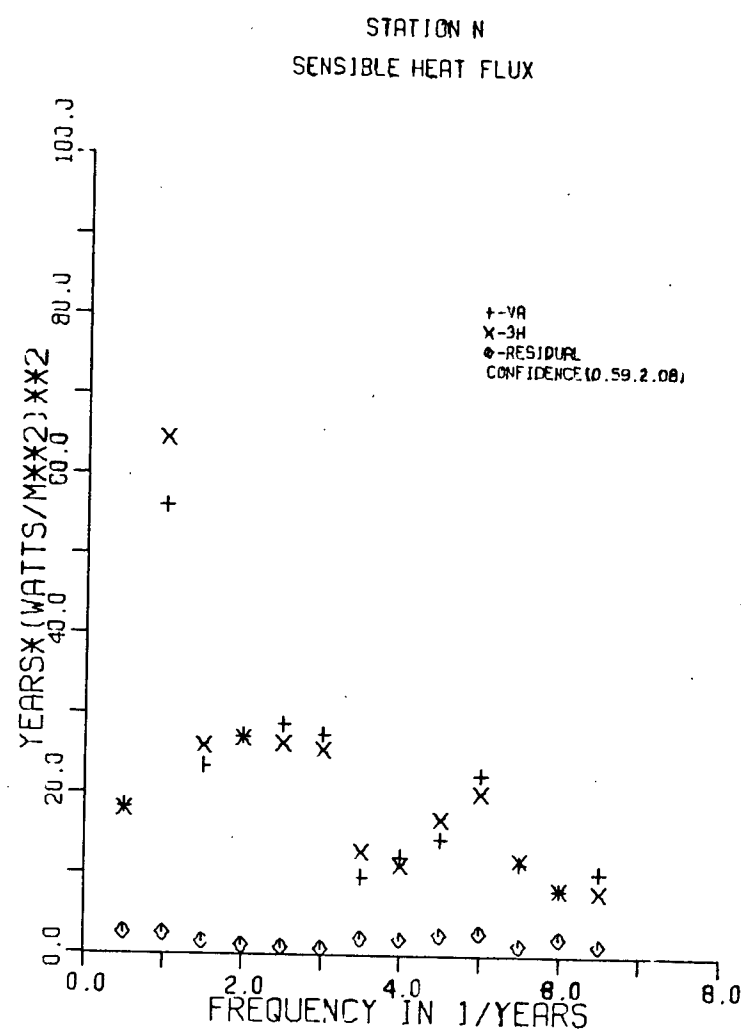


Figure 40 (a)

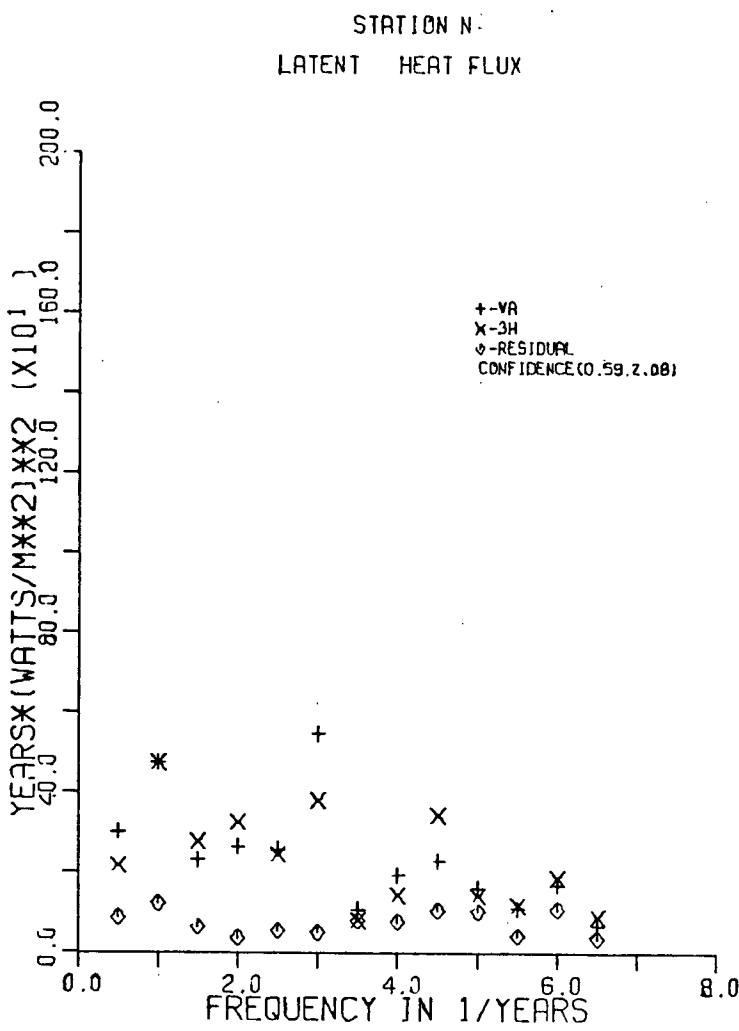


Figure 40 (b)

Figure 40. The heat flux spectra using the seasonally adjusted corrections at Station N,  $L=28.0$  days.

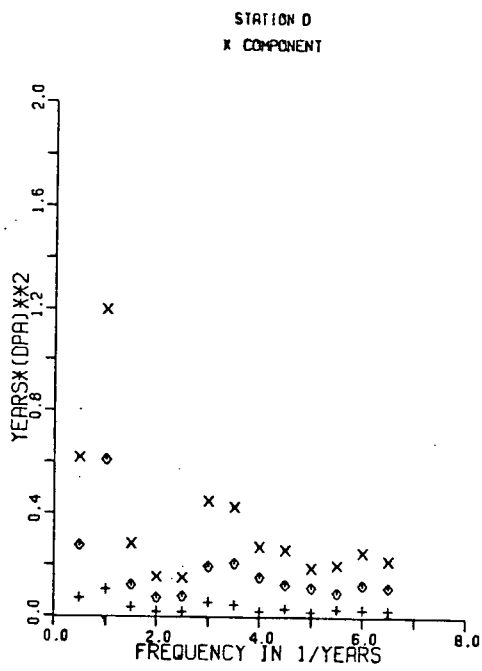


Figure 41(a) Uncorrected

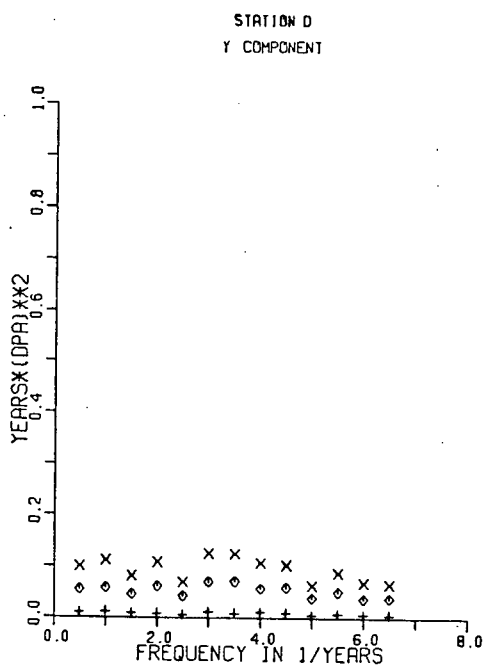


Figure 41(b) Uncorrected

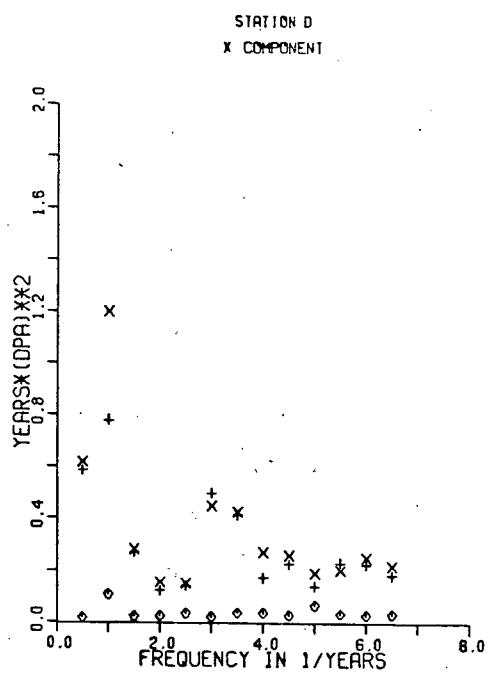


Figure 41(c) Corrected

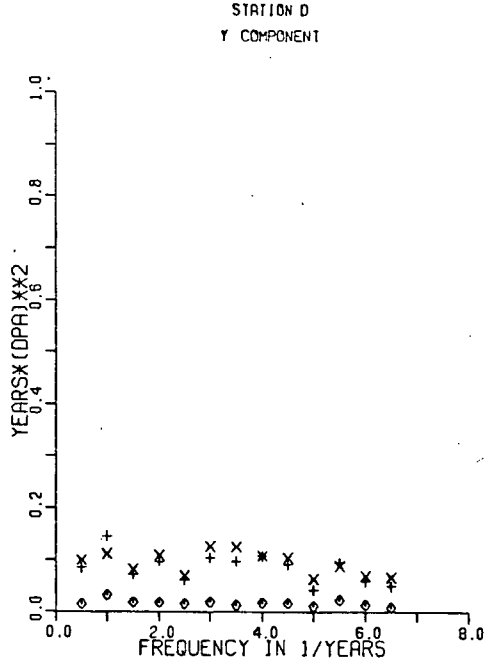


Figure 41(d) Corrected

Figure 41. The x and y component power spectra, linear drag coefficient, for the uncorrected and corrected VA series at Station D, L=28.0 days. The confidence bars are (.57, 2.19)

cycle while the residual spectrum shows a slight peak. At all other frequencies, however, the 3H and VA spectra match quite well. After correction, the y component 3H and VA match fairly well at all frequencies while the residual series is much lower in power. Since the y component power scale is 1/2 of the x component power scale, the variance of the residuals of the y scale are somewhat less than 1/2 of those of the x component. Table V indicates, however, that the actual 3H variance in the y component at Station D is only 1/10 of that in the x component. Thus the generally larger relative residual variances shown in the y component for the linear drag coefficient may be partially attributed to dividing by the smaller 3H variance.

The geographical empirical formula,  $\bar{\eta}$ , was applied to the linear drag coefficient stress at Station D and the resulting spectra appear in Figure 42. The residual spectra are virtually identical to those obtained when the individual correction,  $\eta$ , was applied. The VA spectra, however, systematically underestimates the 3H series spectral densities at all frequencies. This is consistent with the increased difference variances induced by application of the geographical empirical formula.

The Station N residual series, latent flux shows a large amount of power at the annual cycle which can be reduced by applying a semi-annual correction. This suggests that a time dependent correction may be required for the stresses at Station N. The individual Station N stress corrections for the linear drag coefficient were applied and the results are shown in Figure 43. Note that the scale on the y axis (spectral power

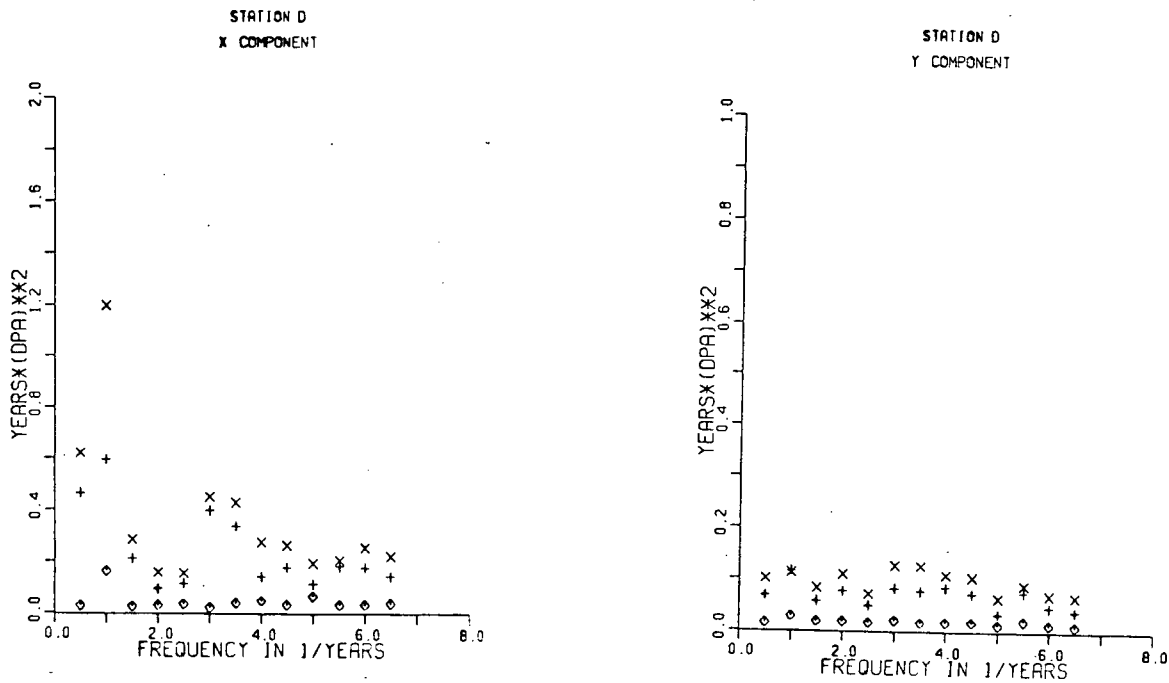


Figure 42. The linear drag coefficient spectra at Station D L=28.0 days, corrected with the geographically averaged formula. The 95% confidence limits are (.57, 2.19).

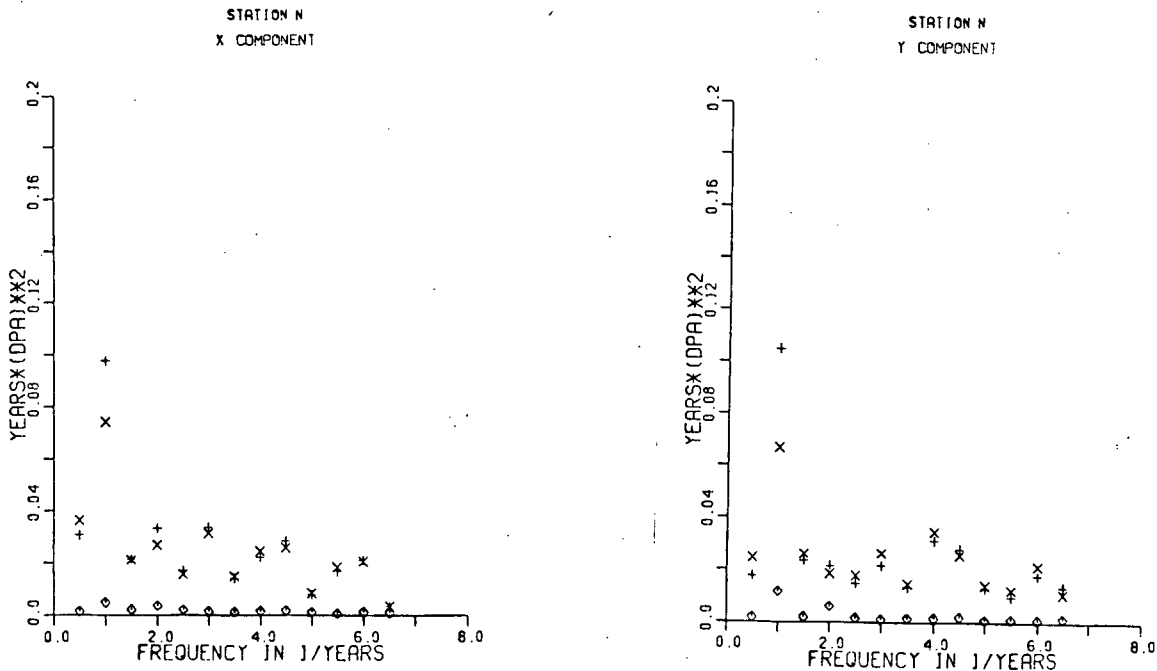


Figure 43. The stress spectra at station N corrected with the Station N empirical formula, L=28.0 days, linear drag coefficient. The 95% confidence limits are (.59, 2.08)

density) has been increased by an order of magnitude over that for Station D consistent with the lower variances reported in Table V. There is a slight mis-match of power between the 3H and VA series as well as a slight rise in the y component stress power densities at the annual cycle. The increase in the residual power is not significant. Consequently a monthly or seasonal dependence in the corrections may not be required for the stresses.

## CHAPTER VI WIND ROSE MEASUREMENTS

### 6.1 Introduction

Over much of the World's oceans, the only source of climatic information is from weather logs of ships of opportunity. The Office of the Chief of Naval Operations, US Navy has compiled and smoothed, in the format of wind roses, the meteorological observations of weatherstations and ships-of-opportunity for each of the twelve months of the year as well as a conglomerate wind rose based on all the available data.

The wind rose is constructed by sorting the data into eight directions and four Beaufort categories. They are then presented as the relative frequency of wind events within the four direction/Beaufort groups and as the relative frequency within nine Beaufort classes irrespective of direction. Further details can be found from the Marine Climatic Atlas (MCA).

Hellerman (1965 and 1967) has used wind roses to estimate world climatic wind stress patterns. Using a discrete and a continuous stress calculation technique and three different drag coefficients to compute stress values, he estimated the wind stress curl and calculated different values of the wind driven western boundary current. He concluded that the selection of drag coefficient had a much larger influence on the magnitude of the western boundary current than errors arising from the type of calculation of stress from wind roses.

The weatherstation data offered an opportunity to investigate in detail the inaccuracies arising in calculation of wind stress from wind roses.

## 6.2 Analysis

To facilitate discussion, the nomenclature of Hellerman (1965) will be used. The variable  $f_{i,j}$  will refer to the relative frequency of wind events in Beaufort category i and direction j while  $F_i$  will refer to the relative frequency of wind events in Beaufort category i irrespective of direction. Note that Hellerman labelled his Beaufort categories from  $i = 0 - 11$  where the present study will use intervals  $i = 1 - 12$ . Beaufort category 13 ( $> 33.5 \text{ m/sec}$ ) will be arbitrarily incorporated into class 12.

The original wind direction was digitized in  $10^\circ$  increments giving 36 directions. The Marine Climatic Atlas was formatted into 8 directions. Because eight is not a factor of 36, the intervals between the two wind roses do not coincide and a bias occurs in the constructions of the 8 direction wind rose as outlined by Lea and Helvey (1971).

To compensate for this bias, a linearly piecewise continuous 36 direction distribution for each Beaufort category was constructed. Hellerman used a similar technique to interpolate wind speeds; we adapted the technique to interpolate directional distributions. For each of the 36 direction intervals,  $f_{i,j}$  was assumed to be centred on the j direction (eg.  $5.0^\circ$ ). The relative frequency was divided by the width of the direction category (in this case  $10^\circ$ ) to arrive at a total frequency density for each direction/Beaufort category. The frequency densities at the ends of each category ( $f'_{i,j}$ ) were determined by interpolation between adjacent centre points as shown in Figure 44. The centre points were then readjusted to

conserve the total frequency density in the interval according to:

$$f'_{i,j} + 2 f^c_{i,j} + f'_{i,j+1} = 4 f_{i,j} \quad 6.1$$

where  $f'_{i,j}$  is the frequency density at the lower end of the  $j^{th}$  direction,  $f'_{i,j+1}$  is the frequency density at the upper end of the category,  $f^c_{i,j}$  is the readjusted centre point,  $f_{i,j}$  is the original centre point frequency density. In the case that  $f_{i,j} = 0.0$  then  $f'_{i,j}$  and  $f'_{i,j+1}$  were set = 0.0. If  $f^c_{i,j} < 0.0$   $f'_{i,j}$  was set = 0.0 and  $f'_{i,j}$  and  $f'_{i,j+1}$  were determined by:

$$\frac{f'_{i,j}}{f'_{i,j+1}} = f_{i,j} / f_{i,j+1} \quad 6.2$$

$$f'_{i,j} + f'_{i,j+1} = 4 f_{i,j}$$

The preceding centre point  $f_{i,j}$  was then again adjusted to conserve the continuity and frequency of the distribution.

The area under the curve was equal to the frequency of occurrence of the wind within each direction interval. The total  $360^\circ$  was then divided into blocks of  $45^\circ$  with the first interval centred on  $0.0^\circ$  and the area within each block was calculated to determine the eight direction frequency function.

The MCA format wind rose groups the Beaufort intervals as follows:

$$f_{3.4}, j; f_{5.6}, j; f_{7.8}, j; f_6 = f_{9,10,11,12}, j; j=1,8 \text{ and:}$$

$$F_{1,2}; F_3; F_4; F_5; F_6; F_7; F_8; F_9; F_{10}.$$

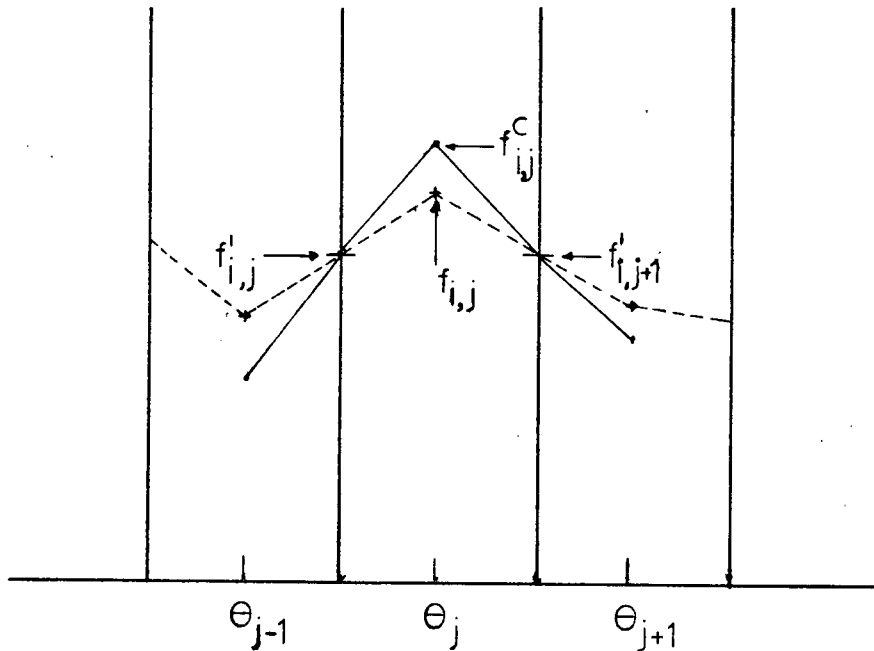


Figure 44. Construction of the piecewise linear distribution for the direction interpolation.

The Modified Scripps procedure (MSc) involves expansion of the of the  $f_{i,j}$  categories through proportionality assumptions from the four speed/direction groupings to 12. The stress is then calculated by:

$$\left. \begin{array}{l} T_x \\ T_y \end{array} \right\} = \bar{\rho} \sum_{j=1}^8 \sum_{i=1}^M f_{i,j} C_d(V_i) V_i^2 \left\{ \begin{array}{l} \sin \theta_j \\ \cos \theta_j \end{array} \right\} \quad 6.3$$

Hellerman expands the gale force wind categories only following the MSc procedures and then applies the frequency density conservation techniques to calculate the stress as:

$$\begin{aligned} \bar{T}_x \\ \bar{T}_y \end{aligned} \left\} = \bar{\rho} \sum_{j=1}^8 \left( \sum_{i=1}^{16} \int_{u_i}^{u_{i+1}} C_d(v_i) f_{ij} v_i^2 dv \right) \begin{cases} \sin \theta_j \\ \cos \theta_j \end{cases} \quad 6.4$$

Ignoring the intrinsic error of the transfer coefficients and accepting those used in the previous chapters, three immediate sources of error can be identified as follows:

- a. errors in the directional construction of the wind rose;
- b. errors in wind magnitude grouping; and
- c. differences in calculation techniques.

Assuming that the 36 direction wind comprises the initial data set, the reduction to 8 directions induces errors to the stress calculations in two ways. First, since the linear piecewise continuous distribution is an approximation of the actual continuous distribution, the assumed overlap calculations may not be accurate. Second, the reduction from 36 to 8 directions reflects a reduction in the number of degrees of freedom of the distribution (and hence the total information available about the statistical structure of the system) by a factor greater than four. A wind speed averaging is inherent in the reduction of number of directions and should result in a decrease in accuracy of the stress calculations.

Errors due to wind speed smoothing arise in a similar manner to the errors due to direction smoothing. The original data for Stations A through N are digitized to 1.0 knot (0.515 m/sec). The initial grouping to 12 Beaufort intervals markedly reduces the number of degrees of freedom of the distribution and induces the vector averaging of the wind. The MCA format increases the wind smoothing by a further reduction in grouping

from 12 Beaufort categories per direction to four. The Modified Scripps technique attempts to overcome this reduction by expansion of the MCA format to 12 Beaufort categories whereas Hellerman expands through interpolation of the given frequency densities.

The Modified Scripps calculation is essentially a discrete calculation in which it is assumed that the frequency densities within each Beaufort category should have little effect on the final flux results. The Hellerman technique assumes that the frequency densities are continuous and that an attempt to interpolate the variations within each Beaufort category may be more effective. A discrete and continuous flux calculation technique can be applied with facility at all levels of wind rose construction.

The total data sample was divided into actual monthly groupings and the stresses and heat fluxes were directly calculated. To simulate irregular samplings by ships-of-opportunity, any 3H reading which contained erroneous data for any variable was rejected from calculations. Wind roses were then constructed in three stages including monthly and total wind groupings. The 36 direction, 12 Beaufort interval was initially constructed. The stress was then calculated by the discrete and continuous methods to determine the loss in accuracy from wind speed smoothing alone. An 8 direction, 12 Beaufort interval wind rose was then constructed from the previous wind rose and the stress calculated by both techniques to indicate the loss in accuracy due to direction smoothing. Finally a MCA type wind rose of 8 directions and 4 Beaufort

intervals was constructed and the stress calculated by the Hellerman continuous technique and the Modified Scripps procedure to determine the loss of accuracy due to further wind speed smoothing and the accuracy one can expect from Marine Climatic Atlas wind roses.

In order to facilitate identification, the type of calculation will be identified by the number of directions and number of Beaufort intervals of the wind rose and the type of flux calculation. The type of flux calculation will be abbreviated as : (1) D - discrete, (2) C - continuous (3) MSC - modified Scripps. Thus the 36-12-D stress will be the stress calculated from the 36 direction 12 Beaufort interval wind rose by the discrete technique. The discrete technique applies Equation 6.3 directly. The MSC method involves the expansion of the four Beaufort categories to 12, then the application of Equation 6.3. The abbreviations and symbols to be used in the stages of calculation of the wind roses appear in Table XIV.

The stress differences were quantified by determining the absolute differences in stress magnitude and direction between the wind rose stress and the 3H stress. The heat fluxes were determined by calculating the monthly average air-sea temperature and humidity differences directly. The wind roses were used to calculate the monthly averaged wind speeds. The wind rose heat flux was then the product of the wind rose wind speed and the monthly average temperature or humidity difference. The difference between the directly determined and wind rose heat fluxes then quantified the inaccuracies.

The differences were determined for each monthly group and

TABLE XIV

Coding for the wind rose levels calculated in Chapter VI.

DIRECTIONS	SPEEDS	CALCULATION TECHNIQUE	ABBREVIATION	SYMBOL
36	12	Continuous	36-12-C	+
36	12	Discrete	36-12-D	○
8	12	Continuous	8-12-C	×
8	12	Discrete	8-12-D	△
8	MCA	Continuous	MCA	
			continuous	◊
8	MCA	MSc	MCA MSC	↑

for the composite record wind rose for each ship. The monthly differences were then averaged in two manners. First, the annual cycle for each ship was averaged and the standard deviations of the monthly discrepancies determined. For example, the discrepancies from January through December for Station A were averaged to determine a typical error for Station A. This averaging will be referred to as the ship average error and the corresponding standard deviation, the ship error standard deviation. The second averaging was performed between ships for each month. For example, the January errors only for all ships were summed, averaged and the standard deviations determined. This technique should indicate if the errors are induced by the annual cycle and will be referred to as the monthly average and monthly error standard deviation.

### 6.3 Results

The stress and heat flux components were calculated through the six stages previously outlined. In all cases the errors involved were generally much smaller than the difference mean errors discussed in Chapters III, IV, and V. In most cases the

error in stress magnitudes were less than  $\pm 0.05$  dPa; the errors in direction were generally less than  $5.0^\circ$ ; and the heat flux errors were generally bounded between  $\pm 5.0$  Watts/m $^2$ .

#### Stress Magnitude Errors

Figures 45 (a) and (b) contain the ship mean and error standard deviations for the constant drag coefficient respectively. Figures 45 (c) and (d) contain the monthly mean and error standard deviations respectively for the linear drag coefficient.

In all cases the 36-12-D calculation is biased slightly negatively at about 0.01 dPa indicating that this technique consistently overestimates the actual stress. This is accompanied by a standard deviation of similar order of magnitude suggesting that the bias is statistically significant. It is doubtful, however, that errors of this magnitude contribute greatly to induce errors in oceanic circulation calculations.

In both the ship and monthly means, the 36-12-C calculations are virtually 0.0 dPa. The error standard deviations are roughly equivalent to the 36-12-D technique.

The 8-12-C has a mean error of about 0.02 dPa larger than the 8-12-D calculations with nearly identical error standard deviations. Furthermore, both cases show a consistent reduction of 0.01 - 0.02 dPa from the respective 36 direction calculation. Thus an effect of reduction of direction degrees of freedom is to induce a slight underestimation of the stress. It is interesting that this induced underestimation in the discrete

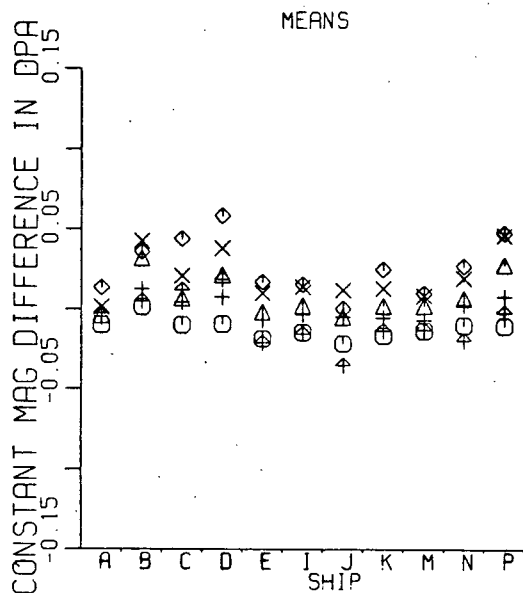


Figure 45 (a) Constant DC

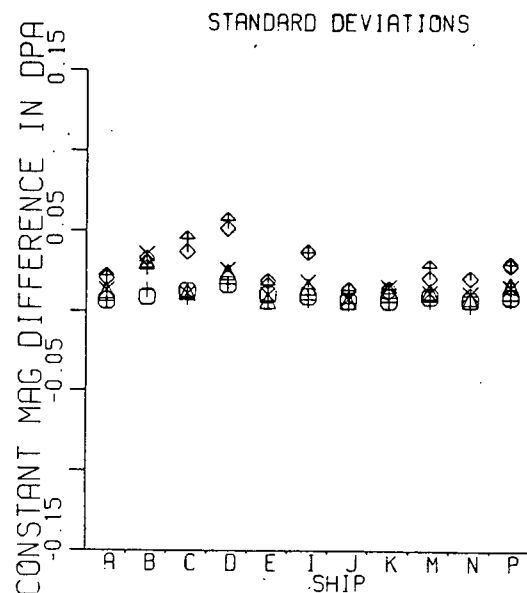


Figure 45 (b) Constant DC

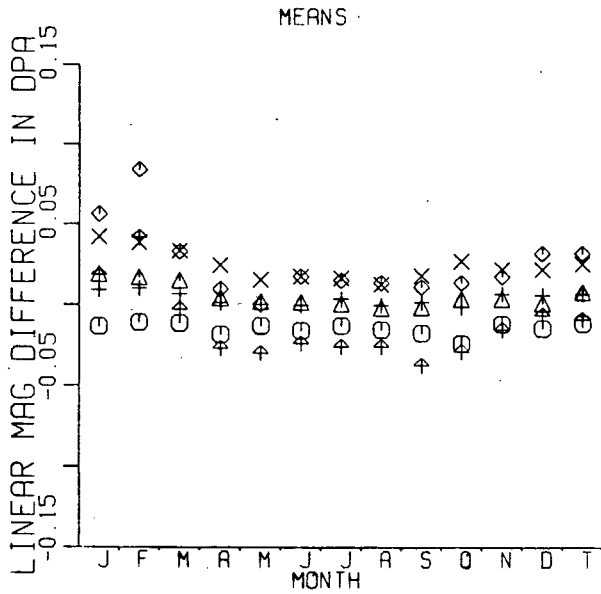


Figure 45 (c) Linear DC

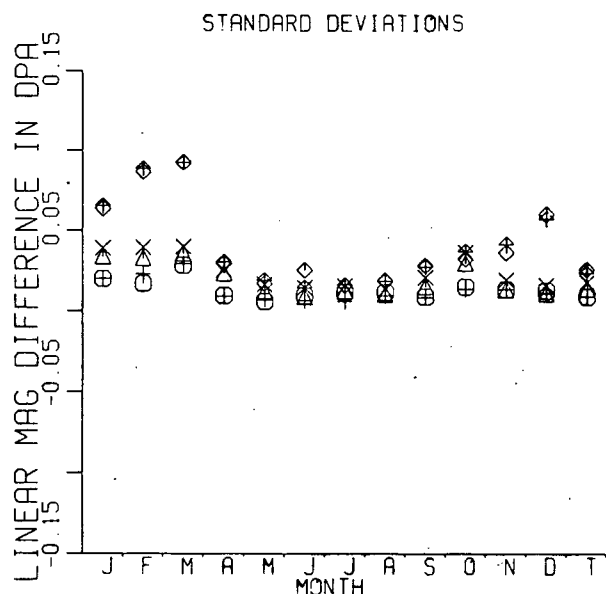


Figure 45 (d) Linear DC

Figure 45. The magnitude mean errors and error standard deviations between the actual stress and wind rose stress as a function of ship and month. The T is the composite wind rose based on all the data. DC denotes drag coefficient.

calculation re-adjusts a systematic overestimation for 36 directions to an over-all mean of nearly 0.0 dPa in the 8 direction case. In the continuous calculation, the means are consistently underestimated by about 0.02 - 0.03 dPa.

The MCA continuous and discrete calculations lead to curious results. The continuous calculation mean errors (with several exceptions), appear to underestimate the total stress to about the same degree as the 8-12-C technique. The MCA MSC mean values are, however, lower than the 8-12-D technique. Indeed, during the summer months the MCA MSC technique overestimates the "actual" stress to an even greater degree than the 36-12-D technique. The standard deviations for the discrete and continuous calculations are nearly identical and display distinct increases (up to 0.1 dPa) in the winter.

The MCA format does not resolve the gale force winds into direction categories. To achieve this, Hellerman divides 1/6 of the total gale force winds into Beaufort categories 11 and 12 irrespective of season and location. Since the stress is calculated as the square of the wind speed (a cubic in the linear case), even small gale force wind frequency densities can make disproportionately large contributions to the total stress. Thus, if the actual ratio of Beaufort categories 11 and 12 is substantially less than 1/6 then a fictitiously high stress will result. For example, at Station J where the discrete calculation yields a particularly high value in January, the gale force winds account for 18.0 % of the distribution. The ratio of Beaufort categories 11 and 12 to the total gale force winds is only 11.3% and not 16.7%. Furthermore, in June and

July there are no recorded values in Beaufort categories 11 and 12.

All errors calculated by all the techniques are very small. The reduction in directional degrees of freedom leads to a slight increase in the underestimation of the "true" stress. The discrete calculation consistently yields larger stress magnitude estimates than the continuous calculation for equivalent degrees of freedom. Inaccuracies associated with the MCA techniques may be due to inadequate interpolation of the gale force winds.

#### Stress Direction Errors

The ship linear angle difference means and standard deviations appear in Figures 46 (a) and (b) respectively while the monthly constant angle difference means appear in Figures 46 (c) and (d).

The mean angle differences are all less than 5.0°. The standard deviations, with the exception of Stations D and K, linear drag coefficient, are also less than 5.0°. The means for the constant drag coefficient as a function of month are biased positively while the linear drag coefficient biases appear less evident.

The mean errors appear to be dependent upon degrees of freedom and not upon discrete or continuous calculation techniques. The 36-12-C, 36-12-D, 8-12-C, and 8-12-D techniques are virtually identical in both means and standard deviations. The two MCA calculations are also very close in their mean values although the parallel is much less evident in the

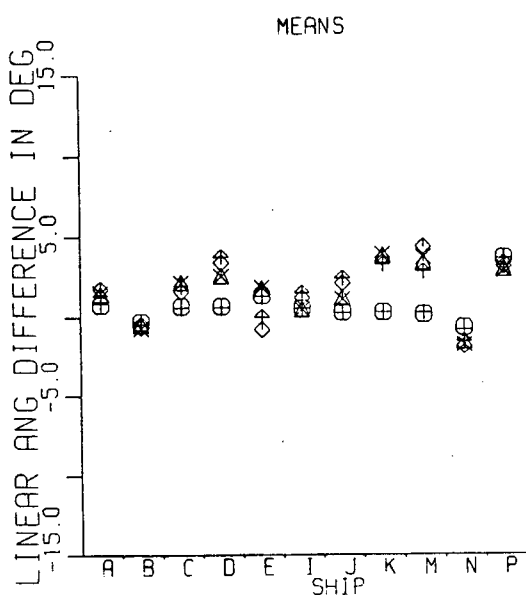


Figure 46 (a) Linear DC

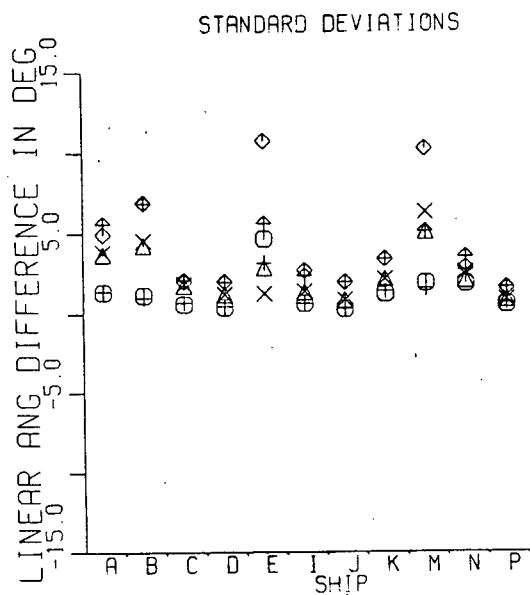


Figure 46 (b) Linear DC

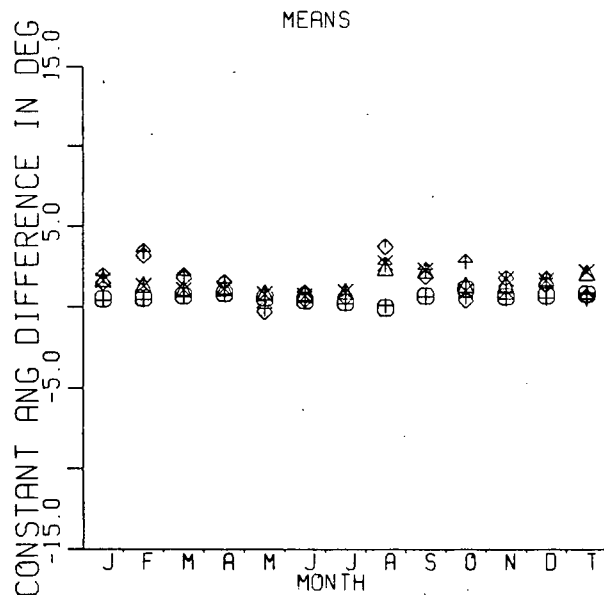


Figure 46 (c) Constant DC

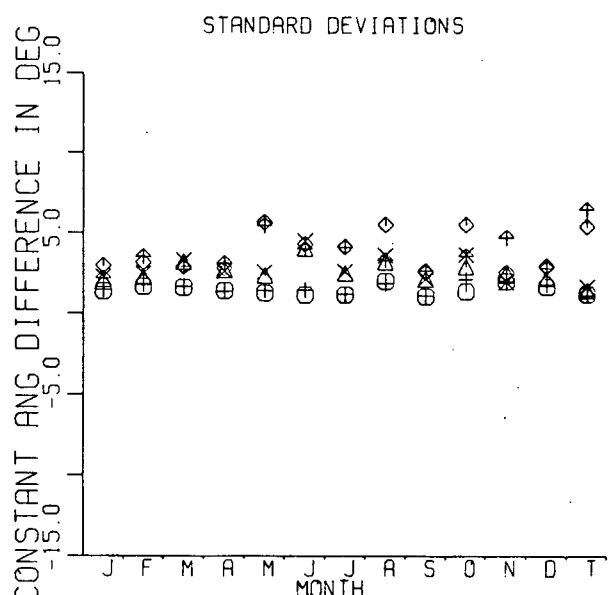


Figure 46 (d) Constant DC

Figure 46. The direction mean errors and error standard deviations between the actual stress and wind rose stress as a function of ship and month. The T is the composite wind rose based on all the data. DC denotes drag coefficient.

standard deviations. Where the two MCA standard deviations diverge, the continuous calculation shows more fluctuations.

### Heat Fluxes

The errors in the sensible heat fluxes appear in Figure 47. Errors are very small -- the means are generally bounded by  $\pm 2.0$  Watts/m<sup>2</sup>. Within each ship or month category the standard deviations for all calculations techniques are virtually identical. The reduction from 36 to 8 directions appears to have a negligible effect on the mean error for either the discrete or continuous calculations. There is, however, a slight positive bias (or underestimation) in the mean error for the 36-12-C, 36-12-D, 8-12-C, and 8-12-D calculations.

Wind speed grouping according to the MCA format induces a small mean error. The continuous MCA calculation consistently underestimates the sensible heat flux in comparison to the other calculations while the MCA MSC calculations yield a consistent overestimation in relation to the other techniques. The effect of this slight overestimation is that the MCA MSC calculation on the average has zero bias in the means for both the ship and monthly average calculations.

The latent heat flux results appear in Figure 48. Many of the observations of the sensible heat flux are also applicable to the latent heat flux. There is little difference in the means between any calculation for the direction reduction and the major discrepancies occur for the MCA format. The continuous MCA calculation again underestimates the latent heat flux in relation to the other techniques while the MCA MSC

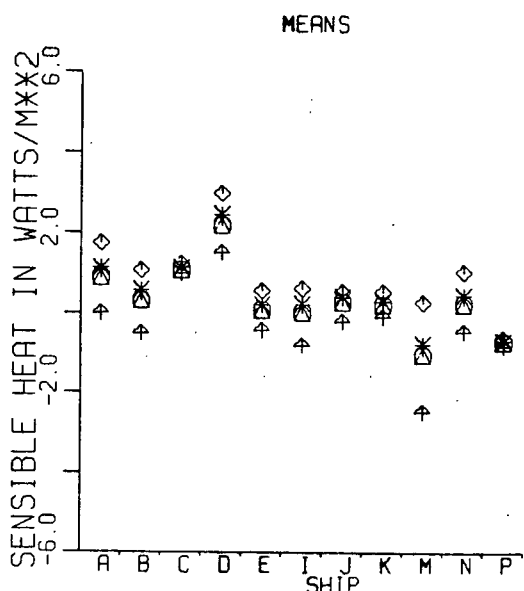


Figure 47 (a)

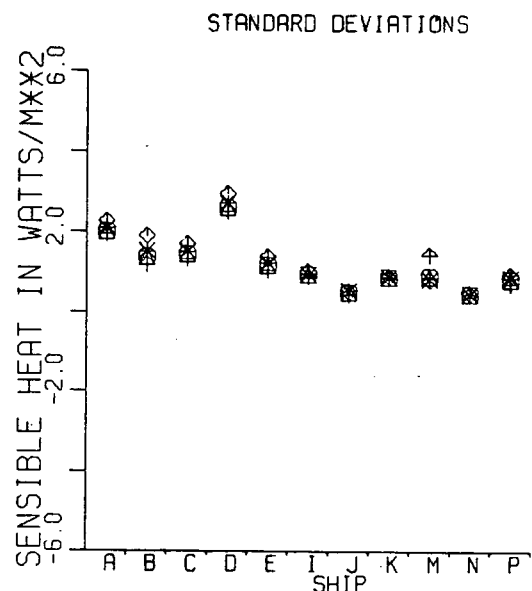


Figure 47 (b)

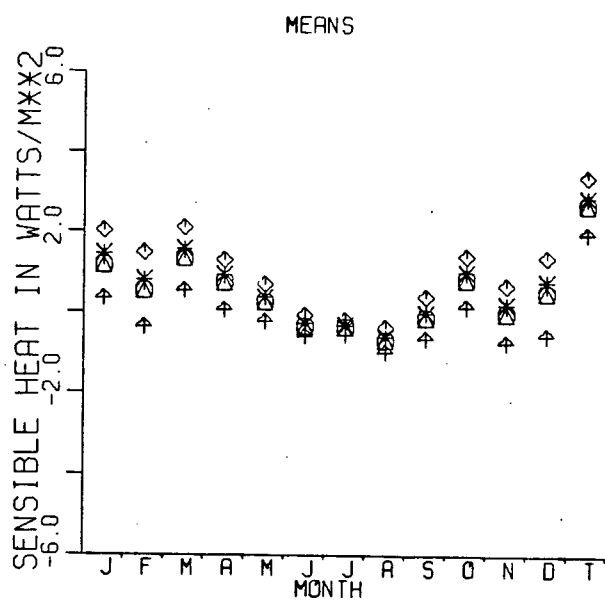


Figure 47 (c)

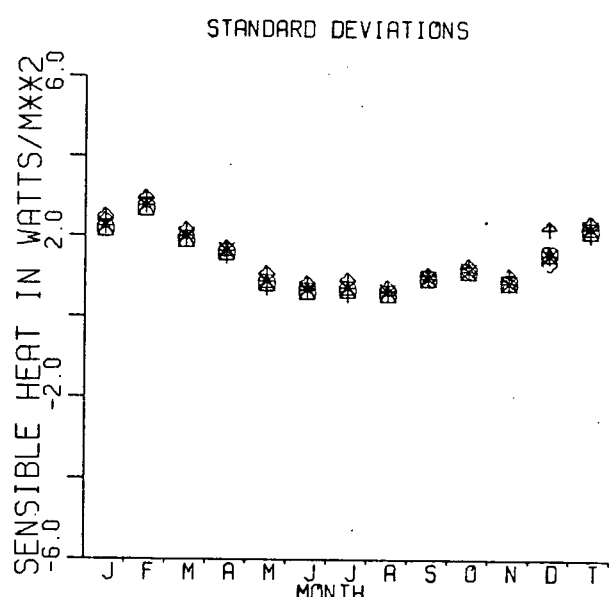


Figure 47 (d)

Figure 47. The mean errors and error standard deviations between the actual sensible heat fluxes and wind rose sensible heat fluxes as a function of ship and month. The T refers to the conglomerate wind rose.

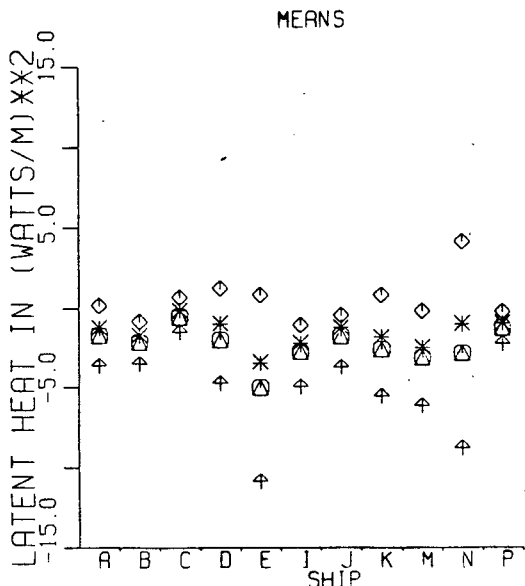


Figure 48(a)

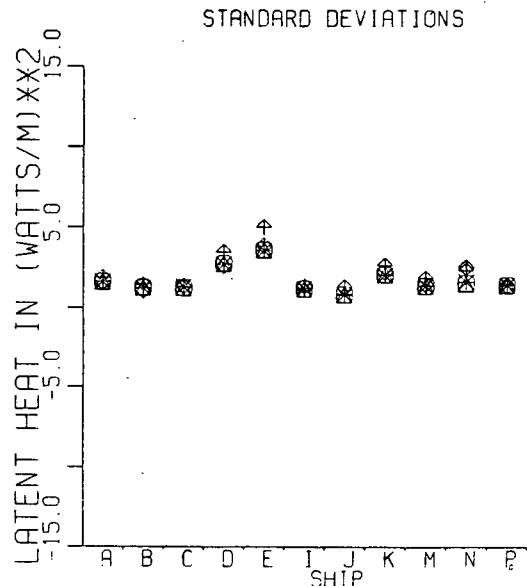


Figure 48(b)

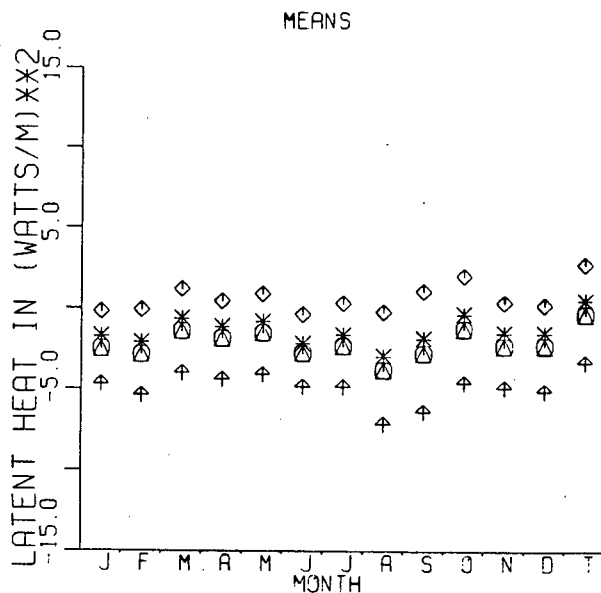


Figure 48(c)

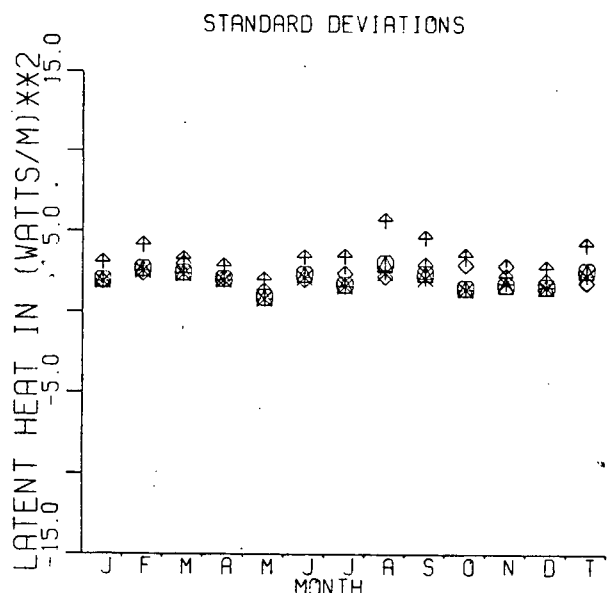


Figure 48(d)

Figure 48. The mean errors and error standard deviations between the actual latent heat fluxes and the wind rose latent heat fluxes as a function of ship and month. The T refers to the conglomerate wind rose.

calculation again overestimates the latent heat flux. The standard deviations for all techniques are virtually identical.

The mean latent heat errors are largely bounded by  $\pm 5$  Watts/m<sup>2</sup> with a general negative bias for all techniques in both the mcnth and ship mean errors. The effect of the negative bias is that the MCA continuous calculation now provides on average, the most accurate estimates of the latent heat flux.

## CHAPTER VII SUMMARY AND CONCLUSIONS

Time series of varying lengths from nine weatherships in the North Atlantic Ocean and from two weatherships on the North Pacific Ocean were examined. The data consisted of three-hourly readings of wind component velocities, barometric pressure, air temperature, dew point temperature, and sea surface temperature from which were calculated three-hourly air densities, air-sea temperature differences, air-sea humidity differences, x and y component wind stresses (using both constant and linear drag coefficients), sensible and latent heat fluxes. The calculated quantities and the wind component velocities were averaged over varying periods. The fluxes were then recalculated using the appropriate averaged constituent variates to arrive at a vector averaged (VA) estimate. The VA flux estimates were then compared to the directly averaged (called 3H) fluxes.

A systematic underprediction of the 3H air-sea fluxes occurs when they are estimated through VA parameters. The required transformations to correct for these losses are similar for all fluxes and are dependent upon the VA wind speed and upon averaging period. (Chapters III and IV)

Four test functions: the difference means, difference variances, residual variances, and correlation coefficients were defined in Equations 2.16 - 2.19 to quantify the differences between the VA and 3H fluxes. In all cases the difference means, difference variances, and residual variances increased roughly exponentially with averaging period while the correlation coefficients showed a similar decrease. The

residual variance measured the point-by-point differences and had maximum uncorrected values at  $L=28.0$  days of 30.0-40.0% for the constant drag coefficient, 40.0-50.0% for the linear drag coefficient, 25.0-45.0% for the sensible heat flux and 40.0%+ for the latent heat flux. (Sections 3.1 and 4.2)

A simple analysis established a lower bound of the point-by-point magnitude reductions in the constant drag coefficient stress,  $R_j(L)$ . They were proportional to the variance of the wind speed lost through averaging, and inversely proportional to the calculated vector averaged wind speed squared. Although not exact, the simple model aided in explaining many distributional features of the 3H-VA discrepancies. The fact that the point-by-point direction differences,  $B_j(L)$ , averaged to 0.0° for moderate wind speeds indicated that a single transformation would suffice for both the x and y stresses. (Section 3.3)

The most precise method of correcting for the 3H-VA discrepancies was to linearly regress the two variates on a Beaufort category/averaging period basis arriving at a transformation  $\xi_{ke}$ . Marked improvements were found in all four test quantities. The residuals increased exponentially to 3.0 days and then remained fairly constant from 3.0 to 28.0 days. At  $L=28.0$  days, the constant drag coefficient residuals were reduced to 5.0-8.0%, the linear drag coefficient residuals were reduced to 10.0-15.0%, the sensible heat flux residuals were reduced to 5.0-10.0% and the latent heat flux residuals were reduced to 10.0-40.0%. Significant (>10.0%) transformations were required for all wind speed categories for averaging periods greater than 0.5 days. (Sections 3.7 and 4.5)

Due to mathematical aspects of the regression, it was found that a positive bias in the difference variances, exactly equal to the residual variances was induced. Because correlations were generally high between the 3H and VA variates, this bias could be corrected without markedly increasing the residuals. (Sections 3.5 and 4.3)

Plots of  $\bar{Z}_{ke}$  indicated that the transformations may be quite regular over varying averaging periods and varying wind speeds for all fluxes. A non-linear regression of the form  $\eta = 1 + \alpha(u^2+v^2)^{\beta/2L}$  was performed and an analysis of the test quantities revealed that application of this formula to the VA fluxes produced identical results to the  $\bar{Z}_{ke}$  test results. The best method of application of the formula was to allow it to correct each VA estimate on a point-by-point basis. (Section 5.2)

The similarity of the results for all fluxes indicated that the vector averaging of the wind in general, and the loss of wind variance information in particular, determined the extent of the reduction for all fluxes. This was confirmed at Station N where a 10 fold reduction in wind speed variance accounted for markedly reduced transformations required for both drag coefficient calculations, and for both heat fluxes. The discrepancy at Station K, sensible heat flux, remains an enigma. (Sections 3.1, 3.4, and 4.4)

It was shown by direct observation that all ships excluding Station N for all fluxes and Station K for the sensible heat flux required similar transformations. The directly calculated difference means, residual variances, and correlation

coefficients were insensitive to a geographic grouping of transformations. The difference variances, in some instances, rose substantially (Section 5.4). This was confirmed in the spectra at Station D where a geographically averaged correction was applied. (Section 5.5)

An analysis of the heat flux spectra at Stations C and N demonstrated some of the internal properties of the transformations. A large annual cycle in both the latent and sensible 3H heat fluxes did not necessitate a seasonal transformation at Station C where the residual variances were lowest. An analysis of the residual spectra at Station N, exactly where the heat flux residuals were highest, revealed that a seasonal transformation could markedly improve the residual variance. Thus, the gross form of the transformation may be dictated by the vector averaging of the wind; deviations from the broad transformations may be dependent upon the correlation of the annual air-sea temperature or humidity differences with the annual winds. Other areas of high residuals (eg. Station E, latent heat flux) may also require a seasonally dependent transformation. (Section 5.5)

An analysis of the uncorrected stress component spectra showed a consistent underestimation of the 3H spectra by the VA spectra at all frequencies. Even though Station D showed the highest residuals after transformation, there was no evidence that a seasonal transformation improved the situation. (Section 5.5)

Any one of the three transformations ( $\xi_{re}$ ,  $\eta$ ,  $\bar{\eta}$ ) will greatly aid calculations based on air-sea fluxes calculated from

averaged constituent data. The  $\xi_{Re}$  transformations for the constant drag coefficient are in the correct range to aid in improving the pressure averaged transports of Figure 1(b) to more closely resemble the averaged transports of Figure 1(a). Consequently application of the transformation may yield more accurate results from numerical models while using more realistic air-sea transfer coefficients. Furthermore, the technique offers the possibility of numerically depicting the time history development of specific wind forced oceanic events. Given the similarity in the test function results between  $\xi_{Re}$ ,  $\eta$ , and  $\bar{u}$ , the two empirical formulae should ease implementation of the transformations with little loss in accuracy.

The improvements in the spectra are very clear. From a situation at  $L=28.0$  days where the uncorrected time series yielded large discrepancies between the VA and 3H spectra and a residual spectrum which was as large or larger than the VA estimated spectrum, the  $\eta$  transformation produced a match between the two estimates on a frequency-by-frequency basis and produced substantial reductions in the residual power density. (Section 5.5)

Several facets, particularly in applying transformations to barometric pressure calculations, require further investigation. First, the barometric pressure maps have an inherent spatial averaging which could not be simulated in this study. Similar calculations at the eleven weathership locations based on geostrophic wind data (such as developed by Willebrand, 1978) could confirm whether similar transformations for geostrophic

wind are required. Application of the transformations to transport calculations similar to those of Aagaard(1970) could add further confirmation. Second, the sub-tropics, tropics, and monsoon regions (where a strongly deterministic annual signal is inherent in the winds) have not been investigated. If confirmation of the technique could be gained from replication on geostrophic winds, then it may be possible to extrapolate transformations to other regions of the world using these data.

The wind rose errors were investigated at all levels of construction. In all cases, the average errors were equal to or less than the corrected difference mean errors for the equivalent  $L=28.0$  days of the vector averaged winds. Slight overprediction could be detected in the discrete versus the continuous calculation. The reduction from 36 to 8 directions induced a slight underestimation in the  $3H$  stress. Errors in the MCA (Marine Climatic Atlas) calculation were probably affected by the allocation of the gale force winds and inherent correlation between the winds and the air-sea temperature and humidity differences. (Chapter VI)

BIBLIOGRAPHY

- Aagaard, K. (1970) Wind-driven transports in the Greenland and Norwegian Seas. *Deep Sea Res.*, 17 (2), pp. 281-291
- Allen, J. S. (1980) Models of wind-driven currents on the continental shelf. *Ann. Rev. Fluid Mech.*, 12, pp. 389-433
- Bendat, J. S., and A. G Piersol (1971). *Random Data*. Wiley-Interscience, New York, 407 pp.
- Deacon, E. L., and E. K. Webb (1962) Small scale interactions. In *The Sea* Vol. I, ed by M. Hill, Interscience publishers, New York, pp. 43-87
- Dorman, C. E. (1974) Analysis of meteorological and oceanographic data from Ocean Station Vessel N (30N 140W). PhD Thesis, Oregon State University. 136 pp.
- Fiedler, F. and H. A. Panofsky (1970). Atmospheric scales and spectral gaps. *Bull. Amer. Met. Soc.*, 51 (12), pp. 1114-1119.
- Fissel, D. B. (1975). A frequency analysis of ten years of surface atmospheric data at Ocean Weatherstation 'Papa'. MSc Thesis, Institute of Oceanography, University of British Columbia. 136 pp.
- , S. Pond, M. Miyake (1977). Computation of surface fluxes from climatological and synoptic data. *Mon. Wea. Rev.*, 105 (1), pp. 26-36.
- Fcfonoff N. P. (1960). Transport computations for the North Pacific Ocean. *Ms. Rep. Ser., Fish. Res. Bd. Can.*, (77), 87 pp
- Hellerman, S. (1965). Computations of wind stress over the Atlantic Ocean. *Mon. Wea. Rev.*, 93 (4), pp. 239-244.
- , (1967). An updated estimate of the wind stress on the world ocean. *Mon. Wea. Rev.* 95 (9), pp. 607-626.
- Hertzman, C., M. Miyake and S. Pond (1974). Ten years of meteorological data a Ocean Station Papa. *Ms. Rep.* No. 29, Institute of Oceanography, University of British Columbia. 46 pp.
- Huang, J. C. K. (1978). Numerical simulation of the oceanic anomalies in the North Pacific basin. I: The ocean model and long-term mean state. *J. Phys. Oceanogr.*, 8, pp 755-778.

- (1979). Numerical studies for oceanic anomalies in the North Pacific Basin: II. Seasonally varying motions and structures. *J. Phys. Oceanogr.* 9, pp. 37-56.
- Hurlburt, H., J. Kindle, J. J. O'Brien (1976). A numerical simulation of the onset of El Niño. *J. Phys. Oceanogr.* 6 pp. 621-631.
- Jenkins, J. M. and D. G. Watts (1968). Spectral Analysis Holden-Day, San Francisco. 325 pp.
- Large, W. G. (1979). The turbulent fluxes of momentum and sensible heat over the open sea during moderate to strong winds. PhD Thesis, Department of Oceanography, University of British Columbia. 180pp.
- Lea, D. A., and Helvey (1971). Directional bias in wind roses due to mixed compass formats. *J. Appl. Met.*, 10 (5), pp. 1037-1039.
- Malkus, J. S. (1962). Large-scale interactions. In The Sea Vol. I ed. by M. Hill, Interscience Publishers, New York, pp. 88-294.
- McCreary, J. P. (1976). Eastern tropical ocean response to changing wind systems: with application to El Niño, *J. Phys. Oceanogr.* 6, pp. 646-664.
- O'Brien J. J. (1971). A two dimensional model of the wind-driven North Pacific, *Invest. Pesq.* 35 (1), pp. 331-349.
- Pfeiffer, P. E. (1965). Concepts of Probability Theory. McGraw-Hill Co., New York. 389 pp.
- Pond, S., G. T. Phelps, J. E. Paquin, G.T. McBean, and R. W. Stewart (1971). Measurements of the turbulent fluxes of momentum, moisture and sensible heat over the ocean. *J. Atmos. Sci.*, 28 (6), pp. 901-917.
- Pond, S., D. B. Fissel, and C. A. Paulson (1974). A note on bulk aerodynamic coefficients for sensible heat and moisture fluxes. *Boundary-Layer Meteorol.* 6, pp. 333-339.
- Roll, H. V. (1965). Physics of the Marine Atmosphere. Academic Press Inc., New York. 426 pp.
- Rossby C. G. and R. B. Montgomery (1935). The layer of frictional influence in wind and ocean currents. Papers in physical oceanography and meteorology. Massachusetts Institute of Technology and Woods Hole Oceanographic Institution. 3 (3), 101 pp.
- Smith, S. D. and E. G. Bank (1975). Variation of the sea surface drag coefficient with wind speed. *Quart. J. R. Met. Soc.* (1975), 101, pp. 665-673

Turner, J. S. (1973). Buoyancy Effects in Fluids. Cambridge University Press: Cambridge, United Kingdom. 368 pp.

Willebrand, J. (1978). Temporal and spatial scales of the wind field over the North Pacific and North Atlantic. J. Phys. Oceanogr., 8 (6), pp. 1080-1094.

## Appendix A

Development of some mathematical aspects of the multiple regression analysis.

### A.1 Equivalence of $S^2$ And $\Delta \sigma^2$

Let  $X$  be the 3H variate and  $X'$  be the VA variate and  $k$  be the Beaufort interval (from 1 to 13). The object is then to minimize the residual variance defined as:

$$\sigma_x^2 S_{ex}^2 = \frac{1}{N} \sum_{k=1}^{13} \sum_{j=1}^{J_k} \left[ X_{kj} - \bar{X}_{ke} X'_{kj} \right]^2 - \left[ \frac{\sum_{k=1}^{13} \sum_{j=1}^{J_k} X_{kj} - \sum_{ke} \bar{X}_{ke} X'_{kj}}{N} \right]^2 \quad 1.1A$$

where  $N$  is the total number of points in the averaging length and  $J_k$  is the number of values in Beaufort category  $k$ .

Setting  $\frac{\partial \sigma_x^2 S_{ex}^2}{\partial \bar{X}_{ke}} = 0$  for each  $k$ :

$$\sum_{j=1}^{J_k} \left[ X_{kj} X'_{kj} - \bar{X}_{ke} X'_{kj} \right]^2 + \sum_{j=1}^{J_k} X'_{kj} \left[ \sum_{k=1}^{13} \sum_{j=1}^{J_k} X_{kj} - \sum_{ke} \bar{X}_{ke} X'_{kj} \right] = 0 \quad 1.2A$$

Redefine:

$$S_{kj} = \sum_{j=1}^{J_k} X_{kj} X'_{kj}$$

$$X_k'^2 = \sum_{j=1}^{J_k} X'_{kj}^2$$

$$X_n^2 = \sum_{j=1}^{J_k} X_{kj}^2$$

$$\bar{X}'_k = \sum_{j=1}^{J_k} X'_{kj}$$

$$\Delta X = \frac{\sum_{k=1}^{13} \sum_{j=1}^{J_k} X_{kj} - \sum_{ke} \bar{X}_{ke} X'_{kj}}{N}$$

Thus:

$$\xi_{ke} = \frac{S_{ke} - \bar{x}_k' \Delta X}{x_k'^2} \quad 1.3A$$

expanding  $\Delta X$  in full gives:

$$\xi_{ke} = \frac{S_{ke} - \bar{x}_k' \left[ \frac{1}{N} \sum_{k=1}^{13} \sum_{j=1}^{In} x_{kj} - \sum_{ke} \bar{x}_{kj} \right]}{x_k'^2}$$

This equation was solved by Gaussian elimination with iterative improvement.

Expanding equation 1.1A gives:

$$\sigma_x^2 S_{ex}^2 = \frac{1}{N} \sum_{k=1}^{13} \left\{ x_k^2 - 2 S_{ke} \xi_{ke} + \xi_{ke}^2 x_k'^2 \right\} - (\Delta X)^2 \quad 1.4A$$

Substituting 1.3A gives:

$$\sigma_x^2 S_{ex}^2 = \frac{1}{N} \sum_{k=1}^{13} \left\{ x_k^2 - \frac{S_{ke}^2}{x_k'^2} + \frac{\bar{x}_k'^2 (\Delta X)^2}{x_k'^2} \right\} - (\Delta X)^2 \quad 1.5A$$

Similarly the difference variance is:

$$\sigma_{\Delta S_{ex}}^2 = \frac{1}{N} \sum_{k=1}^{13} \left\{ x_k^2 - \xi_{ke}^2 x_k'^2 \right\} - \left( \frac{1}{N} \sum_{k=1}^{13} \bar{x}_k' \right)^2 + \left( \frac{1}{N} \sum_{k=1}^{13} \xi_{ke} \bar{x}_k' \right)^2 \quad 1.6A$$

Again substituting 1.3A gives:

$$\begin{aligned} \sigma_{\Delta S_{ex}}^2 &= \frac{1}{N} \sum_{k=1}^{13} \left\{ x_k^2 - \frac{S_{ke}^2}{x_k'^2} + \frac{\bar{x}_k'^2 (\Delta X)^2}{x_k'^2} \right\} + 2 \left( \sum_k \xi_{ke} \bar{x}_k' \right) (\Delta X) \\ &\quad - \left( \frac{1}{N} \sum_n \bar{x}_n' \right)^2 + \left( \frac{1}{N} \sum_k \xi_{ke} \bar{x}_k' \right)^2 \end{aligned}$$

Or:

$$\bar{\sigma}_x^2 \Delta \bar{\sigma}_{ex}^2 = \frac{1}{N} \sum_{k=1}^{13} \left\{ X_k^2 - \frac{S_k^2}{X_k^2} + \frac{\overline{X_k^2}^2 (\Delta X)^2}{X_k^2} \right\} - (\Delta X)^2 \quad 1.7A$$

This is exactly equal to 1.5A or  $\bar{\sigma}_x^2 \Delta \bar{\sigma}_{ex}^2 = \bar{\sigma}_x^2 S_{ex}^2$ . The approximation for the wind stress was that all linear terms (means) are small compared to the quadratic and cross terms in which case:

$$\bar{\sigma}_x^2 S_{ex}^2 = \bar{\sigma}_x^2 \Delta \bar{\sigma}_{ex}^2 = \left[ \frac{1}{N} \sum_{k=1}^{13} X_k^2 - \frac{S_k^2}{X_k^2} \right] \quad 1.8A$$

#### A.2 The Effect Of The Change In $\bar{\sigma}_{ke}$ On $\bar{\sigma}_x^2 S_{ex}^2$

Let  $X$  and  $X'$  be the 3H and WVA variates, and  $(1+\epsilon) = \frac{\bar{\sigma}_y}{\bar{\sigma}_x} = \frac{\bar{\sigma}_x}{\bar{\sigma}_{ke}} = \frac{\bar{\sigma}_{ke}'}{\bar{\sigma}_{ke}}$ ,  $\bar{\sigma}_x^2 S_{ex}^2$  is the residual variance before application of  $(1+\epsilon)$  and  $\bar{\sigma}_x^2 S_{ex}'^2$  is the residual variance after application of  $(1+\epsilon)$ . Then:

$$\bar{\sigma}_x^2 S_{ex}^2 = \overline{(X-X')^2} - \overline{(X-X')^2}' \quad 2.1A$$

$$\bar{\sigma}_x^2 S_{ex}'^2 = \bar{\sigma}_x^2 + (1+\epsilon)^2 \bar{\sigma}_{x'}^2 - 2 R_x (1+\epsilon) \bar{\sigma}_x \bar{\sigma}_{x'} \quad 2.2A$$

Where  $\overline{\quad}$  is the averaging operator.

Which reduces to:

$$\bar{\sigma}_x^2 S_{ex}^2 = \bar{\sigma}_x^2 + \bar{\sigma}_{x'}^2 - 2 R_x \bar{\sigma}_x \bar{\sigma}_{x'} \quad 2.3A$$

$$\bar{V}_x^2 S_{xe}^{12} = \bar{V}_x^2 + (1+\epsilon)^2 \bar{V}_{x'}^2 - 2R_x(1+\epsilon) \bar{V}_x \bar{V}_{x'} \quad 2.4A$$

Where  $R_x$  is the correlation coefficient  $= (\bar{x}_{x'} - \bar{x} \bar{x}') / (\bar{V}_x \bar{V}_{x'})$

Since  $R_x$  is invariant under a scale change and  $(1+\epsilon) \bar{V}_{x'} = \bar{V}_x$ ; subtracting 2.3A from 2.4A gives

$$\begin{aligned} \bar{V}_x^2 (S_{xe}^{12} - S_{xe}^2) &= [2\epsilon + \epsilon^2 - 2R_x(1+\epsilon)] \bar{V}_{x'}^2 \\ &= \epsilon [2 + \epsilon - 2R_x(1+\epsilon)] \bar{V}_{x'}^2 \end{aligned} \quad 2.5A$$

Equation 2.3A can be rewritten in terms of :

$$\bar{V}_x^2 S_{xe}^2 = [2 + 2\epsilon - 2R_x(1+\epsilon)\epsilon^2] \bar{V}_{x'}^2 \quad 2.6A$$

Substituting 2.6A into 2.5A gives

$$\bar{V}_x^2 (S_{xe}^{12} - S_{xe}^2) = \epsilon [ \bar{V}_x^2 S_{xe}^2 - (\epsilon + \epsilon^2) ] \bar{V}_{x'}^2$$

Dividing by  $\bar{V}_x^2 S_{xe}^2$  gives:

$$\frac{S_{xe}^{12} - S_{xe}^2}{S_{xe}^2} = \epsilon - \left[ \frac{(\epsilon^2 + \epsilon^3) \bar{V}_{x'}^2}{\bar{V}_x^2 S_{xe}^2} \right] \quad 2.7A$$

Substituting 2.5A into 2.7A gives:

$$\frac{(S_{xe}^{12} - S_{xe}^2)}{S_{xe}^2} = \epsilon - \left\{ (\epsilon^2 + \epsilon^3) / [2(1+\epsilon)(1-R_x + \epsilon^2)] \right\} \quad 2.8A$$

This result is independent of whether  $\hat{\delta}_{xe}$  is at the minimum or not and thus may be positive or negative.

A.3 The Effect of The Change In  $\Sigma_{ne}$  On  $\delta_{xe}^2$  When  $\delta_{xe}$  Is Minimized.

Considering the primed variates to be uncorrected and the unprimed variates to be the variables corrected for the DV bias, then according to Section A.2:

$$\sigma_x^2 \Delta \sigma_x^2 = \sigma_x^2 - \sigma_{x'}^2$$

3.1A

$$\sigma^2 \delta_{xe}^2 = \sigma_x^2 + \sigma_{x'}^2 - 2 R_x \sigma_x \sigma_{x'}$$

At the minimum:

$$\sigma_x^2 \delta_{xe}^2 = \sigma_x^2 \Delta \sigma_x^2$$

$$\sigma_x^2 - \sigma_{x'}^2 = \sigma_x^2 + \sigma_{x'}^2 - 2 R_x \sigma_x \sigma_{x'}$$

which reduces to

$$R_x = \frac{\sigma_{x'}}{\sigma_x}$$

3.2A

Now:

$$\sigma^2 \delta_{xe}^2 = \sigma_x^2 + \sigma_{x'}^2 - R_x \sigma_x^2$$

$$\sigma_x^2 (\delta_{xe}^2 - \delta_{xe}^2) = \sigma_x^2 - \sigma_{x1}^2 - 2R_x\sigma_x(\sigma_x - \sigma_{x1})$$

3. 3A

Substituting Equation 3. 1A gives:

$$\sigma_x^2 (\delta_{xe}^2 - \delta_{xe}^2) = \sigma_x^2 - \sigma_{x1}^2 - 2\sigma_{x1}(\sigma_x - \sigma_{x1}) = (\sigma_x - \sigma_{x1})^2$$

$$\text{or: } \delta_{xe}^2 - \delta_{xe}^2 = \left( \frac{\sigma_x - \sigma_{x1}}{\sigma_x} \right)^2 = (1 - R_x)^2$$

#### A.4 Proof That A Shift Of $\frac{1}{2}$ Is Induced Between The VA And 3H Variates At Station N.

If we let the spectral components of the VA series at any cycle be  $(a_1 + ib_1)$ , and the 3H series be  $(a_2 + ib_2)$ . Since the Fourier transform of the residuals is a linear operation, the power at the residuals is :

$$\frac{(a_2 - a_1)^2}{2} + \frac{(b_2 - b_1)^2}{2} = \frac{(a_1^2 + b_1^2) + (a_2^2 + b_2^2) - 2(a_1a_2 + b_1b_2)}{2} \quad 4. 1A$$

if we consider that the VA variate must be stretched and rotated to match the 3H variate then

$$(a_2 + ib_2) = m(a_1 + ib_1) e^{i\theta} \quad 4. 2A$$

where: a.  $m$  is the stretch; and

b.  $\theta$  is the angle from the VA to the 3H spectral pairs.

Expanding  $e^{i\theta}$  and matching real and imaginary parts gives:

$$a_2 = m (a_1 \cos\theta - b_1 \sin\theta)$$

$$b_2 = m (a_1 \cos\theta + b_1 \sin\theta)$$

4.3A

Squaring both sides of Equation 4.3A gives the identity

$$(a_2^2 + b_2^2) = m^2 (a_1^2 + b_1^2)^2$$

4.4A

Substituting Equations 4.2A and 4.3A into 4.4A gives

$$(a_2 - a_1)^2 + (b_2 - b_1)^2 = (a_1^2 + b_1^2)(1 - 2m \cos^2\theta + m^2)$$

4.5A

From Figure 5-12, the residual power at the annual cycle is approximately equal to the sum of the power of the 3H and VA series, or:

$$\begin{aligned} (a_2 - a_1)^2 + (b_2 - b_1)^2 &= (a_1^2 + b_1^2) + (a_2^2 + b_2^2) \\ &= (a_1^2 + b_1^2)(1 - 2m \cos^2\theta + m^2) \end{aligned}$$

4.6A

Using 4.4A gives:

$$(a_1^2 + b_1^2) 2m \cos^2\theta = 0$$

Neither  $m$  nor the VA power density equals 0.0 thus  $= \pm$   
or, a  $90^\circ$  phase shift has been induced between the 3H and VA series at the annual cycle.

Appendix B

Difference means in dPa, difference variances, residual variances, and correlation coefficients for the uncorrected VA stress. The first row gives the averaging length in days.

## DIFFERENCE MEANS - CONSTANT D.C. X COMPONENT

SHIP	0.25	0.50	1.0	2.0	4.0	7.0	14.0	28.0
A	.002	.008	.022	.044	.067	.070	.069	.068
B	.010	.022	.051	.098	.145	.175	.220	.247
C	.022	.058	.127	.233	.329	.391	.458	.511
D	.034	.079	.162	.275	.371	.437	.516	.587
E	.015	.034	.066	.112	.151	.182	.227	.261
I	.012	.027	.056	.098	.135	.159	.202	.234
J	.020	.049	.101	.175	.248	.296	.383	.449
K	.018	.043	.083	.128	.164	.204	.257	.313
M	.007	.017	.038	.065	.090	.118	.153	.172
N	.007	.011	.013	.017	.035	.058	.085	.113
P	.014	.034	.065	.098	.127	.136	.152	.177

## DIFFERENCE MEANS - CONSTANT D.C. Y COMPONENT

SHIP	0.25	0.50	1.0	2.0	4.0	7.0	14.0	28.0
A	.002	.007	.009	.009	.007	.012	.007	.016
B	.004	.008	.023	.054	.094	.125	.157	.183
C	.012	.029	.042	.048	.052	.052	.063	.068
D	.015	.036	.056	.073	.077	.089	.100	.109
E	.007	.015	.023	.039	.050	.066	.086	.105
I	.015	.035	.063	.093	.133	.170	.210	.249
J	.014	.034	.068	.093	.127	.161	.199	.224
K	.002	.006	.008	.006	.002	.015	.032	.021
M	.001	.005	.007	.008	.000	.006	.026	.028
N	.004	.005	.006	.009	.017	.022	.033	.044
P	.026	.062	.126	.225	.331	.398	.501	.578

## DIFFERENCE MEANS - LINEAR D.C. X COMPONENT

SHIP	0.25	0.50	1.0	2.0	4.0	7.0	14.0	28.0
A	.005	.017	.043	.082	.115	.117	.113	.113
B	.016	.033	.075	.139	.195	.225	.266	.289
C	.040	.101	.212	.370	.495	.561	.627	.674
D	.057	.133	.265	.420	.538	.609	.686	.753
E	.023	.052	.098	.156	.201	.233	.274	.302
I	.022	.049	.098	.160	.212	.241	.286	.317
J	.035	.082	.162	.270	.363	.417	.508	.565
K	.030	.069	.127	.187	.232	.278	.330	.377
M	.012	.030	.062	.100	.134	.163	.195	.210
N	.006	.009	.009	.012	.027	.044	.065	.086
P	.024	.056	.100	.141	.167	.171	.181	.201

## DIFFERENCE MEANS - LINEAR D.C. Y COMPONENT

SHIP	0.25	0.50	1.0	2.0	4.0	7.0	14.0	28.0
A	.004	.013	.020	.024	.026	.027	.007	.001
B	.010	.019	.048	.103	.164	.200	.233	.256
C	.021	.047	.066	.064	.065	.062	.072	.076
D	.024	.056	.079	.092	.086	.093	.102	.109
E	.009	.020	.028	.042	.047	.059	.075	.089
I	.025	.059	.101	.145	.197	.235	.274	.309
J	.023	.054	.101	.132	.168	.201	.236	.258
K	.004	.011	.012	.010	.003	.013	.026	.017
M	.003	.010	.014	.018	.013	.022	.043	.045
N	.003	.004	.004	.007	.014	.019	.028	.036
P	.043	.104	.206	.349	.484	.560	.660	.723

## DIFFERENCE VARIANCES - CONSTANT D.C. X COMPONENT

SHIP	0.25	0.50	1.0	2.0	4.0	7.0	14.0	28.0
A	.041	.103	.201	.347	.487	.585	.710	.810
B	.042	.099	.197	.335	.507	.624	.725	.811
C	.042	.100	.190	.336	.486	.549	.640	.719
D	.045	.103	.209	.341	.465	.539	.626	.740
E	.044	.098	.182	.313	.444	.552	.641	.694
I	.037	.090	.173	.299	.440	.524	.648	.749
J	.035	.082	.158	.270	.390	.477	.595	.666
K	.040	.091	.171	.258	.369	.490	.634	.726
M	.038	.093	.186	.320	.464	.587	.703	.781
N	.049	.096	.160	.240	.355	.426	.520	.602
P	.048	.115	.234	.366	.489	.607	.710	.781

## DIFFERENCE VARIANCES - CONSTANT D.C. Y COMPONENT

SHIP	0.25	0.50	1.0	2.0	4.0	7.0	14.0	28.0
A	.038	.095	.187	.325	.465	.595	.714	.801
B	.043	.106	.215	.375	.540	.634	.725	.809
C	.058	.137	.255	.405	.561	.652	.728	.793
D	.060	.142	.255	.399	.574	.659	.743	.827
E	.051	.110	.214	.339	.486	.596	.728	.812
I	.045	.106	.197	.321	.461	.561	.648	.703
J	.043	.102	.197	.317	.456	.570	.654	.715
K	.047	.107	.207	.323	.450	.589	.705	.806
M	.037	.090	.177	.293	.445	.539	.697	.785
N	.053	.105	.172	.285	.406	.522	.629	.711
P	.041	.098	.194	.331	.468	.520	.628	.691

## DIFFERENCE VARIANCES - LINEAR D.C. X COMPONENT

SHIP	0.25	0.50	1.0	2.0	4.0	7.0	14.0	28.0
A	.070	.174	.321	.513	.660	.746	.847	.908
B	.073	.165	.311	.480	.690	.787	.860	.910
C	.072	.168	.301	.513	.687	.741	.818	.876
D	.081	.183	.358	.535	.667	.727	.809	.894
E	.077	.163	.297	.470	.617	.717	.796	.833
I	.067	.156	.283	.457	.617	.700	.802	.876
J	.063	.143	.266	.421	.571	.660	.777	.830
K	.072	.162	.295	.411	.548	.667	.781	.850
M	.064	.155	.294	.465	.626	.736	.830	.876
N	.077	.150	.239	.334	.457	.522	.595	.659
P	.089	.198	.376	.546	.674	.779	.850	.891

## DIFFERENCE VARIANCES - LINEAR D.C. Y COMPONENT

SHIP	0.25	0.50	1.0	2.0	4.0	7.0	14.0	28.0
A	.064	.157	.296	.480	.633	.762	.849	.899
B	.073	.175	.338	.536	.707	.785	.852	.906
C	.106	.233	.396	.582	.738	.807	.858	.897
D	.107	.239	.401	.566	.749	.808	.859	.916
E	.094	.189	.334	.489	.641	.740	.830	.884
I	.080	.186	.323	.483	.641	.736	.802	.839
J	.078	.180	.323	.476	.641	.741	.803	.843
K	.083	.188	.338	.490	.618	.750	.826	.890
M	.062	.151	.281	.438	.606	.692	.819	.870
N	.084	.160	.250	.387	.516	.623	.706	.770
P	.075	.168	.318	.515	.670	.723	.819	.856

## RESIDUAL VARIANCE - CONSTANT D.C. X COMPONENT

SHIP	0.25	0.50	1.0	2.0	4.0	7.0	14.0	28.0
A	.003	.010	.030	.072	.132	.187	.271	.367
B	.003	.010	.029	.072	.138	.206	.283	.360
C	.004	.011	.030	.070	.125	.154	.213	.267
D	.004	.013	.037	.076	.121	.160	.205	.287
E	.003	.009	.023	.058	.105	.156	.205	.246
I	.003	.008	.022	.050	.096	.135	.213	.300
J	.003	.008	.021	.046	.082	.117	.178	.227
K	.003	.008	.019	.038	.069	.116	.208	.283
M	.003	.008	.024	.059	.109	.172	.256	.349
N	.003	.007	.016	.037	.077	.110	.164	.220
P	.004	.012	.037	.077	.125	.187	.257	.320

## RESIDUAL VARIANCE - CONSTANT D.C. Y COMPONENT

SHIP	0.25	0.50	1.0	2.0	4.0	7.0	14.0	28.0
A	.002	.008	.025	.062	.119	.185	.276	.366
B	.003	.010	.032	.086	.166	.224	.294	.380
C	.005	.016	.045	.097	.167	.220	.286	.346
D	.007	.020	.049	.101	.186	.243	.312	.393
E	.004	.012	.033	.071	.141	.196	.286	.378
I	.004	.011	.026	.059	.108	.157	.225	.287
J	.003	.010	.029	.062	.108	.166	.220	.270
K	.004	.011	.030	.057	.103	.166	.256	.370
M	.002	.007	.022	.051	.104	.148	.255	.345
N	.004	.010	.020	.050	.095	.148	.218	.286
P	.004	.011	.031	.074	.125	.146	.203	.257

## RESIDUAL VARIANCE - LINEAR D.C. X COMPONENT

SHIP	0.25	0.50	1.0	2.0	4.0	7.0	14.0	28.0
A	.007	.024	.069	.158	.262	.335	.433	.529
B	.008	.023	.068	.149	.272	.365	.449	.528
C	.008	.024	.067	.158	.269	.307	.391	.466
D	.009	.031	.095	.183	.264	.317	.383	.496
E	.008	.022	.054	.127	.200	.274	.344	.385
I	.007	.021	.053	.114	.198	.256	.360	.464
J	.006	.020	.049	.106	.178	.230	.331	.392
K	.006	.020	.052	.090	.153	.224	.337	.422
M	.006	.019	.054	.120	.203	.292	.396	.476
N	.007	.015	.032	.064	.120	.159	.211	.267
P	.011	.033	.094	.175	.256	.345	.425	.489

## RESIDUAL VARIANCE - LINEAR D.C. Y COMPONENT

SHIP	0.25	0.50	1.0	2.0	4.0	7.0	14.0	28.0
A	.005	.020	.057	.132	.232	.336	.437	.519
B	.007	.024	.073	.179	.310	.382	.457	.539
C	.014	.042	.106	.209	.324	.384	.451	.504
D	.017	.051	.117	.211	.349	.412	.478	.561
E	.011	.029	.077	.141	.251	.321	.411	.493
I	.009	.028	.063	.130	.218	.295	.376	.436
J	.009	.027	.070	.133	.223	.305	.365	.415
K	.009	.028	.076	.134	.204	.301	.392	.510
M	.005	.017	.052	.107	.197	.256	.383	.462
N	.009	.019	.038	.084	.147	.211	.282	.349
P	.010	.027	.074	.168	.263	.295	.384	.449

## CORRELATION COEFFICIENT - CONSTANT D.C. X COMPONENT

SHIP	0.25	0.50	1.0	2.0	4.0	7.0	14.0	28.0
A	.999	.996	.990	.978	.964	.953	.946	.945
B	.999	.996	.990	.977	.965	.954	.946	.953
C	.998	.996	.989	.978	.968	.966	.956	.957
D	.998	.995	.986	.975	.967	.958	.956	.954
E	.999	.997	.992	.982	.973	.965	.963	.959
I	.999	.997	.992	.986	.978	.972	.960	.949
J	.999	.997	.993	.985	.978	.972	.964	.957
K	.999	.997	.994	.989	.984	.976	.957	.947
M	.999	.997	.992	.983	.975	.965	.955	.930
N	.999	.997	.995	.988	.976	.966	.949	.933
P	.998	.995	.988	.978	.970	.962	.959	.960

## CORRELATION COEFFICIENT - CONSTANT D.C. Y COMPONENT

SHIP	0.25	0.50	1.0	2.0	4.0	7.0	14.0	28.0
A	.999	.997	.992	.982	.968	.958	.944	.933
B	.999	.996	.989	.973	.954	.944	.936	.929
C	.998	.994	.985	.971	.960	.956	.946	.946
D	.997	.992	.982	.967	.950	.941	.933	.937
E	.998	.996	.988	.978	.957	.950	.944	.934
I	.998	.996	.992	.983	.974	.967	.950	.927
J	.999	.996	.990	.981	.973	.964	.958	.950
K	.998	.996	.990	.984	.976	.971	.957	.935
M	.999	.997	.993	.985	.974	.967	.952	.937
N	.998	.996	.993	.985	.972	.962	.946	.933
P	.998	.996	.988	.975	.965	.962	.958	.946

## CORRELATION COEFFICIENT - LINEAR D.C. X COMPONENT

SHIP	0.25	0.50	1.0	2.0	4.0	7.0	14.0	28.0
A	.997	.991	.977	.952	.925	.912	.920	.929
B	.997	.991	.976	.950	.933	.919	.923	.938
C	.997	.991	.976	.952	.933	.935	.927	.933
D	.996	.988	.965	.940	.926	.915	.924	.935
E	.997	.992	.983	.964	.956	.948	.953	.956
I	.997	.992	.983	.969	.958	.953	.942	.939
J	.997	.992	.983	.968	.955	.952	.944	.943
K	.997	.993	.984	.977	.966	.961	.943	.941
M	.997	.993	.983	.967	.957	.945	.939	.920
N	.997	.995	.991	.981	.966	.954	.938	.920
P	.995	.988	.969	.949	.937	.932	.936	.941

SHIP	CORRELATION COEFFICIENT - LINEAR D.C. Y COMPONENT							
	0.25	0.50	1.0	2.0	4.0	7.0	14.0	28.0
A	.998	.993	.982	.962	.937	.924	.919	.916
B	.997	.991	.976	.943	.908	.899	.899	.905
C	.994	.985	.963	.935	.917	.921	.917	.931
D	.993	.980	.958	.928	.901	.890	.883	.901
E	.995	.989	.974	.958	.924	.921	.921	.915
I	.996	.990	.981	.965	.952	.943	.924	.903
J	.996	.990	.976	.961	.948	.937	.938	.937
K	.996	.990	.975	.963	.953	.949	.937	.904
M	.998	.994	.983	.970	.954	.948	.938	.925
N	.996	.993	.989	.976	.961	.949	.933	.918
P	.995	.990	.974	.946	.929	.933	.937	.916

Appendix C - Part I

The  $\bar{Z}_{ne}$  values for the stresses after correction for the systematic bias in the variance differences. 0.0 indicates no data.

## STATION - A CONSTANT D.C.

SPEED	0.25	0.50	1.0	2.0	4.0	7.0	14.0	28.0
0.4	4.82	7.56	9.38	42.93	0.0	45.11	181.5	14.81
1.6	2.33	4.28	8.17	9.38	14.35	20.58	17.53	18.62
3.4	1.31	1.70	2.42	3.05	3.83	4.13	4.63	5.05
5.5	1.13	1.31	1.60	2.02	2.46	2.65	2.96	3.12
8.0	1.06	1.16	1.33	1.56	1.77	2.00	2.07	2.26
10.8	1.04	1.10	1.21	1.36	1.51	1.54	1.69	1.83
13.9	1.03	1.07	1.13	1.23	1.32	1.43	1.48	1.46
17.2	1.02	1.05	1.10	1.17	1.21	1.17	0.0	0.0
20.8	1.01	1.04	1.09	1.11	1.13	1.06	0.0	0.0
24.5	1.02	1.03	1.06	1.11	1.08	0.0	0.0	0.0
28.5	1.01	1.03	1.05	0.0	0.0	0.0	0.0	0.0
33.5	1.01	1.03	0.0	0.0	0.0	0.0	0.0	0.0
35.0	1.00	0.0	0.0	0.0	0.0	0.0	0.0	0.0

## STATION - B CONSTANT D.C.

SPEED	0.25	0.50	1.0	2.0	4.0	7.0	14.0	28.0
0.4	7.30	9.73	46.06	34.76	106.7	97.29	78.98	69.30
1.6	2.78	4.85	9.83	13.87	19.86	16.39	15.62	14.82
3.4	1.31	1.67	2.33	3.32	4.01	4.35	4.58	4.85
5.5	1.14	1.30	1.67	2.15	2.49	2.78	2.97	3.22
8.0	1.07	1.18	1.36	1.63	1.90	2.02	2.21	2.19
10.8	1.05	1.11	1.23	1.40	1.56	1.68	1.74	1.85
13.9	1.03	1.07	1.15	1.28	1.36	1.41	1.42	0.0
17.2	1.02	1.06	1.11	1.17	1.24	1.28	1.23	0.0
20.8	1.02	1.04	1.08	1.11	1.17	1.11	0.0	0.0
24.5	1.02	1.03	1.07	1.08	0.0	0.0	0.0	0.0
28.5	1.01	1.03	1.04	1.06	0.0	0.0	0.0	0.0
33.5	1.01	1.02	1.02	1.04	0.0	0.0	0.0	0.0
35.0	1.00	0.0	0.0	0.0	0.0	0.0	0.0	0.0

## STATION - C CONSTANT D.C.

SPEED	0.25	0.50	1.0	2.0	4.0	7.0	14.0	28.0
0.4	12.66	14.65	30.89	27.14	56.65	280.2	65.84	274.9
1.6	3.28	5.49	8.09	15.35	17.66	17.00	26.85	21.48
3.4	1.36	1.79	2.49	3.12	3.68	3.98	4.40	4.72
5.5	1.17	1.36	1.72	2.12	2.35	2.52	2.78	2.83
8.0	1.09	1.19	1.39	1.61	1.81	1.95	2.05	2.16
10.8	1.05	1.12	1.24	1.37	1.52	1.62	1.72	1.87
13.9	1.04	1.08	1.16	1.26	1.40	1.43	1.49	1.65
17.2	1.03	1.06	1.12	1.23	1.29	1.35	1.42	0.0
20.8	1.02	1.05	1.10	1.14	1.18	1.23	0.0	0.0
24.5	1.02	1.04	1.07	1.13	0.0	0.0	0.0	0.0
28.5	1.02	1.04	1.06	0.0	0.0	0.0	0.0	0.0
33.5	1.02	1.04	1.05	0.0	0.0	0.0	0.0	0.0
35.0	1.01	1.02	0.0	0.0	0.0	0.0	0.0	0.0

## STATION - D CONSTANT D.C.

SPEED	0.25	0.50	1.0	2.0	4.0	7.0	14.0	28.0
0.4	14.33	9.74	38.77	75.11	173.1	91.56	555.1	325.8
1.6	3.00	6.40	8.66	13.43	18.13	19.68	22.87	16.40
3.4	1.38	1.81	2.50	3.46	3.77	3.97	4.22	4.31
5.5	1.18	1.36	1.72	2.05	2.38	2.48	2.70	2.80
8.0	1.08	1.20	1.37	1.58	1.81	1.93	2.08	2.36
10.8	1.05	1.13	1.23	1.40	1.53	1.68	1.78	2.02
13.9	1.04	1.09	1.18	1.28	1.42	1.49	1.65	1.64
17.2	1.03	1.07	1.13	1.21	1.31	1.31	1.41	0.0
20.8	1.02	1.05	1.11	1.12	1.15	1.17	1.28	0.0
24.5	1.02	1.04	1.05	1.12	1.16	0.0	0.0	0.0
28.5	1.02	1.04	1.06	1.28	0.0	0.0	0.0	0.0
33.5	1.02	1.03	1.20	0.0	0.0	0.0	0.0	0.0
35.0	1.03	1.06	0.0	0.0	0.0	0.0	0.0	0.0

## STATION - E CONSTANT D.C.

SPEED	0.25	0.50	1.0	2.0	4.0	7.0	14.0	28.0
0.4	8.03	6.20	10.29	15.52	47.59	51.96	30.76	28.10
1.6	1.98	3.90	4.59	8.34	12.14	13.58	15.86	12.45
3.4	1.18	1.39	1.75	2.42	2.90	3.16	3.46	3.34
5.5	1.10	1.20	1.37	1.63	1.93	2.04	2.26	2.57
8.0	1.05	1.11	1.21	1.37	1.54	1.73	1.84	2.07
10.8	1.04	1.08	1.16	1.25	1.38	1.47	1.62	1.64
13.9	1.03	1.06	1.12	1.20	1.28	1.36	1.37	1.50
17.2	1.02	1.05	1.09	1.13	1.22	1.18	0.0	0.0
20.8	1.02	1.04	1.06	1.14	1.15	0.0	0.0	0.0
24.5	1.02	1.03	1.08	1.05	0.0	0.0	0.0	0.0
28.5	1.01	1.02	0.0	0.0	0.0	0.0	0.0	0.0
33.5	1.07	1.20	1.09	0.0	0.0	0.0	0.0	0.0
35.0	1.01	1.01	0.0	0.0	0.0	0.0	0.0	0.0

## STATION - I CONSTANT D.C.

SPEED	0.25	0.50	1.0	2.0	4.0	7.0	14.0	28.0
0.4	6.29	24.89	12.18	174.5	49.46	0.0	0.0	0.0
1.6	2.22	3.61	10.92	12.04	15.23	16.61	19.63	22.02
3.4	1.48	1.82	2.50	2.91	3.52	3.76	4.30	4.51
5.5	1.15	1.33	1.58	1.93	2.27	2.50	2.77	2.96
8.0	1.06	1.15	1.31	1.52	1.71	1.85	1.99	2.08
10.8	1.05	1.11	1.20	1.31	1.45	1.53	1.64	1.61
13.9	1.03	1.07	1.12	1.21	1.29	1.36	1.43	1.62
17.2	1.02	1.05	1.09	1.15	1.23	1.28	1.32	0.0
20.8	1.02	1.04	1.07	1.14	1.14	1.28	0.0	0.0
24.5	1.02	1.04	1.07	1.08	1.18	0.0	0.0	0.0
28.5	1.02	1.04	1.05	1.07	0.0	0.0	0.0	0.0
33.5	1.01	1.04	0.0	0.0	0.0	0.0	0.0	0.0
35.0	1.00	0.0	0.0	0.0	0.0	0.0	0.0	0.0

## STATION - J CONSTANT D.C.

SPEED	0.25	0.50	1.0	2.0	4.0	7.0	14.0	28.0
0.4	5.68	7.79	11.42	59.90	53.68	0.0	0.0	69.29
1.6	2.19	4.89	5.20	16.74	19.87	19.98	20.25	6.94
3.4	1.39	1.76	2.30	2.90	3.39	3.62	4.22	4.12
5.5	1.14	1.30	1.54	1.87	2.20	2.39	2.53	2.71
8.0	1.05	1.14	1.29	1.47	1.60	1.78	1.87	1.99
10.8	1.04	1.09	1.18	1.28	1.40	1.49	1.60	1.65
13.9	1.02	1.06	1.12	1.19	1.28	1.34	1.39	1.46
17.2	1.02	1.04	1.09	1.14	1.21	1.29	0.0	0.0
20.8	1.02	1.04	1.07	1.12	1.15	1.10	0.0	0.0
24.5	1.02	1.03	1.07	1.07	1.03	0.0	0.0	0.0
28.5	1.01	1.04	1.03	1.02	0.0	0.0	0.0	0.0
33.5	1.01	1.01	0.0	0.0	0.0	0.0	0.0	0.0
35.0	1.02	0.0	0.0	0.0	0.0	0.0	0.0	0.0

## STATION - K CONSTANT D.C.

SPEED	0.25	0.50	1.0	2.0	4.0	7.0	14.0	28.0
0.4	5.26	8.51	11.57	70.47	52.89	114.9	612.0	94.15
1.6	1.43	3.20	5.50	8.96	8.83	10.20	16.15	17.90
3.4	1.27	1.45	1.83	2.37	2.87	3.20	3.59	3.86
5.5	1.11	1.22	1.41	1.65	1.93	2.16	2.44	2.72
8.0	1.05	1.12	1.22	1.35	1.51	1.68	1.91	2.01
10.8	1.03	1.08	1.15	1.22	1.34	1.45	1.60	1.69
13.9	1.02	1.06	1.11	1.19	1.26	1.36	1.39	0.0
17.2	1.02	1.05	1.08	1.13	1.18	1.24	0.0	0.0
20.8	1.02	1.04	1.08	1.12	1.13	0.0	0.0	0.0
24.5	1.02	1.03	1.12	1.14	0.0	0.0	0.0	0.0
28.5	1.02	1.06	1.04	0.0	0.0	0.0	0.0	0.0
33.5	1.02	1.03	0.0	0.0	0.0	0.0	0.0	0.0
35.0	1.04	0.0	0.0	0.0	0.0	0.0	0.0	0.0

## STATION - M CONSTANT D.C.

SPEED	0.25	0.50	1.0	2.0	4.0	7.0	14.0	28.0
0.4	2.65	6.05	10.02	42.93	54.42	74.38	46.18	47.17
1.6	1.82	3.73	6.67	9.66	14.21	15.96	18.08	13.69
3.4	1.30	1.64	2.10	2.72	3.33	3.55	4.11	4.28
5.5	1.12	1.26	1.49	1.81	2.10	2.30	2.57	2.95
8.0	1.05	1.13	1.27	1.46	1.64	1.80	1.98	2.05
10.8	1.03	1.08	1.17	1.27	1.38	1.48	1.53	1.60
13.9	1.02	1.05	1.10	1.18	1.26	1.33	1.50	1.49
17.2	1.02	1.04	1.08	1.12	1.18	1.12	0.0	0.0
20.8	1.01	1.03	1.06	1.12	1.27	1.22	0.0	0.0
24.5	1.01	1.03	1.07	1.15	0.0	0.0	0.0	0.0
28.5	1.01	1.04	1.03	0.0	0.0	0.0	0.0	0.0
33.5	1.01	1.06	0.0	0.0	0.0	0.0	0.0	0.0
35.0	1.02	0.0	0.0	0.0	0.0	0.0	0.0	0.0

## STATION - N CONSTANT D.C.

SPEED	0.25	0.50	1.0	2.0	4.0	7.0	14.0	28.0
0.4	5.24	5.66	9.55	20.05	21.98	31.36	46.07	81.31
1.6	2.02	3.08	4.15	6.15	7.58	8.90	15.69	12.95
3.4	1.18	1.35	1.57	1.95	2.49	2.86	2.90	3.28
5.5	1.08	1.14	1.23	1.40	1.59	1.73	1.87	1.92
8.0	1.04	1.07	1.12	1.20	1.29	1.36	1.44	1.49
10.8	1.03	1.05	1.09	1.14	1.20	1.28	1.27	1.22
13.9	1.02	1.05	1.09	1.13	1.20	1.10	0.0	0.0
17.2	1.02	1.04	1.07	1.13	1.19	0.0	0.0	0.0
20.8	1.02	1.03	1.05	1.07	0.0	0.0	0.0	0.0
24.5	1.01	1.02	0.0	0.0	0.0	0.0	0.0	0.0
28.5	0.0	0.0	0.0	0.0	0.0	0.0	0.0	0.0
33.5	0.0	0.0	0.0	0.0	0.0	0.0	0.0	0.0
35.0	0.0	0.0	0.0	0.0	0.0	0.0	0.0	0.0

## STATION - P CONSTANT D.C.

SPEED	0.25	0.50	1.0	2.0	4.0	7.0	14.0	28.0
0.4	10.71	4.53	45.24	20.22	16.54	9.90	0.0	0.0
1.6	2.49	3.80	7.39	9.60	24.39	23.14	33.49	0.0
3.4	1.29	1.76	2.21	3.01	3.51	4.01	4.07	4.06
5.5	1.13	1.31	1.61	1.97	2.27	2.54	2.58	2.78
8.0	1.07	1.18	1.34	1.60	1.78	1.84	2.04	2.22
10.8	1.05	1.12	1.23	1.36	1.48	1.58	1.67	1.82
13.9	1.03	1.08	1.16	1.25	1.35	1.40	1.57	1.44
17.2	1.02	1.06	1.11	1.19	1.26	1.30	0.0	0.0
20.8	1.02	1.05	1.09	1.14	1.16	0.0	0.0	0.0
24.5	1.02	1.03	1.07	1.13	0.0	0.0	0.0	0.0
28.5	1.01	1.04	1.06	0.0	0.0	0.0	0.0	0.0
33.5	1.01	1.02	0.0	0.0	0.0	0.0	0.0	0.0
35.0	1.02	1.02	0.0	0.0	0.0	0.0	0.0	0.0

## STATION - A LINEAR D.C.

SPEED	0.25	0.50	1.0	2.0	4.0	7.0	14.0	28.0
0.4	4.83	7.59	9.47	50.75	0.0	58.34	183.8	15.62
1.6	2.33	4.33	10.63	13.30	21.22	33.06	26.24	29.29
3.4	1.32	1.73	2.69	3.55	4.81	5.21	6.40	7.01
5.5	1.14	1.35	1.73	2.36	3.14	3.51	4.04	4.25
8.0	1.07	1.20	1.46	1.86	2.27	2.74	2.90	3.31
10.8	1.08	1.18	1.41	1.72	2.07	2.12	2.43	2.77
13.9	1.06	1.14	1.26	1.49	1.71	1.96	2.06	1.99
17.2	1.04	1.11	1.21	1.38	1.47	1.37	0.0	0.0
20.8	1.03	1.09	1.19	1.24	1.28	1.13	0.0	0.0
24.5	1.03	1.07	1.13	1.24	1.19	0.0	0.0	0.0
28.5	1.02	1.05	1.12	0.0	0.0	0.0	0.0	0.0
33.5	1.02	1.08	0.0	0.0	0.0	0.0	0.0	0.0
35.0	1.01	0.0	0.0	0.0	0.0	0.0	0.0	0.0

STATION - B LINEAR D.C.									
SPEED	0.25	0.50	1.0	2.0	4.0	7.0	14.0	28.0	
0.4	7.31	9.78	57.34	37.94	182.0	146.5	112.7	139.4	
1.6	2.78	5.29	11.65	17.11	29.73	25.06	25.11	22.23	
3.4	1.32	1.72	2.58	4.10	5.17	5.82	6.29	6.64	
5.5	1.15	1.33	1.85	2.59	3.19	3.78	4.08	4.58	
8.0	1.09	1.24	1.51	2.00	2.53	2.78	3.13	3.12	
10.8	1.09	1.21	1.44	1.82	2.18	2.44	2.58	2.78	
13.9	1.06	1.15	1.32	1.60	1.79	1.91	1.95	0.0	
17.2	1.05	1.12	1.23	1.38	1.52	1.63	1.49	0.0	
20.8	1.04	1.09	1.18	1.24	1.38	1.23	0.0	0.0	
24.5	1.04	1.07	1.16	1.20	0.0	0.0	0.0	0.0	
28.5	1.03	1.07	1.09	1.13	0.0	0.0	0.0	0.0	
33.5	1.02	1.05	1.05	1.09	0.0	0.0	0.0	0.0	
35.0	1.00	0.0	0.0	0.0	0.0	0.0	0.0	0.0	
STATION - C LINEAR D.C.									
SPEED	0.25	0.50	1.0	2.0	4.0	7.0	14.0	28.0	
0.4	12.71	14.79	35.98	28.31	91.02	443.7	88.52	384.9	
1.6	3.36	5.80	9.64	21.07	28.05	25.22	48.62	40.70	
3.4	1.39	1.87	2.83	3.72	4.58	4.96	5.76	6.32	
5.5	1.18	1.42	1.92	2.56	2.93	3.22	3.72	3.78	
8.0	1.11	1.26	1.57	1.98	2.36	2.66	2.84	3.11	
10.8	1.10	1.24	1.47	1.75	2.11	2.34	2.58	2.88	
13.9	1.07	1.17	1.35	1.58	1.92	1.96	2.11	2.53	
17.2	1.06	1.14	1.27	1.51	1.67	1.79	2.00	0.0	
20.8	1.05	1.12	1.22	1.31	1.41	1.53	0.0	0.0	
24.5	1.04	1.09	1.16	1.30	0.0	0.0	0.0	0.0	
28.5	1.04	1.09	1.13	0.0	0.0	0.0	0.0	0.0	
33.5	1.04	1.09	1.12	0.0	0.0	0.0	0.0	0.0	
35.0	1.03	1.04	0.0	0.0	0.0	0.0	0.0	0.0	
STATION - D LINEAR D.C.									
SPEED	0.25	0.50	1.0	2.0	4.0	7.0	14.0	28.0	
0.4	19.36	9.84	40.49	88.10	362.7	137.4	1034.	457.0	
1.6	3.04	7.42	9.74	16.64	29.11	29.75	38.98	31.79	
3.4	1.41	1.94	2.87	4.34	4.66	4.99	5.44	5.66	
5.5	1.20	1.42	1.97	2.45	2.97	3.15	3.59	3.74	
8.0	1.11	1.28	1.57	1.93	2.37	2.61	2.89	3.48	
10.8	1.10	1.24	1.45	1.83	2.13	2.46	2.73	3.30	
13.9	1.08	1.19	1.39	1.63	1.95	2.11	2.50	2.45	
17.2	1.06	1.15	1.29	1.47	1.69	1.68	1.89	0.0	
20.8	1.05	1.12	1.24	1.28	1.32	1.38	1.64	0.0	
24.5	1.04	1.10	1.13	1.27	1.35	0.0	0.0	0.0	
28.5	1.03	1.10	1.14	1.82	0.0	0.0	0.0	0.0	
33.5	1.04	1.08	1.49	0.0	0.0	0.0	0.0	0.0	
35.0	1.05	1.13	0.0	0.0	0.0	0.0	0.0	0.0	

## STATION - E LINEAR D.C.

SPEED	0.25	0.50	1.0	2.0	4.0	7.0	14.0	28.0
0.4	8.05	6.22	10.40	20.20	80.28	61.55	33.35	43.63
1.6	1.98	4.17	5.01	10.97	16.07	18.03	20.22	16.46
3.4	1.19	1.42	1.81	2.67	3.27	3.65	4.10	3.81
5.5	1.10	1.22	1.43	1.77	2.20	2.33	2.70	3.19
8.0	1.05	1.13	1.28	1.52	1.81	2.15	2.33	2.79
10.8	1.07	1.14	1.30	1.49	1.73	1.94	2.26	2.27
13.9	1.05	1.12	1.25	1.43	1.59	1.78	1.82	2.10
17.2	1.05	1.10	1.18	1.28	1.49	1.41	0.0	0.0
20.8	1.03	1.09	1.14	1.31	1.32	0.0	0.0	0.0
24.5	1.03	1.06	1.18	1.12	0.0	0.0	0.0	0.0
28.5	1.03	1.05	0.0	0.0	0.0	0.0	0.0	0.0
33.5	1.14	1.43	1.22	0.0	0.0	0.0	0.0	0.0
35.0	1.02	1.03	0.0	0.0	0.0	0.0	0.0	0.0

## STATION - I LINEAR D.C.

SPEED	0.25	0.50	1.0	2.0	4.0	7.0	14.0	28.0
0.4	6.30	32.38	12.31	227.81	76.01	0.0	0.0	0.0
1.6	2.22	3.63	13.09	15.37	20.41	30.98	30.83	36.96
3.4	1.49	1.89	2.75	3.29	4.18	4.66	5.60	5.78
5.5	1.16	1.37	1.69	2.19	2.74	3.16	3.67	4.07
8.0	1.08	1.19	1.44	1.78	2.13	2.38	2.66	2.86
10.8	1.09	1.20	1.38	1.62	1.91	2.07	2.33	2.29
13.9	1.05	1.13	1.26	1.43	1.63	1.77	1.93	2.38
17.2	1.04	1.10	1.19	1.33	1.50	1.62	1.67	0.0
20.8	1.03	1.08	1.16	1.31	1.31	1.62	0.0	0.0
24.5	1.04	1.08	1.17	1.19	1.42	0.0	0.0	0.0
28.5	1.04	1.08	1.11	1.16	0.0	0.0	0.0	0.0
33.5	1.02	1.08	0.0	0.0	0.0	0.0	0.0	0.0
35.0	1.01	0.0	0.0	0.0	0.0	0.0	0.0	0.0

## STATION - J LINEAR D.C.

SPEED	0.25	0.50	1.0	2.0	4.0	7.0	14.0	28.0
0.4	5.69	8.36	11.55	84.01	95.85	0.0	0.0	102.2
1.6	2.21	5.26	5.32	20.26	26.00	28.94	28.06	16.79
3.4	1.40	1.81	2.45	3.26	3.93	4.36	5.55	5.20
5.5	1.15	1.33	1.64	2.12	2.66	2.94	3.21	3.45
8.0	1.06	1.18	1.40	1.71	1.92	2.29	2.43	2.67
10.8	1.08	1.18	1.34	1.55	1.81	1.97	2.24	2.36
13.9	1.05	1.13	1.25	1.41	1.61	1.73	1.87	2.02
17.2	1.04	1.09	1.18	1.30	1.46	1.64	0.0	0.0
20.8	1.03	1.08	1.15	1.27	1.33	1.22	0.0	0.0
24.5	1.03	1.08	1.17	1.16	1.08	0.0	0.0	0.0
28.5	1.02	1.08	1.07	1.04	0.0	0.0	0.0	0.0
33.5	1.03	1.03	0.0	0.0	0.0	0.0	0.0	0.0
35.0	1.04	0.0	0.0	0.0	0.0	0.0	0.0	0.0



## STATION - P LINEAR D.C.

SPEED	0.25	0.50	1.0	2.0	4.0	7.0	14.0	28.0
0.4	10.74	4.56	48.14	20.79	17.04	14.01	0.0	0.0
1.6	2.50	3.82	8.64	11.13	41.57	42.75	63.84	0.0
3.4	1.31	1.87	2.44	3.62	4.26	5.22	5.11	5.17
5.5	1.14	1.36	1.77	2.34	2.81	3.30	3.35	3.79
8.0	1.09	1.24	1.50	1.97	2.31	2.42	2.81	3.16
10.8	1.10	1.24	1.46	1.74	1.98	2.23	2.38	2.74
13.9	1.07	1.17	1.34	1.54	1.77	1.89	2.31	1.97
17.2	1.05	1.12	1.24	1.42	1.58	1.67	0.0	0.0
20.8	1.04	1.10	1.20	1.32	1.36	0.0	0.0	0.0
24.5	1.04	1.07	1.16	1.31	0.0	0.0	0.0	0.0
28.5	1.03	1.10	1.15	0.0	0.0	0.0	0.0	0.0
33.5	1.03	1.05	0.0	0.0	0.0	0.0	0.0	0.0
35.0	1.04	1.04	0.0	0.0	0.0	0.0	0.0	0.0

## AVERAGE VALUE - CONSTANT D.C.

SPEED	0.25	0.50	1.0	2.0	4.0	7.0	14.0	28.0
0.4	6.84	9.77	19.68	41.17	71.48	84.77	147.8	75.72
1.6	2.28	4.34	7.32	11.40	15.73	16.43	18.75	17.03
3.4	1.31	1.65	2.21	2.92	3.48	3.78	4.16	4.32
5.5	1.13	1.29	1.56	1.92	2.24	2.42	2.66	2.86
8.0	1.07	1.16	1.31	1.52	1.71	1.87	2.01	2.15
10.8	1.04	1.10	1.20	1.33	1.46	1.56	1.66	1.78
13.9	1.03	1.07	1.14	1.23	1.32	1.39	1.46	1.58
17.2	1.02	1.05	1.10	1.17	1.24	1.28	1.37	0.0
20.8	1.02	1.04	1.08	1.13	1.15	1.19	1.28	0.0
24.5	1.02	1.04	1.07	1.11	1.12	0.0	0.0	0.0
28.5	1.01	1.04	1.05	1.11	0.0	0.0	0.0	0.0
33.5	1.02	1.03	1.08	1.04	0.0	0.0	0.0	0.0
35.0	1.02	1.03	0.0	0.0	0.0	0.0	0.0	0.0

## AVERAGE VALUE - LINEAR D.C.

SPEED	0.25	0.50	1.0	2.0	4.0	7.0	14.0	28.0
0.4	7.14	10.69	21.45	56.38	125.8	126.7	216.6	120.0
1.6	2.29	4.59	8.57	14.58	22.79	24.62	28.56	27.85
3.4	1.32	1.70	2.42	3.41	4.21	4.68	5.36	5.58
5.5	1.15	1.33	1.70	2.22	2.74	3.05	3.47	3.80
8.0	1.08	1.20	1.44	1.79	2.16	2.46	2.72	3.02
10.8	1.08	1.19	1.39	1.66	1.95	2.16	2.40	2.65
13.9	1.06	1.15	1.29	1.50	1.71	1.86	2.04	2.31
17.2	1.05	1.11	1.22	1.37	1.53	1.62	1.81	0.0
20.8	1.04	1.09	1.19	1.28	1.34	1.42	1.64	0.0
24.5	1.04	1.08	1.16	1.25	1.26	0.0	0.0	0.0
28.5	1.03	1.08	1.12	1.29	0.0	0.0	0.0	0.0
33.5	1.03	1.08	1.20	1.09	0.0	0.0	0.0	0.0
35.0	1.03	1.08	0.0	0.0	0.0	0.0	0.0	0.0

Appendix C - Part II

Errors of  $\bar{e}_{ke}$  calculated by the Student 't' test.

## STATION - A CONSTANT D.C.

SPEED	0.25	0.50	1.0	2.0	4.0	7.0	14.0	28.0
0.4	0.74	3.54	8.26	25.75	0.0	0.0	0.0	0.0
1.6	0.30	0.67	3.20	6.76	5.95	8.40	7.24	5.11
3.4	0.02	0.05	0.12	0.17	0.25	0.23	0.29	0.33
5.5	0.01	0.02	0.04	0.06	0.09	0.11	0.13	0.14
8.0	0.00	0.01	0.02	0.03	0.05	0.06	0.10	0.18
10.8	0.00	0.01	0.01	0.02	0.04	0.05	0.11	0.20
13.9	0.00	0.00	0.01	0.02	0.03	0.06	0.10	0.0
17.2	0.00	0.00	0.01	0.02	0.04	0.07	0.0	0.0
20.8	0.00	0.00	0.01	0.02	0.09	0.0	0.0	0.0
24.5	0.00	0.01	0.02	0.05	0.0	0.0	0.0	0.0
28.5	0.00	0.01	0.03	0.0	0.0	0.0	0.0	0.0
33.5	0.01	0.03	0.0	0.0	0.0	0.0	0.0	0.0
35.0	0.0	0.0	0.0	0.0	0.0	0.0	0.0	0.0

## STATION - B CONSTANT D.C.

SPEED	0.25	0.50	1.0	2.0	4.0	7.0	14.0	28.0
0.4	1.10	10.35	34.55	30.98	160.2	320.7	339.1	69.30
1.6	0.41	1.52	2.74	3.62	6.36	5.53	6.38	5.71
3.4	0.02	0.05	0.10	0.19	0.24	0.24	0.25	0.30
5.5	0.01	0.02	0.04	0.06	0.08	0.11	0.13	0.15
8.0	0.00	0.01	0.02	0.03	0.05	0.06	0.07	0.09
10.8	0.00	0.01	0.01	0.02	0.03	0.04	0.07	0.13
13.9	0.00	0.00	0.01	0.02	0.03	0.06	0.10	0.0
17.2	0.00	0.00	0.01	0.02	0.03	0.08	0.0	0.0
20.8	0.00	0.00	0.01	0.02	0.16	0.0	0.0	0.0
24.5	0.00	0.00	0.01	0.04	0.0	0.0	0.0	0.0
28.5	0.00	0.01	0.03	0.0	0.0	0.0	0.0	0.0
33.5	0.00	0.01	0.0	0.0	0.0	0.0	0.0	0.0
35.0	0.0	0.0	0.0	0.0	0.0	0.0	0.0	0.0

## STATION - C CONSTANT D.C.

SPEED	0.25	0.50	1.0	2.0	4.0	7.0	14.0	28.0
0.4	3.36	10.34	39.41	51.84	87.83	0.0	0.0	0.0
1.6	0.56	1.26	2.43	4.66	9.85	5.10	23.70	5.61
3.4	0.03	0.06	0.13	0.17	0.24	0.20	0.30	0.39
5.5	0.01	0.02	0.04	0.07	0.08	0.10	0.11	0.13
8.0	0.01	0.01	0.02	0.03	0.04	0.05	0.07	0.10
10.8	0.00	0.01	0.01	0.02	0.03	0.04	0.08	0.12
13.9	0.00	0.00	0.01	0.02	0.04	0.05	0.07	0.19
17.2	0.00	0.00	0.01	0.03	0.04	0.08	0.0	0.0
20.8	0.00	0.00	0.01	0.03	0.17	0.0	0.0	0.0
24.5	0.00	0.01	0.01	0.04	0.0	0.0	0.0	0.0
28.5	0.00	0.01	0.03	0.0	0.0	0.0	0.0	0.0
33.5	0.01	0.02	0.07	0.0	0.0	0.0	0.0	0.0
35.0	0.01	0.0	0.0	0.0	0.0	0.0	0.0	0.0







## STATION - B LINEAR D.C.

SPEED	0.25	0.50	1.0	2.0	4.0	7.0	14.0	28.0
0.4	1.10	10.35	40.96	39.60	272.7	568.7	622.3	148.7
1.6	0.41	2.22	4.05	5.58	12.23	11.34	11.79	11.22
3.4	0.03	0.06	0.16	0.34	0.46	0.46	0.50	0.59
5.5	0.01	0.02	0.07	0.11	0.15	0.22	0.25	0.33
8.0	0.01	0.01	0.03	0.06	0.09	0.12	0.15	0.18
10.8	0.01	0.01	0.02	0.05	0.08	0.10	0.16	0.28
13.9	0.00	0.01	0.02	0.04	0.07	0.19	0.0	0.0
17.2	0.00	0.01	0.02	0.04	0.07	0.19	0.0	0.0
20.8	0.00	0.01	0.02	0.03	0.36	0.0	0.0	0.0
24.5	0.00	0.01	0.03	0.10	0.0	0.0	0.0	0.0
28.5	0.01	0.02	0.06	0.0	0.0	0.0	0.0	0.0
33.5	0.01	0.03	0.0	0.0	0.0	0.0	0.0	0.0
35.0	0.0	0.0	0.0	0.0	0.0	0.0	0.0	0.0

## STATION - C LINEAR D.C.

SPEED	0.25	0.50	1.0	2.0	4.0	7.0	14.0	28.0
0.4	3.36	10.34	52.26	54.70	168.7	0.0	0.0	0.0
1.6	0.66	1.52	4.84	8.34	22.11	8.59	73.55	13.01
3.4	0.05	0.09	0.23	0.29	0.42	0.33	0.62	0.73
5.5	0.02	0.03	0.07	0.12	0.14	0.19	0.23	0.25
8.0	0.01	0.02	0.03	0.06	0.08	0.12	0.15	0.21
10.8	0.00	0.01	0.02	0.04	0.07	0.09	0.19	0.30
13.9	0.00	0.01	0.02	0.04	0.09	0.12	0.17	0.53
17.2	0.00	0.01	0.02	0.06	0.09	0.19	0.0	0.0
20.8	0.00	0.01	0.03	0.06	0.39	0.0	0.0	0.0
24.5	0.01	0.01	0.03	0.09	0.0	0.0	0.0	0.0
28.5	0.01	0.02	0.05	0.0	0.0	0.0	0.0	0.0
33.5	0.02	0.04	0.17	0.0	0.0	0.0	0.0	0.0
35.0	0.02	0.0	0.0	0.0	0.0	0.0	0.0	0.0

## STATION - D LINEAR D.C.

SPEED	0.25	0.50	1.0	2.0	4.0	7.0	14.0	28.0
0.4	12.41	2.60	45.54	0.0	1281.	1534.	0.0	0.0
1.6	0.53	3.16	4.16	6.67	17.83	12.57	30.32	0.0
3.4	0.04	0.12	0.23	0.34	0.33	0.39	0.53	0.63
5.5	0.02	0.03	0.09	0.11	0.14	0.17	0.23	0.25
8.0	0.01	0.02	0.04	0.06	0.09	0.11	0.14	0.23
10.8	0.01	0.01	0.02	0.05	0.07	0.11	0.18	0.31
13.9	0.00	0.01	0.03	0.05	0.10	0.16	0.42	0.0
17.2	0.00	0.01	0.02	0.05	0.10	0.23	0.56	0.0
20.8	0.00	0.01	0.03	0.08	0.18	0.44	0.0	0.0
24.5	0.01	0.02	0.02	0.09	0.0	0.0	0.0	0.0
28.5	0.01	0.02	0.06	0.0	0.0	0.0	0.0	0.0
33.5	0.02	0.04	0.0	0.0	0.0	0.0	0.0	0.0
35.0	0.07	0.0	0.0	0.0	0.0	0.0	0.0	0.0







#### Appendix D

Difference means, difference variances, residual variances, and correlation coefficients for the final values of the  $\xi_{ve}$  transformation after the systematic error in the variance difference has been removed. The units of the difference means are decipascals while the difference variances are in percent. The residual variances and correlation coefficients are dimensionless.

## DIFFERENCE MEANS - CONSTANT D.C. X COMPONENT

SHIP	0.25	0.50	1.0	2.0	4.0	7.0	14.0	28.0
A	.003	.009	.023	.044	.065	.061	.069	.066
B	.003	.010	.017	.024	.031	.037	.042	.034
C	.005	.008	.001	.015	.016	.023	.031	.030
D	.001	.002	.006	.015	.003	.006	.005	.021
E	.002	.006	.012	.020	.016	.008	.015	.016
I	.001	.000	.004	.010	.006	.001	.008	.003
J	.001	.002	.001	.008	.003	.014	.004	.013
K	.004	.010	.021	.030	.021	.011	.009	.000
M	.002	.005	.014	.022	.024	.030	.043	.035
N	.005	.012	.026	.047	.061	.065	.067	.060
P	.002	.006	.010	.004	.005	.018	.029	.018

## DIFFERENCE MEANS - CONSTANT D.C. Y COMPONENT

SHIP	0.25	0.50	1.0	2.0	4.0	7.0	14.0	28.0
A	.002	.008	.013	.013	.017	.016	.013	.013
B	.001	.006	.004	.007	.022	.031	.036	.043
C	.005	.012	.008	.010	.032	.041	.044	.048
D	.005	.014	.011	.004	.027	.035	.041	.050
E	.001	.002	.011	.020	.037	.042	.044	.043
I	.001	.002	.002	.014	.026	.032	.037	.042
J	.002	.004	.009	.007	.017	.022	.027	.031
K	.005	.011	.017	.020	.020	.013	.000	.014
M	.000	.002	.002	.002	.008	.006	.004	.008
N	.001	.004	.009	.016	.021	.026	.021	.021
P	.006	.016	.028	.031	.028	.033	.008	.019

## DIFFERENCE MEANS - LINEAR D.C. X COMPONENT

SHIP	0.25	0.50	1.0	2.0	4.0	7.0	14.0	28.0
A	.003	.013	.037	.076	.110	.105	.113	.111
B	.006	.021	.036	.051	.071	.085	.089	.078
C	.013	.022	.015	.006	.001	.014	.024	.017
D	.007	.015	.008	.002	.030	.040	.045	.070
E	.002	.007	.012	.021	.015	.002	.007	.011
I	.001	.001	.006	.015	.009	.001	.008	.005
J	.003	.008	.009	.001	.011	.040	.025	.003
K	.005	.013	.026	.037	.025	.009	.005	.001
M	.003	.007	.018	.029	.033	.040	.054	.047
N	.006	.014	.029	.053	.069	.078	.078	.074
P	.005	.012	.018	.007	.010	.035	.054	.049

## DIFFERENCE MEANS - LINEAR D.C. Y COMPONENT

SHIP	0.25	0.50	1.0	2.0	4.0	7.0	14.0	28.0
A	.004	.015	.026	.031	.037	.032	.028	.026
B	.004	.013	.013	.004	.027	.041	.053	.063
C	.011	.024	.020	.012	.045	.064	.071	.081
D	.011	.025	.020	.008	.048	.063	.071	.087
E	.001	.001	.012	.026	.054	.063	.066	.065
I	.002	.003	.005	.028	.049	.059	.072	.078
J	.002	.006	.010	.018	.042	.052	.064	.066
K	.007	.017	.024	.027	.025	.013	.000	.020
M	.001	.004	.004	.001	.013	.012	.008	.007
N	.002	.006	.011	.018	.025	.029	.025	.025
P	.015	.034	.061	.075	.070	.082	.048	.072

## DIFFERENCE VARIANCES - CONSTANT D.C. X COMPONENT

SHIP	0.25	0.50	1.0	2.0	4.0	7.0	14.0	28.0
A	0.22	0.54	1.02	1.45	1.62	0.35	0.47	-1.25
B	0.04	-0.10	-0.38	-0.72	0.09	1.69	2.09	1.89
C	-0.58	-1.29	-1.72	-1.31	-1.49	-2.71	-0.39	-1.33
D	-0.44	-1.00	-0.41	0.69	-0.77	-0.26	-0.05	-1.17
E	-0.10	0.00	-0.75	0.32	0.70	1.32	0.24	-2.87
I	-0.32	-0.65	-0.85	-0.30	0.23	-0.74	3.38	4.91
J	-0.26	-0.63	-1.14	-0.98	-1.43	-2.65	-0.39	0.17
K	-0.26	-0.62	-1.52	-2.84	-3.04	-3.52	-0.73	-0.74
M	0.05	0.20	0.44	1.51	1.76	3.55	2.02	4.81
N	-0.20	-0.51	-0.67	-2.77	-2.67	-5.66	-6.73	-4.82
P	0.09	0.13	0.54	-0.69	-2.89	0.33	0.73	1.78

## DIFFERENCE VARIANCES - CONSTANT D.C. Y COMPONENT

SHIP	0.25	0.50	1.0	2.0	4.0	7.0	14.0	28.0
A	-0.22	-0.54	-1.04	-1.48	-1.65	-0.35	-0.47	1.23
B	-0.04	0.10	0.38	0.71	-0.09	-1.73	-2.15	-1.95
C	0.58	1.26	1.68	1.28	1.46	2.60	0.38	1.30
D	0.43	0.99	0.41	-0.69	0.76	0.26	0.05	1.15
E	0.10	-0.00	0.74	-0.32	-0.71	-1.35	-0.24	2.75
I	0.32	0.65	0.84	0.30	-0.23	0.73	-3.57	-5.30
J	0.26	0.63	1.12	0.96	1.40	2.55	0.39	-0.17
K	0.26	0.61	1.49	2.72	2.91	3.34	0.72	0.73
M	-0.05	-0.20	-0.44	-1.55	-1.80	-3.75	-2.08	-5.18
N	0.20	0.50	0.66	2.66	2.57	5.21	6.12	4.49
P	-0.09	-0.13	-0.54	0.69	2.77	-0.33	-0.74	-1.83

## DIFFERENCE VARIANCES - LINEAR D.C. X COMPONENT

SHIP	0.25	0.50	1.0	2.0	4.0	7.0	14.0	28.0
A	0.44	1.21	2.05	2.92	3.37	1.00	0.61	-0.77
B	0.09	-0.24	-0.77	-1.63	0.73	2.80	2.87	3.85
C	-1.54	-3.10	-3.62	-2.23	-2.17	-3.79	-0.42	0.22
D	-1.05	-2.16	-0.87	2.12	-0.32	0.71	0.46	-0.46
E	-0.16	0.37	-1.18	1.33	1.42	2.31	0.41	-2.22
I	-0.66	-1.53	-2.10	-0.87	0.23	-1.51	4.81	9.49
J	-0.58	-1.49	-2.29	-1.35	-1.85	-4.16	0.83	2.87
K	-0.47	-1.30	-2.53	-5.41	-4.78	-6.63	-2.40	-2.15
M	0.12	0.37	0.86	2.32	2.83	5.80	3.98	7.40
N	-0.40	-0.70	-0.69	-4.27	-4.01	-8.98	-10.7	-9.02
P	0.41	0.78	1.56	-0.94	-5.26	0.71	0.51	-0.65

## DIFFERENCE VARIANCES - LINEAR D.C. Y COMPONENT

SHIP	0.25	0.50	1.0	2.0	4.0	7.0	14.0	28.0
A	-0.45	-1.23	-2.11	-3.06	-3.55	-1.01	-0.62	0.76
B	-0.09	0.24	0.76	1.59	-0.74	-2.93	-3.00	-4.09
C	1.50	2.96	3.43	2.16	2.10	3.58	0.42	-0.22
D	1.04	2.09	0.85	-2.19	0.31	-0.72	-0.46	0.45
E	0.16	-0.38	1.16	-1.36	-1.45	-2.39	-0.42	2.14
I	0.65	1.49	2.04	0.86	-0.23	1.48	-5.19	-11.11
J	0.58	1.46	2.22	1.32	1.80	3.91	-0.84	-3.00
K	0.47	1.28	2.43	5.01	4.46	6.03	2.32	2.08
M	-0.12	-0.37	-0.87	-2.40	-2.95	-6.35	-4.23	-8.32
N	0.40	0.70	0.69	4.01	3.79	7.91	9.23	7.94
P	-0.41	-0.78	-1.59	0.93	4.87	-0.72	-0.52	0.65

## RESIDUAL VARIANCES - CONSTANT D.C. X COMPONENT

SHIP	0.25	0.50	1.0	2.0	4.0	7.0	14.0	28.0
A	.002	.007	.017	.031	.043	.047	.049	.042
B	.002	.007	.017	.032	.042	.046	.039	.035
C	.003	.008	.019	.034	.047	.045	.052	.053
D	.003	.010	.024	.040	.047	.051	.051	.059
E	.003	.006	.014	.029	.037	.043	.039	.037
I	.002	.006	.013	.022	.028	.032	.038	.044
J	.002	.006	.013	.023	.031	.035	.044	.047
K	.002	.006	.012	.018	.025	.032	.043	.056
M	.002	.006	.013	.024	.031	.037	.046	.049
N	.003	.004	.009	.019	.032	.041	.053	.067
P	.003	.008	.021	.035	.042	.045	.050	.035

## RESIDUAL VARIANCES - CONSTANT D.C. Y COMPONENT

SHIP	0.25	0.50	1.0	2.0	4.0	7.0	14.0	28.0
A	.002	.006	.014	.027	.040	.047	.051	.039
B	.002	.007	.018	.038	.057	.059	.055	.060
C	.004	.011	.026	.044	.054	.051	.053	.053
D	.006	.014	.031	.050	.072	.079	.078	.083
E	.004	.008	.021	.036	.065	.070	.070	.079
I	.003	.008	.014	.025	.032	.037	.043	.054
J	.003	.008	.018	.028	.036	.043	.039	.042
K	.003	.008	.018	.027	.035	.039	.057	.073
M	.002	.005	.012	.022	.033	.036	.048	.047
N	.003	.006	.011	.025	.039	.045	.064	.070
P	.003	.008	.020	.040	.051	.052	.060	.070

## RESIDUAL VARIANCES - LINEAR D.C. X COMPONENT

SHIP	0.25	0.50	1.0	2.0	4.0	7.0	14.0	28.0
A	.006	.017	.041	.079	.107	.110	.107	.090
B	.006	.016	.042	.076	.103	.107	.089	.078
C	.007	.018	.044	.086	.117	.109	.121	.117
D	.008	.024	.062	.101	.119	.116	.104	.104
E	.006	.014	.032	.065	.078	.082	.075	.061
I	.006	.015	.032	.053	.066	.073	.081	.089
J	.005	.015	.032	.056	.074	.077	.093	.093
K	.005	.014	.031	.046	.061	.069	.084	.095
M	.005	.013	.031	.056	.070	.078	.092	.087
N	.005	.009	.018	.035	.057	.072	.082	.095
P	.009	.023	.057	.091	.105	.108	.108	.084

## RESIDUAL VARIANCES - LINEAR D.C. Y COMPONENT

SHIP	0.25	0.50	1.0	2.0	4.0	7.0	14.0	28.0
A	.004	.014	.034	.064	.096	.109	.112	.084
B	.006	.017	.043	.089	.134	.134	.123	.127
C	.011	.029	.066	.111	.141	.124	.128	.115
D	.014	.038	.078	.125	.171	.180	.174	.178
E	.009	.019	.050	.079	.136	.141	.132	.139
I	.008	.020	.035	.060	.077	.087	.096	.120
J	.007	.019	.044	.067	.087	.097	.086	.086
K	.007	.019	.048	.069	.082	.092	.113	.147
M	.004	.011	.031	.053	.074	.077	.093	.089
N	.007	.013	.022	.044	.067	.076	.100	.106
P	.009	.019	.049	.098	.120	.113	.116	.135

## CORRELATION COEFFICIENTS - CONSTANT D.C. X COMPONENT

SHIP	0.25	0.50	1.0	2.0	4.0	7.0	14.0	28.0
A	.999	.997	.992	.984	.978	.977	.976	.979
B	.999	.997	.992	.984	.979	.977	.980	.982
C	.999	.996	.991	.983	.977	.978	.974	.974
D	.998	.995	.988	.980	.976	.975	.974	.971
E	.999	.997	.993	.986	.981	.979	.980	.982
I	.999	.997	.994	.989	.986	.984	.981	.978
J	.999	.997	.994	.988	.985	.983	.978	.976
K	.999	.997	.994	.991	.988	.985	.978	.972
M	.999	.997	.993	.988	.984	.981	.977	.975
N	.999	.998	.996	.991	.984	.980	.975	.968
P	.998	.996	.990	.983	.979	.978	.975	.982

## CORRELATION COEFFICIENTS - CONSTANT D.C. Y COMPONENT

SHIP	0.25	0.50	1.0	2.0	4.0	7.0	14.0	28.0
A	.999	.997	.993	.987	.980	.977	.975	.980
B	.999	.997	.991	.981	.972	.971	.973	.970
C	.998	.994	.987	.978	.973	.974	.973	.973
D	.997	.993	.985	.975	.964	.961	.961	.958
E	.998	.996	.990	.982	.967	.965	.965	.960
I	.998	.996	.993	.988	.984	.981	.979	.974
J	.999	.996	.991	.986	.982	.979	.981	.979
K	.998	.996	.991	.986	.982	.980	.972	.963
M	.999	.998	.994	.989	.984	.982	.976	.977
N	.998	.997	.994	.988	.980	.977	.968	.965
P	.998	.996	.990	.980	.974	.974	.970	.965

## CORRELATION COEFFICIENTS - LINEAR D.C. X COMPONENT

SHIP	0.25	0.50	1.0	2.0	4.0	7.0	14.0	28.0
A	.997	.992	.979	.960	.946	.945	.946	.955
B	.997	.992	.979	.962	.948	.946	.955	.960
C	.997	.991	.978	.958	.942	.947	.940	.942
D	.996	.988	.969	.949	.941	.942	.948	.948
E	.997	.993	.984	.967	.961	.958	.962	.970
I	.997	.993	.984	.973	.967	.964	.959	.954
J	.998	.993	.984	.972	.963	.962	.953	.953
K	.997	.993	.985	.978	.970	.967	.959	.953
M	.997	.994	.984	.972	.965	.960	.953	.955
N	.997	.995	.991	.983	.972	.966	.962	.956
P	.995	.989	.971	.955	.949	.946	.946	.958

SHIP	0.25	0.50	1.0	2.0	4.0	7.0	14.0	28.0
A	.998	.993	.983	.968	.953	.946	.944	.958
B	.997	.992	.979	.955	.933	.934	.940	.938
C	.994	.985	.967	.944	.929	.937	.936	.943
D	.993	.981	.961	.938	.914	.911	.913	.911
E	.996	.990	.975	.961	.932	.931	.934	.930
I	.996	.990	.982	.970	.962	.956	.953	.944
J	.996	.990	.978	.966	.956	.951	.957	.958
K	.996	.990	.976	.965	.958	.953	.943	.926
M	.998	.994	.985	.974	.964	.963	.955	.958
N	.996	.993	.989	.978	.966	.961	.948	.946
P	.996	.990	.976	.951	.939	.944	.942	.932

#### Appendix E

The raw difference means, difference variances, residual variances, and correlation coefficients for the heat fluxes with no correction applied. The difference means are in Watts/m<sup>2</sup> while the other test parameters are dimensionless.

DIFFERENCE MEANS - SENSIBLE HEAT FLUX									
SHIP	0.25	0.50	1.0	2.0	4.0	7.0	14.0	28.0	
A	0.8	1.9	4.1	7.5	11.1	14.3	18.1	21.7	
B	0.8	1.9	4.1	7.8	12.0	15.3	19.6	23.2	
C	0.2	0.5	1.2	2.5	3.5	4.3	5.2	6.1	
D	1.1	2.5	5.5	10.4	15.1	18.4	21.6	24.8	
E	0.4	0.8	1.5	3.0	4.8	6.1	7.1	8.0	
I	0.8	1.8	3.5	6.0	8.9	11.5	15.3	18.8	
J	0.4	1.0	1.9	3.3	4.8	6.0	8.0	9.4	
K	0.1	0.3	0.4	0.8	1.1	1.8	2.8	3.6	
M	0.7	1.7	3.5	6.3	10.2	13.4	18.0	22.1	
N	0.3	0.6	1.0	1.8	3.0	3.9	5.3	6.6	
P	0.1	0.2	0.4	0.7	1.0	1.4	1.9	2.2	
DIFFERENCE MEANS - LATENT HEAT FLUX									
SHIP	0.25	0.50	1.0	2.0	4.0	7.0	14.0	28.0	
A	1.3	3.2	6.8	12.7	19.5	25.2	32.3	39.3	
B	1.2	2.8	6.0	11.6	18.0	23.0	28.9	33.7	
C	1.2	2.8	5.9	11.3	16.5	20.3	24.8	28.7	
D	3.4	7.9	16.8	31.2	45.8	55.9	65.9	74.4	
E	2.7	5.9	11.9	23.1	37.1	48.2	58.8	68.5	
I	1.6	3.7	7.6	13.7	20.4	26.7	35.5	43.6	
J	1.2	3.1	6.3	11.5	17.1	22.0	29.2	34.3	
K	1.2	2.8	5.5	10.3	15.6	22.6	33.2	42.0	
M	1.2	3.0	6.4	12.2	19.7	26.5	35.3	43.0	
N	2.1	4.1	7.2	12.8	21.3	28.3	38.4	46.4	
P	0.7	1.7	3.7	7.1	10.6	13.6	16.9	19.3	
DIFFERENCE VARIANCES - SENSIBLE HEAT FLUX									
SHIP	0.25	0.50	1.0	2.0	4.0	7.0	14.0	28.0	
A	.025	.059	.129	.267	.401	.536	.652	.774	
B	.024	.059	.118	.222	.368	.449	.574	.707	
C	.037	.084	.175	.314	.433	.501	.594	.703	
D	.028	.065	.146	.282	.411	.487	.549	.658	
E	.034	.073	.162	.296	.464	.574	.664	.729	
I	.026	.064	.124	.222	.384	.465	.602	.711	
J	.024	.060	.123	.217	.330	.418	.524	.589	
K	.029	.068	.141	.240	.344	.448	.608	.675	
M	.025	.057	.121	.218	.371	.472	.620	.761	
N	.029	.055	.088	.156	.250	.307	.439	.567	
P	.026	.070	.154	.276	.392	.475	.613	.683	

## DIFFERENCE VARIANCES - LATENT HEAT FLUX

SHIP	0.25	0.50	1.0	2.0	4.0	7.0	14.0	28.0
A	.016	.039	.088	.197	.314	.436	.558	.688
B	.019	.044	.093	.184	.316	.393	.508	.627
C	.027	.059	.127	.244	.361	.430	.505	.560
D	.020	.046	.108	.231	.355	.425	.492	.600
E	.018	.039	.096	.195	.331	.424	.502	.539
I	.013	.034	.072	.148	.270	.312	.414	.502
J	.014	.033	.076	.152	.224	.268	.322	.388
K	.020	.045	.095	.168	.249	.348	.561	.644
M	.015	.034	.075	.140	.276	.347	.479	.637
N	.007	.009	.008	.012	.008	-.049	-.070	-.239
P	.017	.046	.099	.205	.312	.365	.489	.573

## RESIDUAL VARIANCES - SENSIBLE HEAT FLUX

SHIP	0.25	0.50	1.0	2.0	4.0	7.0	14.0	28.0
A	.004	.010	.032	.075	.130	.215	.299	.432
B	.003	.008	.023	.057	.102	.135	.201	.282
C	.005	.013	.033	.069	.113	.145	.197	.267
D	.004	.012	.036	.079	.124	.162	.197	.262
E	.005	.011	.032	.083	.165	.230	.315	.415
I	.005	.012	.031	.071	.121	.185	.308	.425
J	.004	.012	.027	.054	.086	.126	.192	.249
K	.003	.008	.019	.041	.078	.111	.215	.271
M	.004	.012	.030	.067	.140	.185	.323	.457
N	.006	.013	.024	.057	.117	.154	.271	.464
P	.003	.010	.029	.060	.096	.129	.208	.232

## RESIDUAL VARIANCES - LATENT HEAT FLUX

SHIP	0.25	0.50	1.0	2.0	4.0	7.0	14.0	28.0
A	.005	.014	.046	.108	.187	.289	.382	.498
B	.004	.012	.037	.087	.145	.180	.245	.295
C	.005	.015	.041	.087	.135	.175	.224	.273
D	.006	.018	.051	.111	.169	.213	.264	.333
E	.006	.014	.043	.124	.243	.347	.449	.573
I	.006	.017	.047	.107	.180	.255	.408	.552
J	.004	.013	.035	.081	.134	.185	.292	.385
K	.004	.010	.025	.062	.115	.188	.347	.473
M	.005	.016	.044	.102	.215	.278	.437	.555
N	.006	.012	.031	.093	.229	.332	.661	1.16
P	.003	.010	.031	.073	.116	.150	.203	.210

## CORRELATION COEFFICIENTS - SENSIBLE HEAT FLUX

SHIP	0.25	0.50	1.0	2.0	4.0	7.0	14.0	28.0
A	.998	.995	.985	.968	.949	.917	.889	.835
B	.999	.996	.990	.976	.963	.954	.938	.933
C	.998	.994	.987	.976	.965	.959	.948	.945
D	.998	.994	.983	.967	.954	.943	.934	.923
E	.997	.995	.987	.966	.936	.916	.880	.822
I	.998	.994	.986	.968	.953	.923	.864	.803
J	.998	.995	.988	.977	.967	.954	.930	.906
K	.999	.996	.993	.986	.974	.970	.940	.924
M	.998	.994	.986	.970	.939	.924	.858	.801
N	.997	.994	.989	.972	.943	.924	.861	.736
P	.999	.995	.988	.978	.970	.963	.948	.964

## CORRELATION COEFFICIENTS - LATENT HEAT FLUX

SHIP	0.25	0.50	1.0	2.0	4.0	7.0	14.0	28.0
A	.998	.993	.977	.946	.905	.849	.797	.729
B	.998	.994	.982	.957	.931	.916	.889	.883
C	.997	.993	.980	.960	.941	.924	.904	.880
D	.997	.991	.975	.946	.919	.898	.872	.843
E	.997	.993	.979	.937	.872	.810	.744	.654
I	.997	.992	.976	.945	.907	.864	.770	.671
J	.998	.994	.983	.959	.932	.904	.841	.784
K	.998	.995	.988	.970	.944	.907	.824	.740
M	.998	.992	.978	.948	.887	.851	.751	.671
N	.997	.994	.984	.953	.885	.838	.681	.483
P	.998	.995	.985	.965	.947	.932	.915	.931

Appendix F

Part I - The individually calculated  $\zeta_{he}$  values for the heat fluxes. 0.0 indicates no data.

## STATION A - SENSIBLE HEAT FLUX

SPEED	0.25	0.50	1.0	2.0	4.0	7.0	14.0	28.0
0.4	6.61	6.72	6.58	24.10	0.0	20.29	29.07	32.26
1.6	1.88	2.55	6.91	9.90	14.50	12.90	15.45	13.65
3.4	1.19	1.47	2.21	2.65	3.25	3.82	3.98	4.29
5.5	1.08	1.21	1.41	1.74	2.02	2.38	2.69	2.67
8.0	1.04	1.10	1.22	1.40	1.61	1.85	1.98	2.01
10.8	1.03	1.06	1.13	1.24	1.34	1.42	1.60	1.61
13.9	1.02	1.04	1.09	1.18	1.26	1.34	1.29	1.43
17.2	1.01	1.03	1.06	1.12	1.18	1.18	0.0	0.0
20.8	1.01	1.02	1.06	1.11	1.17	1.01	0.0	0.0
24.5	1.01	1.02	1.05	1.10	1.09	0.0	0.0	0.0
28.5	1.01	1.02	1.03	0.0	0.0	0.0	0.0	0.0
33.5	1.01	1.01	0.0	0.0	0.0	0.0	0.0	0.0
35.0	1.01	0.0	0.0	0.0	0.0	0.0	0.0	0.0

## STATION B - SENSIBLE HEAT FLUX

SPEED	0.25	0.50	1.0	2.0	4.0	7.0	14.0	28.0
0.4	4.30	8.44	7.80	18.54	13.02	31.33	41.84	30.63
1.6	2.65	2.67	6.10	7.18	11.49	12.52	11.15	10.21
3.4	1.19	1.48	1.98	3.01	3.55	3.65	3.94	4.19
5.5	1.07	1.19	1.42	1.75	2.08	2.34	2.42	2.64
8.0	1.04	1.09	1.20	1.34	1.59	1.62	1.82	1.84
10.8	1.02	1.06	1.12	1.23	1.33	1.41	1.51	1.64
13.9	1.02	1.03	1.06	1.14	1.21	1.24	1.22	0.0
17.2	1.01	1.03	1.05	1.09	1.16	1.18	1.11	0.0
20.8	1.01	1.02	1.05	1.07	1.06	1.07	0.0	0.0
24.5	1.01	1.02	1.05	1.04	0.0	0.0	0.0	0.0
28.5	1.01	1.03	1.04	1.06	0.0	0.0	0.0	0.0
33.5	1.01	1.02	1.01	1.02	0.0	0.0	0.0	0.0
35.0	1.00	0.0	0.0	0.0	0.0	0.0	0.0	0.0

## STATION C - SENSIBLE HEAT FLUX

SPEED	0.25	0.50	1.0	2.0	4.0	7.0	14.0	28.0
0.4	6.94	9.26	27.16	21.41	18.93	18.88	26.05	226.31
1.6	1.96	3.15	5.47	7.69	7.12	10.14	14.45	10.57
3.4	1.25	1.57	1.89	2.44	2.77	3.23	3.30	3.89
5.5	1.08	1.25	1.41	1.61	1.99	2.09	2.34	2.23
8.0	1.05	1.11	1.29	1.41	1.53	1.63	1.73	1.79
10.8	1.03	1.07	1.14	1.25	1.33	1.41	1.53	1.68
13.9	1.02	1.05	1.10	1.17	1.27	1.29	1.30	1.40
17.2	1.02	1.04	1.08	1.14	1.19	1.19	1.28	0.0
20.8	1.01	1.03	1.06	1.13	1.11	1.32	0.0	0.0
24.5	1.01	1.02	1.04	1.10	0.0	0.0	0.0	0.0
28.5	1.01	1.02	1.04	0.0	0.0	0.0	0.0	0.0
33.5	1.01	1.01	1.05	0.0	0.0	0.0	0.0	0.0
35.0	1.01	1.01	0.0	0.0	0.0	0.0	0.0	0.0

## STATION D - SENSIBLE HEAT FLUX

SPEED	0.25	0.50	1.0	2.0	4.0	7.0	14.0	28.0
0.4	3.35	10.33	18.60	21.87	32.07	29.00	60.11	45.07
1.6	1.99	5.35	6.17	11.25	9.32	14.15	12.39	15.54
3.4	1.24	1.61	2.20	3.03	3.39	3.42	3.69	3.88
5.5	1.10	1.20	1.55	1.83	2.11	2.29	2.49	2.67
8.0	1.04	1.11	1.24	1.44	1.64	1.74	1.78	1.94
10.8	1.03	1.06	1.13	1.29	1.39	1.50	1.51	1.66
13.9	1.02	1.05	1.11	1.20	1.30	1.34	1.41	1.43
17.2	1.02	1.03	1.07	1.15	1.20	1.21	1.28	0.0
20.8	1.01	1.03	1.06	1.08	1.14	1.12	1.17	0.0
24.5	1.01	1.02	1.04	1.09	1.14	0.0	0.0	0.0
28.5	1.01	1.03	1.04	1.13	0.0	0.0	0.0	0.0
33.5	1.01	1.02	1.11	0.0	0.0	0.0	0.0	0.0
35.0	1.01	1.05	0.0	0.0	0.0	0.0	0.0	0.0

## STATION E - SENSIBLE HEAT FLUX

SPEED	0.25	0.50	1.0	2.0	4.0	7.0	14.0	28.0
0.4	4.61	4.13	5.23	9.31	19.13	19.40	31.86	27.39
1.6	1.61	2.58	3.47	8.29	10.23	8.91	9.53	11.96
3.4	1.16	1.27	1.59	2.32	2.77	3.30	3.42	3.82
5.5	1.05	1.13	1.27	1.43	1.82	1.87	2.09	2.47
8.0	1.03	1.06	1.15	1.30	1.45	1.59	1.67	1.73
10.8	1.03	1.05	1.11	1.19	1.31	1.38	1.43	1.52
13.9	1.02	1.03	1.08	1.16	1.24	1.30	1.33	1.29
17.2	1.01	1.03	1.07	1.09	1.20	1.28	0.0	0.0
20.8	1.01	1.03	1.07	1.16	1.17	0.0	0.0	0.0
24.5	1.01	1.03	1.06	1.14	0.0	0.0	0.0	0.0
28.5	1.01	1.02	0.0	0.0	0.0	0.0	0.0	0.0
33.5	1.06	1.25	1.07	0.0	0.0	0.0	0.0	0.0
35.0	1.01	1.02	0.0	0.0	0.0	0.0	0.0	0.0

## STATION I - SENSIBLE HEAT FLUX

SPEED	0.25	0.50	1.0	2.0	4.0	7.0	14.0	28.0
0.4	6.84	11.56	4.99	19.05	28.43	0.0	0.0	0.0
1.6	2.78	3.28	6.51	6.75	9.96	12.90	12.86	14.61
3.4	1.31	1.61	2.25	2.96	3.27	3.90	4.11	4.83
5.5	1.11	1.22	1.42	1.79	2.09	2.37	2.75	2.79
8.0	1.04	1.10	1.22	1.39	1.56	1.62	1.80	1.88
10.8	1.03	1.07	1.13	1.20	1.34	1.42	1.51	1.46
13.9	1.02	1.04	1.08	1.14	1.21	1.27	1.32	1.50
17.2	1.01	1.03	1.06	1.10	1.25	1.22	1.33	0.0
20.8	1.01	1.03	1.06	1.13	1.09	1.29	0.0	0.0
24.5	1.01	1.03	1.05	1.06	1.21	0.0	0.0	0.0
28.5	1.01	1.05	1.04	1.08	0.0	0.0	0.0	0.0
33.5	1.01	1.02	0.0	0.0	0.0	0.0	0.0	0.0
35.0	1.00	0.0	0.0	0.0	0.0	0.0	0.0	0.0

## STATION J - SENSIBLE HEAT FLUX

SPEED	0.25	0.50	1.0	2.0	4.0	7.0	14.0	28.0
0.4	5.05	5.68	5.71	24.94	108.0	0.0	0.0	26.18
1.6	1.48	3.13	3.70	8.62	9.36	10.58	16.31	22.76
3.4	1.20	1.51	2.06	2.59	3.25	3.24	3.89	4.30
5.5	1.10	1.20	1.40	1.59	1.92	2.09	2.17	2.42
8.0	1.04	1.09	1.19	1.35	1.44	1.60	1.67	1.78
10.8	1.02	1.06	1.11	1.20	1.27	1.35	1.45	1.51
13.9	1.01	1.04	1.08	1.12	1.22	1.26	1.31	1.37
17.2	1.01	1.03	1.05	1.11	1.17	1.23	0.0	0.0
20.8	1.01	1.02	1.05	1.09	1.13	1.10	0.0	0.0
24.5	1.01	1.03	1.05	1.07	1.04	0.0	0.0	0.0
28.5	1.01	1.02	1.03	1.02	0.0	0.0	0.0	0.0
33.5	1.01	1.00	0.0	0.0	0.0	0.0	0.0	0.0
35.0	0.94	0.0	0.0	0.0	0.0	0.0	0.0	0.0

## STATION K - SENSIBLE HEAT FLUX

SPEED	0.25	0.50	1.0	2.0	4.0	7.0	14.0	28.0
0.4	2.94	3.94	10.23	4.57	20.15	24.91	1187.	6.54
1.6	1.49	2.10	3.59	4.66	7.29	4.10	11.02	10.39
3.4	1.13	1.27	1.49	1.70	2.62	2.87	3.01	3.78
5.5	1.04	1.12	1.21	1.40	1.49	1.77	1.77	1.83
8.0	1.02	1.06	1.10	1.19	1.32	1.35	1.46	1.44
10.8	1.02	1.04	1.09	1.12	1.16	1.24	1.36	1.35
13.9	1.01	1.03	1.07	1.14	1.16	1.19	1.22	0.0
17.2	1.01	1.03	1.05	1.08	1.13	1.10	0.0	0.0
20.8	1.01	1.02	1.04	1.10	1.18	0.0	0.0	0.0
24.5	1.01	1.02	1.11	1.15	0.0	0.0	0.0	0.0
28.5	1.01	1.04	0.0	0.0	0.0	0.0	0.0	0.0
33.5	1.00	1.01	0.0	0.0	0.0	0.0	0.0	0.0
35.0	0.0	0.0	0.0	0.0	0.0	0.0	0.0	0.0

## STATION M - SENSIBLE HEAT FLUX

SPEED	0.25	0.50	1.0	2.0	4.0	7.0	14.0	28.0
0.4	2.17	2.50	4.12	9.71	18.81	19.02	27.65	23.90
1.6	1.38	2.79	5.08	6.86	11.68	11.55	13.33	12.44
3.4	1.12	1.37	1.82	2.28	3.21	3.05	3.79	3.95
5.5	1.07	1.17	1.30	1.50	1.83	2.07	2.37	2.58
8.0	1.03	1.07	1.18	1.32	1.45	1.60	1.81	1.91
10.8	1.02	1.05	1.10	1.19	1.31	1.35	1.34	1.38
13.9	1.01	1.03	1.07	1.10	1.19	1.23	1.22	1.50
17.2	1.01	1.03	1.05	1.09	1.15	1.16	0.0	0.0
20.8	1.01	1.02	1.05	1.10	1.03	1.12	0.0	0.0
24.5	1.01	1.02	1.05	1.09	0.0	0.0	0.0	0.0
28.5	1.01	1.01	1.04	0.0	0.0	0.0	0.0	0.0
33.5	1.00	1.03	0.0	0.0	0.0	0.0	0.0	0.0
35.0	1.02	0.0	0.0	0.0	0.0	0.0	0.0	0.0

## STATION N - SENSIBLE HEAT FLUX

SPEED	0.25	0.50	1.0	2.0	4.0	7.0	14.0	28.0
0.4	5.09	2.23	4.76	10.34	10.69	20.29	15.84	32.64
1.6	1.47	2.01	2.76	3.92	5.98	5.22	7.68	9.36
3.4	1.07	1.20	1.33	1.68	2.03	2.25	2.40	3.13
5.5	1.04	1.07	1.13	1.21	1.41	1.46	1.58	1.83
8.0	1.02	1.04	1.07	1.12	1.19	1.23	1.27	1.34
10.8	1.01	1.03	1.04	1.09	1.12	1.13	1.14	1.36
13.9	1.01	1.02	1.05	1.06	1.08	1.05	0.0	0.0
17.2	1.01	1.03	1.04	1.06	0.0	0.0	0.0	0.0
20.8	1.01	1.02	1.09	0.0	0.0	0.0	0.0	0.0
24.5	1.00	1.02	0.0	0.0	0.0	0.0	0.0	0.0
28.5	0.0	0.0	0.0	0.0	0.0	0.0	0.0	0.0
33.5	0.0	0.0	0.0	0.0	0.0	0.0	0.0	0.0
35.0	0.0	0.0	0.0	0.0	0.0	0.0	0.0	0.0

## STATION P - SENSIBLE HEAT FLUX

SPEED	0.25	0.50	1.0	2.0	4.0	7.0	14.0	28.0
0.4	6.38	2.45	7.13	35.97	20.68	31.32	0.0	0.0
1.6	1.48	1.91	4.36	9.56	9.93	9.34	13.94	0.0
3.4	1.14	1.47	1.75	2.27	2.66	3.18	3.34	3.49
5.5	1.06	1.18	1.39	1.59	1.88	2.14	2.26	2.28
8.0	1.04	1.10	1.19	1.41	1.55	1.56	1.78	1.88
10.8	1.02	1.06	1.12	1.22	1.31	1.39	1.49	1.51
13.9	1.02	1.04	1.11	1.15	1.23	1.30	1.37	1.20
17.2	1.01	1.03	1.07	1.16	1.14	1.14	0.0	0.0
20.8	1.01	1.03	1.06	1.09	1.13	0.0	0.0	0.0
24.5	1.01	1.02	1.04	1.07	0.0	0.0	0.0	0.0
28.5	1.00	1.02	1.05	0.0	0.0	0.0	0.0	0.0
33.5	1.01	1.01	0.0	0.0	0.0	0.0	0.0	0.0
35.0	1.00	1.03	0.0	0.0	0.0	0.0	0.0	0.0

## STATION A - LATENT HEAT FLUX

SPEED	0.25	0.50	1.0	2.0	4.0	7.0	14.0	28.0
0.4	4.32	4.64	4.67	23.08	0.0	15.91	29.24	33.08
1.6	1.69	2.04	4.11	6.42	10.93	11.51	12.42	10.10
3.4	1.12	1.34	1.88	2.41	2.90	3.60	3.81	3.89
5.5	1.06	1.15	1.30	1.63	1.95	2.23	2.55	2.43
8.0	1.03	1.08	1.17	1.34	1.52	1.75	1.89	1.94
10.8	1.02	1.05	1.10	1.21	1.33	1.41	1.55	1.55
13.9	1.01	1.03	1.07	1.16	1.24	1.34	1.35	1.36
17.2	1.01	1.03	1.06	1.12	1.17	1.21	0.0	0.0
20.8	1.01	1.02	1.06	1.10	1.17	1.09	0.0	0.0
24.5	1.01	1.02	1.04	1.09	1.10	0.0	0.0	0.0
28.5	1.01	1.01	1.03	0.0	0.0	0.0	0.0	0.0
33.5	1.01	1.00	0.0	0.0	0.0	0.0	0.0	0.0
35.0	1.00	0.0	0.0	0.0	0.0	0.0	0.0	0.0

### STATION C = LATENT HEAT FLUX

SPEED	0.25	0.50	1.0	2.0	4.0	7.0	14.0	28.0
0.4	6.61	4.97	18.51	18.02	31.95	24.50	24.96	94.36
1.6	1.96	2.48	4.59	6.59	8.00	11.03	13.10	10.82
3.4	1.17	1.41	1.75	2.36	2.62	3.06	3.39	4.07
5.5	1.07	1.18	1.35	1.60	1.87	2.11	2.29	2.30
8.0	1.04	1.09	1.21	1.37	1.53	1.63	1.75	1.78
10.8	1.02	1.06	1.12	1.23	1.32	1.40	1.49	1.58
13.9	1.02	1.04	1.08	1.16	1.24	1.28	1.31	1.41
17.2	1.02	1.03	1.07	1.13	1.17	1.20	1.25	0.0
20.8	1.01	1.03	1.05	1.09	1.12	1.21	0.0	0.0
24.5	1.01	1.02	1.03	1.07	0.0	0.0	0.0	0.0
28.5	1.01	1.02	1.03	0.0	0.0	0.0	0.0	0.0
33.5	1.01	1.01	1.03	0.0	0.0	0.0	0.0	0.0
35.0	1.01	1.02	0.0	0.0	0.0	0.0	0.0	0.0

STATION D - LATENT HEAT FLUX

SPEED	0.25	0.50	1.0	2.0	4.0	7.0	14.0	28.0
0.4	4.03	7.33	14.52	17.60	25.60	34.81	55.75	49.72
1.6	1.84	3.34	4.75	7.37	8.43	11.52	11.38	14.44
3.4	1.15	1.36	1.81	2.57	3.10	3.12	3.45	3.64
5.5	1.06	1.14	1.34	1.62	1.95	2.07	2.26	2.35
8.0	1.03	1.08	1.18	1.36	1.56	1.68	1.76	1.93
10.8	1.02	1.05	1.11	1.26	1.38	1.48	1.52	1.67
13.9	1.02	1.04	1.09	1.18	1.28	1.32	1.40	1.42
17.2	1.01	1.03	1.07	1.14	1.21	1.21	1.29	0.0
20.8	1.01	1.02	1.05	1.09	1.13	1.12	1.17	0.0
24.5	1.01	1.02	1.04	1.08	1.17	0.0	0.0	0.0
28.5	1.01	1.02	1.04	1.11	0.0	0.0	0.0	0.0
33.5	1.01	1.02	1.10	0.0	0.0	0.0	0.0	0.0
35.0	1.01	1.04	0.0	0.0	0.0	0.0	0.0	0.0

## STATION E - LATENT HEAT FLUX

SPEED	0.25	0.50	1.0	2.0	4.0	7.0	14.0	28.0
0.4	4.52	2.41	3.97	6.11	16.51	18.77	32.10	21.24
1.6	1.28	1.63	2.31	4.21	7.24	7.98	8.01	9.20
3.4	1.07	1.12	1.31	1.74	2.24	2.74	2.74	2.50
5.5	1.03	1.06	1.14	1.32	1.63	1.77	1.89	2.13
8.0	1.02	1.04	1.09	1.22	1.40	1.57	1.67	1.68
10.8	1.02	1.03	1.08	1.17	1.31	1.42	1.50	1.54
13.9	1.01	1.03	1.06	1.15	1.26	1.35	1.37	1.36
17.2	1.01	1.02	1.05	1.10	1.22	1.24	0.0	0.0
20.8	1.01	1.02	1.05	1.14	1.19	0.0	0.0	0.0
24.5	1.01	1.02	1.05	1.09	0.0	0.0	0.0	0.0
28.5	1.01	1.00	0.0	0.0	0.0	0.0	0.0	0.0
33.5	1.05	1.17	1.07	0.0	0.0	0.0	0.0	0.0
35.0	1.01	1.01	0.0	0.0	0.0	0.0	0.0	0.0

## STATION I - LATENT HEAT FLUX

SPEED	0.25	0.50	1.0	2.0	4.0	7.0	14.0	28.0
0.4	4.21	7.69	5.92	21.42	25.30	0.0	0.0	0.0
1.6	1.95	1.92	4.97	6.62	9.29	11.31	12.60	12.18
3.4	1.18	1.40	1.87	2.39	2.91	3.21	3.82	4.21
5.5	1.07	1.16	1.32	1.63	1.90	2.09	2.47	2.64
8.0	1.03	1.07	1.17	1.34	1.52	1.58	1.79	1.90
10.8	1.02	1.05	1.10	1.19	1.32	1.39	1.53	1.52
13.9	1.01	1.03	1.07	1.14	1.22	1.28	1.38	1.53
17.2	1.01	1.03	1.06	1.11	1.22	1.23	1.37	0.0
20.8	1.01	1.02	1.05	1.13	1.12	1.28	0.0	0.0
24.5	1.01	1.02	1.05	1.07	1.19	0.0	0.0	0.0
28.5	1.01	1.03	1.04	1.08	0.0	0.0	0.0	0.0
33.5	1.01	1.02	0.0	0.0	0.0	0.0	0.0	0.0
35.0	1.00	0.0	0.0	0.0	0.0	0.0	0.0	0.0

## STATION J - LATENT HEAT FLUX

SPEED	0.25	0.50	1.0	2.0	4.0	7.0	14.0	28.0
0.4	4.50	4.34	4.31	21.99	23.37	0.0	0.0	21.05
1.6	1.44	2.16	3.33	7.43	8.86	9.45	14.62	23.89
3.4	1.12	1.34	1.68	2.20	2.78	2.85	3.38	3.39
5.5	1.06	1.13	1.26	1.47	1.73	1.88	1.98	2.20
8.0	1.02	1.05	1.14	1.27	1.37	1.52	1.59	1.68
10.8	1.02	1.04	1.08	1.18	1.25	1.31	1.42	1.50
13.9	1.01	1.03	1.06	1.12	1.20	1.24	1.29	1.37
17.2	1.01	1.02	1.05	1.10	1.15	1.20	0.0	0.0
20.8	1.01	1.02	1.04	1.09	1.13	1.11	0.0	0.0
24.5	1.00	1.02	1.04	1.05	1.05	0.0	0.0	0.0
28.5	1.01	1.02	1.03	1.03	0.0	0.0	0.0	0.0
33.5	1.01	1.00	0.0	0.0	0.0	0.0	0.0	0.0
35.0	0.91	0.0	0.0	0.0	0.0	0.0	0.0	0.0

STATION K - LATENT HEAT FLUX

## STATION M - LATENT HEAT FLUX

SPEED	0.25	0.50	1.0	2.0	4.0	7.0	14.0	28.0
0.4	1.49	2.09	3.08	7.42	16.75	19.93	25.70	22.43
1.6	1.31	2.18	2.86	5.05	10.59	9.80	10.87	10.67
3.4	1.07	1.22	1.57	2.00	2.73	2.82	3.39	3.52
5.5	1.04	1.10	1.21	1.40	1.74	1.93	2.26	2.38
8.0	1.02	1.05	1.13	1.25	1.44	1.58	1.77	1.84
10.8	1.02	1.04	1.09	1.16	1.30	1.36	1.38	1.42
13.9	1.01	1.03	1.06	1.10	1.21	1.25	1.31	1.42
17.2	1.01	1.02	1.05	1.09	1.17	1.17	0.0	0.0
20.8	1.01	1.02	1.05	1.09	1.23	1.23	0.0	0.0
24.5	1.01	1.01	1.05	1.11	0.0	0.0	0.0	0.0
28.5	1.00	1.03	1.02	0.0	0.0	0.0	0.0	0.0
33.5	1.00	1.04	0.0	0.0	0.0	0.0	0.0	0.0
35.0	1.02	0.0	0.0	0.0	0.0	0.0	0.0	0.0

### STATION N = LATENT HEAT FLUX

## STATION P - LATENT HEAT FLUX

SPEED	0.25	0.50	1.0	2.0	4.0	7.0	14.0	28.0
0.4	7.87	1.58	7.57	7.07	13.69	24.60	0.0	0.0
1.6	1.74	1.79	2.69	6.06	9.54	10.19	12.21	0.0
3.4	1.12	1.33	1.60	2.00	2.67	3.02	3.15	3.19
5.5	1.05	1.12	1.29	1.50	1.78	2.00	2.04	2.09
8.0	1.03	1.07	1.15	1.34	1.46	1.51	1.68	1.77
10.8	1.02	1.05	1.10	1.17	1.30	1.34	1.45	1.51
13.9	1.01	1.03	1.07	1.14	1.21	1.26	1.36	1.23
17.2	1.01	1.02	1.05	1.11	1.15	1.18	0.0	0.0
20.8	1.01	1.02	1.04	1.09	1.12	0.0	0.0	0.0
24.5	1.01	1.01	1.04	1.05	0.0	0.0	0.0	0.0
28.5	1.00	1.01	1.03	0.0	0.0	0.0	0.0	0.0
33.5	1.01	1.02	0.0	0.0	0.0	0.0	0.0	0.0
35.0	1.00	1.02	0.0	0.0	0.0	0.0	0.0	0.0

## AVERAGE VALUE - SENSIBLE HEAT FLUX

SPEED	0.25	0.50	1.0	2.0	4.0	7.0	14.0	28.0
0.4	4.83	6.39	8.33	17.17	24.19	23.94	35.70	41.02
1.6	1.88	2.97	5.20	8.35	10.46	11.33	12.59	12.57
3.4	1.20	1.46	1.95	2.61	3.12	3.43	3.72	4.08
5.5	1.08	1.19	1.39	1.64	1.97	2.17	2.40	2.53
8.0	1.04	1.09	1.21	1.37	1.54	1.65	1.78	1.85
10.8	1.02	1.06	1.12	1.23	1.33	1.40	1.49	1.57
13.9	1.02	1.04	1.08	1.15	1.24	1.29	1.31	1.41
17.2	1.01	1.03	1.06	1.12	1.19	1.20	1.27	0.0
20.8	1.01	1.03	1.06	1.10	1.12	1.18	1.17	0.0
24.5	1.01	1.02	1.05	1.08	1.12	0.0	0.0	0.0
28.5	1.01	1.03	1.04	1.07	0.0	0.0	0.0	0.0
33.5	1.01	1.02	1.05	1.02	0.0	0.0	0.0	0.0
35.0	1.00	1.03	0.0	0.0	0.0	0.0	0.0	0.0

## AVERAGE VALUE - LATENT HEAT FLUX

SPEED	0.25	0.50	1.0	2.0	4.0	7.0	14.0	28.0
0.4	3.95	4.40	6.75	12.56	20.46	23.19	40.27	30.00
1.6	1.64	2.13	3.66	5.94	8.89	9.86	11.24	10.69
3.4	1.12	1.30	1.66	2.20	2.74	3.06	3.38	3.55
5.5	1.05	1.12	1.27	1.52	1.82	2.01	2.21	2.32
8.0	1.03	1.07	1.15	1.31	1.48	1.59	1.73	1.80
10.8	1.02	1.04	1.10	1.20	1.31	1.38	1.47	1.55
13.9	1.01	1.03	1.07	1.14	1.22	1.28	1.32	1.42
17.2	1.01	1.03	1.06	1.11	1.18	1.19	1.29	0.0
20.8	1.01	1.02	1.05	1.10	1.13	1.17	1.17	0.0
24.5	1.01	1.02	1.04	1.07	1.13	0.0	0.0	0.0
28.5	1.01	1.02	1.03	1.06	0.0	0.0	0.0	0.0
33.5	1.01	1.02	1.04	1.01	0.0	0.0	0.0	0.0
35.0	1.01	1.03	0.0	0.0	0.0	0.0	0.0	0.0

Part II

The error estimates of the slopes calculated by the Student 't' test outlined in Equation 3.10.

## STATION A - SENSIBLE HEAT FLUX

SPEED	0.25	0.50	1.0	2.0	4.0	7.0	14.0	28.0
0.4	1.15	2.00	2.04	24.75	0.0	0.0	0.0	0.0
1.6	0.22	0.41	1.89	4.14	4.31	4.71	4.72	4.83
3.4	0.02	0.04	0.11	0.18	0.19	0.31	0.27	0.45
5.5	0.01	0.02	0.03	0.07	0.09	0.16	0.18	0.28
8.0	0.00	0.01	0.02	0.03	0.06	0.10	0.13	0.30
10.8	0.00	0.00	0.01	0.02	0.04	0.07	0.14	0.39
13.9	0.00	0.00	0.01	0.02	0.03	0.07	0.10	0.0
17.2	0.00	0.00	0.01	0.02	0.05	0.12	0.0	0.0
20.8	0.00	0.00	0.01	0.03	0.13	0.0	0.0	0.0
24.5	0.00	0.00	0.01	0.07	0.0	0.0	0.0	0.0
28.5	0.00	0.01	0.02	0.0	0.0	0.0	0.0	0.0
33.5	0.00	0.06	0.0	0.0	0.0	0.0	0.0	0.0
35.0	0.0	0.0	0.0	0.0	0.0	0.0	0.0	0.0

## STATION B - SENSIBLE HEAT FLUX

SPEED	0.25	0.50	1.0	2.0	4.0	7.0	14.0	28.0
0.4	0.80	2.36	3.74	14.43	189.2	246.0	295.4	34.88
1.6	0.42	0.44	1.56	2.34	3.36	3.95	2.88	5.31
3.4	0.02	0.05	0.10	0.23	0.27	0.30	0.28	0.42
5.5	0.01	0.01	0.03	0.07	0.09	0.14	0.15	0.30
8.0	0.00	0.01	0.01	0.03	0.05	0.07	0.11	0.18
10.8	0.00	0.00	0.01	0.02	0.03	0.06	0.10	0.30
13.9	0.00	0.00	0.01	0.02	0.03	0.06	0.11	0.0
17.2	0.00	0.00	0.01	0.02	0.04	0.10	0.0	0.0
20.8	0.00	0.00	0.01	0.02	0.08	0.0	0.0	0.0
24.5	0.00	0.00	0.02	0.03	0.0	0.0	0.0	0.0
28.5	0.00	0.01	0.07	0.0	0.0	0.0	0.0	0.0
33.5	0.00	0.01	0.0	0.0	0.0	0.0	0.0	0.0
35.0	0.0	0.0	0.0	0.0	0.0	0.0	0.0	0.0

## STATION C - SENSIBLE HEAT FLUX

SPEED	0.25	0.50	1.0	2.0	4.0	7.0	14.0	28.0
0.4	1.80	3.24	19.37	50.36	28.91	0.0	0.0	0.0
1.6	0.21	0.56	1.10	2.15	1.78	4.19	10.91	2.59
3.4	0.03	0.05	0.09	0.16	0.20	0.27	0.24	0.58
5.5	0.01	0.02	0.03	0.06	0.10	0.13	0.17	0.20
8.0	0.00	0.01	0.02	0.03	0.04	0.07	0.09	0.16
10.8	0.00	0.01	0.01	0.02	0.03	0.06	0.10	0.26
13.9	0.00	0.00	0.01	0.02	0.04	0.07	0.10	0.60
17.2	0.00	0.00	0.01	0.03	0.04	0.09	0.0	0.0
20.8	0.00	0.00	0.01	0.04	0.09	0.0	0.0	0.0
24.5	0.00	0.01	0.01	0.06	0.0	0.0	0.0	0.0
28.5	0.00	0.01	0.01	0.0	0.0	0.0	0.0	0.0
33.5	0.01	0.01	0.12	0.0	0.0	0.0	0.0	0.0
35.0	0.01	0.0	0.0	0.0	0.0	0.0	0.0	0.0







## STATION B - LATENT HEAT FLUX

SPEED	0.25	0.50	1.0	2.0	4.0	7.0	14.0	28.0
0.4	1.91	2.08	16.31	13.49	367.5	125.7	178.2	8.11
1.6	1.36	1.38	2.39	1.60	2.02	2.08	2.26	3.87
3.4	0.10	0.11	0.16	0.15	0.19	0.17	0.22	0.23
5.5	0.04	0.04	0.07	0.06	0.07	0.06	0.10	0.12
8.0	0.02	0.02	0.03	0.03	0.04	0.04	0.05	0.07
10.8	0.01	0.01	0.02	0.02	0.03	0.03	0.07	0.10
13.9	0.01	0.01	0.01	0.01	0.02	0.04	1.03	0.0
17.2	0.00	0.01	0.01	0.01	0.02	0.07	0.0	0.0
20.8	0.00	0.00	0.01	0.02	1.19	0.0	0.0	0.0
24.5	0.08	0.13	0.24	1.01	0.0	0.0	0.0	0.0
28.5	0.16	0.31	3.05	0.0	0.0	0.0	0.0	0.0
33.5	0.30	0.64	0.0	0.0	0.0	0.0	0.0	0.0
35.0	0.0	0.0	0.0	0.0	0.0	0.0	0.0	0.0

## STATION C - LATENT HEAT FLUX

SPEED	0.25	0.50	1.0	2.0	4.0	7.0	14.0	28.0
0.4	3.42	12.02	9.64	25.18	60.92	0.0	0.0	0.0
1.6	0.85	1.15	1.57	1.87	3.23	2.36	6.26	1.19
3.4	0.07	0.07	0.14	0.13	0.17	0.15	0.22	0.32
5.5	0.03	0.03	0.05	0.06	0.07	0.08	0.09	0.09
8.0	0.01	0.02	0.02	0.03	0.04	0.04	0.05	0.07
10.8	0.01	0.01	0.02	0.02	0.03	0.03	0.07	0.07
13.9	0.01	0.01	0.01	0.02	0.03	0.04	0.07	0.15
17.2	0.01	0.01	0.01	0.02	0.04	0.06	0.0	0.0
20.8	0.00	0.01	0.04	0.03	1.25	0.0	0.0	0.0
24.5	0.08	0.14	0.24	0.58	0.0	0.0	0.0	0.0
28.5	0.14	0.24	0.52	0.0	0.0	0.0	0.0	0.0
33.5	0.27	0.47	3.07	0.0	0.0	0.0	0.0	0.0
35.0	0.90	0.0	0.0	0.0	0.0	0.0	0.0	0.0

## STATION D - LATENT HEAT FLUX

SPEED	0.25	0.50	1.0	2.0	4.0	7.0	14.0	28.0
0.4	6.66	7.24	14.83	0.0	103.3	0.0	0.0	0.0
1.6	1.28	1.29	3.25	2.35	3.28	3.06	6.62	0.0
3.4	0.10	0.10	0.14	0.13	0.17	0.19	0.26	0.35
5.5	0.04	0.04	0.06	0.05	0.08	0.07	0.11	0.10
8.0	0.02	0.02	0.03	0.03	0.04	0.04	0.06	0.07
10.8	0.01	0.01	0.02	0.02	0.03	0.03	0.07	0.07
13.9	0.01	0.01	0.02	0.02	0.03	0.04	0.11	0.0
17.2	0.01	0.01	0.01	0.02	0.04	0.09	2.23	0.0
20.8	0.01	0.01	0.01	0.02	0.08	0.12	0.0	0.0
24.5	0.01	0.01	0.28	0.66	0.0	0.0	0.0	0.0
28.5	0.15	0.24	0.68	0.0	0.0	0.0	0.0	0.0
33.5	0.29	0.67	0.0	0.0	0.0	0.0	0.0	0.0
35.0	1.16	0.0	0.0	0.0	0.0	0.0	0.0	0.0







Appendix G

The test values for the corrected  $\xi_{\text{ke}}$  calculations for the heat fluxes. The difference means are given in Watts/m<sup>2</sup> and the difference variances were forced to 0.0 in all cases and are not shown.

## DIFFERENCE MEANS - SENSIBLE HEAT FLUX

SHIP	0.25	0.50	1.0	2.0	4.0	7.0	14.0	28.0
A	0.03	0.06	0.37	0.78	1.01	2.28	2.49	1.12
B	0.05	0.01	0.02	0.13	0.61	0.48	0.12	0.26
C	0.04	0.08	0.00	0.34	0.73	0.82	1.03	1.34
D	0.01	0.09	0.45	0.99	0.97	0.80	0.35	0.83
E	0.02	0.02	0.21	0.41	0.60	0.60	0.73	1.87
I	0.12	0.23	0.59	1.27	2.21	2.61	3.12	2.98
J	0.03	0.09	0.33	0.58	0.89	1.16	1.10	1.24
K	0.02	0.03	0.03	0.08	0.09	0.41	1.14	1.36
M	0.08	0.26	0.64	0.88	2.26	1.84	2.30	1.76
N	0.02	0.12	0.16	0.41	0.85	0.70	0.51	1.91
P	0.06	0.16	0.31	0.54	0.67	0.68	0.66	0.89

## DIFFERENCE MEANS - LATENT HEAT FLUX

SHIP	0.25	0.50	1.0	2.0	4.0	7.0	14.0	28.0
A	0.00	0.00	0.49	2.16	3.29	6.75	7.19	1.12
B	0.03	0.03	0.24	0.72	2.31	1.54	1.23	0.26
C	0.12	0.23	0.45	0.79	0.74	1.53	1.25	0.91
D	0.48	0.79	0.23	3.76	6.95	6.75	6.76	8.61
E	0.39	0.98	0.33	2.97	9.73	13.8	9.89	2.02
I	0.09	0.22	1.12	3.15	6.31	5.83	9.96	8.51
J	0.05	0.10	0.27	1.87	2.77	3.28	2.79	2.35
K	0.05	0.11	0.14	0.55	0.97	1.07	1.52	3.92
M	0.07	0.08	0.35	0.57	4.82	3.47	3.65	0.24
N	0.86	1.64	3.12	3.27	0.02	6.25	10.4	17.7
P	0.04	0.14	0.41	0.92	2.11	1.91	1.76	1.43

## RESIDUAL VARIANCES - SENSIBLE HEAT FLUX

SHIP	0.25	0.50	1.0	2.0	4.0	7.0	14.0	28.0
A	.003	.008	.022	.043	.056	.072	.070	.099
B	.003	.006	.017	.033	.040	.035	.039	.042
C	.004	.010	.021	.035	.045	.042	.042	.048
D	.004	.010	.026	.042	.051	.056	.054	.062
E	.005	.010	.024	.049	.076	.089	.109	.135
I	.004	.010	.021	.038	.052	.064	.085	.127
J	.003	.010	.019	.032	.040	.050	.064	.074
K	.003	.007	.013	.023	.034	.035	.043	.081
M	.004	.010	.021	.042	.066	.080	.119	.164
N	.006	.011	.020	.042	.071	.086	.145	.233
P	.003	.008	.021	.035	.039	.038	.045	.025

## RESIDUAL VARIANCES - LATENT HEAT FLUX

SHIP	0.25	0.50	1.0	2.0	4.0	7.0	14.0	28.0
A	.004	.012	.038	.079	.122	.165	.201	.254
B	.004	.010	.030	.062	.083	.084	.095	.102
C	.005	.013	.032	.057	.078	.083	.092	.099
D	.006	.017	.043	.078	.095	.120	.138	.184
E	.006	.013	.041	.111	.199	.270	.382	.499
I	.006	.015	.039	.076	.116	.157	.226	.383
J	.004	.012	.030	.060	.093	.121	.192	.270
K	.004	.009	.022	.049	.084	.122	.198	.315
M	.005	.015	.038	.084	.154	.197	.317	.411
N	.006	.012	.029	.086	.191	.268	.534	.834
P	.003	.009	.026	.056	.070	.076	.098	.075

## CORRELATION COEFFICIENTS - SENSIBLE HEAT FLUX

SHIP	0.25	0.50	1.0	2.0	4.0	7.0	14.0	28.0
A	.998	.996	.989	.978	.972	.964	.965	.951
B	.999	.997	.992	.984	.980	.983	.981	.979
C	.998	.995	.989	.982	.977	.979	.979	.976
D	.998	.995	.987	.979	.975	.972	.973	.969
E	.998	.995	.988	.976	.962	.956	.946	.932
I	.998	.995	.989	.981	.974	.968	.958	.936
J	.998	.995	.990	.984	.980	.975	.968	.963
K	.999	.997	.994	.988	.983	.982	.979	.960
M	.998	.995	.989	.979	.967	.960	.940	.918
N	.997	.994	.990	.979	.964	.957	.928	.884
P	.999	.996	.989	.982	.980	.981	.977	.987

## CORRELATION COEFFICIENTS - LATENT HEAT FLUX

SHIP	0.25	0.50	1.0	2.0	4.0	7.0	14.0	28.0
A	.998	.994	.981	.961	.939	.918	.899	.873
B	.998	.995	.985	.969	.958	.958	.952	.949
C	.997	.994	.984	.971	.961	.959	.954	.951
D	.997	.992	.978	.961	.952	.940	.931	.908
E	.997	.993	.980	.945	.901	.865	.809	.750
I	.997	.993	.981	.962	.942	.922	.887	.809
J	.998	.994	.985	.970	.954	.939	.904	.865
K	.998	.995	.989	.975	.958	.939	.901	.842
M	.998	.993	.981	.958	.923	.901	.842	.794
N	.997	.994	.985	.957	.905	.866	.733	.583
P	.999	.996	.987	.972	.965	.962	.951	.962

#### Appendix H

The ships' regression coefficients for the empirical equation of the form  $\chi = C + \alpha(u_j^2 + v_j^2)^{3/2} L^8$ . The geographically averaged values appear at the end. The C indicates the constant drag coefficient, the L indicates the linear drag coefficient, the H refers to the heat flux with S for the sensible heat and L for the latent heat. The X and Y refer to the x and y stress components respectively.

SHIP	TYPE	REGION I				REGION II			
		.25 - 2.0 DAYS				4.0 - 28.0 DAYS			
		$\alpha$	$\beta$	$\gamma$	$\delta$	$\alpha$	$\beta$	$\gamma$	$\delta$
A	C X	4.108	-1.365	0.941	15.866	-1.212	0.210		
	C Y	4.190	-1.410	0.951	15.537	-1.250	0.263		
	L X	3.081	-0.982	0.984	15.694	-0.944	0.256		
	L Y	3.046	-1.022	0.991	15.216	-0.980	0.318		
	H S	3.227	-1.440	0.980	14.279	-1.204	0.243		
	H L	2.945	-1.433	1.014	13.967	-1.215	0.250		
B	C X	4.951	-1.423	0.947	16.053	-1.189	0.209		
	C Y	4.127	-1.341	0.970	15.662	-1.162	0.203		
	L X	4.259	-1.101	0.980	16.084	-0.926	0.249		
	L Y	3.295	-0.988	1.022	15.430	-0.890	0.248		
	H S	3.997	-1.589	1.014	14.991	-1.315	0.208		
	H L	3.164	-1.487	1.039	14.388	-1.275	0.214		
C	C X	4.564	-1.376	0.912	14.772	-1.137	0.238		
	C Y	4.487	-1.318	0.884	15.890	-1.168	0.189		
	L X	3.222	-0.975	0.972	13.664	-0.745	0.280		
	L Y	3.132	-0.890	0.935	15.157	-0.819	0.216		
	H S	2.766	-1.336	0.929	13.358	-1.155	0.248		
	H L	2.463	-1.351	1.003	13.199	-1.171	0.268		
D	C X	3.561	-1.250	0.908	14.030	-1.036	0.244		
	C Y	4.618	-1.334	0.860	16.302	-1.167	0.166		
	L X	2.895	-0.885	0.976	12.758	-0.627	0.305		
	L Y	3.152	-0.900	0.897	15.317	-0.803	0.197		
	H S	4.034	-1.484	1.027	14.510	-1.190	0.201		
	H L	2.639	-1.366	1.029	14.068	-1.153	0.200		
E	C X	1.661	-1.090	0.916	12.612	-1.013	0.287		
	C Y	2.060	-1.172	0.879	13.515	-1.083	0.216		
	L X	0.769	-0.526	0.968	11.787	-0.632	0.359		
	L Y	1.032	-0.616	0.907	12.527	-0.733	0.287		
	H S	2.059	-1.327	0.990	13.698	-1.226	0.217		
	H L	1.204	-1.145	1.029	13.045	-1.126	0.218		
I	C X	4.413	-1.443	0.924	15.100	-1.237	0.260		
	C Y	5.079	-1.474	0.872	15.928	-1.291	0.225		
	L X	3.155	-1.041	0.966	14.409	-0.914	0.299		
	L Y	3.592	-1.054	0.912	15.140	-0.966	0.261		
	H S	4.991	-1.622	0.905	15.065	-1.355	0.278		
	H L	3.903	-1.526	0.958	14.182	-1.296	0.300		

J	C X	3.770	-1.420	0.915	4.448	-1.256	0.280	
	C Y	4.515	-1.458	0.895	5.964	-1.320	0.229	
	L X	2.426	-0.979	0.956	2.931	-0.813	0.319	
	L Y	3.019	-1.016	0.925	4.770	-0.948	0.252	
	H S	3.755	-1.565	0.940	4.685	-1.391	0.277	
	H L	2.517	-1.473	1.005	3.879	-1.348	0.297	
K	C X	2.123	-1.219	0.860	2.407	-1.114	0.388	
	C Y	2.242	-1.194	0.856	2.830	-1.103	0.341	
	L X	1.016	-0.657	0.891	1.485	-0.685	0.458	
	L Y	1.077	-0.624	0.904	1.970	-0.709	0.402	
	H S	1.248	-1.231	0.921	3.618	-1.468	0.246	
	H L	1.199	-1.247	0.979	1.807	-1.253	0.419	
M	C X	3.843	-1.437	0.958	3.622	-1.146	0.302	
	C Y	3.837	-1.465	0.920	4.414	-1.228	0.250	
	L X	2.400	-0.982	0.996	2.644	-0.811	0.385	
	L Y	2.381	-1.009	0.943	3.439	-0.912	0.315	
	H S	2.598	-1.458	0.965	3.711	-1.269	0.271	
	H L	2.010	-1.357	1.019	2.998	-1.213	0.309	
N	C X	2.210	-1.474	0.682	4.177	-1.553	0.230	
	C Y	1.943	-1.341	0.764	3.507	-1.378	0.240	
	L X	0.860	-0.810	0.690	4.305	-1.393	0.218	
	L Y	0.827	-0.720	0.785	3.217	-1.170	0.262	
	H S	1.533	-1.516	0.836	2.082	-1.520	0.329	
	H L	1.950	-1.423	0.857	1.376	-1.603	0.327	
P	C X	4.118	-1.339	0.887	5.487	-1.237	0.251	
	C Y	3.989	-1.330	0.903	4.825	-1.159	0.243	
	L X	3.315	-0.966	0.933	4.464	-0.863	0.280	
	L Y	3.494	-1.006	0.937	3.749	-0.773	0.279	
	H S	2.265	-1.315	0.998	3.657	-1.233	0.264	
	H L	1.902	-1.345	1.020	3.387	-1.230	0.265	
AVG	C X	3.337	-1.322	0.920	4.237	-1.150	0.261	
	C Y	3.437	-1.336	0.901	4.639	-1.183	0.231	
	L X	2.325	-0.910	0.967	3.276	-0.795	0.310	
	L Y	2.322	-0.910	0.940	3.754	-0.853	0.275	
	H S	2.874	-1.469	0.984	3.946	-1.244	0.244	
	H L	1.365	-1.251	1.021	2.335	-1.108	0.263	

Appendix I

The four test values for the stresses and the heat fluxes when the individual ships' equation  $1 + \alpha(u_j^2 + v_j^2)^{0.5} L^k$  was applied to each velocity individually. The stress DMs are in dPa and the heat flux DMs are in Watts/m<sup>2</sup>.

## DIFFERENCE MEANS - X COMPONENT CONSTANT D.C.

SHIP	0.25	0.50	1.0	2.0	4.0	7.0	14.0	28.0
A	0.003	0.009	0.023	0.045	0.066	0.069	0.069	0.067
B	0.004	0.004	0.001	0.003	0.000	0.005	0.012	0.006
C	0.002	0.011	0.036	0.051	0.064	0.078	0.076	0.043
D	0.005	0.023	0.054	0.060	0.060	0.071	0.068	0.039
E	0.001	0.004	0.007	0.004	0.014	0.012	0.013	0.033
I	0.001	0.003	0.010	0.008	0.003	0.005	0.013	0.003
J	0.006	0.001	0.003	0.015	0.030	0.030	0.017	0.041
K	0.001	0.009	0.017	0.002	0.022	0.014	0.012	0.020
M	0.000	0.003	0.011	0.012	0.011	0.024	0.036	0.028
N	0.014	0.030	0.065	0.131	0.163	0.174	0.198	0.233
P	0.002	0.012	0.024	0.015	0.009	0.001	0.016	0.031

## DIFFERENCE MEANS - Y COMPONENT CONSTANT D.C.

SHIP	0.25	0.50	1.0	2.0	4.0	7.0	14.0	28.0
A	0.003	0.008	0.012	0.014	0.015	0.020	0.005	0.001
B	0.002	0.003	0.001	0.012	0.030	0.050	0.065	0.071
C	0.006	0.016	0.017	0.001	0.015	0.025	0.029	0.042
D	0.007	0.020	0.024	0.010	0.009	0.013	0.021	0.036
E	0.005	0.006	0.017	0.038	0.055	0.057	0.062	0.077
I	0.001	0.005	0.005	0.018	0.028	0.017	0.016	0.023
J	0.002	0.004	0.011	0.018	0.031	0.024	0.024	0.042
K	0.005	0.012	0.018	0.025	0.026	0.015	0.006	0.022
M	0.000	0.002	0.002	0.002	0.015	0.012	0.003	0.002
N	0.005	0.011	0.024	0.047	0.059	0.065	0.070	0.080
P	0.006	0.001	0.010	0.001	0.006	0.020	0.044	0.027

## DIFFERENCE MEANS - X COMPONENT LINEAR D.C.

SHIP	0.25	0.50	1.0	2.0	4.0	7.0	14.0	28.0
A	0.003	0.012	0.037	0.076	0.114	0.118	0.111	0.112
B	0.007	0.011	0.009	0.015	0.009	0.007	0.004	0.036
C	0.006	0.014	0.051	0.080	0.109	0.125	0.114	0.065
D	0.006	0.035	0.084	0.089	0.092	0.104	0.092	0.052
E	0.002	0.004	0.007	0.012	0.028	0.029	0.032	0.064
I	0.001	0.005	0.016	0.009	0.007	0.007	0.017	0.000
J	0.011	0.006	0.003	0.036	0.055	0.063	0.047	0.096
K	0.000	0.012	0.022	0.009	0.039	0.028	0.029	0.044
M	0.001	0.004	0.013	0.011	0.012	0.030	0.042	0.028
N	0.018	0.037	0.080	0.163	0.210	0.232	0.269	0.317
P	0.007	0.024	0.041	0.032	0.020	0.003	0.032	0.053

## DIFFERENCE MEANS - Y COMPONENT LINEAR D.C.

SHIP	0.25	0.50	1.0	2.0	4.0	7.0	14.0	28.0
A	0.005	0.015	0.025	0.032	0.038	0.041	0.017	0.011
B	0.005	0.009	0.003	0.014	0.052	0.081	0.100	0.103
C	0.012	0.030	0.035	0.066	0.017	0.035	0.043	0.061
D	0.013	0.035	0.041	0.020	0.016	0.025	0.039	0.060
E	0.005	0.005	0.019	0.048	0.077	0.083	0.093	0.108
I	0.002	0.008	0.006	0.032	0.040	0.031	0.034	0.052
J	0.003	0.006	0.014	0.030	0.052	0.047	0.053	0.085
K	0.008	0.018	0.025	0.034	0.034	0.018	0.007	0.024
M	0.000	0.003	0.002	0.005	0.021	0.016	0.005	0.003
N	0.007	0.015	0.031	0.060	0.077	0.086	0.096	0.111
P	0.013	0.003	0.009	0.007	0.017	0.037	0.060	0.017

## DIFFERENCE VARIANCES - X COMPONENT CONSTANT D.C.

SHIP	0.25	0.50	1.0	2.0	4.0	7.0	14.0	28.0
A	-.007	0.010	0.020	-.015	-.037	0.007	0.064	0.088
B	-.004	0.008	0.017	-.026	-.040	0.038	0.057	0.032
C	-.006	0.008	0.015	-.008	-.000	0.004	0.015	0.003
D	-.007	0.006	0.024	-.011	-.043	-.012	0.019	0.103
E	-.004	0.007	0.010	-.012	-.023	0.035	0.042	-.016
I	-.005	0.008	0.015	-.013	-.016	0.009	0.044	0.030
J	-.005	0.007	0.014	-.014	-.009	0.019	0.045	0.007
K	-.005	0.009	0.019	-.026	-.023	0.017	0.059	-.022
M	-.005	0.009	0.018	-.018	-.023	0.038	0.037	0.001
N	-.006	0.007	0.014	-.002	0.008	0.032	0.033	-.005
P	-.009	0.008	0.032	-.021	-.016	0.030	0.037	-.006

## DIFFERENCE VARIANCES - Y COMPONENT CONSTANT D.C.

SHIP	0.25	0.50	1.0	2.0	4.0	7.0	14.0	28.0
A	-.006	0.009	0.018	-.013	-.029	0.036	0.062	0.031
B	-.006	0.008	0.021	-.017	-.016	0.033	0.041	0.015
C	-.008	0.014	0.024	-.035	-.009	0.042	0.037	0.023
D	-.007	0.017	0.021	-.041	-.029	0.018	0.052	0.071
E	-.005	0.006	0.021	-.021	-.062	0.007	0.089	0.128
I	-.006	0.011	0.019	-.021	-.003	0.041	0.040	-.010
J	-.006	0.010	0.021	-.024	-.010	0.056	0.050	-.009
K	-.007	0.008	0.023	-.017	-.014	0.051	0.051	-.024
M	-.006	0.009	0.019	-.018	-.031	0.011	0.077	0.029
N	-.003	0.009	0.006	-.005	-.004	0.057	0.064	0.005
P	-.008	0.007	0.020	-.003	0.001	-.009	0.027	0.002

## DIFFERENCE VARIANCES - X COMPONENT LINEAR D.C.

SHIP	0.25	0.50	1.0	2.0	4.0	7.0	14.0	28.0
A	-0.012	0.018	0.029	-.022	-.048	-.003	0.075	0.078
B	-.007	0.013	0.027	-.049	-.050	0.055	0.061	-.006
C	-.010	0.013	0.015	0.003	-.009	-.014	0.018	0.017
D	-.011	0.009	0.045	-.028	-.070	-.056	0.004	0.158
E	-.006	0.008	0.017	-.014	-.012	0.054	0.048	-.099
I	-.008	0.014	0.019	-.028	-.035	-.003	0.044	0.047
J	-.007	0.011	0.021	-.029	-.039	0.001	0.077	0.015
K	-.012	0.013	0.039	-.044	-.015	0.032	0.052	-.075
M	-.009	0.015	0.027	-.036	-.007	0.058	0.034	-.094
N	-.011	0.010	0.021	-.010	0.036	0.050	0.011	-.070
P	-.013	0.012	0.048	-.042	-.040	0.044	0.046	-.035

## DIFFERENCE VARIANCES - Y COMPONENT LINEAR D.C.

SHIP	0.25	0.50	1.0	2.0	4.0	7.0	14.0	28.0
A	-.011	0.014	0.027	-.018	-.044	0.062	0.070	-.021
B	-.010	0.013	0.032	-.032	-.015	0.042	0.031	-.020
C	-.010	0.024	0.025	-.061	-.020	0.043	0.028	0.002
D	-.013	0.028	0.032	-.066	-.051	0.002	0.028	0.085
E	-.006	0.010	0.024	-.040	-.052	0.023	0.064	0.055
I	-.011	0.021	0.027	-.047	-.005	0.066	0.041	-.060
J	-.010	0.018	0.032	-.051	-.016	0.075	0.049	-.050
K	-.015	0.013	0.038	-.023	-.016	0.083	0.028	-.084
M	-.011	0.014	0.029	-.026	-.014	0.022	0.076	-.058
N	-.004	0.012	0.003	-.015	0.025	0.075	0.035	-.071
P	-.012	0.007	0.029	0.010	-.014	-.025	0.062	-.017

## RESIDUAL VARIANCES - X COMPONENT CONSTANT D.C.

SHIP	0.25	0.50	1.0	2.0	4.0	7.0	14.0	28.0
A	0.002	0.007	0.017	0.031	0.045	0.047	0.044	0.038
B	0.003	0.007	0.017	0.032	0.043	0.045	0.038	0.031
C	0.003	0.008	0.018	0.034	0.045	0.042	0.048	0.048
D	0.004	0.009	0.024	0.040	0.048	0.051	0.047	0.051
E	0.003	0.006	0.014	0.029	0.037	0.041	0.038	0.032
I	0.002	0.006	0.013	0.022	0.029	0.030	0.035	0.035
J	0.002	0.006	0.013	0.023	0.030	0.033	0.042	0.038
K	0.002	0.006	0.012	0.018	0.024	0.030	0.039	0.044
M	0.002	0.006	0.013	0.024	0.031	0.035	0.043	0.040
N	0.003	0.004	0.008	0.017	0.029	0.035	0.041	0.041
P	0.003	0.008	0.020	0.034	0.040	0.043	0.042	0.035

RESIDUAL VARIANCES - Y COMPONENT CCNSTANT D.C.									
SHIP	0.25	0.50	1.0	2.0	4.0	7.0	14.0	28.0	
A	0.002	0.005	0.014	0.026	0.040	0.046	0.048	0.035	
B	0.003	0.007	0.017	0.037	0.056	0.058	0.054	0.049	
C	0.004	0.011	0.025	0.044	0.054	0.049	0.049	0.044	
D	0.006	0.014	0.030	0.050	0.070	0.074	0.074	0.075	
E	0.004	0.008	0.021	0.036	0.065	0.067	0.064	0.064	
I	0.003	0.008	0.014	0.024	0.031	0.035	0.040	0.042	
J	0.003	0.008	0.017	0.028	0.036	0.041	0.037	0.033	
K	0.003	0.008	0.018	0.027	0.036	0.040	0.048	0.066	
M	0.002	0.005	0.012	0.022	0.033	0.034	0.041	0.040	
N	0.003	0.006	0.011	0.024	0.038	0.045	0.052	0.055	
P	0.003	0.008	0.019	0.039	0.050	0.050	0.053	0.067	
RESIDUAL VARIANCES - X COMPONENT LINEAR D.C.									
SHIP	0.25	0.50	1.0	2.0	4.0	7.0	14.0	28.0	
A	0.006	0.017	0.041	0.082	0.117	0.118	0.100	0.087	
B	0.006	0.016	0.041	0.079	0.107	0.108	0.090	0.079	
C	0.007	0.017	0.043	0.085	0.118	0.107	0.119	0.118	
D	0.008	0.024	0.065	0.111	0.133	0.138	0.115	0.107	
E	0.006	0.015	0.032	0.068	0.079	0.084	0.077	0.064	
I	0.006	0.015	0.032	0.054	0.069	0.070	0.079	0.085	
J	0.005	0.015	0.031	0.057	0.077	0.076	0.094	0.089	
K	0.005	0.014	0.031	0.046	0.061	0.066	0.081	0.091	
M	0.005	0.013	0.031	0.058	0.069	0.078	0.094	0.089	
N	0.005	0.009	0.018	0.034	0.053	0.063	0.065	0.067	
P	0.009	0.023	0.057	0.092	0.105	0.109	0.099	0.089	
RESIDUAL VARIANCES - Y COMPONENT LINEAR D.C.									
SHIP	0.25	0.50	1.0	2.0	4.0	7.0	14.0	28.0	
A	0.004	0.014	0.033	0.064	0.097	0.111	0.107	0.086	
B	0.006	0.017	0.042	0.093	0.138	0.136	0.125	0.116	
C	0.012	0.029	0.066	0.117	0.143	0.124	0.125	0.111	
D	0.015	0.038	0.078	0.128	0.175	0.179	0.177	0.173	
E	0.010	0.021	0.050	0.080	0.138	0.137	0.131	0.124	
I	0.008	0.020	0.036	0.062	0.076	0.084	0.096	0.102	
J	0.007	0.020	0.044	0.070	0.089	0.096	0.086	0.079	
K	0.007	0.020	0.049	0.072	0.085	0.093	0.104	0.159	
M	0.004	0.011	0.031	0.053	0.075	0.075	0.084	0.086	
N	0.007	0.013	0.022	0.045	0.068	0.080	0.090	0.101	
P	0.009	0.019	0.048	0.096	0.122	0.114	0.112	0.144	

## CORRELATION COEFFICIENTS - X COMPONENT CONSTANT D.C.

SHIP	0.25	0.50	1.0	2.0	4.0	7.0	14.0	28.0
A	0.999	0.997	0.992	0.984	0.978	0.976	0.978	0.981
B	0.999	0.997	0.992	0.984	0.979	0.977	0.981	0.985
C	0.998	0.996	0.991	0.983	0.978	0.979	0.976	0.976
D	0.998	0.995	0.988	0.980	0.977	0.975	0.976	0.974
E	0.999	0.997	0.993	0.986	0.982	0.979	0.981	0.984
I	0.999	0.997	0.994	0.989	0.986	0.985	0.983	0.982
J	0.999	0.997	0.994	0.989	0.985	0.984	0.979	0.981
K	0.999	0.997	0.994	0.991	0.988	0.985	0.980	0.978
M	0.999	0.997	0.993	0.988	0.985	0.983	0.978	0.980
N	0.999	0.998	0.996	0.991	0.986	0.982	0.979	0.980
P	0.998	0.996	0.990	0.983	0.980	0.978	0.979	0.982

## CORRELATION COEFFICIENTS - Y COMPONENT CONSTANT D.C.

SHIP	0.25	0.50	1.0	2.0	4.0	7.0	14.0	28.0
A	0.999	0.997	0.993	0.987	0.981	0.977	0.976	0.982
B	0.999	0.997	0.991	0.981	0.972	0.971	0.973	0.975
C	0.998	0.994	0.987	0.979	0.973	0.975	0.975	0.978
D	0.997	0.993	0.985	0.976	0.965	0.963	0.963	0.962
E	0.998	0.996	0.990	0.982	0.969	0.966	0.968	0.968
I	0.998	0.996	0.993	0.988	0.985	0.983	0.980	0.979
J	0.999	0.996	0.991	0.986	0.982	0.979	0.981	0.983
K	0.998	0.996	0.991	0.986	0.982	0.980	0.976	0.967
M	0.999	0.998	0.994	0.989	0.984	0.983	0.979	0.980
N	0.998	0.997	0.994	0.988	0.981	0.977	0.973	0.972
P	0.998	0.996	0.990	0.980	0.975	0.975	0.973	0.967

## CORRELATION COEFFICIENTS - X COMPONENT LINEAR D.C.

SHIP	0.25	0.50	1.0	2.0	4.0	7.0	14.0	28.0
A	0.997	0.992	0.979	0.959	0.943	0.941	0.949	0.956
B	0.997	0.992	0.979	0.962	0.948	0.945	0.954	0.960
C	0.997	0.991	0.978	0.957	0.941	0.947	0.940	0.941
D	0.996	0.988	0.967	0.946	0.936	0.933	0.942	0.946
E	0.997	0.992	0.984	0.966	0.961	0.957	0.961	0.970
I	0.997	0.993	0.984	0.973	0.966	0.965	0.960	0.957
J	0.998	0.993	0.984	0.972	0.962	0.962	0.952	0.955
K	0.997	0.993	0.984	0.978	0.970	0.967	0.959	0.957
M	0.997	0.994	0.984	0.972	0.965	0.960	0.952	0.959
N	0.997	0.995	0.991	0.983	0.973	0.968	0.967	0.968
P	0.995	0.988	0.971	0.955	0.949	0.945	0.949	0.957

## CORRELATION COEFFICIENTS - Y COMPONENT LINEAR D.C.

SHIP	0.25	0.50	1.0	2.0	4.0	7.0	14.0	28.0
A	0.998	0.993	0.983	0.968	0.953	0.943	0.945	0.958
B	0.997	0.992	0.979	0.954	0.931	0.931	0.937	0.943
C	0.994	0.985	0.967	0.944	0.929	0.937	0.937	0.944
D	0.993	0.981	0.961	0.939	0.915	0.911	0.910	0.911
E	0.995	0.989	0.975	0.961	0.933	0.931	0.933	0.937
I	0.996	0.990	0.982	0.970	0.962	0.957	0.951	0.951
J	0.996	0.990	0.978	0.966	0.956	0.951	0.956	0.962
K	0.996	0.990	0.975	0.964	0.958	0.952	0.948	0.925
M	0.998	0.994	0.984	0.974	0.963	0.962	0.957	0.959
N	0.996	0.993	0.989	0.978	0.966	0.959	0.954	0.952
P	0.996	0.990	0.976	0.952	0.939	0.944	0.943	0.929

## DIFFERENCE MEANS - SENSIBLE HEAT FLUX

SHIP	0.25	0.50	1.0	2.0	4.0	7.0	14.0	28.0
A	0.235	0.120	0.041	1.013	1.487	0.589	0.324	1.282
B	0.107	0.011	0.067	0.706	0.381	0.802	1.756	1.563
C	0.067	0.046	0.121	0.302	0.640	0.924	1.145	1.192
D	0.218	0.157	0.148	1.743	0.773	0.248	0.348	0.197
E	0.081	0.116	0.265	0.719	0.747	0.437	0.619	1.497
I	0.361	0.417	0.739	2.254	2.253	2.196	2.465	4.619
J	0.159	0.106	0.239	0.958	1.002	0.882	0.999	2.007
K	0.006	0.055	0.027	0.061	0.113	0.523	1.130	1.109
M	0.302	0.299	0.471	1.645	2.064	1.467	1.165	2.746
N	0.134	0.235	0.476	0.976	0.511	0.469	0.589	1.452
P	0.093	0.130	0.249	0.561	0.716	0.676	0.570	0.710

## DIFFERENCE MEANS - LATENT HEAT FLUX

SHIP	0.25	0.50	1.0	2.0	4.0	7.0	14.0	28.0
A	0.628	0.731	1.287	4.264	4.687	3.532	3.443	5.762
B	0.305	0.342	0.530	2.546	1.736	0.105	0.572	0.793
C	0.302	0.251	0.221	1.566	0.676	0.002	0.199	2.546
D	0.532	0.260	0.347	5.249	9.077	6.566	7.050	10.70
E	0.937	1.645	3.537	8.837	19.16	16.61	17.67	22.88
I	1.132	1.634	3.047	7.801	7.558	7.697	9.290	15.22
J	0.481	0.397	0.735	3.140	4.806	4.557	5.516	10.14
K	0.314	0.274	0.606	2.003	1.310	0.509	1.917	3.327
M	0.620	0.750	1.345	4.086	4.606	3.462	3.706	7.933
N	3.272	5.933	11.31	21.51	3.827	6.403	8.751	6.815
P	0.228	0.165	0.268	1.087	2.444	2.027	2.150	3.802

## DIFFERENCE VARIANCES - SENSIBLE HEAT FLUX

SHIP	0.25	0.50	1.0	2.0	4.0	7.0	14.0	28.0
A	-0.004	0.002	0.012	0.016	-0.041	0.049	0.102	0.120
B	-0.001	0.006	0.007	-0.020	-0.030	0.006	0.065	0.103
C	-0.005	0.004	0.019	-0.001	0.003	0.015	0.015	0.005
D	-0.002	0.002	0.014	-0.004	-0.010	0.027	0.028	0.064
E	-0.002	0.001	0.017	-0.005	-0.001	0.058	0.059	0.004
I	-0.003	0.008	0.013	-0.010	0.012	0.028	0.084	0.045
J	-0.004	0.005	0.015	-0.002	-0.001	0.037	0.046	-0.041
K	-0.005	0.004	0.017	-0.004	0.001	0.037	0.084	-0.021
M	-0.001	0.004	0.011	-0.015	-0.023	0.026	0.104	0.137
N	0.001	0.008	0.002	-0.012	0.041	0.053	0.086	0.027
P	-0.006	0.004	0.020	-0.001	-0.004	0.009	0.055	0.014

## DIFFERENCE VARIANCES - LATENT HEAT FLUX

SHIP	0.25	0.50	1.0	2.0	4.0	7.0	14.0	28.0
A	-0.002	0.003	0.010	0.015	-0.022	0.078	0.172	0.260
B	0.000	0.004	0.005	-0.015	-0.022	0.019	0.089	0.148
C	-0.001	0.002	0.009	-0.000	0.001	0.033	0.038	0.030
D	-0.002	-0.000	0.009	0.022	-0.013	0.039	0.068	0.136
E	-0.002	-0.001	0.012	0.020	0.022	0.123	0.182	0.203
I	-0.002	0.006	0.012	0.014	0.027	0.049	0.147	0.222
J	-0.002	0.001	0.010	0.017	0.006	0.032	0.104	0.113
K	-0.002	0.003	0.010	-0.004	0.010	0.043	0.127	-0.011
M	-0.000	0.003	0.008	-0.012	0.007	0.063	0.176	0.307
N	0.003	0.012	0.009	-0.003	0.095	0.089	0.163	0.136
P	-0.004	0.002	0.009	0.017	-0.007	-0.001	0.059	0.061

## RESIDUAL VARIANCES - SENSIBLE HEAT FLUX

SHIP	0.25	0.50	1.0	2.0	4.0	7.0	14.0	28.0
A	0.003	0.008	0.022	0.040	0.056	0.070	0.063	0.053
B	0.003	0.006	0.016	0.032	0.039	0.034	0.031	0.024
C	0.004	0.010	0.021	0.034	0.042	0.040	0.039	0.038
D	0.004	0.010	0.026	0.039	0.045	0.047	0.044	0.037
E	0.005	0.009	0.023	0.046	0.069	0.075	0.076	0.081
I	0.004	0.011	0.021	0.038	0.044	0.054	0.065	0.057
J	0.003	0.010	0.019	0.032	0.037	0.045	0.059	0.063
K	0.003	0.007	0.013	0.023	0.031	0.037	0.037	0.032
M	0.004	0.010	0.021	0.043	0.065	0.069	0.087	0.070
N	0.006	0.011	0.019	0.042	0.072	0.071	0.094	0.126
P	0.003	0.008	0.021	0.035	0.039	0.036	0.041	0.030

RESIDUAL VARIANCES - LATENT HEAT FLUX									
SHIP	0.25	0.50	1.0	2.0	4.0	7.0	14.0	28.0	
A	0.004	0.013	0.038	0.077	0.112	0.141	0.148	0.147	
B	0.004	0.010	0.029	0.059	0.077	0.074	0.071	0.060	
C	0.005	0.012	0.031	0.054	0.070	0.075	0.077	0.076	
D	0.006	0.016	0.042	0.071	0.083	0.094	0.098	0.095	
E	0.006	0.014	0.040	0.104	0.180	0.218	0.259	0.316	
I	0.006	0.016	0.039	0.077	0.096	0.114	0.147	0.180	
J	0.004	0.012	0.030	0.060	0.079	0.103	0.139	0.156	
K	0.004	0.009	0.021	0.047	0.078	0.111	0.157	0.165	
M	0.005	0.015	0.038	0.081	0.142	0.159	0.215	0.204	
N	0.007	0.015	0.040	0.116	0.189	0.232	0.396	0.589	
P	0.003	0.009	0.026	0.053	0.067	0.068	0.078	0.073	
CORRELATION COEFFICIENTS - SENSIBLE HEAT FLUX									
SHIP	0.25	0.50	1.0	2.0	4.0	7.0	14.0	28.0	
A	0.998	0.996	0.989	0.980	0.973	0.964	0.968	0.974	
B	0.999	0.997	0.992	0.984	0.981	0.983	0.984	0.989	
C	0.998	0.995	0.989	0.983	0.979	0.980	0.980	0.981	
D	0.998	0.995	0.987	0.980	0.978	0.977	0.978	0.982	
E	0.998	0.995	0.989	0.977	0.965	0.962	0.961	0.960	
I	0.998	0.995	0.990	0.981	0.978	0.973	0.967	0.971	
J	0.998	0.995	0.991	0.984	0.982	0.977	0.970	0.970	
K	0.999	0.997	0.994	0.989	0.984	0.981	0.981	0.984	
M	0.998	0.995	0.989	0.979	0.968	0.965	0.956	0.965	
N	0.997	0.994	0.990	0.979	0.963	0.964	0.952	0.936	
P	0.999	0.996	0.989	0.983	0.981	0.982	0.979	0.985	
CORRELATION COEFFICIENTS - LATENT HEAT FLUX									
SHIP	0.25	0.50	1.0	2.0	4.0	7.0	14.0	28.0	
A	0.998	0.994	0.981	0.961	0.944	0.928	0.923	0.926	
B	0.998	0.995	0.985	0.971	0.962	0.963	0.964	0.971	
C	0.997	0.994	0.984	0.973	0.965	0.962	0.961	0.962	
D	0.997	0.992	0.979	0.964	0.959	0.952	0.950	0.952	
E	0.997	0.993	0.980	0.948	0.909	0.885	0.862	0.829	
I	0.997	0.992	0.980	0.961	0.952	0.942	0.923	0.906	
J	0.998	0.994	0.985	0.970	0.960	0.948	0.928	0.919	
K	0.998	0.995	0.989	0.976	0.961	0.943	0.918	0.918	
M	0.998	0.993	0.981	0.960	0.929	0.919	0.886	0.894	
N	0.997	0.993	0.980	0.942	0.902	0.879	0.788	0.686	
P	0.999	0.996	0.987	0.973	0.967	0.966	0.960	0.963	

Appendix J

The four test values for the stresses and the heat fluxes when the geographically averaged equation,  $\bar{\eta}$ , was applied to the velocities individually. The stress DMs are in dPa and the heat flux DMs are in Watts/m<sup>2</sup>.

## DIFFERENCE MEANS - X COMPONENT CONSTANT D.C.

SHIP	0.25	0.50	1.0	2.0	4.0	7.0	14.0	28.0
A	0.003	0.009	0.023	0.045	0.066	0.069	0.069	0.067
B	0.004	0.004	0.001	0.003	0.000	0.005	0.012	0.006
C	0.002	0.011	0.036	0.051	0.064	0.078	0.076	0.043
D	0.005	0.023	0.054	0.060	0.060	0.071	0.068	0.039
E	0.001	0.004	0.007	0.004	0.014	0.012	0.013	0.033
I	0.001	0.003	0.010	0.008	0.003	0.005	0.013	0.003
J	0.006	0.001	0.003	0.015	0.030	0.030	0.017	0.041
K	0.001	0.009	0.017	0.002	0.022	0.014	0.012	0.020
M	0.000	0.003	0.011	0.012	0.011	0.024	0.036	0.028
N	0.014	0.030	0.065	0.131	0.163	0.174	0.198	0.233
P	0.002	0.012	0.024	0.015	0.009	0.001	0.016	0.031

## DIFFERENCE MEANS - Y COMPONENT CONSTANT D.C.

SHIP	0.25	0.50	1.0	2.0	4.0	7.0	14.0	28.0
A	0.003	0.008	0.012	0.014	0.015	0.020	0.005	0.001
B	0.002	0.003	0.001	0.012	0.030	0.050	0.065	0.071
C	0.006	0.016	0.017	0.001	0.015	0.025	0.029	0.042
D	0.007	0.020	0.024	0.010	0.009	0.013	0.021	0.036
E	0.005	0.006	0.017	0.038	0.055	0.057	0.062	0.077
I	0.001	0.005	0.005	0.018	0.028	0.017	0.016	0.023
J	0.002	0.004	0.011	0.018	0.031	0.024	0.024	0.042
K	0.005	0.012	0.018	0.025	0.026	0.015	0.006	0.022
M	0.000	0.002	0.002	0.002	0.015	0.012	0.003	0.002
N	0.005	0.011	0.024	0.047	0.059	0.065	0.070	0.080
P	0.006	0.001	0.010	0.001	0.006	0.020	0.044	0.027

## DIFFERENCE MEANS - X COMPONENT LINEAR D.C.

SHIP	0.25	0.50	1.0	2.0	4.0	7.0	14.0	28.0
A	0.003	0.012	0.037	0.076	0.114	0.118	0.111	0.112
B	0.007	0.011	0.009	0.015	0.009	0.007	0.004	0.036
C	0.006	0.014	0.051	0.080	0.109	0.125	0.114	0.065
D	0.006	0.035	0.084	0.089	0.092	0.104	0.092	0.052
E	0.002	0.004	0.007	0.012	0.028	0.029	0.032	0.064
I	0.001	0.005	0.016	0.009	0.007	0.007	0.017	0.000
J	0.011	0.006	0.003	0.036	0.055	0.063	0.047	0.096
K	0.000	0.012	0.022	0.009	0.039	0.028	0.029	0.044
M	0.001	0.004	0.013	0.011	0.012	0.030	0.042	0.028
N	0.018	0.037	0.080	0.163	0.210	0.232	0.269	0.317
P	0.007	0.024	0.041	0.032	0.020	0.003	0.032	0.053

## DIFFERENCE MEANS - Y COMPONENT LINEAR D.C.

SHIP	0.25	0.50	1.0	2.0	4.0	7.0	14.0	28.0
A	0.005	0.015	0.025	0.032	0.038	0.041	0.017	0.011
B	0.005	0.009	0.003	0.014	0.052	0.081	0.100	0.103
C	0.012	0.030	0.035	0.006	0.017	0.035	0.043	0.061
D	0.013	0.035	0.041	0.020	0.016	0.025	0.039	0.060
E	0.005	0.005	0.019	0.048	0.077	0.083	0.093	0.108
I	0.002	0.008	0.006	0.032	0.040	0.031	0.034	0.052
J	0.003	0.006	0.014	0.030	0.052	0.047	0.053	0.085
K	0.008	0.018	0.025	0.034	0.034	0.018	0.007	0.024
M	0.000	0.003	0.002	0.005	0.021	0.016	0.005	0.003
N	0.007	0.015	0.031	0.060	0.077	0.086	0.096	0.111
P	0.013	0.003	0.009	0.007	0.017	0.037	0.060	0.017

## DIFFERENCE VARIANCES - X COMPONENT CONSTANT D.C.

SHIP	0.25	0.50	1.0	2.0	4.0	7.0	14.0	28.0
A	-.004	0.018	0.038	0.031	0.027	0.068	0.118	0.132
B	-.001	0.017	0.041	0.035	0.072	0.149	0.170	0.145
C	0.002	0.023	0.044	0.052	0.062	0.068	0.079	0.064
D	0.006	0.030	0.069	0.073	0.068	0.103	0.139	0.217
E	-.009	-.003	-.014	-.073	-.108	-.066	-.074	-.152
I	-.008	0.004	0.009	-.020	-.029	-.002	0.042	0.043
J	-.010	-.004	-.008	-.057	-.104	-.080	-.060	-.103
K	-.010	-.005	-.015	-.114	-.189	-.140	-.070	-.104
M	-.016	-.008	-.010	-.059	-.080	-.011	-.001	-.015
N	-.036	-.067	-.163	-.424	-.599	-.685	-.876	-.1.19
P	0.002	0.027	0.065	0.038	0.009	0.066	0.086	0.056

## DIFFERENCE VARIANCES - Y COMPONENT CONSTANT D.C.

SHIP	0.25	0.50	1.0	2.0	4.0	7.0	14.0	28.0
A	-.010	0.006	0.019	0.006	0.007	0.096	0.163	0.191
B	-.003	0.020	0.053	0.069	0.107	0.160	0.175	0.157
C	0.012	0.049	0.089	0.091	0.120	0.170	0.165	0.144
D	0.013	0.053	0.086	0.077	0.130	0.169	0.188	0.185
E	-.009	-.004	-.006	-.093	-.125	-.082	-.049	-.067
I	-.003	0.016	0.026	-.008	-.011	0.037	0.043	0.002
J	-.008	0.006	0.015	-.034	-.048	0.023	0.021	-.031
K	-.007	0.004	0.007	-.070	-.114	-.033	0.000	-.024
M	-.018	-.013	-.020	-.088	-.106	-.063	0.005	-.038
N	-.031	-.054	-.139	-.341	-.481	-.478	-.578	-.790
P	-.000	0.021	0.048	0.053	0.058	0.061	0.113	0.109

DIFFERENCE VARIANCES - X COMPONENT LINEAR D.C.									
SHIP	0.25	0.50	1.0	2.0	4.0	7.0	14.0	28.0	
A	-0.008	0.028	0.054	0.041	0.048	0.094	0.181	0.198	
B	-0.004	0.020	0.049	0.015	0.127	0.227	0.248	0.206	
C	-0.000	0.033	0.056	0.088	0.145	0.142	0.167	0.155	
D	0.012	0.055	0.131	0.138	0.138	0.163	0.222	0.340	
E	-0.008	0.001	-0.008	-0.096	-0.144	-0.085	-0.103	-0.261	
I	-0.014	0.004	0.002	-0.051	-0.049	-0.014	0.048	0.074	
J	-0.018	-0.010	-0.021	-0.113	-0.161	-0.130	-0.060	-0.143	
K	-0.012	0.002	-0.005	-0.181	-0.283	-0.207	-0.135	-0.195	
M	-0.026	-0.015	-0.023	-0.117	-0.138	-0.042	-0.022	-0.083	
N	-0.053	-0.104	-0.268	-0.741	-1.101	-1.341	-1.851	-2.631	
P	0.009	0.051	0.114	0.077	0.048	0.136	0.142	0.067	
DIFFERENCE VARIANCES - Y COMPONENT LINEAR D.C.									
SHIP	0.25	0.50	1.0	2.0	4.0	7.0	14.0	28.0	
A	-0.021	0.001	0.016	-0.009	0.020	0.170	0.248	0.257	
B	-0.009	0.024	0.074	0.092	0.179	0.242	0.253	0.235	
C	0.026	0.090	0.146	0.160	0.237	0.284	0.263	0.221	
D	0.027	0.095	0.146	0.126	0.248	0.277	0.273	0.281	
E	-0.003	0.008	0.000	-0.130	-0.163	-0.112	-0.117	-0.174	
I	-0.005	0.031	0.042	-0.018	0.012	0.091	0.076	-0.013	
J	-0.011	0.015	0.026	-0.061	-0.031	0.060	0.028	-0.082	
K	-0.007	0.019	0.030	-0.079	-0.136	-0.006	-0.011	-0.056	
M	-0.032	-0.026	-0.045	-0.162	-0.161	-0.114	-0.032	-0.139	
N	-0.044	-0.085	-0.229	-0.567	-0.826	-0.875	-1.131	-1.531	
P	-0.002	0.027	0.069	0.090	0.143	0.150	0.240	0.194	
RESIDUAL VARIANCES - X COMPONENT CONSTANT D.C.									
SHIP	0.25	0.50	1.0	2.0	4.0	7.0	14.0	28.0	
A	0.002	0.007	0.017	0.031	0.045	0.049	0.047	0.040	
B	0.002	0.007	0.017	0.032	0.044	0.051	0.046	0.035	
C	0.003	0.008	0.018	0.034	0.045	0.042	0.049	0.048	
D	0.004	0.010	0.025	0.040	0.046	0.051	0.049	0.059	
E	0.003	0.006	0.014	0.032	0.041	0.042	0.040	0.038	
I	0.002	0.006	0.013	0.022	0.029	0.031	0.036	0.036	
J	0.002	0.006	0.013	0.024	0.034	0.036	0.044	0.043	
K	0.002	0.006	0.012	0.023	0.035	0.036	0.040	0.048	
M	0.002	0.006	0.013	0.025	0.033	0.035	0.043	0.040	
N	0.003	0.006	0.016	0.060	0.106	0.134	0.191	0.292	
P	0.003	0.008	0.021	0.034	0.040	0.045	0.043	0.036	

## RESIDUAL VARIANCES - Y COMPONENT CONSTANT D.C.

SHIP	0.25	0.50	1.0	2.0	4.0	7.0	14.0	28.0
A	0.002	0.005	0.014	0.026	0.040	0.049	0.055	0.045
B	0.003	0.007	0.018	0.038	0.058	0.063	0.060	0.053
C	0.004	0.012	0.027	0.043	0.055	0.054	0.054	0.047
D	0.006	0.015	0.031	0.049	0.071	0.077	0.078	0.078
E	0.004	0.008	0.021	0.040	0.068	0.070	0.065	0.069
I	0.003	0.008	0.014	0.024	0.032	0.036	0.043	0.047
J	0.003	0.008	0.018	0.029	0.038	0.042	0.038	0.035
K	0.003	0.008	0.019	0.030	0.040	0.041	0.048	0.065
M	0.002	0.005	0.013	0.024	0.037	0.036	0.041	0.041
N	0.004	0.007	0.017	0.055	0.094	0.101	0.130	0.186
P	0.003	0.008	0.020	0.039	0.050	0.049	0.054	0.066

## RESIDUAL VARIANCES - X COMPONENT LINEAR D.C.

SHIP	0.25	0.50	1.0	2.0	4.0	7.0	14.0	28.0
A	0.006	0.017	0.042	0.081	0.116	0.122	0.106	0.091
B	0.006	0.016	0.042	0.079	0.105	0.118	0.103	0.085
C	0.007	0.017	0.043	0.084	0.114	0.104	0.117	0.116
D	0.008	0.024	0.066	0.107	0.122	0.128	0.113	0.124
E	0.006	0.015	0.033	0.074	0.089	0.090	0.086	0.080
I	0.006	0.015	0.032	0.055	0.071	0.072	0.080	0.084
J	0.005	0.015	0.032	0.062	0.087	0.085	0.100	0.100
K	0.005	0.014	0.032	0.058	0.087	0.083	0.090	0.103
M	0.005	0.013	0.032	0.063	0.078	0.081	0.097	0.089
N	0.006	0.013	0.038	0.151	0.284	0.383	0.598	0.976
P	0.009	0.023	0.058	0.088	0.102	0.109	0.100	0.086

## RESIDUAL VARIANCES - Y COMPONENT LINEAR D.C.

SHIP	0.25	0.50	1.0	2.0	4.0	7.0	14.0	28.0
A	0.005	0.014	0.033	0.064	0.096	0.114	0.116	0.097
B	0.006	0.017	0.043	0.092	0.138	0.143	0.132	0.119
C	0.011	0.030	0.068	0.111	0.141	0.131	0.129	0.111
D	0.014	0.039	0.079	0.121	0.166	0.175	0.175	0.174
E	0.010	0.021	0.051	0.088	0.149	0.149	0.144	0.145
I	0.008	0.020	0.036	0.061	0.077	0.085	0.098	0.107
J	0.007	0.020	0.044	0.071	0.090	0.097	0.088	0.083
K	0.007	0.020	0.049	0.077	0.094	0.097	0.106	0.153
M	0.005	0.011	0.032	0.062	0.086	0.083	0.088	0.094
N	0.008	0.016	0.038	0.124	0.220	0.251	0.346	0.509
P	0.009	0.020	0.048	0.095	0.118	0.109	0.116	0.139

## CORRELATION COEFFICIENTS - X COMPONENT CONSTANT D.C.

SHIP	0.25	0.50	1.0	2.0	4.0	7.0	14.0	28.0
A	0.999	0.997	0.992	0.984	0.977	0.975	0.977	0.981
B	0.999	0.997	0.992	0.984	0.978	0.976	0.979	0.984
C	0.998	0.996	0.991	0.983	0.977	0.979	0.975	0.976
D	0.998	0.995	0.988	0.980	0.977	0.975	0.976	0.974
E	0.999	0.997	0.993	0.985	0.982	0.980	0.981	0.985
I	0.999	0.997	0.994	0.989	0.986	0.984	0.982	0.982
J	0.999	0.997	0.994	0.989	0.985	0.983	0.979	0.981
K	0.999	0.997	0.994	0.991	0.988	0.985	0.981	0.979
M	0.999	0.997	0.993	0.988	0.985	0.983	0.979	0.980
N	0.999	0.998	0.995	0.990	0.986	0.983	0.980	0.979
P	0.998	0.996	0.990	0.983	0.980	0.977	0.978	0.982

## CORRELATION COEFFICIENTS - Y COMPONENT CONSTANT D.C.

SHIP	0.25	0.50	1.0	2.0	4.0	7.0	14.0	28.0
A	0.999	0.997	0.993	0.987	0.980	0.976	0.974	0.981
B	0.999	0.997	0.991	0.981	0.971	0.970	0.971	0.975
C	0.998	0.994	0.987	0.978	0.973	0.975	0.975	0.978
D	0.997	0.993	0.985	0.975	0.965	0.962	0.962	0.962
E	0.998	0.996	0.990	0.982	0.969	0.967	0.968	0.967
I	0.998	0.996	0.993	0.988	0.984	0.982	0.978	0.977
J	0.999	0.996	0.991	0.986	0.982	0.979	0.981	0.983
K	0.998	0.996	0.991	0.986	0.983	0.980	0.976	0.968
M	0.999	0.998	0.994	0.989	0.984	0.983	0.979	0.980
N	0.998	0.997	0.994	0.987	0.981	0.978	0.974	0.973
P	0.998	0.996	0.990	0.980	0.975	0.975	0.973	0.966

## CORRELATION COEFFICIENTS - X COMPONENT LINEAR D.C.

SHIP	0.25	0.50	1.0	2.0	4.0	7.0	14.0	28.0
A	0.997	0.992	0.979	0.959	0.941	0.937	0.946	0.955
B	0.997	0.992	0.979	0.960	0.946	0.941	0.951	0.959
C	0.997	0.991	0.978	0.957	0.941	0.947	0.940	0.941
D	0.996	0.988	0.967	0.945	0.937	0.934	0.944	0.945
E	0.997	0.992	0.984	0.966	0.961	0.958	0.960	0.971
I	0.997	0.993	0.984	0.973	0.966	0.964	0.959	0.957
J	0.998	0.993	0.984	0.972	0.963	0.962	0.952	0.955
K	0.997	0.993	0.984	0.977	0.969	0.967	0.960	0.957
M	0.997	0.994	0.984	0.972	0.966	0.960	0.952	0.958
N	0.997	0.995	0.990	0.981	0.972	0.967	0.964	0.959
P	0.995	0.988	0.971	0.955	0.948	0.944	0.949	0.956

## CORRELATION COEFFICIENTS - Y COMPONENT LINEAR D.C.

SHIP	0.25	0.50	1.0	2.0	4.0	7.0	14.0	28.0
A	0.998	0.993	0.983	0.968	0.951	0.942	0.943	0.955
B	0.997	0.992	0.978	0.953	0.929	0.928	0.934	0.941
C	0.994	0.985	0.966	0.943	0.929	0.937	0.937	0.945
D	0.993	0.981	0.960	0.938	0.914	0.910	0.910	0.911
E	0.995	0.989	0.975	0.960	0.934	0.931	0.933	0.936
I	0.996	0.990	0.982	0.970	0.961	0.957	0.950	0.947
J	0.996	0.990	0.978	0.966	0.956	0.950	0.955	0.961
K	0.996	0.990	0.975	0.964	0.958	0.952	0.947	0.926
M	0.998	0.994	0.985	0.974	0.963	0.962	0.957	0.958
N	0.996	0.993	0.988	0.976	0.964	0.958	0.954	0.950
P	0.996	0.990	0.976	0.951	0.939	0.944	0.943	0.928

## DIFFERENCE MEANS - SENSIBLE HEAT FLUX

SHIP	0.25	0.50	1.0	2.0	4.0	7.0	14.0	28.0
A	0.070	0.204	0.603	0.275	0.281	1.411	2.001	1.392
B	0.069	0.130	0.408	0.229	0.198	1.337	2.240	1.836
C	0.017	0.095	0.366	0.687	0.739	1.025	1.257	1.291
D	0.068	0.499	1.364	1.752	1.772	2.694	2.562	1.605
E	0.125	0.208	0.466	1.180	1.180	1.072	1.551	2.876
I	0.012	0.179	0.241	0.616	1.245	0.531	0.383	0.086
J	0.088	0.009	0.074	0.720	1.383	1.137	0.872	1.375
K	0.029	0.024	0.144	0.322	0.531	0.165	0.328	0.296
M	0.356	0.436	0.800	2.439	2.884	2.156	1.553	2.608
N	0.423	0.908	1.986	4.355	5.495	6.009	6.822	8.334
P	0.087	0.118	0.220	0.490	0.763	0.713	0.579	0.677

## DIFFERENCE MEANS - LATENT HEAT FLUX

SHIP	0.25	0.50	1.0	2.0	4.0	7.0	14.0	28.0
A	0.027	0.643	1.592	1.871	2.093	4.750	7.173	8.262
B	0.123	0.592	1.562	2.300	2.818	5.207	7.036	6.980
C	0.195	0.749	1.780	2.630	2.562	3.992	4.959	4.311
D	0.816	2.587	5.764	8.111	8.618	12.29	13.02	10.20
E	0.782	1.326	2.887	7.584	10.05	7.326	8.728	14.31
I	0.084	0.698	1.343	0.770	0.429	2.230	5.462	6.749
J	0.190	0.196	0.425	0.655	2.528	0.960	1.122	0.205
K	0.417	0.575	1.408	4.019	6.961	3.866	0.661	1.604
M	0.306	0.083	0.028	1.092	1.447	1.564	4.627	5.199
N	1.805	3.984	9.403	21.30	30.13	31.79	33.81	42.42
P	0.103	0.099	0.280	0.091	0.620	0.383	0.892	0.015

DIFFERENCE VARIANCES - SENSIBLE HEAT FLUX									
SHIP	0.25	0.50	1.0	2.0	4.0	7.0	14.0	28.0	
A	0.002	0.013	0.034	0.064	0.041	0.140	0.206	0.241	
B	-0.002	0.006	0.010	-0.001	-0.020	0.010	0.063	0.095	
C	0.009	0.026	0.059	0.067	0.021	0.032	0.028	0.005	
D	0.005	0.017	0.050	0.087	0.080	0.116	0.114	0.139	
E	-0.002	0.001	0.015	-0.021	-0.041	-0.002	-0.038	-0.166	
I	0.003	0.018	0.029	0.023	0.028	0.066	0.163	0.204	
J	-0.002	0.008	0.018	0.000	-0.055	-0.011	0.016	-0.015	
K	-0.012	-0.015	-0.033	-0.139	-0.282	-0.294	-0.298	-0.497	
M	-0.003	0.001	0.002	-0.041	-0.062	-0.009	0.078	0.132	
N	-0.020	-0.038	-0.109	-0.307	-0.514	-0.604	-0.713	-0.892	
P	-0.002	0.013	0.038	0.035	-0.015	0.002	0.054	0.024	

DIFFERENCE VARIANCES - LATENT HEAT FLUX									
SHIP	0.25	0.50	1.0	2.0	4.0	7.0	14.0	28.0	
A	0.001	0.008	0.023	0.060	0.056	0.165	0.274	0.394	
B	0.001	0.008	0.016	0.024	0.023	0.060	0.132	0.193	
C	0.007	0.018	0.043	0.075	0.065	0.107	0.132	0.141	
D	0.004	0.012	0.037	0.091	0.112	0.162	0.193	0.263	
E	0.003	0.009	0.032	0.059	0.078	0.173	0.230	0.250	
I	-0.001	0.005	0.014	0.031	0.043	0.069	0.176	0.281	
J	-0.004	-0.002	0.003	0.008	-0.040	-0.017	0.027	0.080	
K	-0.003	-0.001	-0.002	-0.035	-0.131	-0.086	0.052	0.034	
M	-0.000	0.002	0.009	-0.003	0.009	0.069	0.196	0.377	
N	-0.005	-0.010	-0.035	-0.085	-0.272	-0.381	-0.453	-0.670	
P	-0.003	0.005	0.015	0.034	0.016	0.028	0.103	0.114	

RESIDUAL VARIANCES - SENSIBLE HEAT FLUX									
SHIP	0.25	0.50	1.0	2.0	4.0	7.0	14.0	28.0	
A	0.003	0.008	0.022	0.041	0.055	0.074	0.072	0.065	
B	0.003	0.006	0.017	0.031	0.040	0.037	0.033	0.024	
C	0.004	0.010	0.022	0.035	0.041	0.039	0.038	0.039	
D	0.004	0.010	0.026	0.040	0.046	0.049	0.046	0.039	
E	0.005	0.010	0.024	0.049	0.071	0.076	0.078	0.100	
I	0.004	0.010	0.021	0.037	0.047	0.061	0.082	0.077	
J	0.003	0.010	0.019	0.031	0.040	0.047	0.059	0.048	
K	0.003	0.007	0.015	0.035	0.055	0.061	0.063	0.088	
M	0.004	0.010	0.021	0.046	0.067	0.069	0.087	0.071	
N	0.006	0.014	0.030	0.097	0.137	0.157	0.201	0.271	
P	0.003	0.008	0.021	0.035	0.039	0.036	0.041	0.030	

## RESIDUAL VARIANCES - LATENT HEAT FLUX

SHIP	0.25	0.50	1.0	2.0	4.0	7.0	14.0	28.0
A	0.004	0.012	0.038	0.077	0.122	0.167	0.190	0.204
B	0.004	0.010	0.030	0.062	0.088	0.092	0.098	0.080
C	0.005	0.013	0.033	0.056	0.074	0.083	0.089	0.090
D	0.006	0.017	0.043	0.077	0.094	0.110	0.119	0.123
E	0.006	0.014	0.040	0.103	0.176	0.221	0.263	0.317
I	0.006	0.015	0.040	0.076	0.113	0.148	0.223	0.276
J	0.004	0.012	0.030	0.059	0.091	0.120	0.178	0.188
K	0.004	0.009	0.022	0.049	0.089	0.121	0.172	0.182
M	0.005	0.015	0.038	0.079	0.151	0.175	0.252	0.254
N	0.006	0.012	0.033	0.095	0.221	0.301	0.527	0.894
P	0.003	0.009	0.026	0.054	0.069	0.075	0.087	0.075

## CORRELATION COEFFICIENTS - SENSIBLE HEAT FLUX

SHIP	0.25	0.50	1.0	2.0	4.0	7.0	14.0	28.0
A	0.998	0.996	0.989	0.980	0.972	0.963	0.967	0.972
B	0.999	0.997	0.992	0.985	0.980	0.982	0.983	0.989
C	0.998	0.995	0.989	0.983	0.979	0.980	0.981	0.980
D	0.998	0.995	0.987	0.980	0.977	0.976	0.978	0.982
E	0.997	0.995	0.988	0.976	0.966	0.962	0.962	0.957
I	0.998	0.995	0.990	0.982	0.976	0.969	0.959	0.963
J	0.998	0.995	0.991	0.985	0.981	0.976	0.970	0.976
K	0.999	0.996	0.993	0.986	0.984	0.982	0.981	0.984
M	0.998	0.995	0.989	0.978	0.968	0.966	0.956	0.965
N	0.997	0.994	0.987	0.966	0.966	0.966	0.960	0.953
P	0.999	0.996	0.989	0.982	0.981	0.982	0.979	0.985

## CORRELATION COEFFICIENTS - LATENT HEAT FLUX

SHIP	0.25	0.50	1.0	2.0	4.0	7.0	14.0	28.0
A	0.998	0.994	0.981	0.961	0.938	0.913	0.901	0.900
B	0.998	0.995	0.985	0.969	0.956	0.953	0.950	0.961
C	0.997	0.994	0.984	0.972	0.963	0.958	0.955	0.955
D	0.997	0.992	0.978	0.961	0.952	0.944	0.939	0.940
E	0.997	0.993	0.980	0.947	0.909	0.883	0.859	0.828
I	0.997	0.993	0.980	0.962	0.942	0.924	0.882	0.851
J	0.998	0.994	0.985	0.970	0.956	0.941	0.910	0.903
K	0.998	0.995	0.989	0.976	0.960	0.943	0.912	0.908
M	0.998	0.993	0.981	0.961	0.924	0.910	0.865	0.867
N	0.997	0.994	0.984	0.955	0.909	0.885	0.799	0.687
P	0.999	0.996	0.987	0.973	0.965	0.962	0.955	0.962